Sequence Specific Cleavage of Double Helical DNA

N-Bromoacetyldistamycin

Thesis by

Brenda Faye Baker

In Partial Fulfillment of the Requirements
for the
Degree of Doctor of Philosophy

California Institute of Technology
Pasadena, California

1988

(Submitted May 23, 1988)

© 1988

Brenda Faye Baker

All Rights Reserved

Acknowledgements

My deepest gratitude goes to my mentor and friend, Professor Peter Dervan, who shared his endless and **intense** energy with me throughout my graduate studies. I also thank the other members of my committee, Professors John Roberts, John Richards and Dennis Dougherty, for their encouragement through example.

I give special thanks to Professors Robert Williams and Elaine Roberts at Colorado State University who inspired me to continue my education and scientific growth through graduate studies at Caltech.

I am very appreciative of the technical and professional assistance provided by those of the Caltech community. Especially, those folks involved in the athletic and graphic art facilities, the libraries, and the division of chemistry -- without whom I would still be scrambling.

Dervanites -- Past, Present, and Future -- YOOOWWWWWWW!!!!!!!!!!!!!.

And those at large -- thanks for being on the boogie side.

Finally, thanks to Mom and Dad, Dave, Tom, Bonnie, Bev, and Mitch for **being there** through both the highs and the lows.

Love,

Brenda

Abstract

This thesis is concerned with the design, synthesis, and mechanism of interaction of sequence specific double helical DNA cleaving molecules. The design of sequence specific cleaving molecules for double helical DNA requires the attachment of DNA cleaving moieties to sequence specific DNA binding molecules. The degree of cleavage specificity is in part controlled by the cleavage moiety. With this in mind attention is focused on attachment of a nondiffusible cleavage moiety, specifically an electrophile, to a sequence specific binding unit. Electrophilic attack of DNA nucleophiles, such as the N-3 of adenine or the N-7 of guanine, results in cleavage of the backbone via depurination.

N-Bromoacetyldistamycin (BD) is designed to place an electrophile in the minor groove within adenine-thymine rich regions in close proximity to the N3 of adenine. The electrophile, bromoacetyl, is attached at the amino end of tris-N-methylpyrrolcarboxamide, a tripeptide binding unit from the natural product distamycin A.

A general synthetic scheme has been devised which allows for synthesis of the isotopically labeled compounds (carbon 13 and 14) and the other halide derivatives, iodo and chloro, for purposes of product characterization and kinetic analysis.

Affinity cleavage studies by high resolution gel electrophoresis show that BD has a high degree of cleavage specificity. Out of 334 bases in a 167 b.p. restriction fragment, from the pBR322 plasmid, cleavage occurs primarily (80%) at a single adenine after 10 hours at 37 degrees. In order to understand this high degree of specificity the mechanistic details of the reaction have been explored.

Under longer reaction times and higher temperatures cleavage occurs at other adenines of the 167 b.p. restriction fragment. The amount of cleavage at any given adenine is dependent upon the leaving group as shown with the hydroxy, chloro, iodo and mesyl derivatives, where Br>I≃Ms>Cl>>>OH.

Electrophilic attack of double helical DNA by BD occurs at the N3 of adenine. In

this regard, carbon 14 labeled BD was utilized to compare the products from the BD/free base adenine reaction and the BD/DNA reactions. 99% enriched [^{15}N3]-adenine, 99% enriched N-Bromo-[2-^{13}C]-acetyldistamycin, and subsequently the four isotopic combinations of the distamycin-adenine adduct were synthesized to determine the site of alkylation by proton, carbon 13, and nitrogen 15 NMR. The adenine adduct exists in the amino form (N6) as shown by NMR of the ^{15}N6 labeled adduct.

3-(Acetyldistamycin)-adenine is the sole released product from the reaction of BD with a 15 base pair oligonucleotide, which contains the site of major cleavage from the 167 b.p. restriction fragment.

DNA products at each stage of the reaction and workup procedure were monitored by high resolution gel electrophoreses of radioactively labeled DNA. The alkylated DNA-distamycin intermediate has been detected. The DNA end products were determined enzymatically with phosphatases verifying that both the 3' and 5' DNA termini are phosphates as expected for an alkylation/depurination reaction followed by base workup.

The reaction of the N-haloacetyldistamycins (Cl, Br, and I) with double helical DNA which results in strand cleavage has four experimentally distinguishable steps: 1) binding, 2) covalent attachment to adenine, 3) release of the adenine adduct, and 4) strand cleavage. Steps one through three were quantitatively analyzed using a synthetic oligonucleotide that contained the site of major cleavage (one binding site) of the 167 restriction fragment. In this system the binding constant for BD measures as $K = 5.5 \times 10^5\ M^{-1}$. The rate of akylation is first order ($k = 1.94 \times 10^{-2}\ h^{-1}$, 37°C) and the rate of adenine adduct release is first order ($7.76 \times 10^{-2}\ h^{-1}$, 37°C).

The cleavage specificities of the synthetic molecule, N-Bromoacetyldistamycin, and the natural product, CC1065 were compared on the 167 b.p. restriction fragment After a reaction time of one hour at 37°C, CC1065 cleaves at 21 adenines whereas BD shows only a minute amount of cleavage at one adenine.

Table of Contents

I) Introduction 1

II) Results and Discussion
- A. N-Bromoacetyldistamycin (BD) 25
- B. Cleavage of Double Helical DNA by BD 30
- C. Dependence of DNA Cleavage on Time and Temperature 35
- D. Dependence of Cleavage Rate and Specificity on Leaving Group 47
- E. Released Product Analysis 54
- F. Characterization of the Distamycin-Adenine Adduct 64
  - 1. Determination of the Site of Alkylation 67
  - 2. Determination of the Tautomeric Species 82
  - 3. Resonance *vs.* Self Base Pairing 86
  - 4. Peak Assignment of the Carbon 13 Spectrum 92
- G. DNA Product Analysis 100
- H. Kinetic Analysis 113
  - 1. Binding/Complexation 114
    - Equilibrium Dialysis 114
    - Melting Temperature of the 15mer 115
  - 2. Alkylation/Covalent Attachment 124
    - Rate of Alkylation of Adenine 48 127
    - Rate of Alkylation of Adenine 58 and 59 138
  - 3. Depurination/Base Release 151
- I. A Comparison to CC1065 161

III) Conclusion 165

IV) Experimental 170

V) References 194

List of Figures

I) Introduction

Figure 1: Right-Handed Double Helical DNA....2

Figure 2: Watson-Crick Base Pairs....4

Figure 3: Proposed Mechanism for Oxidative Cleavage of DNA....7

Figure 4: Proposed Mechanism of Hydrolytic Cleavage of DNA....7

Figure 5: Proposed Mechanism of Electrophilic Cleavage of DNA....9

Figure 6: Mechanism of Electrophilic Attack of Double Helical DNA by Anthramycin and Mitomycin C....13

Figure 7: Mechanism of Covalent Binding to DNA by CC1065....15

Figure 8: Model of the N-methyltripyrrole Binding Unit Complexed to Double Helical DNA....19

Figure 9: Proposed Placement of an Electrophile in the Minor Groove of Double Helical DNA....19

II) Results and Discussion

Figure 1: Proton Spectrum of N-Bromoacetyldistamycin in DMSO....28

Figure 2: Proton Spectrum of N-Bromoacetyldistamycin in D_2O....29

Figure 3: Autoradiogram of BD Cleavage and MPE Footprinting on the 167 b.p. restriction fragment....31

Figure 4: Histogram of Sites of Cleavage and Binding of BD on the 167 b.p. restriction fragment....33

Figure 5: Autoradiogram of the Dependence of Cleavage on Time....36

Figure 6: Histogram of Time Studies....38

Figure 7: Autoradiogram of the Dependence of Cleavage on Temperature....39

Figure 8: Histogram of Temperature Studies....41

Figure 9: Proton Spectrum of N-Chloroacetyldistamycin in D_2O 47

Figure 10: A) N-Hydroxyacetyldistamycin B) N-Chloroacetyldistamycin C) N-Iodoacetyldistamycin D) N-Mesylacetyldistamycin 48

Figure 11: Autoradiogram of the Dependence of Cleavage and MPE Footprinting on the167 b.p. restriction fragment of HOD, CD, BD, and ID 52

Figure 12: Autoradiograms of the TLC plates for the reaction between ^{14}C-BD and adenine 55

Figure 13: Autoradiograms of the TLC plates for the reaction between ^{14}C-BD and the 15mer 58

Figure 14: Comparison of the UV-vis spectra of the synthetic BD-adenine adduct with that of the 15mer-BD adduct 60

Figure 15: Common product from the free base adenine and oligonucleotide reaction with BD 61

Figure 16: Proton Spectrum of the Authentic Distamycin-Adenine Adduct 63

Figure 17: Ultraviolet Spectrum of the Adenine Adduct acquired by the Photodiode Array Detector during Chromatography 65

Figure 18: Isotopically Labeled Distamycin-Adenine Adducts 71

Figure 19: Proton Spectrum of the Unlabeled Adenine Adduct 73

Figure 20: Proton Spectrum of the [^{12}C-^{15}N] Adenine Adduct 74

Figure 21: Proton Spectrum of the [^{13}C-^{14}N] Adenine Adduct 75

Figure 22: Proton Spectrum of the [^{13}C-^{15}N] Adenine Adduct 76

Figure 23: Proton Spectrum of the Unlabeled Adenine Adduct with the Pertinent Peak Assignments 77

Figure 24: Nitrogen 15 Spectra of [^{13}C-^{15}N] and [^{12}C-^{15}N] 3-(Acetyldistamycin)-adenine 79

Figure 25: Carbon 13 Spectra of [^{13}C-^{15}N] and [^{13}C-^{14}N] 3-(Acetyldistamycin)-adenine 81

Figure 26: Tautomer: Imino *vs.* Amino 83

Figure 27: 3-(Acetyldistamycin)-[$^{15}N6$]-adenine 84

Figure 28: Nitrogen 15 Spectrum of 3-(Acetyldistamycin-[$^{15}N6$]-adenine 85

Figure 29: Resonance *vs.* Self Base Pairing.. 86

Figure 30: Proton Spectrum of 3-(Acetyldistamycin)-[^{15}N6]-adenine............ 87

Figure 31: 3-(N-[2-Bromoacetamido] N'N'-dimethyl-1,3-propane diamine)-adenine **23** (DOA)... 93

Figure 32: Proton Decoupled and Coupled Carbon 13 Spectra of DOA... 94

Figure 33: Selected Proton Decoupled Carbon 13 Spectra of DOA... 95

Figure 34: Assigned N3 Adenine Adducts for (I) BD (II) Simple BD Model (III) CC1065 (IV) 9-Anthryloxirane, (V) Methyltoluenesulfonate, (VI) Butylbromide, and (VII) Benzylbromide 97

Figure 35: Autoradiogram of the Sequential Analysis of the Oligonucleotide Reaction Products...................................... 102

Figure 36: Diagram of the Gel Band Assignment of the Sequential Analysis of the Oligonucleotide Products.............................. 104

Figure 37: Diagram of the Enzymatic Characterization of the Cleaved Oligonucleotide Products............................... 106

Figure 38: Autoradiogram of the Enzymatic Characterization of the Cleaved Oligonucleotide Products...................................... 107

Figure 39: Autoradiogram of the Moderation of the Oligo/^{14}C-BD Reaction Pathway through Time... 110

Figure 40: Diagram of the spot assignment, by structure, of the TLC autoradiogram of the Oligo/BD reaction....................... 112

Figure 41: Oligonucleotide sequences utilized for binding and kinetic analysis.. 113

Figure 42: Equilibration Time of N-Acetyldistamycin............................. 117

Figure 43: Diagram of the Equilibrium Dialysis System and Technique... 118

Figure 44: Graph of the Melting Temperature of the 15mer at 10mM NaPhosphate.. 121

Figure 45: Graph of the Melting Temperature of the 15mer at 100mM NaPhosphate... 122

Figure 46: HPLC Chromatograms of the BD/15mer reaction...................... 125

Figure 47: Concentration and the Rate of Alkylation: Graph of Time *vs.* -ln ([BD] / $[BD]_o$)... 130

Figure 48: Verification of the Maximization of the Rate of Alkylation: Graph of Time *vs*. $-\ln([BD] / [BD]_o)$ 131

Figure 49: Absolute Rate of Alkylation of Adenine 48: Graph of Time *vs*. $-\ln([BD] / [BD]_o)$ 132

Figure 50: HPLC Chromatograms of the ID/15mer reaction 133

Figure 51: Rate of Alkylation of ID/15mer at 45°C: Graph of Time *vs*. $-\ln([ID] / [ID]_o)$ 136

Figure 52: Rate of Alkylation of BD/15mer at 45°C: Graph of Time *vs*. $-\ln([BD] / [BD]_o$ 137

Figure 53: Rate of Alkylation of BD/21mer at 45°C: Graph of Time *vs*. $-\ln([BD] / [BD]_o$ 142

Figure 54: Autoradiogram of the 21mer: Measurement of Cleavage at Adenine 58 and 59 by ID and BD 143

Figure 55: HPLC Chromatograms of the BD/21mer reaction 147

Figure 56: HPLC Chromatogram of the BD/21mer reaction after 168 hours 149

Figure 57: Graph of Relative Amounts of the Reaction Species through Time 157

Figure 58: Equation-Derived Graph of Relative Amounts of the Reaction through Time 158

Figure 59: Graph Overlay of Real and Derived Data of the Relative Amounts of the Reaction Species through Time 159

Figure 60: Comparison of CC1065 and BD on the 167 b.p. Restriction Fragment: Autoradiogram of the Gel 162

Figure 61: Histrogram of Sites of Cleavage: CC1065 *vs*. BD 164

Figure 62: Methidiumpropyl EDTA-Fe(II), Distamycin EDTA-Fe(II) and N-Bromoacetyldistamycin 166

Figure 63: Histogram of the MPE footprints for Distamycin A and BD and the Cleavage Sites of BD and DE on the 167 b.p. restriction fragment 167

III) Experimental

Figure 1: Autoradiogram of the Binding Sites for BD and Distamycin A on the 167 b.p. restriction fragment 181

Figure 2: Workup Conditions for Optimizing Cleavage 183

List of Tables

I) Introduction

Table 1: Alkylation Product Distribution of Double Helical DNA by Simple Electrophiles 10

Table 2: Comparison of the Intra and Intermolecular S_N2 Reaction Rates 22

Table 3: Dependence of the Rate of S_N2 Displacement Reactions on the Leaving Group 23

II) Results and Discussion

Table 1: Application of Calladine's Rules to the 167 b.p. restriction fragment 46

Table 2: Carbon 13 Spectral Assignments for N3 Adenine Adducts 99

Table 3: Proton (H2 and H8) Spectral Assignments for N3 Adenine Adducts 99

Table 4: Equilibrium Dialysis / Scintillation Counting Data 120

Table 5: Equilibrium Dialysis / % Bound and % Free 120

Table 6: Percentage of Single Stranded 15mer with Temperature 123

Table 7: Concentration and the Rate of Alkylation 130

Table 8: The Absolute Rate of Alkylation at Adenine 48: Verification of the DNA:BD Ratio 131

Table 9: The Absolute Rate of Alkylation at Adenine 48 132

Table 10: Relative Rates of Alkylation at Adenine 48, ID/BD: N-Iodoacetyldistamycin 135

Table 11: Relative Rates of Alkylation at Adenine 48, ID/BD: N-Bromoacetyldistamycin 135

Table 12: Overall Rate of Alkylation: Adenine 58 plus 59 by BD 142

Table 13: Relative Rates of Alkylation by BD: Adenine 58 *vs* 59 145

Table 14: Relative Rates of Alkylation, ID/BD: Adenines 58 and 59 146

Table 15: Determination of the Extinction Coefficients of BD Under HPLC conditions 154

Table 16: Determination of the Extinction Coefficients of DA Under HPLC conditions.. 154

Table 17: Relative Amounts of Product (DA) and Reactant (BD) during the reaction time.. 155

Table 18: Averaged Values of Relative Amounts of DA and BD during the reaction time.. 156

List of Schemes

Scheme 1: Synthetic Scheme of N-Bromoacetyldistamycin........................... 27

Scheme 2: Synthetic Scheme of [^{15}N3]-Adenine....................................... 68

Scheme 3: Synthetic Scheme of [^{15}N6]-Adenine....................................... 84

INTRODUCTION

The design of sequence specific DNA cleaving reagents entails the attachment of a DNA cleaving moiety to a sequence specific DNA binding molecule. The cleavage specificity achieved by the molecule is determined by both the sequence specificity of the molecule and the mechanism of cleavage. The design is limited by our current understanding of the structure of deoxyribonucleic acid in solution and the mechanism of DNA cleavage. An in depth analysis of the mechanism of the interactions and reactions between these novel engineered compounds and DNA provides a base for new designs in order to achieve any desired degree and type of specificity with regard to cleavage of double helical DNA. This dissertation embodies the design, synthesis, and mechanism of action of the sequence specific DNA cleaving molecule N-bromoacetyldistamycin.

DNA

Deoxyribonucleic acids are complex macromolecules which exist in many states (crystalline, fibrous, solution), forms (single stranded, double stranded, triple stranded), shapes (supercoiled, circular, linear), and conformations (A, B, P, C, Z). This research has been directed towards double stranded, linear, B form DNA in aqueous solution.

Double helical DNA can be divided into three domains -- the major groove, the minor groove, and the sugar/phosphate backbone (Figure 1).[1,2] Each domain has its own set of recognition elements. These sets include elements such as the dimensions and geometries (groove width and depth), and the type and array of functional groups. Double stranded DNA is formed and stabilized through hydrogen bonding between complimentary bases[1] (Figure 2, Watson-Crick pairing) and the stacking forces between bases on the same strand.[2] The repulsive electrostatic forces between the two phosphate backbones are stabilized by cations.

Local double helical DNA conformations are dependent upon the base sequence. This dependence is evident from the x-ray crystal analysis (1.9A resolution) of the B DNA dodecamer, 5'-d(CGCGAATTCGCG).[3] In this duplex, variability is apparent in the helical twist angle at each base pair step. For instance, the angle of the C3-G4 step measures as 27.4° and that of the A5-A6 step as 37.7°. Significant conformational variations are also observed in the torsion angle, δ (the dihedral angle between C5'-C4'-C3'-O3') and the N-glycosyl angle, χ (O1'-C1'-N9-C4 for purines and O1'-C1'-N1-C2 for pyrimidines). Values range from 100° to 160° for the torsion angle and -85° to -140° for the glycosyl angle. In general it is observed that the purines prefer higher δ and χ values than the

Figure 1: Computer graphic of right-handed double helical DNA generated by Biograf software on an Evans and Sutherland PS 340 system. Bases are light purple, sugars are blue, and the phosphates are yellow. *Top*, a view of the macromolecule down the helix axis. *Bottom left*, the major groove is centered on the front face. *Bottom right,* the minor groove is centered on the front face.

3

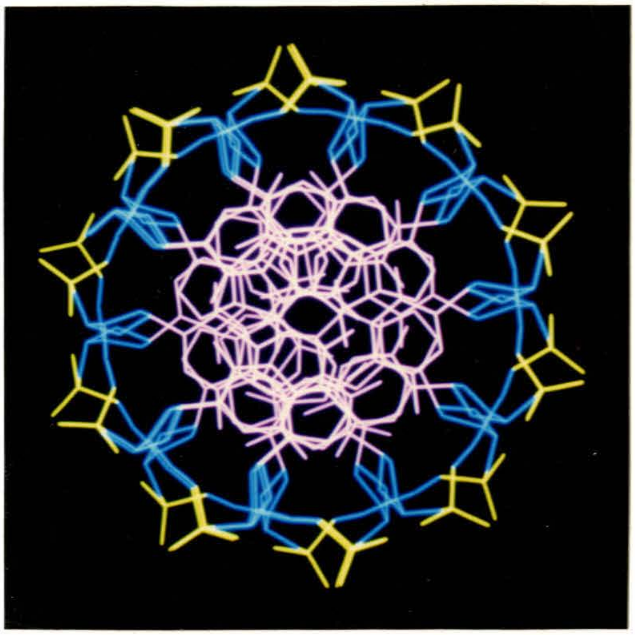

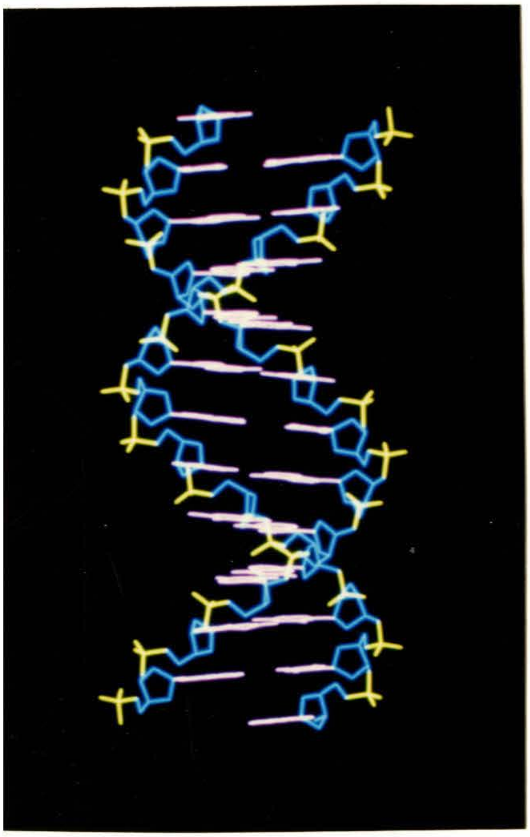

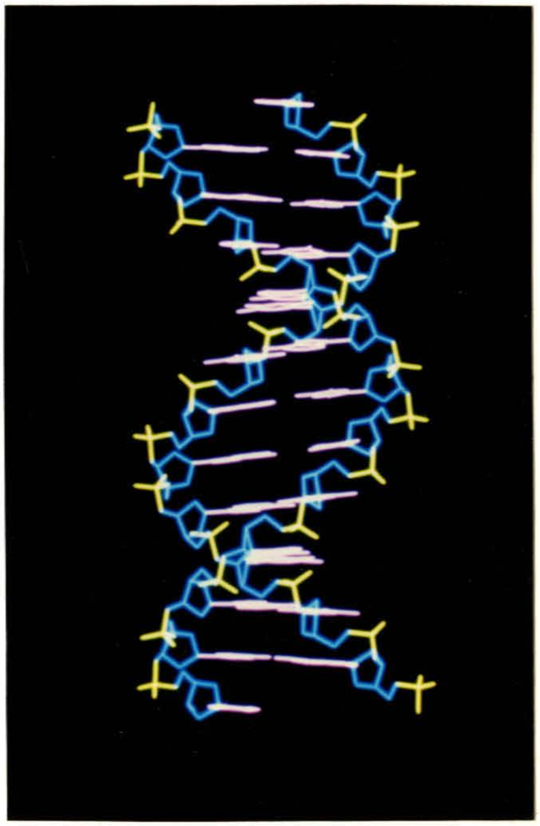

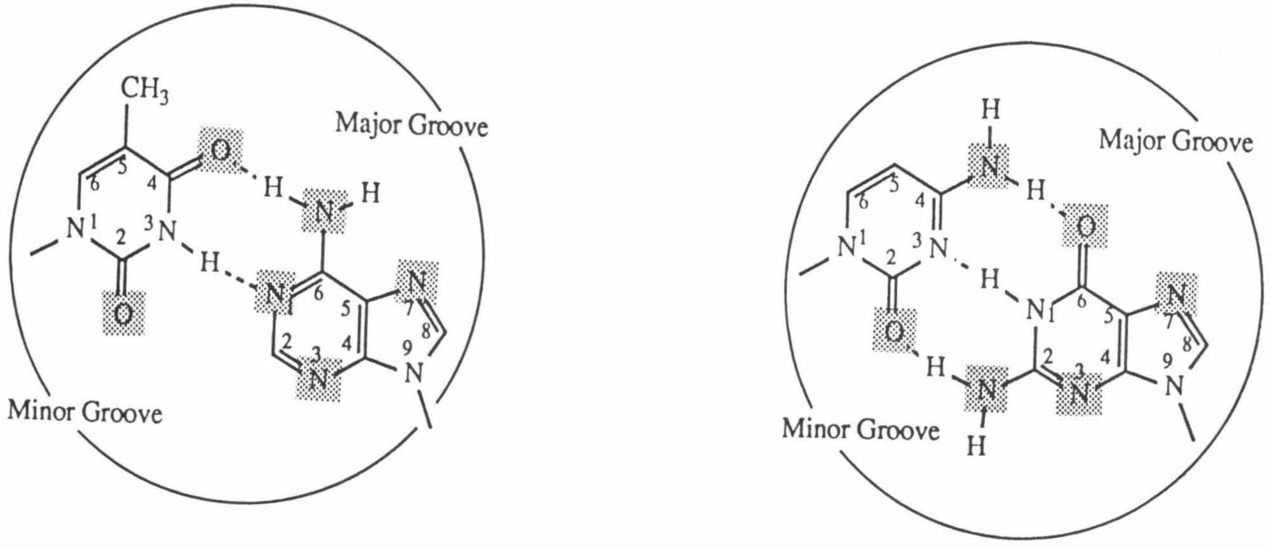

Thymine-Adenine

Cytosine-Guanine

CH3
Major Groove
Minor Groove
Major Groove
Minor Groove

Figure 2: Watson-Crick Base Pairs.

pyrimidines. For example, for A18, $\chi = 108^\circ$ and $\delta = 130^\circ$, and for T8, $\chi = 126^\circ$ and $\delta = 109^\circ$. In addition, one observes differences in the propellar twist of individual base pairs. These angles range from 4.9° to 18.6°. The propellar twist is greater for A-T pairs (avg = 17°) than G-C pairs (avg = 11.5°). This difference is a consequence of the different steric interactions between bases of opposite strands and the different number of hydrogen bonds of each base pair, two for A-T versus three for G-C. Finally, the angles between base-plane normals of successive bases change as one progresses along the helix. Purine-pyrimidine base steps systematically open out towards the major groove and pyrimidine-purine steps open towards the minor groove. The degree of roll is dependent on the flanking sequences. Homopolymer steps are relatively resistant to rolling in either direction.

In a formal sense the sequence specific local structural variations as described for the Dickerson dodecamer could affect the rates, mechanisms, and products of DNA cleavage reactions. For example, a good correlation has been drawn between the sites of DNase I cleavage of the dodecamer backbone and the degree of local helical twist.[4] In this system, the rates of backbone cleavage (in solution) were fastest at base steps that have the largest helical twist angles (x-ray crystal).

Sequence specific dynamics and thermal fluctuations might also affect the rates, mechanisms, and products of DNA cleavage reactions. For example, DNA breathing is part of the mechanism by which formaldehyde reversibly denatures double stranded DNA as based upon product and kinetic data.[5]

The length and base composition of a linear piece of DNA determines the equilibrium between the single and double stranded states.[6-8] The average melting temperature (double to single stranded) is lower for A-T pairs than G-C pairs based on the number of hydrogen bonds formed. For example, the melting temperature for the 12 base pair oligonucleotide, 5'-CGATTATAATCG, is 17° C lower than that of 5'-CGCGTATACGCG, an oligomer of similar length, but with a lower percentage of AT base pairs (55° C *vs.* 72° C respectively).

The dynamics of base pair opening in the interior of nucleic acid duplexes can be determined by monitoring the exchange kinetics of the imino protons by NMR[7] or by isotopic labelling.[9] These rates are sequence dependent. For example, Patel and coworkers found that the exchange rate for the TATA sequence is 2.5 times faster than the one for the AATT sequence when sequestered in the center of the same flanking sequences, 5'-CGCG____CGCG. These 12mers have equivalent T_m's of 72° C. This result reflects the forces other than hydrogen bonding which stabilize the duplex. As mentioned, stacking interactions provide stabilization. They depend on the permanent dipole moments and pi electron systems of the individual bases. Optimum overlap or stacking is attained between bases up and down the same strand when they are twisted 10 to 20 degrees out of the plane of the base pair.[2] However, optimal overlap is counteracted by the steric interactions between bases on opposite strands. The worst clash occurs between purines of adjacent base pairs.[10]

Finally, the conformation and stability of a duplex are dependent upon the extrinsic solvent and solute conditions. Cations, such as the alkali metal ions, play a critical role in stabilizing the double helix.[11] They counter the high charge density created by the phosphate groups. The monovalent cations, like Na^+ and Rb^+, adhere to the polyelectrolyte theory, as shown experimentally by NMR.[12,13] These ions form an ionic cloud around the DNA, with no specific interactions. Reduction of the ion concentration decreases the melting temperature of the DNA -- without counterions to dissipate the charge or shield the phosphate backbones from one another the duplex denatures to the single stranded state.

Cleaving Moiety

The DNA constituents (sugars, phosphates, and bases) provide a number of routes to cleavage of the DNA backbone. The choice of the cleavage moiety of a sequence specific cleaving reagent is centered on understanding the mechanisms of these cleavage reactions. It has been found that cleavage can occur by oxidative degradation of the sugar,[14-18] by nucleophilic substitution at phosphorous,[19] or by electrophilic attack of a base.[20,21]

Synthetic cleavage moieties that have been utilized for oxidative chemistry include EDTA coordinated with ferrous ion[16] and [1,10]-phenanthroline coordinated with cuprous ions.[17]

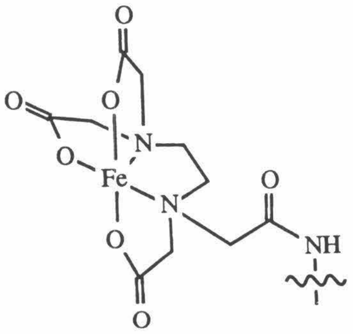

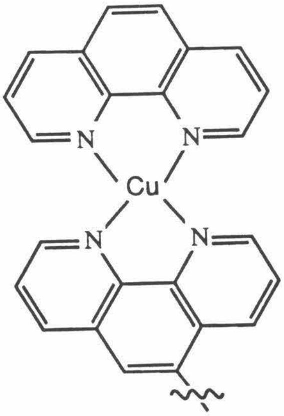

In some cases a redox active metal generates a radical species (such as a metal oxo or hydroxyl radical) which abstracts a hydrogen atom from the sugar residue. Hydrogen atom abstraction from the deoxyribose results in its degradation and scission of one or both of the sugar phosphate bonds, depending on which proton is abstracted and the reaction conditions. For example, the following mechanistic scheme (Figure 3) is proposed for EDTA-Fe(II) when placed in the minor groove.[15,16]

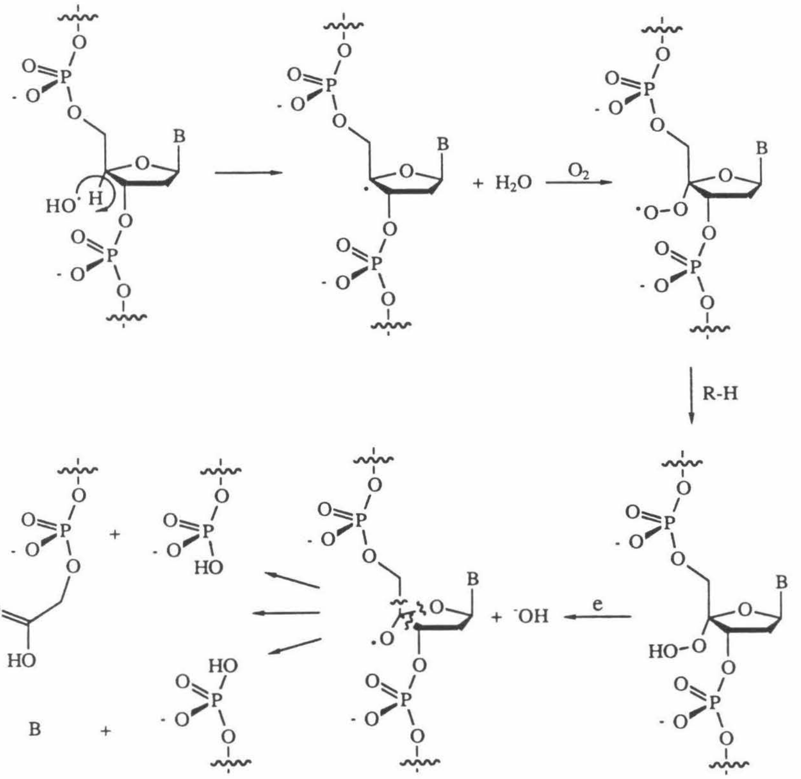

Figure 3: A proposed mechanism for oxidative cleavage of the DNA backbone by EDTA•Fe(II) from the minor groove.

Another means of cleaving the DNA backbone is by hydrolysis of the phosphodiester bond.[24,25] A tetrahedral phosphorous is transformed to a pentacoordinate intermediate upon bond formation with the incoming nucleophile (Figure 4). Departure of either of the sugar hydroxyls (3' or 5') results in cleavage of the DNA backbone.

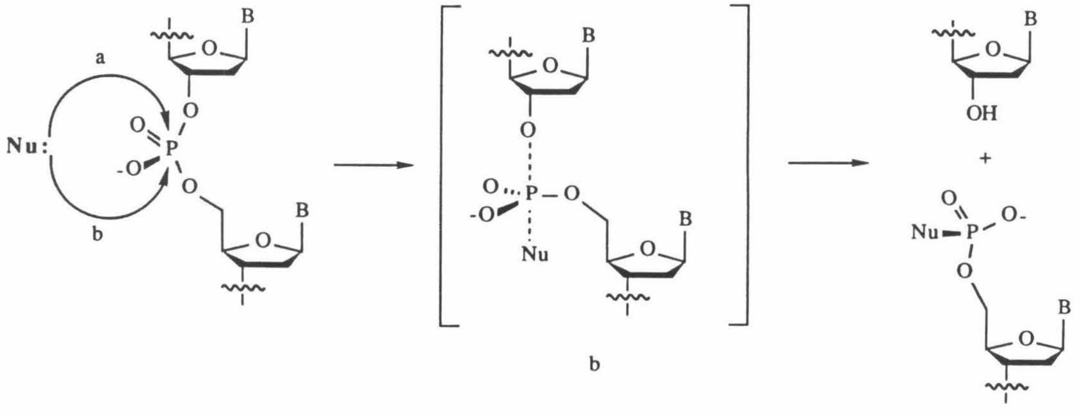

Figure 4: Proposed mechanism of cleavage of the DNA backbone by hydrolysis of the phosphodiester bond.

This type of reaction is predominant in nature,[24] *i.e.*, enzymatic cleavage of nucleic acids and other phosphate esters. In these biological systems metal cations coordinate with the oxygens, which deactivates or delocalizes the negative charge of the phosphate functional group. In addition the metals potentially deliver a good nucleophile, such as a hydroxide, by coordination with water. Recently Professor Barton and coworkers[19] have utilized two polyamine tridentate arms chelated with nonredox metal cations, Zn(II), Cd(II), or Pb(II), as the cleaving moiety to elicit this type of reaction. As with enzymes, it is thought that the metal cations in addition to the nitrogens are coordinated to hydroxide, which acts as the nucleophile to cleave the phosphodiester bond.

Finally, cleavage of the DNA backbone may be achieved by electrophilic attack of the third DNA constituent, the base. Many of the atoms or functional groups of the bases are nucleophilic as shown by shading in Figure 2. The degree of nucleophilicity varies with the accessibility (base pairing, steric interactions, degree of solvation) and the stereoelectronic properties or electronic distribution at the atom (directionality, density). Alkylation or protonation of a select few of these nucleophilic sites, *e.g.*, N7 or N3 of the purines, results in release of the base from the DNA backbone (Figure 5).[26,27] Electrophilic attack disrupts the electronic integrity of the aromatic base creating a good leaving group and thus labilizing the N-glycosidic bond. Upon loss of its base the deoxyribose is a highly unstable cyclic carboxonium ion that undergoes rapid hydrolysis to yield a diastereomeric mixture of 2-deoxy-α-D-ribose and 2-deoxy-β-D-ribose. These deoxyriboses exist in equilibrium between the acyclic free aldehyde form and the cyclic furanose form.[28] Cleavage of the DNA backbone occurs in the aldehyde form by β-elimination of the 3' phosphate.

There are numerous examples of simple electrophiles (such as dimethyl sulfate, methyl- and ethylmethane sulfonate, and N-methyl and N-ethyl-N-nitrosourea) which may display base or phosphate specificity, as shown in Table 1. However, these compounds show no sequence specificity.[26,27]

There are also examples of natural products which deliver electrophiles to specific regions of double helical DNA, such as mitomycin C,[20] anthramycin,[21] and CC1065.[21]

However, upon commencement of this thesis there were no designed synthetic examples of the attachment of an electrophile to a double helical DNA binding unit in order to elicit a cleavage event at a specific site with regard to both base and sequence.

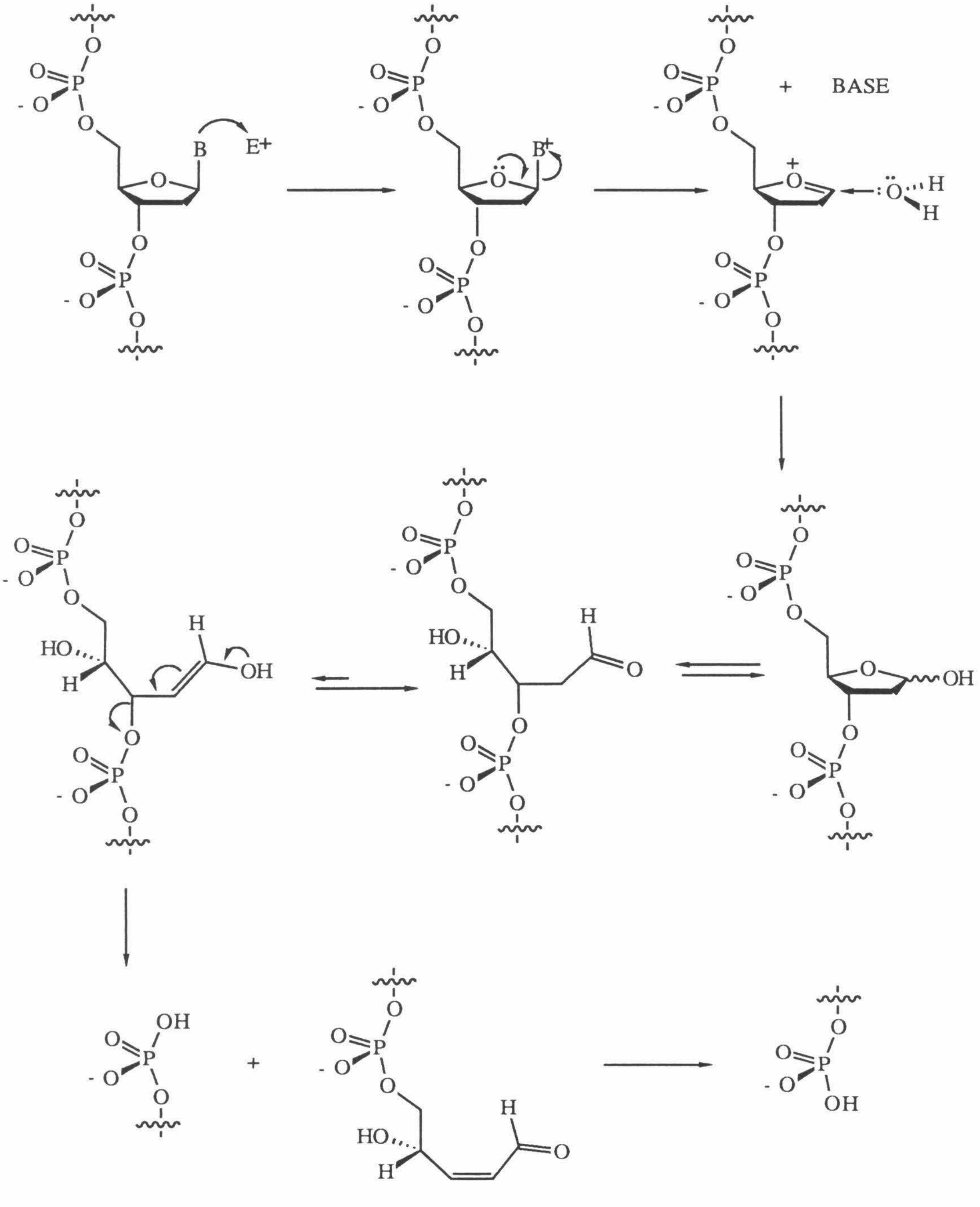
B
E+
B+
+ BASE
OH
OH
H
HO
O

Figure 5: Proposed mechanism of cleavage of the DNA backbone via an electrophilic attack of a base.

Table 1: Percentage of Alkylation of Specific Base and Phosphate Sites by Simple Electrophiles in Relation to the Total Amount of DNA Alkylated.

Site of Alkylation	Me-Methanesulfonate	Et-Methanesulfonate	N-Me-N-nitrosourea	N-Et-N-nitrosourea
N1-Adenine	1.89	1.68	0.87	0.29
N3-Adenine	11.33	4.24	8.44	2.78
N6-Adenine	n.d.	n.d.	n.d.	n.d.
N7-Adenine	1.83	1.88	1.98	0.38
N1-Guanine	n.d.	n.d.	n.d.	n.d.
N2-Guanine	n.d.	n.d.	n.d.	n.d.
N3-Guanine	0.62	0.27	0.63	0.61
N7-Guanine	81.43	58.37	66.39	10.98
O6-Guanine	0.31	2.03	5.90	7.91
O2-Thymine	n.d.	n.d.	0.11	7.79
N3-Thymine	0.08	n.d.	n.d.	n.d.
O4-Thymine	n.d.	n.d.	0.67	0.95
O2-Cytosine	n.d.	0.30	n.d.	2.85
N3-Cytosine	n.d.	0.35	0.51	0.24
Phosphodiester	0.82	12.0	12.1	55.35
TOTAL	98	81	98	91

Reaction Conditions: 5 mM Phosphate DNA, 20 mM Reagent, 100 mM Tris-HCl pH 8.0 at 37°C for 2.5 hours.

Natural products (antibiotics and enzymes) have previously provided the impetus and necessary insight for the design of new cleavage moieties and consequently new sequence specific DNA cleaving reagents. In light of this, the structure and mechanism of action of three pertinent antibiotics, mitomycin C, anthramycin and CC1065, will be discussed.

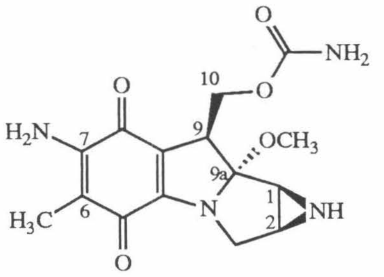

Mitomycin C[29] has four reactive functional groups: the aziridine (C1-C2), the methoxy (C9a), the carbamate (C10), and the quinone. The apparent electrophilic centers include C10, C9a, C1, and C2. However, this molecule is special in that it does not act as an electrophile as is. For example, the aziridine centers are both tertiary carbons which by inductive and steric effects are less reactive than the terminal functional group analog. Mitomycin C must be activated to a more reactive intermediate either by reductive or mild acidic conditions in order to become electrophilic towards DNA nucleophiles and simple nucleophiles such as the hydroxide ion.[30]

Mitomycin C reacts primarily with the N2 of guanine of double helical right handed DNA (90% yield for calf thymus DNA) under suitable reducing conditions.[31] Reductants have included enzyme systems, such as cytochrome C reductase/NADPH and xanthine oxidase/NADH, and metals with hydrogen, like H_2/PtO_2. The activated electrophilic intermediate is created by 1) a one electron reduction of the quinone to a radical anion, 2) release of methanol at the C9a position and 3) opening of the aziridine at the C1 position.[20,31,32] Attack of the now sufficiently positive center at C-1 by the exocyclic amino group of guanine creates a stable covalent bond between the small molecule and the DNA helix. Reoxidation of the radical anion to the quinone by oxygen leads directly to the monoalkylated adduct. This covalent adduct, referred to as a mitosene, has been characterized by FTIR and NMR.[20] The mechanism is shown Figure 6.

From the perspective of the design of new DNA cleavage reagents, the advantage of this molecule is that it must be activated in order to elicit a reaction. The disadvantage, though, is that the electronic integrity of the base is insensitive to alkylation at this site. Therefore, the N-glycosidic bond is not labilized and cleavage of the backbone does not occur.

Anthramycin is a member of the pyrrolo- 1,4-benzodiazepine class of antitumor antibiotics.[21] This molecule is characterized by a reactive carbinolamine (N-10, C-11), which may either undergo an S_N2 reaction at carbon 11 or an S_N1 reaction which is enhanced by resonance stabilization through the imine. Additionally, it may undergo a Michael addition at C3 or C12. It differs from the others in its class by the aromatic substitution pattern, degree of saturation in the pyrrolo ring, and type of sidechain at the C2 position. However they all display the same type of reaction towards DNA. The stereochemistry at C11a determines the twist of the molecule. The naturally occurring form is only the R isomer. It has a 45° right handed twist from the aromatic ring to the pyrrolo ring.

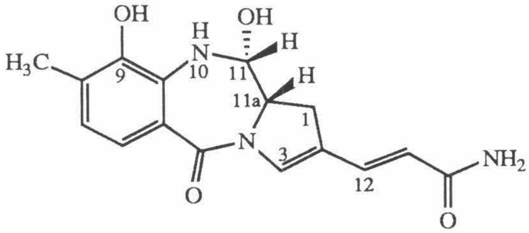

Anthramycin binds in the minor groove of double helical right handed DNA as shown by its ability to bind to T7 phage DNA, which is glucosylated in the major groove.[33] It also binds to A DNA like poly (dG)-(dC), which is classified as the A form by fiber diffraction experiments. MPE footprinting studies indicate that this compound covers three base pairs. All of the binding sites contain a guanine at the central position.[34] The most preferred sites, determined from analysis of 515 base pairs of restriction fragments, are PuGPu (54 of 65, 83%). The least preferred are PyGPy (16 of 22, 26%). These results indicate a relatively low level of sequence specificity, but a definite base specificity. The basis of the specificity for guanine is the covalent attachment of the small molecule to the exocyclic amine at the 2 position of the purine through the C11 carbon (Figure 6).

The DNA adduct has been characterized by carbon 13 and proton NMR utilizing labeled compounds (C11, C14, and C15) covalently bound to a 6 base pair oligonucleotide, 5'-dATGCAT.[35] Upon covalent attachment the C11 peak of anthramycin shifts 16 ppm upfield, the C14 resonance peak shifts downfield 4 ppm, and the C15 shifts downfield 1.5 ppm, relative to anthramycin alone in a mixture of Me_2SO/D_2O (4:1). Further supporting evidence for the mechanism of electrophilic attack of this base site exists in the inability of anthramycin to covalently attach to poly (dI)-(dC). Inosine lacks the exocyclic amino functional group. In addition, oxidation of the carbinolamine to the amide or its reduction to the methylenamine precludes the DNA reaction.

As with mitomycin C, even though the electrophile of this small molecule is delivered to and reacts with a specific nucleophilic site of the DNA, cleavage of the backbone does not occur. From these two examples it appears that electrophiles positioned in proximity to

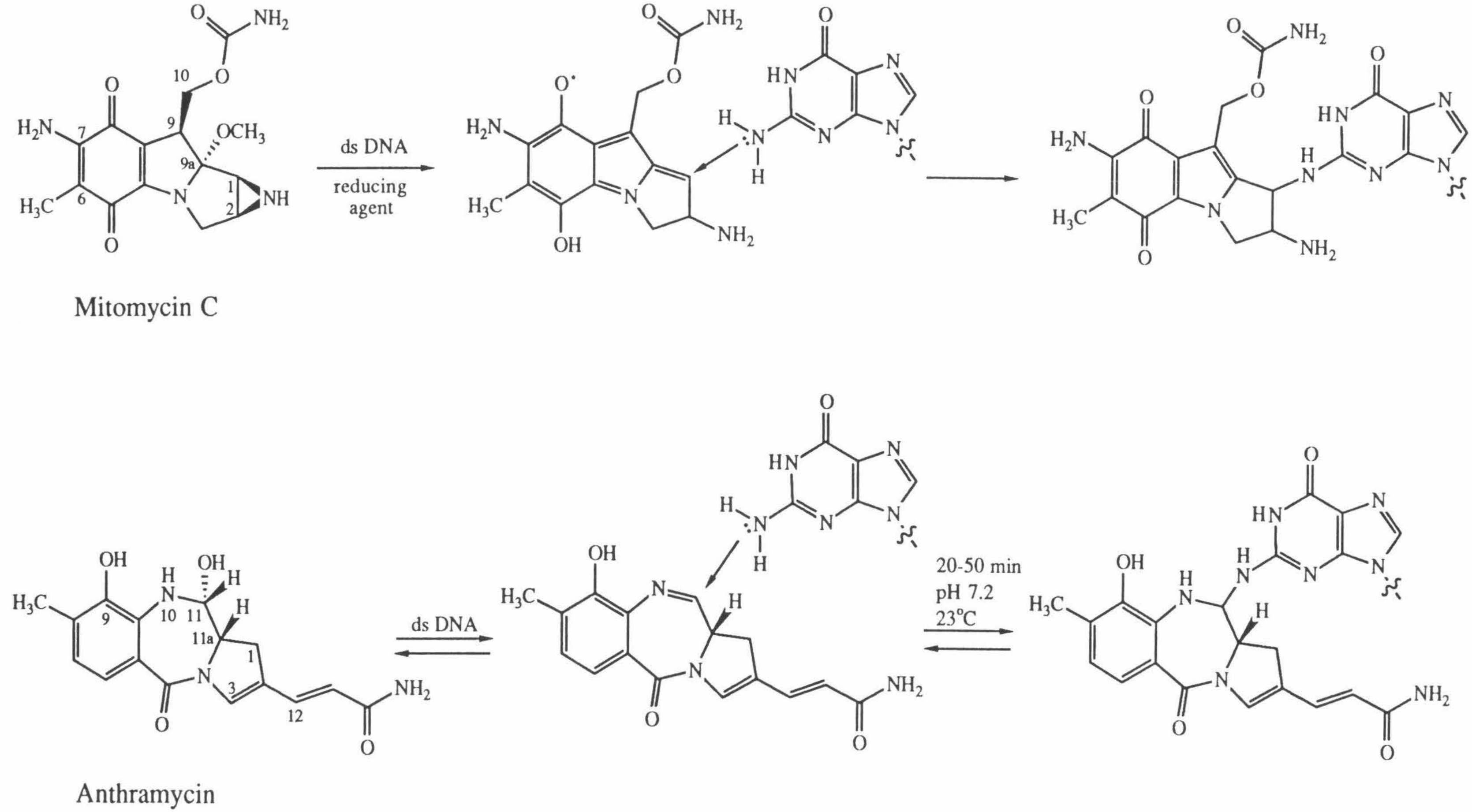
ds DNA
reducing agent
Mitomycin C
ds DNA
20-50 min
pH 7.2
23°C
Anthramycin

Figure 6: Mechanism of Electrophilic Attack of Double Helical DNA by Anthramycin and Mitomycin C.

guanines along the floor of the minor groove preferentially react with the exocyclic amine at position 2 over nitrogen 3. This may be due to both the relative accessibilities and degree of nucleophilicity for these two sites.

Of the natural products which deliver an electrophile to specific locations on double helical DNA, CC1065 is the example of one that directs electrophilic attack of an appropriate DNA nucleophile for cleavage of the phosphodiester backbone (as outlined in the given mechanism).[22,36]

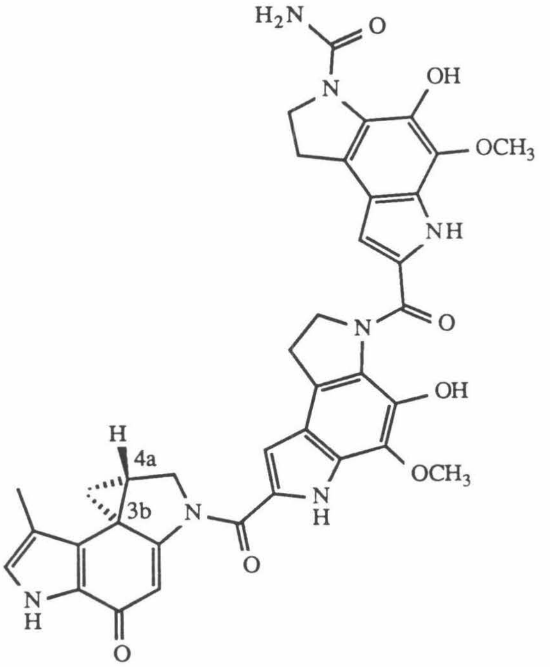

CC1065 consists of three substituted benzodipyrrole moieties linked by amide bonds. It contains two chiral centers at the cyclopropyl ring junctions, assigned as C3b(R) and C4a(S). The general concave shape, right handed twist, and hydrophobic nature of CC1065 is similar to Distamycin A and other small molecules, like Hoechst 33258,[37] which bind to A-T rich regions in the minor groove. The cyclopropyl ring is a potential site of reactivity. Due to the strain energy of the cyclopropyl ring and the potential resonance stabilization of products the carbons of the cyclopropyl group are electrophilic.

Competitive binding studies with netropsin and its ability to bind and react with T4 DNA which has been glucosylated in the major groove classifies CC1065 as a nonintercalative minor groove binder. Hurley and coworkers found by isotopic labelling (tritiated bases) and isolation of a CC1065 DNA adduct (heating of the reaction followed by butanol extraction), that CC1065 binds covalently to DNA at the N-3 of adenine.[38] Nucleophilic attack by N-3 of adenine occurs at the cyclopropyl methylene carbon of the A subunit with concommitment ring opening and reduction of the indole quinone to an indole phenol (Figure 7). The assignment of the nucleophilic and electrophilic site was determined by comparison of the ^{13}C spectra of 3-methyladenine with that of the CC1065-DNA adduct.

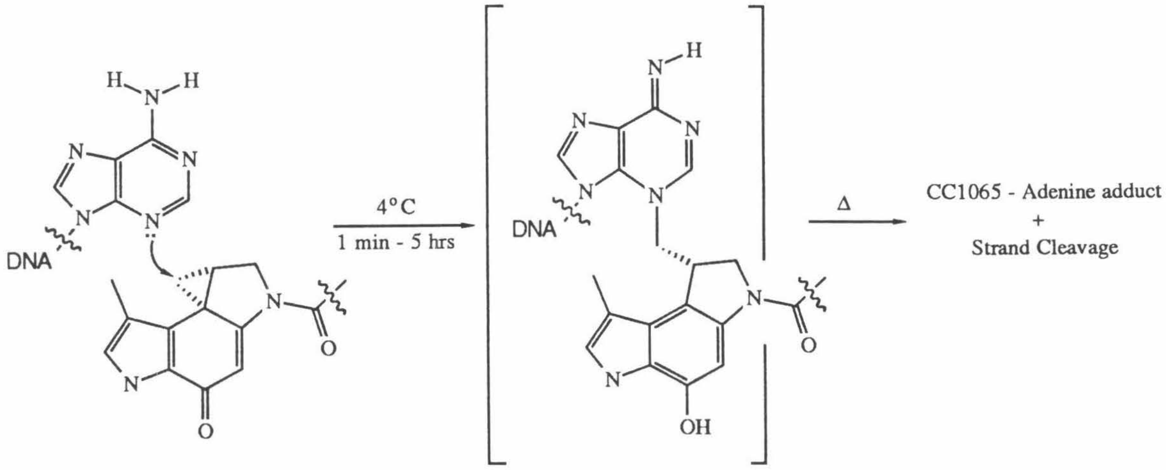

Figure 7: Mechanism of Covalent Binding to DNA by CC1065.

DNA binding sites have been assigned by MPE and DNase footprinting of the covalent complex and by sequence analysis of the cleavage sites.[38,39] Note, analogs identical to the natural antibiotic, but lacking the cyclopropyl ring (therefore nonreactive), do not footprint. This indicates that the "binding unit" of CC1065 interacts weakly with the DNA and that tight binding is conferred only by covalent attachment to the DNA.[40] This differentiates this compound from distamycin and netropsin. CC1065's lack of a positively charged moiety and lack of amide linkages capable of hydrogen bonding with the base pairs appear to be the basis of this difference.

Review of the cleavage sites on a 2060 base pair SV40 plasmid demonstrates that two classes of covalent binding sites are prevalent, 5'PuNTT**A** and 5'AAAA**A**, where the adenine at the 3' end (in bold) is the site of alkylation.[41] Binding always occurs to the 5' side of the alkylation site. Alkylation may be detected after one minute at 4°C and maximizes after 3 to 5 hours.

In conclusion, the degree of cleavage specificity is partially controlled by the cleavage moiety. Moieties which react with the sugars or phosphates are nonsequence specific, whereas those which react with the bases are sequence specific. In addition, those moieties which generate diffusible reactive species (such as EDTA-Fe(II)) are less specific -- how much less specific depends on the lifetime of the reactive species. This attribute (diffusion) gives some flexibility in the proximal placement of the moiety next to the DNA reactive site. In contrast, the nondiffusible reactive species is more particular with regard to its placement and exact positioning next to the DNA site in order to elicit a reaction.

Binding Unit

The binding unit of a sequence specific DNA cleaving molecule directs the placement of the cleavage moiety. Therefore it contributes significantly to the level of cleavage specificity attained.[42] The mode of binding and the number, type, and order of base pairs that a molecule recognizes or effectively interacts with determines the binding specificity. For instance, simple flat aromatic molecules, like methidium, bind to DNA by intercalation or insertion between the base pairs with little or no regard to the sequence. However, the position of the intercalator will govern which groove the cleaving moiety is placed in and consequently the mechanism by which cleavage of the backbone occurs. Methidium intercalates with the phenyl ring in the minor groove. Therefore, as shown by Hertzberg and Dervan, attachment of EDTA-Fe(II) to the phenyl ring of methidium places this cleaving moiety in the proximity of the narrow groove and the deoxyribose ring.[16] This strategy yields a relatively nonsequence specific cleaving reagent because both the binding unit and cleavage moiety are nonsequence specific. A higher degree of specificity is achieved by attaching the same cleavage moiety to a groove binder. The variegation of functional groups and stereoelectronic features along the floor and walls of the grooves allow for more complexity in recognition. For instance, the tripeptide distamycin binds to five base pairs in the minor groove and preferentially to A-T rich regions. Attachment of distamycin to EDTA-Fe(II) places the cleavage moiety solely in these regions of the minor groove to yield a relatively sequence specific DNA cleaving molecule -- based upon the increase in the number and type of base pairs recognized and spanned by the binding unit.[43] One may reach still higher levels of recognition and thus cleavage specificity by continually increasing the number of base pairs covered. For example, this strategy has been developed and effectively utilized by Scott Youngquist with his synthetic polypyrrole molecules, which may bind up to 16 contiguous A-T basepairs.[44]

Synthetic Nondiffusible Sequence Specific DNA Cleaving Molecules

This thesis is focused on utilizing a sequence specific DNA binding molecule to deliver an electrophile to a specific nucleophilic DNA site. With respect to affinity cleaving the intent is to develop and utilize a nondiffusable sequence specific cleavage moiety in order to achieve a level of DNA cleavage specificity beyond that of the diffusible cleavage moieties, like EDTA, which display multiple cleavage patterns per site. Proper placement of a nondiffusable sequence specific cleavage moiety, such as an electrophile, near the appropriate DNA site requires a detailed understanding of the molecular structure of the binding unit when it is complexed with the DNA.

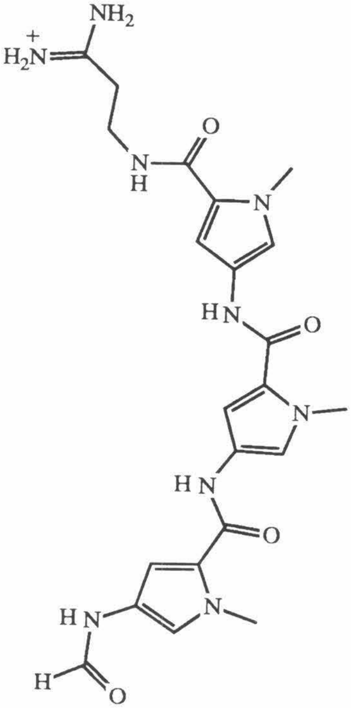

Distamycin: The binding unit chosen for this research is modelled after the natural product Distamycin A, a well-characterized peptide composed of three N-methyl pyrrole carboxamide units.[45] Distamycin A has a crescent shape and is slightly spiral with a right-handed twist. The amide groups are in the trans configuration with the N-methyls of the pyrrole rings and the oxygen atoms of the amides oriented in the same direction.[46]

Distamycin binds nonintercalatively in the minor groove of the double helix with a strong preference for A-T rich regions.[45] Footprinting of distamycin with the synthetic cleaving reagent MPE[47,48] and affinity cleavage by distamycin-EDTA and EDTA-distamycin[49] have defined the binding site size to be 5 base pairs. Binding sites were usually composed only of adenine/thymine base pairs. However, on rare occasions binding was detected at sites that contained a G-C base pair. In addition, data revealed that the peptide could orient itself in either direction at each binding site. This bidirectional binding mode has also been observed in the NMR spectra of a complex of distamycin with the Dickerson dodecamer.[50] At 27° C in 10 mM NaCl/10 mM phosphate buffer a distamycin molecule flips on a DNA duplex two times per second. In addition, two out of ten molecules dissociate from the DNA duplex every 50 msec, $k_{off}=4\ s^{-1}$.

The molecular basis for recognition of DNA by distamycin was originally extrapolated from x-ray[51] and NMR[52] analysis of the oligonucleotide, d(CGCGAATTCGCG), and netropsin complex. Netropsin is a dipeptide composed of the same pyrrolecarboxamide units as distamycin and shows similar biological and biopysical properties. In the cocrystal netropsin has displaced the water molecules of the spine of hydration and lies symmetrically in the minor groove. The amide NH groups of netropsin form bifurcated hydrogen bonds between adjacent adenine N3 or thymine O2 atoms of opposite strands. Close Van der Waal interactions exist between the adenine C2 hydrogens and the CH groups on the pyrrole rings. These interactions, hydrogen bonding and Van der Waal interactions, are proposed to be the basis of specificity, *i.e.*, preference, for A-T rich regions. Due to sterics, guanine, with its exocyclic amine group at the C-2 position, is unable to accomodate the peptide. CPK models clearly demonstrate this steric hindrance.

More recently the cocrystal structure of the oligonucleotide, d(CGCAAATTTGCG), and distamycin was solved to 2.2 A resolution.[53] Again the antibiotic lies in the minor groove near the center of the fragment. It covers five of the six A-T base pairs, with similar hydrogen, electrostatic, and Van der Waal interactions. However, it was observed that the periodicity of the tripeptide unit is not perfectly meshed with the hydrogen bonding acceptors on the floor of the minor groove. The second amide from the amino terminus is 4.4 and 3.9 å away from its potential hydrogen bond acceptors. Whereas the others range from 2.6 to 3.2 A. Also of importance, the DNA was found to have an unusual conformation in the $d(A)_3$-$d(T)_3$ regions. These base pairs had a large positive propeller twist, an average of 20° (in contrast to 17 normally and 14° for G-C pairs). This conformation is stabilized by bifurcating hydrogen bonds in the major groove between the N6 of adenine and the O4 of two adjacent thymines and the enhanced base stacking.

The entropic gain achieved by displacement and release of the water molecules composing the spine of hydration is an important driving force for the binding of these polypyrrole carboxamides in the minor groove of the DNA.[54] G-C rich regions lack this ordered hydration state because the exocyclic amine group of guanine disrupts the spine. This observation lends an energetic basis, specifically entropic, for A-T specificity. Another contribution to binding is the hydrophobic interactions between the pyrrole rings and the sugar residues of the DNA. The conformation of the helix in A-T rich regions probably maximizes these interactions by providing the best hydrophobic fit based on the groove width and depth. Crystal structures show that there is no room for any solvent molecule to be interposed between the distamycin and the DNA.

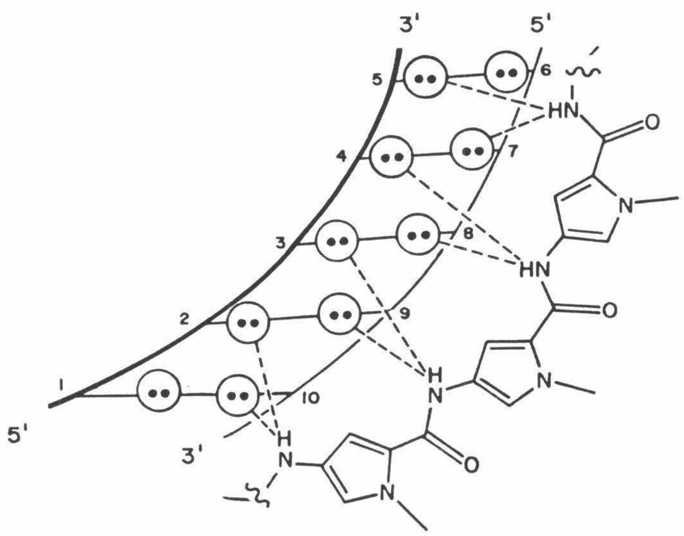
3'
5'
1
2
3
4
5
6
7
8
9
10
5'
3'
HN
O
N
HN
O
H
N
N
H
N
O
N

Figure 8: Model for the N-methyltripyrrole binding unit complexed to double helical DNA within the minor groove. The circles with two dots represent the lone pair of electrons of N3 of adenine or O2 of thymine.

N-Bromoacetyldistamycin: Based on our understanding of distamycin and its interaction with double helical DNA, attachment of an electrophile on the amino end of the tripeptide tris-N-methyl pyrrole carboxamide should place the electrophile in proximity to nucleophiles, such as the N3 of adenine or O2 of thymine (Figure 9).

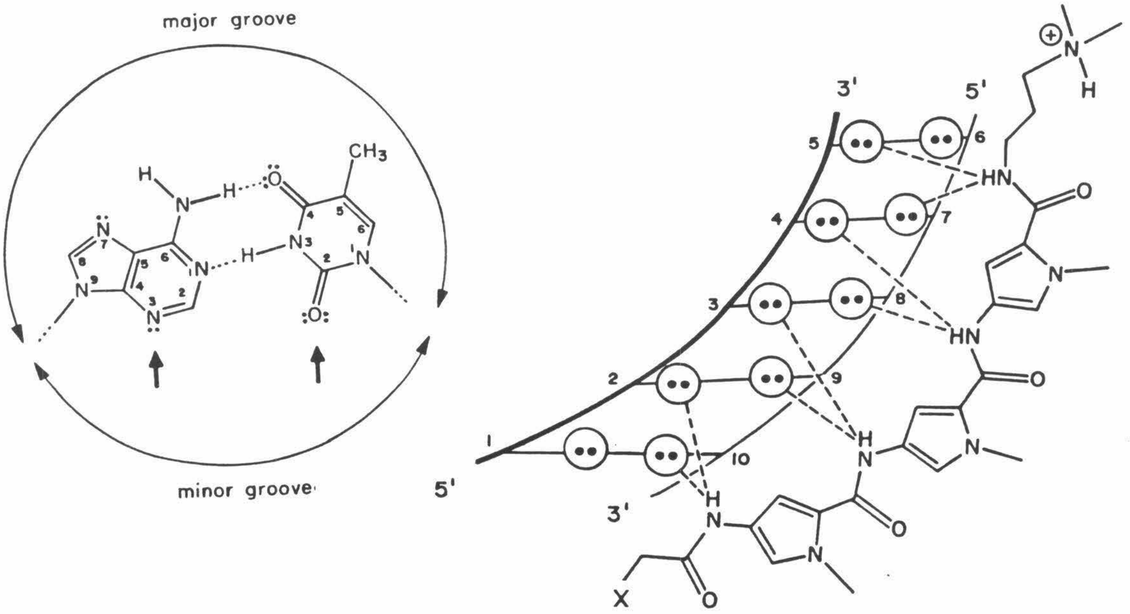
major groove
minor groove
CH_3
H
N
H
O
N3
N
N
O
3'
5'
1
2
3
4
5
6
7
8
9
10
5'
3'
N
H
HN
O
N
HN
O
H
N
N
H
N
O
N
X
O

Figure 9: Proposed placement of an electrophile in the minor groove.

We chose to attach an α-bromoacetyl group to the binding unit to create N-Bromoacetyldistamycin (BD). According to CPK modeling of the DNA/BD complex the electrophilic α-carbon is in close proximity to the floor of the minor groove within reach and proper orientation to the N3 atom of adenine. Alkylation of the N3 of adenine, via a backside nucleophilic displacement of the bromide ion, should lead to strand scission under the appropriate reaction conditions. Heat and base workup after the reaction causes depurination and phosphodiester cleavage at adenines that have been alkylated at this site.[26,27]

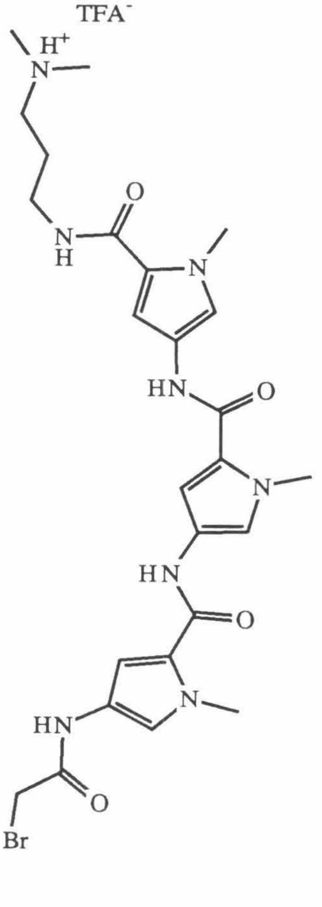

N-Bromoacetyldistamycin

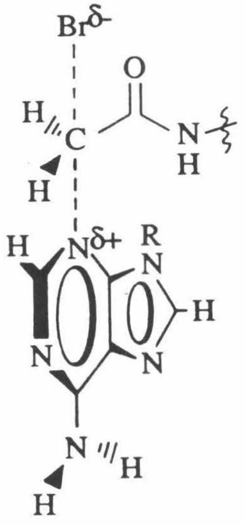

Proposed
Transition State
Structure

In order to understand DNA cleavage specificity of designed molecules the mechanism of the cleavage reactions must be elucidated. This thesis addresses the design, synthesis, sequence specificity, and mechanistic details of the reaction of N-bromoacetyldistamycin and its derivatives with double helical DNA.

S_N2 Reactions

Before the results are given in the next section a few comments on the rates of S_N2 reactions are appropriate. S_N2 stands for substitution nucleophilic bimolecular. Importantly, with regard to this research, the two means bimolecular and not necessarily second order. If a large excess of nucleophile is present, for example as a solvent, or the nucleophile is part of the same molecule as the electrophile, *i.e.*, intramolecular, then the mechanism may still be bimolecular even though the experimentally determined kinetics are first order. In a formal sense the reaction between BD bound to double helical DNA is intramolecular, therefore we expect the reaction to be described by first order rate equations.

Differences in orientation,[55,56] distance[57] and time of localization[58] will result in different rates of reaction between a nucleophile and an electrophile. First, the rates of an S_N2 reaction are dependent upon the direction of the incoming nucleophile. As shown in the early characterizations of the S_N2 reaction by Hughes and coworkers,[59] the nucleophile does a backside displacement of the leaving group, which results in inversion of the stereochemistry at the electrophilic carbon. Later, Echenmoser and coworkers[60] initiated the sizing of the reaction window (or scope of the allowed displacement angle) through their discovery that S_N2 endocyclic intramolecular cyclizations are not feasible. In this case the intramolecular reaction is overridden by the intermolecular exocyclic reaction which allows for an in line backside displacement. This result is attributed to improper juxtapositioning of the endocyclic reaction centers. Exceptional flexibility is observed in cyclization reactions which form 3 membered rings (proximity effect) and reactions where the nucleophile has multidirectional or relatively diffusive orbitals, such as oxygen and sulfur.[57]

The proximity of the reaction centers to one another is important in S_N2 reactions as shown by comparison of intramolecular reactions with their intermolecular counterparts. For instance, cyclization of 6-chlorohexoxide occurs 280 times faster than the analogous bimolecular reaction.[57] The basis of the increased rate of the intramolecular reactions may be viewed as an increase in the effective concentration and localization of the nucleophile in the vicinity of the electrophilic center, which translates into a higher frequency of encounters and orbital overlap. The rate of an intramolecular reaction in relation to its intermolecular equivalent can be quite different from system to system as shown in Table 2.

Finally the rate of the S_N2 reaction is dependent on the leaving group. Since N3 of adenine is a pyridinic nitrogen, relevant rate measurements of S_N2 displacement reactions include those of pyridine. Table 3 lists the results obtained for the reaction of pyridine with the n-halobutanes, chloro, bromo, and iodo.[61] From these studies it is apparent that the rate of displacement follows the order I>Br>Cl.

Table 2: Comparison of the Intra and Intermolecular S_N2 Reaction Rates.[a,b]

Compound	k_{obs} (s^{-1})	T (° C)	Intra/Inter (k_1/k_2)
$HO(CH_2)_4Cl$	0.104	30	60 000
$HO(CH_2)_5Cl$	5.0×10^{-4}	30	280
$H_2N(CH_2)_4Cl$	5.84×10^{-3}	25	3000
$H_2N(CH_2)_4Br$	0.5	25	7000
$H_2N(CH_2)_5Br$	8.3×10^{-3}	25	100
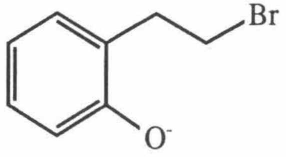	38.4	50	13 100
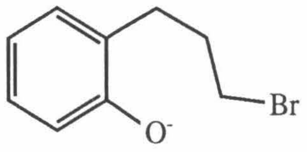	1.92	50	6560

a) from reference 57 b) the data are for reactions followed in aqueous solution

Table 3: Dependence of the Rate of S_N2 Displacement Reactions on the Leaving Group: The displacement of halogens by pyridine.

Halogen	Solvent	$10^6 k_2$ (l-mol^{-1}-s^{-1}), 0° C	$10^6 k_2$ (l-mol^{-1}-s^{-1}), 75°C	E_a(kcal-mol^{-1})	k_{rel}, 0°C	k_{rel}, 75°C
Cl	MeOH/H_2O	8.8×10^{-4}	2.20	20.6	0.025	0.03
Cl	DMF	5.5×10^{-4}	1.34	19.7	0.002	0.01
Br	MeOH/H_2O	3.5×10^{-2}	70.5	19.1	1.0	1.0
Br	DMF	2.8×10^{-1}	133	15.6	1.0	1.0
I	MeOH/H_2O	3.8×10^{-2}	110	20.2	1.1	1.6
I	DMF	1.3	739	15.9	4.6	5.6

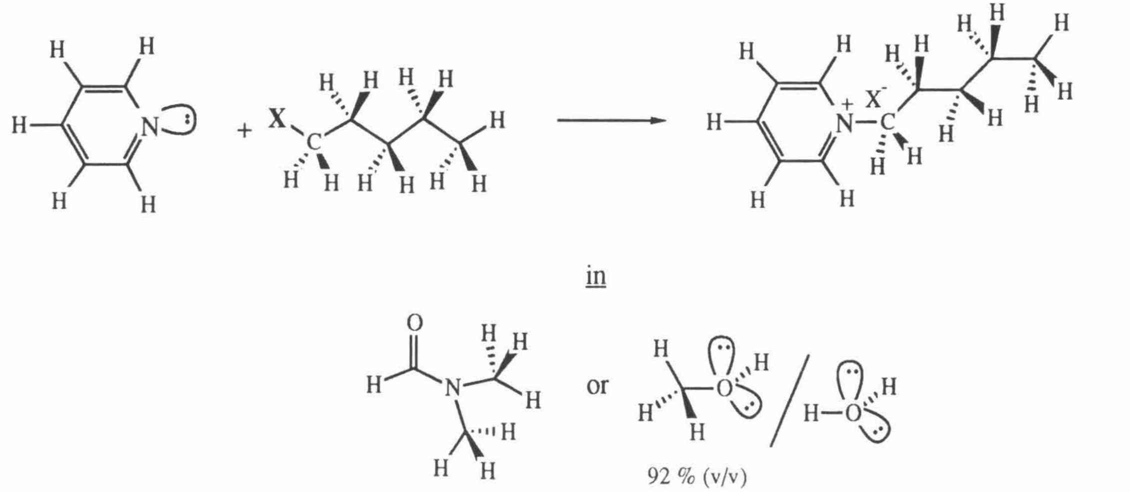

Results and Discussion

A. Synthesis of N-Bromoacetyldistamycin: The synthetic route to N-bromoacetyldistamycin **3a** (BD) is shown in Scheme 1. The tripeptide **1** is prepared in eight steps from N-methylpyrrole-2-carboxylic acid using a modification of a published procedure.[62-64] Reaction of the mixed anhydride,[65] triflouroacetyl bromoacetic anhydride **4a**, with the chromatographed tripeptide diamine **2** in dichloromethane at 0° C under argon yields the desired molecule. The tertiary amine at the C-terminus of the distamycin moiety acts as an internal base in the coupling reaction and its protonation prevents polymerization. The reaction is quantitative when analyzed by thin layer chromatography. Triflouroacetic acid is added after the coupling is complete to ensure salt formation. Addition of diethyl ether causes the TFA salt to precipitate out of solution as a white fluffy solid (60-85% yield). The purity of the recovered solid was analyzed by reverse phase high pressure liquid chromatography and shown to be 98% N-bromoacetyldistamycin **3a** and 2% N-hydroxyacetyldistamycin. Coupling the bromoacetyl group to the amino terminus of the tripeptide may also be accomplished with dicyclohexylcarbodiimide (DCC) or with the acyl halide. However, the purity of the product was consistently poorer by these methods. In the DCC reaction the difficulty arose in completely removing dicyclohexylurea. In the acyl halide reaction polymerization or acylation of the tertiary amine consistently occurred. These problems are unacceptable since the product cannot be chromatographed. In addition the acyl halide is a liquid and much more reactive, making it more difficult to handle than the crystalline mixed anhydride.

N-Bromoacetyldistamycin **3a** (BD) was characterized by ultraviolet and infrared spectroscopy, and mass and nuclear magnetic resonance spectrometry. The mass spectrum, obtained by fast atom bombardment, displays a doublet of peaks, separated by two mass units for the parent molecule. Bromine atoms have two natural isotopes of relatively equivalent abundance, 79 and 81.[66] Therefore, this result is a clear indication of the presence of a bromine atom in the molecule. The proton spectra of N-bromoacetyldistamycin **3a** (BD) in deuterated dimethyl sulfoxide is shown in Figure 1. The NMR spectra of the compound in aqueous solutions, Figure 2, are different from those obtained in dimethyl sulfoxide. The dimethyl sulfoxide spectrum reflects a very homogeneous solution, whereas the aqueous is heterogeneous. That is, in D_2O on the NMR timescale, the molecule exists in more than one environment or conformation. Either the molecule forms aggregates because of its hydrophobicity or it exists freely in several conformations.

The stability of the molecule in aqueous phosphate buffered solutions at room temperature was examined by nuclear magnetic resonance and high pressure liquid chromatography. In the NMR spectrum after 3 hours in 100 mM Na phosphate buffer, pH 7.0 there is a loss of peak definition (line broadening). Peak width (among other parameters) is proportional to the correlation or tumbling time of the proton(s). Polymerization or aggregation will increase this time.

When monitored by HPLC, after eight hours, 80% of the compound remains. Therefore it appears that the molecule aggregates and precipitates out of solution at a relatively fast rate and at a slower rate transforms to other undefined compounds, excluding the α-hydroxyacetyl derivative. Hydrolysis does occur though in the solid form -- 50% is hydrolyzed after approximately one month in the dark at room temperature.

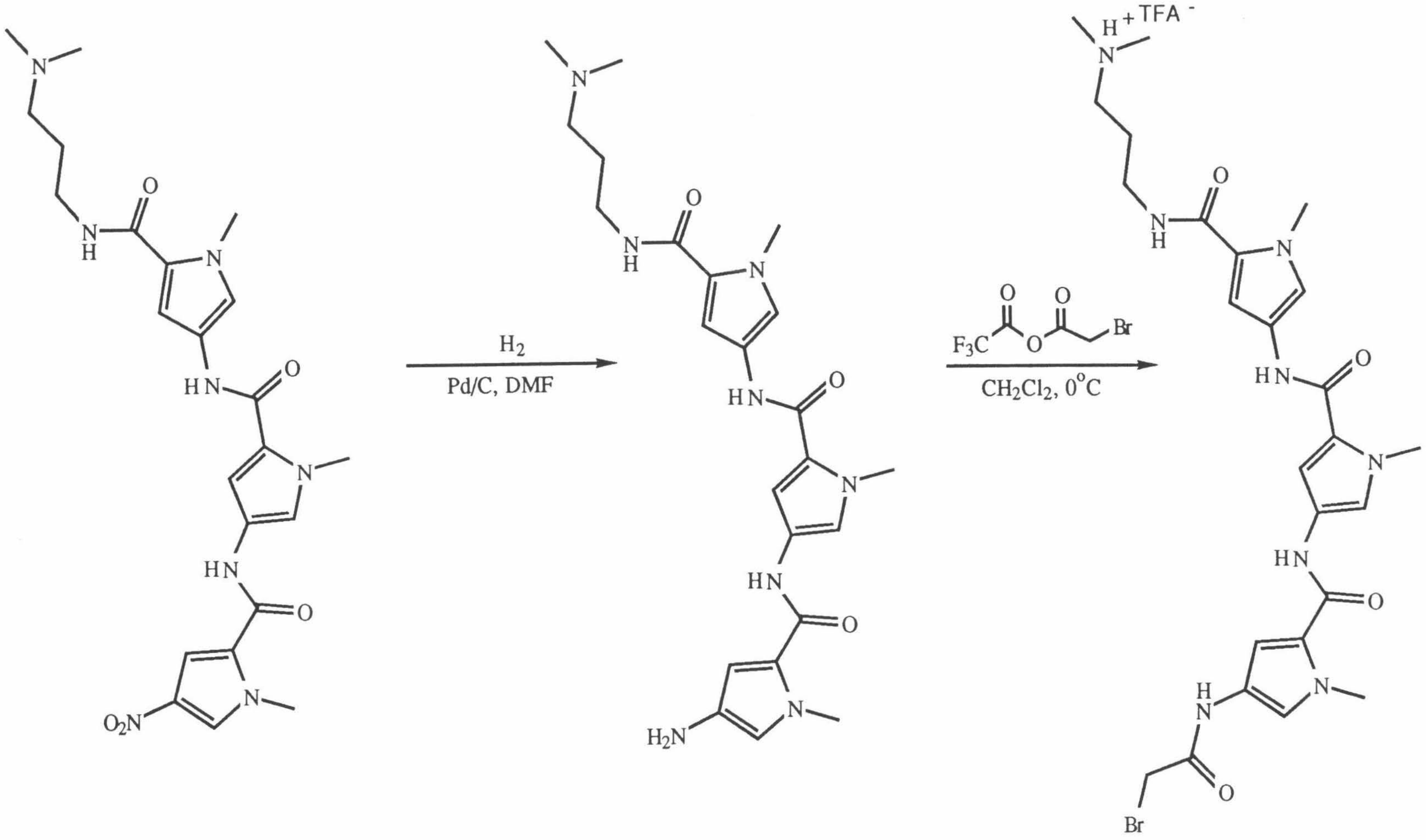
H+ TFA -
H_2
Pd/C, DMF
F_3C
Br
CH_2Cl_2, 0°C

1

2

3

Scheme 1: Synthetic Scheme of N-Bromoacetyldistamycin

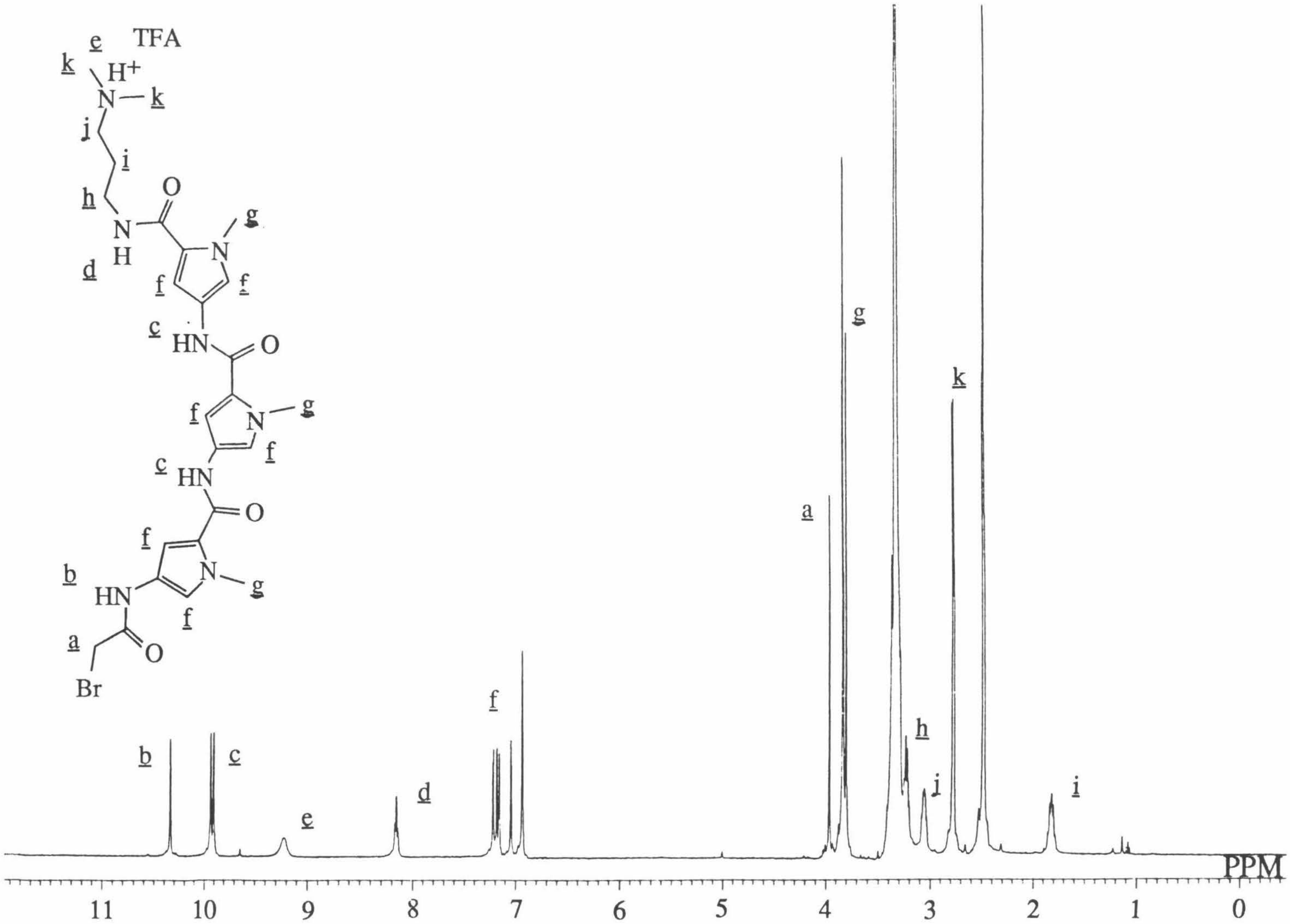

Figure 1: Proton Spectrum of N-Bromoacetyldistamycin **3a** (Me_2SO-d_6).

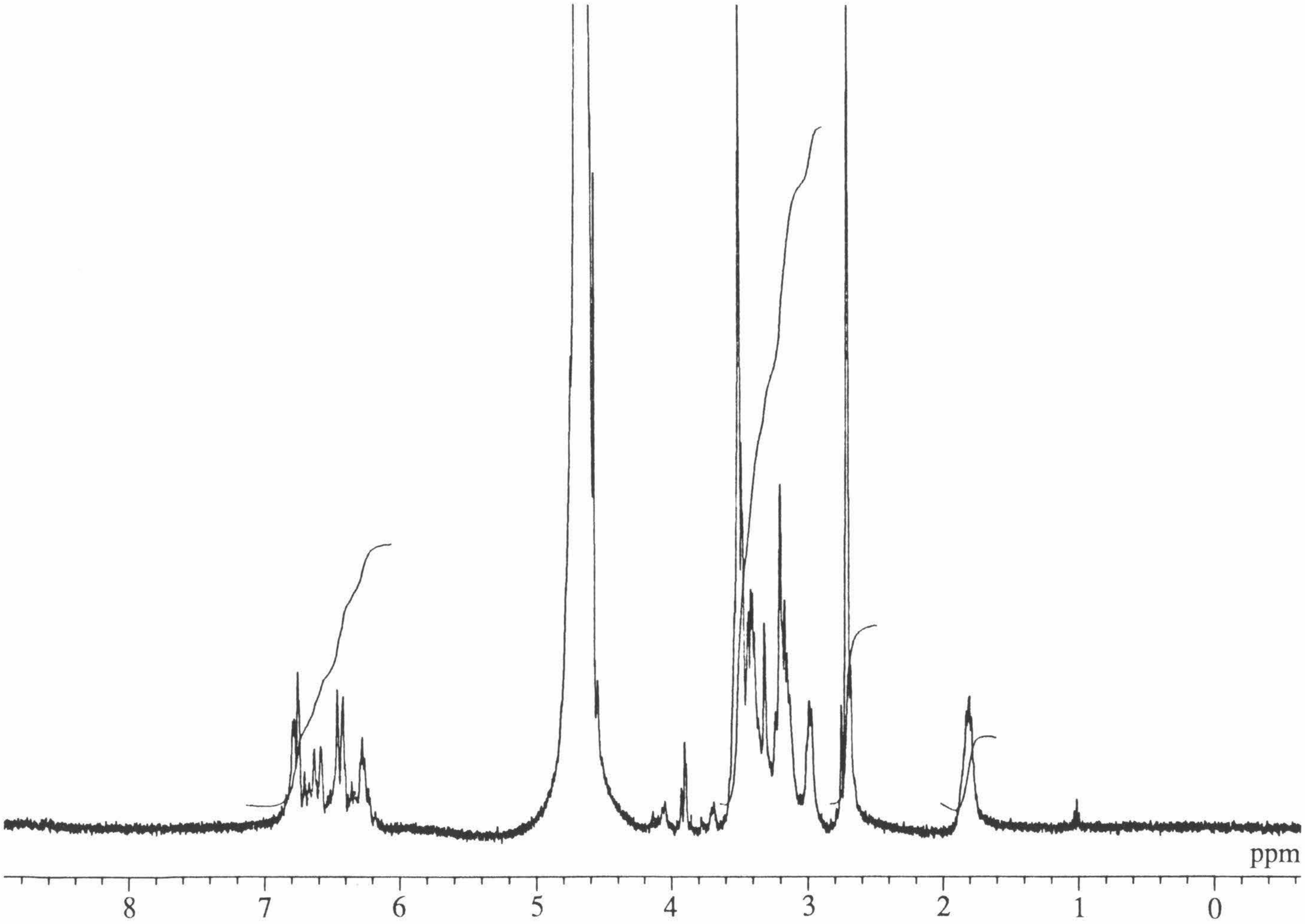

Figure 2: Proton Spectrum of N-Bromoacetyldistamycin (D_2O).

B. Cleavage of Double Helical DNA by N-Bromoacetyldistamycin 3a (BD): To test for the sequence specific cleavage of DNA, N-bromoacetyldistamycin (BD) was incubated with a ^{32}P end labeled 167 base pair restriction fragment (ECO RI/RSA I) from pBR322 plasmid DNA. The tripeptide tris-N-methylpyrrolecarboxamide has been shown by footprinting[47] and affinity cleaving[49] methods to bind four five-basepair sites on this fragment. N-Bromoacetyldistamycin at 5.0 uM concentration was allowed to interact with the ^{32}P-end labeled fragment at 37° C in 10 mM NaPhosphate buffer (pH 7.0), with sonicated calf thymus DNA acting as the carrier DNA (100 uM b.p.). After reaction times of 0.5, 5, and 10 hours, the DNA was precipitated with EtOH, heated at 90° C for 15 minutes in buffer, and then heated at 90° C for 15 minutes in 1.0 M piperidine.

Sites of cleavage were determined by high resolution denaturing gel electrophoresis. After 0.5 hours no cleavage was detected (Figure 3, lanes 3 and 4), however after 5 and 10 hour reaction times preferential cleavage was detected at a single adenine at base pair #48 (Figure 4, lanes 5-8; Figure 4, Histogram). Footprinting with the synthetic DNA cleaving reagent MPE-Fe(II),[23] under conditions of little or no observable cleavage by BD (0.5 h, 37° C), reveals that BD at a concentration of 5 uM is binding four five-basepair sites on this restriction fragment, (5'-3') TTTAA, GTTTA, AAATT, and GAAAT (Figure 3, lanes 9 and 10; Figure 4, histogram). The major cleavage site is contained within one of these four equilibrium binding sites on the complementary strand of the 5'-GTTTA-3' site.

Footprinting control experiments show that distamycin A and N-bromoacetyl-distamycin bind to identical sites on the 167 base pair restriction fragment, (5'-3') TTTAA, GTTTA, AAATT, and GAAAT (Figure 1, experimental section). This demonstrates that the α-bromoacetyl moiety does not detectably change the equilibrium binding specificity of the tripeptide binding unit.

The highly selective cleavage of the backbone exhibited by BD might be a reflection of the sequence dependent microheterogeneity of DNA and the individual alignment, distance, and residence time of the cleavage moiety (the electrophile) with respect to the

Figure 3: Autoradiogram of a high-resolution denaturing gel which indicates the sites of cleavage on the 167 b.p restriction fragment by BD. Odd and even numbered lanes are DNA end labeled with ^{32}P at the 5' and 3' position, respectively. Arrows on the left of the autoradiogram reading bottom to top is the sequence left to right in Figure 4. Arrow on the right at the middle of the gel points to the site of major cleavage (see Lane 8).

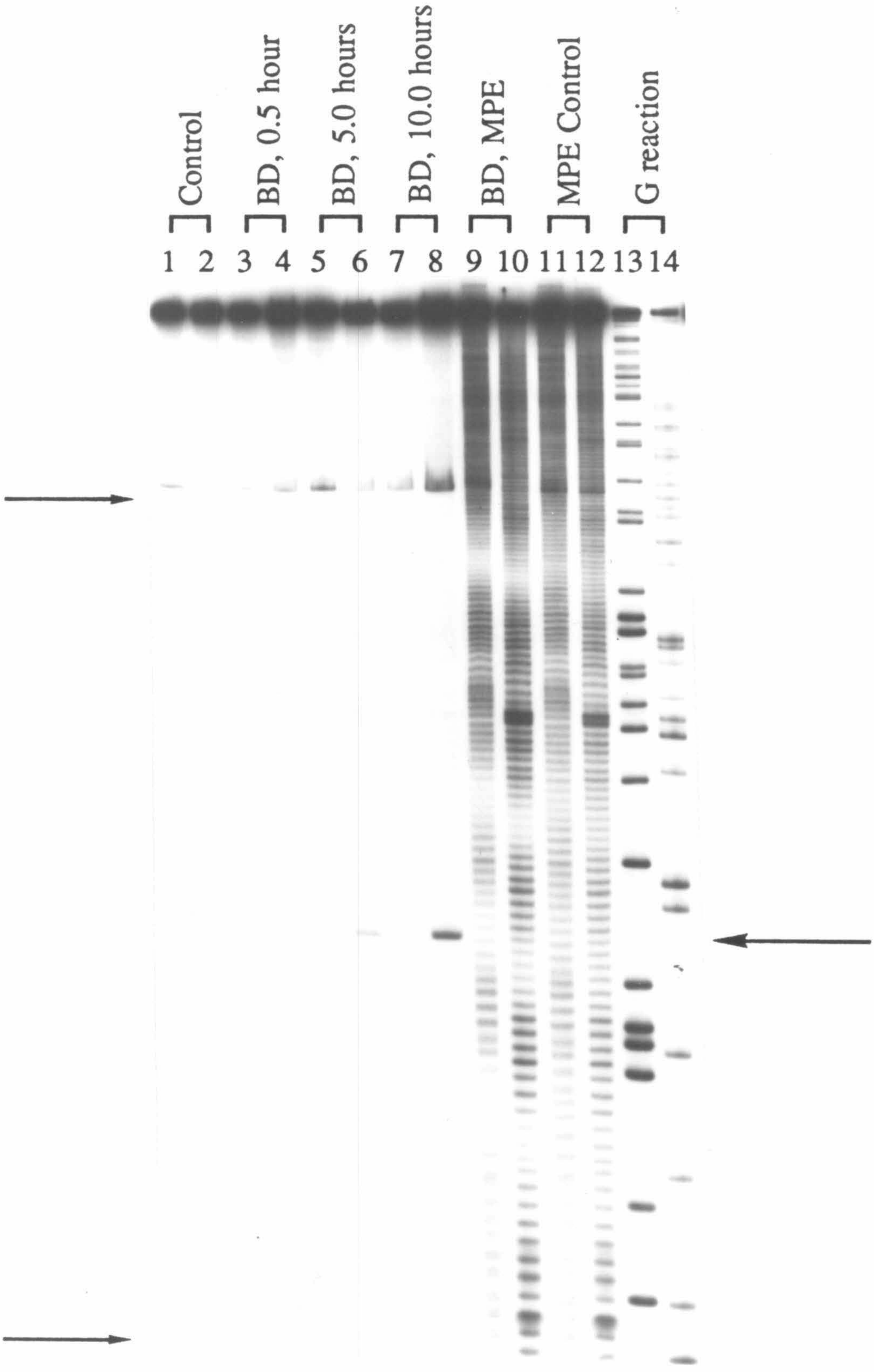
Control
BD, 0.5 hour
BD, 5.0 hours
BD, 10.0 hours
BD, MPE
MPE Control
G reaction
1 2 3 4 5 6 7 8 9 10 11 12 13 14

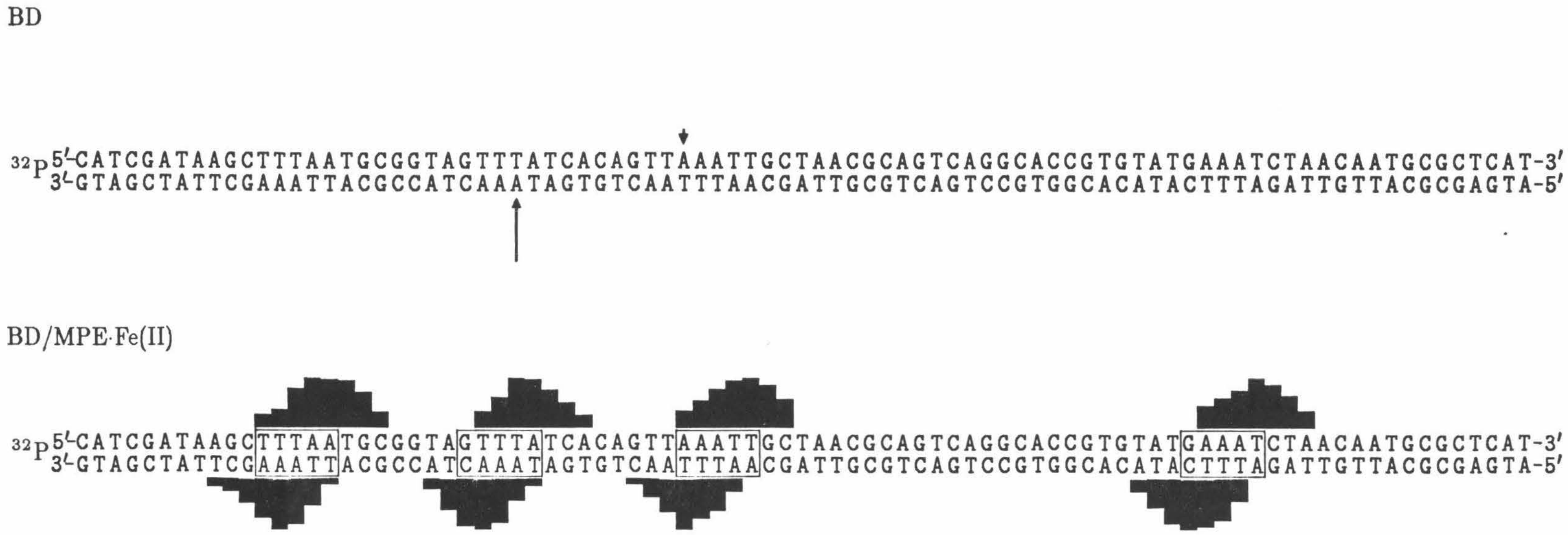
BD
32P 5'-CATCGATAAGCTTTAATGCGGTAGTTTATCACAGTTAAATTGCTAACGCAGTCAGGCACCGTGTATGAAATCTAACAATGCGCTCAT-3'
3'-GTAGCTATTCGAAATTACGCCATCAAATAGTGTCAATTTAACGATTGCGTCAGTCCGTGGCACATACTTTAGATTGTTACGCGAGTA-5'
BD/MPE·Fe(II)
32P 5'-CATCGATAAGCTTTAATGCGGTAGTTTATCACAGTTAAATTGCTAACGCAGTCAGGCACCGTGTATGAAATCTAACAATGCGCTCAT-3'
3'-GTAGCTATTCGAAATTACGCCATCAAATAGTGTCAATTTAACGATTGCGTCAGTCCGTGGCACATACTTTAGATTGTTACGCGAGTA-5'

Figure 4: Histogram of Sites of Cleavage and Binding on the 167 b.p. restriction fragment, base pairs 22-108. (Top) Arrows indicate the sites of cleavage resulting from the reaction of BD on the restriction fragment at 37°C after 10 hours. (Bottom) MPE-Fe(II) footprints of BD at 5 uM concentration bound to the 167 restriction fragment at 37°C. Assymmetric histograms on each strand represent regions on the end labeled DNA restriction fragment protected by BD from cleavage by MPE-Fe(II), Figure 3, lanes 9 and 10. Boxes are equilibrium binding sites of BD whose assignment is based on the MPE-Fe(II) model described in reference 25.

potential nucleophilic centers within each binding site on the restriction fragment.

The directionality of the molecular orbitals of both reactants are fixed by the conformation of each in the complex. Each base may tilt, roll, and twist from the plane perpendicular to the vertical helical axis, which will vary the unidirectionality of the individual orbitals of the lone pair of electrons of the postulated nucleophile, nitrogen 3 of adenine, at each site. The direction of the orbit may be viewed grossly parallel to that of the carbonyl groups of the tripeptide binding unit. Due to the assumed differences in the conformation of the N-bromoacetyldistamycin DNA complex at different binding sites it is not unreasonable to imagine that the high degree of selectivity displayed at adenine 48 results from placement of the electrophile in closer proximity to the nucleophilic centers of this particular base to create a higher effective molarity and consequently faster rate of reactivity.

The relative rates of alkylation at all potential nucleophilic centers determines the ultimate specificity of the N-bromoacetyldistamycin DNA cleavage reaction. To further understand the degree of cleavage specificity yielded by this small molecule, cleavage of the 167 b.p. restriction fragment was monitored over longer periods of time and over a wide range of temperature.

C. Dependence of DNA Cleavage on Time and Temperature: Cleavage of the 167 b.p. fragment by N-bromoacetyldistamycin was monitored over a 40 hour time period at 35° C (Figure 5). Cleavage is detectable after 5 hours at basepair #48, adenine. The amount of cleavage at this site continually increases to the 40 hour cut off time. A second cleavage product (b.p. #58, an adenine one helix turn away, on the opposite strand) appears after 10 hours and also increases in amount over the 40 hour reaction time. A third cleavage product appears in minute quantities after 20 hours (adjacent to the major site) at basepair #47, also an adenine. (Figure 6, histogram).

The temperature dependence of the N-bromoacetyldistamycin reaction on the 167 fragment was investigated over the range of 5 to 65° C in 10° C increments (Figure 7). The reaction time was 5 hours. New sites appear at each increasing increment. There is one product at 35° C (b.p. #48), two at 45° C (48, 58), eight at 55° C (35, 47, 48, 58, 59, 89, 90, 91), and nine at 65° C (35, 47, 48, 58, 59, 60, 89, 90, 91), see histogram (Figure 8). Therefore, as the temperature increases the degree of specificity decreases, as one expects based on the Arrhenius equation and principles of transition state theory. The reactions all occur at adenine and all within the binding sites of the tripeptide. In addition, there is an increase in the yield of cleaved DNA at all the specified sites with an increase in temperature.

These time and temperature studies on the 167 b.p. restriction fragment reveal that there are subsets of binding sites within or adjacent to the thermodynamically most stable and conformationally most complementary complexes as determined by MPE footprinting studies. The most dramatic example is at 65° C, where the rate of cleavage is equal at all three adenines within the MPE binding site, 5' GAAAT. In this case it appears that a GC base pair must be incorporated into the binding site regardless of which way the molecule shifts. Alternatively or concurrently dramatic alterations in the DNA helical twist, base propellar twist, roll angle and torsion angle may be occurring to allow accessiblity to the

Figure 5: Autoradiogram of the Dependence of Cleavage on Time. Determination of BD cleavage sites on the 167 b.p. restriction fragment through a 40 hour time course at 37° C. Odd and even numbered lanes are DNA end labeled with ^{32}P at the 5' and 3' position, respectively. All reactions are 100 uM b.p. calf thymus DNA, 5 uM BD in 10 mM NaPhosphate pH 7.0.

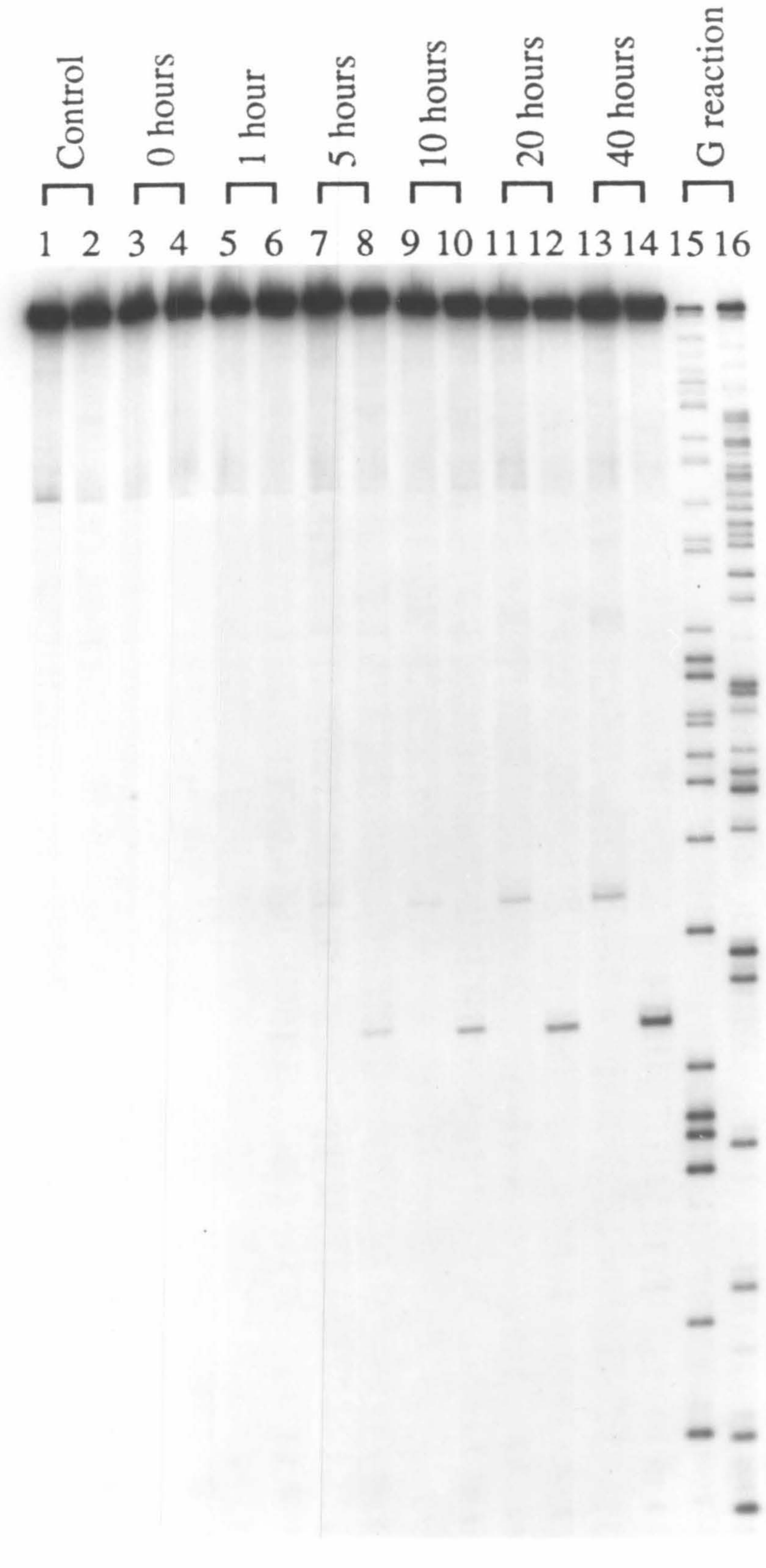
Control
0 hours
1 hour
5 hours
10 hours
20 hours
40 hours
G reaction
1 2 3 4 5 6 7 8 9 10 11 12 13 14 15 16

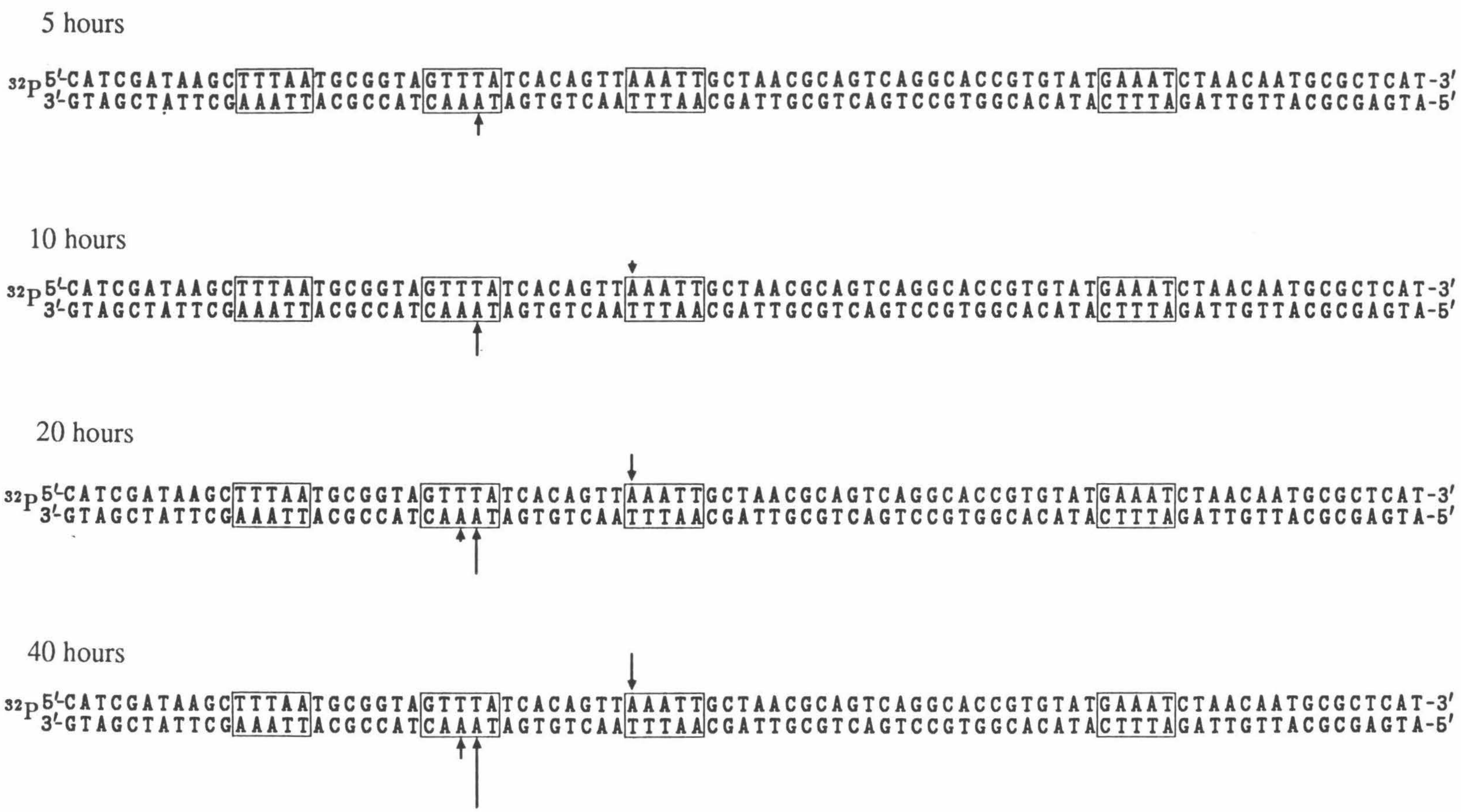
5 hours
32P 5′-CATCGATAAGCTTTAATGCGGTAGTTTATCACAGTTAAATTGCTAACGCAGTCAGGCACCGTGTATGAAATCTAACAATGCGCTCAT-3′
3′-GTAGCTATTCGAAATTACGCCATCAAATAGTGTCAATTTAACGATTGCGTCAGTCCGTGGCACATACTTTAGATTGTTACGCGAGTA-5′
10 hours
32P 5′-CATCGATAAGCTTTAATGCGGTAGTTTATCACAGTTAAATTGCTAACGCAGTCAGGCACCGTGTATGAAATCTAACAATGCGCTCAT-3′
3′-GTAGCTATTCGAAATTACGCCATCAAATAGTGTCAATTTAACGATTGCGTCAGTCCGTGGCACATACTTTAGATTGTTACGCGAGTA-5′
20 hours
32P 5′-CATCGATAAGCTTTAATGCGGTAGTTTATCACAGTTAAATTGCTAACGCAGTCAGGCACCGTGTATGAAATCTAACAATGCGCTCAT-3′
3′-GTAGCTATTCGAAATTACGCCATCAAATAGTGTCAATTTAACGATTGCGTCAGTCCGTGGCACATACTTTAGATTGTTACGCGAGTA-5′
40 hours
32P 5′-CATCGATAAGCTTTAATGCGGTAGTTTATCACAGTTAAATTGCTAACGCAGTCAGGCACCGTGTATGAAATCTAACAATGCGCTCAT-3′
3′-GTAGCTATTCGAAATTACGCCATCAAATAGTGTCAATTTAACGATTGCGTCAGTCCGTGGCACATACTTTAGATTGTTACGCGAGTA-5′

Figure 6: Time Histogram of base pairs 22-108 from the pBR322 plasmid. Arrows indicate the sites of cleavage resulting from the reaction of BD on the 167 b.p. restriction fragment at 37°C after the indicated reaction times.

Figure 7: Autoradiogram of the Dependence of Cleavage on Temperature. Determination of sites of cleavage of BD in increments from 5 to 65^{o} C after 5 hours. Odd and even numbered lanes are DNA end labeled with ^{32}P at the 5' and 3' position, respectively. All reactions are 100 uM b.p. calf thymus DNA , 5 uM BD in 10 mM NaPhosphate pH 7.0.

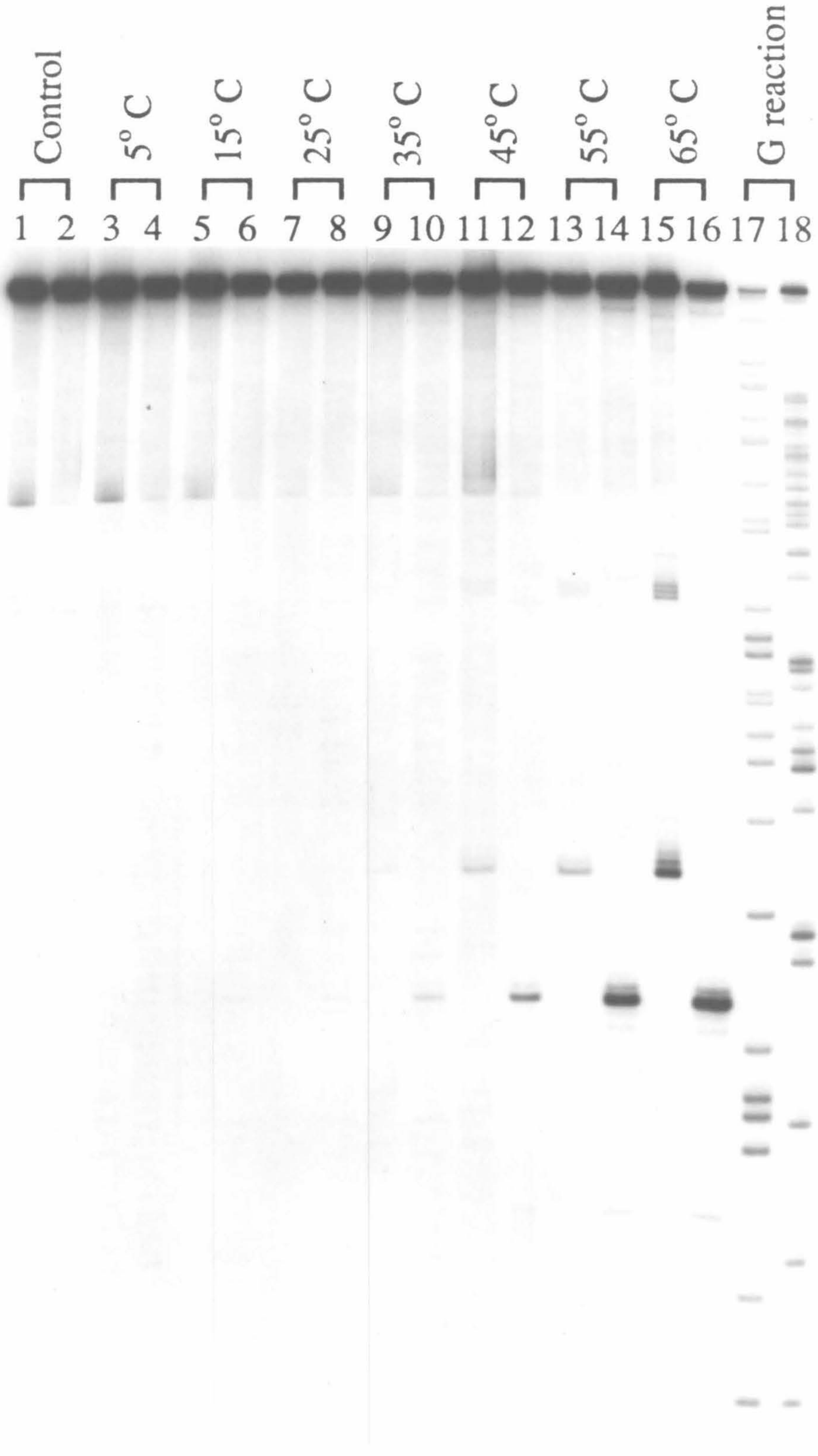
Control
5° C
15° C
25° C
35° C
45° C
55° C
65° C
G reaction
1 2 3 4 5 6 7 8 9 10 11 12 13 14 15 16 17 18

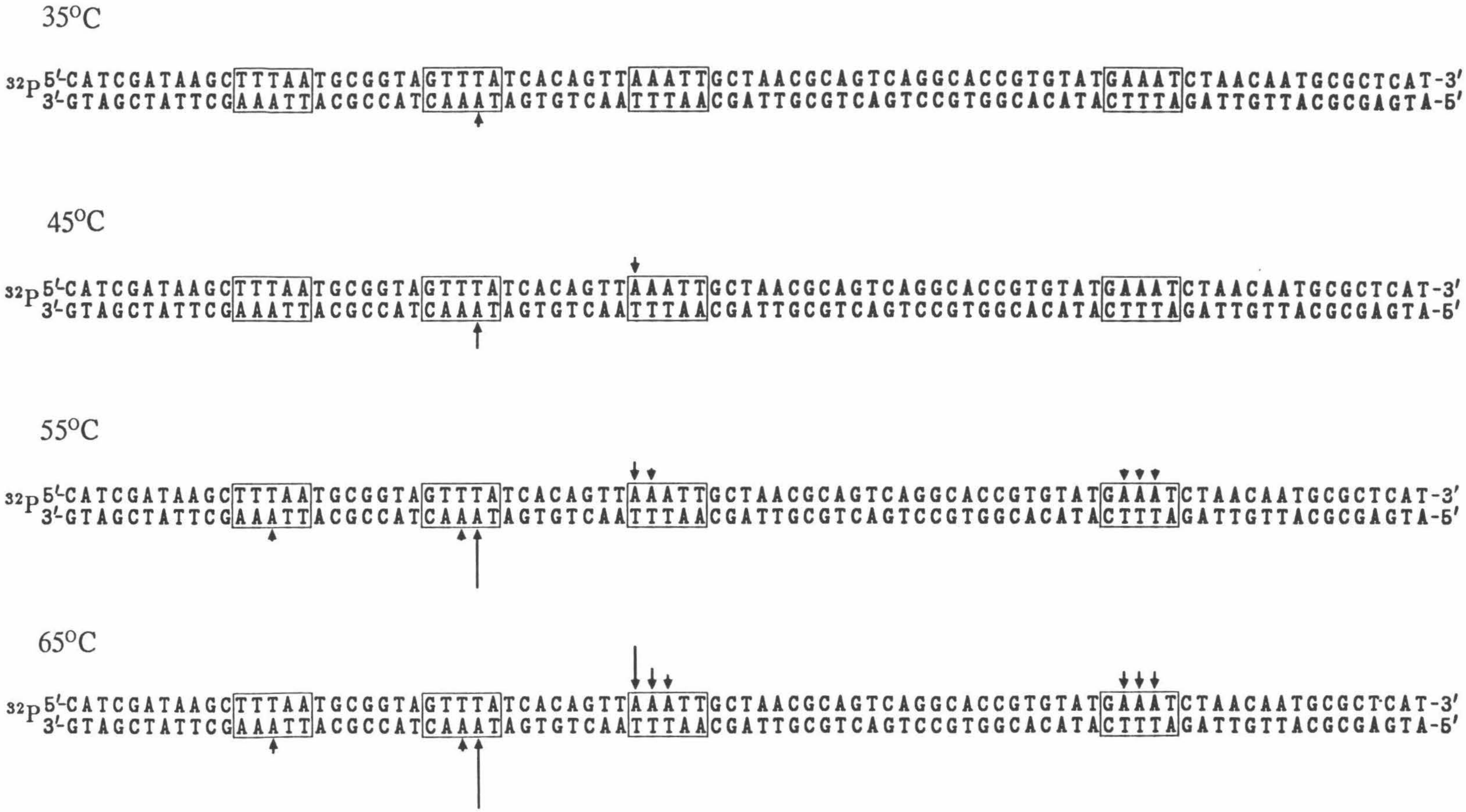
35°C
32P 5'-CATCGATAAGCTTTAATGCGGTAGTTTATCACAGTTAAATTGCTAACGCAGTCAGGCACCGTGTATGAAATCTAACAATGCGCTCAT-3'
3'-GTAGCTATTCGAAATTACGCCATCAAATAGTGTCAATTTAACGATTGCGTCAGTCCGTGGCACATACTTTAGATTGTTACGCGAGTA-5'
45°C
32P 5'-CATCGATAAGCTTTAATGCGGTAGTTTATCACAGTTAAATTGCTAACGCAGTCAGGCACCGTGTATGAAATCTAACAATGCGCTCAT-3'
3'-GTAGCTATTCGAAATTACGCCATCAAATAGTGTCAATTTAACGATTGCGTCAGTCCGTGGCACATACTTTAGATTGTTACGCGAGTA-5'
55°C
32P 5'-CATCGATAAGCTTTAATGCGGTAGTTTATCACAGTTAAATTGCTAACGCAGTCAGGCACCGTGTATGAAATCTAACAATGCGCTCAT-3'
3'-GTAGCTATTCGAAATTACGCCATCAAATAGTGTCAATTTAACGATTGCGTCAGTCCGTGGCACATACTTTAGATTGTTACGCGAGTA-5'
65°C
32P 5'-CATCGATAAGCTTTAATGCGGTAGTTTATCACAGTTAAATTGCTAACGCAGTCAGGCACCGTGTATGAAATCTAACAATGCGCTCAT-3'
3'-GTAGCTATTCGAAATTACGCCATCAAATAGTGTCAATTTAACGATTGCGTCAGTCCGTGGCACATACTTTAGATTGTTACGCGAGTA-5'

Figure 8: Temperature Histogram of base pairs 22-108 from the pBR322 plasmid. Arrows indicate the sites of DNA cleavage resulting from the reaction of BD on the 167 b.p. restriction fragment after 5 hours at the designated reaction temperatures.

other internal nucleophiles. By increasing the temperature or expanding the reaction time coordinate we are able to visualize by cleavage other conformational states of higher energy (with regard to alkylation) of both the DNA and N-bromoacetyldistamycin. In addition, we have a much better idea of the actual degree of specificity and relative rates.

To further understand the basis of cleavage specifity the two binding sites in which cleavage occurs after 40 hours at 37° C will be compared. In Table 1 the cleaved strands, which contain each binding site and the 4 base pair flanking sequences, have been ordered 5' to 3' in columns with the binding sites aligned with one another. The sites of cleavage are shaded. In addition, the cleaved strands are listed in columns by the purine and pyrimidine sequence.

In these two binding sites cleavage by N-bromoacetyldistamycin preferentially occurs at the 5' end. Recall that CC1065 preferentially alkylates adenines at the 3' end of its binding sites. The orientation and placement of the electrophilic carbon of CC1065 is fixed and determined by the stereochemistry at carbons 3b and 4a along with the direction and degree of curvature of the whole molecule. N-Bromoacetyldistamycin does not have any inherent stereochemistry at its electrophilic carbon. However, the halogen atom and its conformation with respect to the amide and tripyrrole binding unit might confer stereochemistry. The halogen atom may fix and specify the orientation and placement of the electrophile upon binding. For instance, only one of the two gauche conformers may bind within the minor groove of right handed B DNA, thus establishing a directional/strand preference for alkylation and cleavage. However, at this time this is a concept since the data base is limited. This concept is analogous to the orbital steering and proximity concepts thought to be important for reaction rate enhancements by enzymes.[25]

The sequence and consequently conformational attributes of the DNA were assessed by an application of Calladine's rules to the two binding sites sequestered within their two four base pair flanking sequences. These rules are based upon the crystal data and structural analysis of the Dickerson dodecamer.[10] This model is an application of quantitative mechanics of an elastic beam system to the double helix.[67] It attributes the conformation of the DNA to steric repulsive forces betweeen adjacent purine bases on opposite strands. These clashes are due to the larger size of the purine bases, which extends them beyond the center of the base pair, and the persistent propellar twist, which rotates the bases on opposite strands in opposite directions. In this model there are four basic means by which to relieve these steric interactions.

1. Rotate the base pair around the axis of the helix to decrease the local helix twist. A decrease in the twist angle lessens minor groove steric hindrance by increasing the distance between the N3 atoms of adjacent purines on opposite strands. In addition, it alters the widths of the grooves.

2. Rotate or roll the base pair as a unit. θ_R is defined from the mean base pair plane and is the magnitude of the total angle between successive base plane normals. The value is positive if the two planes being compared open out towards the minor groove and negative if towards the major groove. To relieve steric interactions, the roll angle is opened up on the side on which the clash occurs.

3. Decrease the propellar twist. Propellar twist is the dihedral angle between individual base planes. Looking down the long axis of the base pair, θ_P is defined positive if the near base is rotated clockwise with respect to the far one.

4. Translate or shift the base pair sideways towards the purine end of the base pairs, which changes the sugar torsional angles. This will pull the purine out of the stack and away from adjacent purines on opposite strands.

Numerical algorithms have been devised for this model and applied to the resolved crystal structure of the Dickerson Dodecamer.[68,69] The linear correlation coefficients are $R = 0.994$ for the helical twist, $R = 0.917$ for the base roll, $R = 0.777$ for torsion angle, and $R = 0.680$ for the propellar twist.

The same rules and algorithms have been applied to the two binding sites and sequences of the 167 restriction fragment in which cleavage occurs after 40 hours at 37° C.

The purpose is to compare and contrast (by modeling) the topography of the DNA in these regions.

Table 1 lists the numerical results for each attribute (helical twist, base roll, base propeller twist, and torsional angle). First note that cleavage occurs in both cases at a 5'-3' pyrimidine/purine junction. The helical twist at this junction, 5' from the site of cleavage, is low. The difference of a few degrees between the two sites is attributed to the different 5' flanking sequences which also have contrasting degrees of helical twist at each base step. The base roll or the magnitude of the total angle between successive base plane normals is positive at this junction. Recall, positive values indicate a roll towards the major groove and negative values towards the minor groove. A roll towards the major groove opens up the minor groove, which places the base edges and consequently functional groups of adjacent base pairs farther away from one another in the minor groove. Again the subtle difference, between the two sites at the 5' junction, is attributed to the different 5' flanking sequences and their contrasting values at each base pair step.

In the 3' direction from the two sites of cleavage and within each binding site there are no differences in the helical twist and base roll from base pair to base pair.

The propellar twist and torsion angle values of the base pair where cleavage occurs are identical in each case. Additionally, those sequentially from the 3' side of the cleavage sites are the same. Based on these values alone one expects the alignment of the small molecule to be the same.

These calculations strictly give a perspective of the microheterogeneity of the DNA from site to site. Based on the correlation coefficients, these algorithms are reliable for predicting the helical twist and base roll. For instance, other experimental evidence which correlates with the degree and change of conformation with sequence has been shown by the cleavage patterns produced by iron(II) EDTA and DNase I on restriction fragments. By this method, Tullius and Dombroski[70] measured the number of base pairs per helical turn. Importantly, they observed lower than expected reactivity in sequences in which a pyrimidine occurs to the 5' side of a purine. On the other hand, calculations of the propellar twist and torsion angle may be relatively unreliable, as indicated by the correlation coefficients. For example, application of the propeller twist algorithm to the dodecamer recently cocrystallized with distamycin A, 5'-d(CGCAAATTTGCG), is especially erroneous for base pair 9, which experimentally is determined as 26° and theoretically by this algorithm as 17.1°.

SITE #	Base Sequence #2	Base Sequence #3	Purine(R)/ Pyrimidine(Y) #2	Purine(R)/ Pyrimidine(Y) #3	Helical Twist #2	Helical Twist #3	Base Roll #2	Base Roll #3	Propellar Twist #2	Propellar Twist #3	Torsion Angle #2	Torsion Angle #3
5'	G	A	R	R								
					39.8	41.9	- 7.7	- 2.2	13.5	20.7	46.8	15.6
	T	G	Y	R								
					29.3	31.4	+4.4	- 3.3	17.1	20.7	31.2	15.6
C	G	T	R	Y								
l					41.9	41.9	- 2.2	- 2.2	20.7	17.1	15.6	31.2
e a	A	T	R	Y								
v					35.6	27.2	- 5.5	+3.3	13.5	17.1	46.8	31.2
e	T	A	Y	R								
d					29.3	39.8	+4.4	- 3.3	17.1	24.3	31.2	00
	A	A	R	R								
					39.8	37.7	- 3.3	0	24.3	20.7	00	15.6
S	A	A	R	R								
t					37.7	31.4	0	- 3.3	20.7	20.7	15.6	15.6
r	A	T	R	Y								
a					31.4	41.9	- 3.3	- 2.2	20.7	17.1	15.6	31.2
n	C	T	Y	Y								
d					41.9	29.3	- 2.2	+4.4	17.1	17.1	31.2	46.8
	T	G	Y	R								
					29.3	35.6	+4.4	- 5.5	13.5	24.3	46.8	15.6
	A	C	R	Y								
					35.6	41.9	- 5.5	- 2.2	20.7	20.7	15.6	31.2
	C	T	Y	Y								
					41.9	27.2	- 2.2	+ 3.3				
↓	C	A	Y	R								

Table 1: Application of Calladine's Numerical Algorithms to the 167 base pair restriction fragment.

D. Dependence of Cleavage Rate and Specificity on the Leaving Group: To assess the dependence of cleavage on the leaving group a comparison and contrast was made between the hydroxy (HOD), chloro (CD), bromo (BD), iodo (ID), and mesyl (MsD) derivatives (Figure 10).

Synthesis of N-Chloro **3b** and N-Iodoacetyldistamycin **3c**: The chloro **3b** (CD) and iodo **3c** (ID) derivatives were synthesized by the same method as that used for the synthesis of N-bromoacetyldistamycin **3a** (BD), *i.e.,* coupling via the triflouroacetic mixed anhydride **4**.

N-Chloroacetyldistamycin **3b** (CD): The mass spectrum displays a doublet of peaks separated by two mass units for the parent molecule. Chlorine atoms have two natural isotopes, 35 and 37.[45] The proton spectra is similar to that of N-bromoacetyldistamycin **3a**, except the methylene protons adjacent to the halide ion are shifted downfield to 4.19 ppm, resulting from the more electronegative halide substituent. This molecule is more hydrophilic than the bromo derivative as shown by NMR and HPLC. All peaks in the proton spectra are well defined in D_2O (Figure 9). In addition, the elution time on a reverse phase high pressure column is 0.97x that of N-bromoacetyldistamycin **3a**.

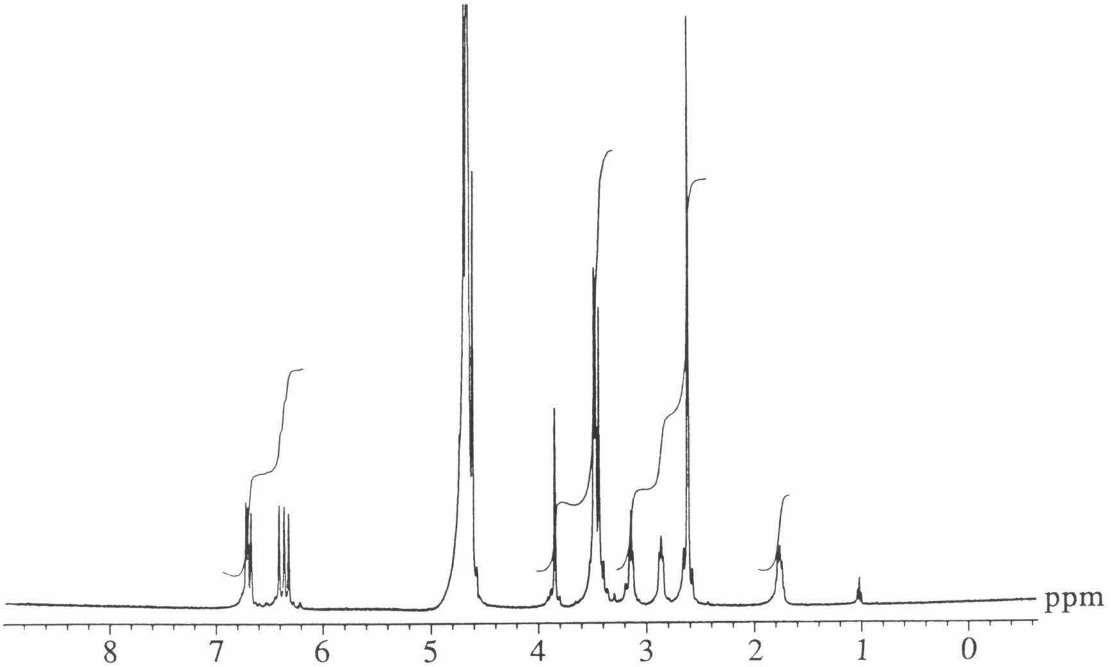

Figure 9: Proton Spectrum of N-Chloroacetyldistamycin **3b** (D_2O).

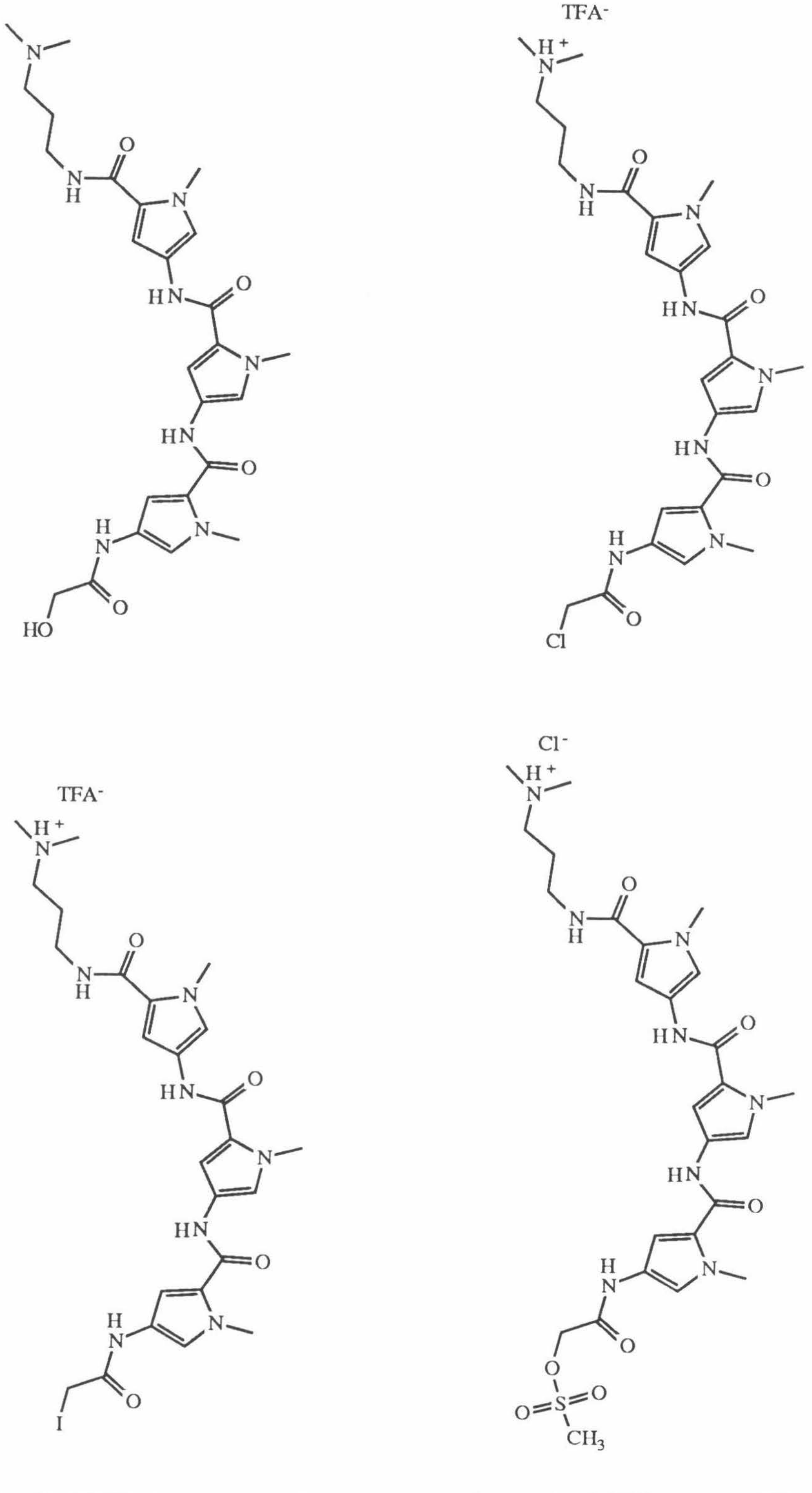
TFA-
HO
TFA-
Cl
TFA-
I
Cl-
CH3

Figure 10: A) N-Hydroxyaceytldistamycin (HOD) B) N-Chloroacetyldistamycin (CD) C) N-Iodoacetyldistamycin (ID) D) N-Mesylacetyldistamycin (MsD)

N-Iodoacetyldistamycin **3c** (ID): The solid form of this compound is slightly yellow -- iodide. The methylene protons next to the iodine atom are sequestered under the peaks of the N-methylpyrrole protons, upfield from both the bromo **3a** and the chloro **3b** compounds. The proton spectra of N-iodoacetyldistamycin **3c** in D_2O is similar to that of N-bromoacetyldistamycin **3a**, with regard to peak definition and resolution. The elution time for N-iodoacetyldistamycin **3c** on a reverse phase high pressure column is 1.05x that of N-bromoacetyldistamycin **3a**, therefore it is a slightly more hydrophobic compound.

Synthesis of N-Hydroxyacetyldistamycin **5** (HOD): This derivative was synthesized in 86% yield from the tripeptide amine **2** and glycolic acid by the dicyclohexylcarbodiimide/N-hydroxybenzotriazole method.[71,72] Distinguishable characteristics of the proton spectra (dimethyl sulfoxide) include a triplet at 5.59 ppm corresponding to the hydroxyl proton and a doublet at 3.95 ppm corresponding to the adjacent methylene protons. It is distinguishable by TLC and reverse phase HPLC. One observes a lower R_f by TLC ($R_f = 0.40$ for HOD **5**, whereas for BD **3a** $R_f = 0.52$ / 1% NH_4OH/MeOH) and a faster elution time by reverse phase HPLC (0.66x that of BD **3a**).

Synthesis of N-Mesylacetyldistamycin **6** (MsD): This compound was synthesized from N-hydroxyacetyldistamycin **5** and 450 equivalents of mesyl chloride in a 1:1 mixture of acetonitrile and pyridine. It was removed from solution by precipitation with diethyl ether. The TLC of the precipitate was one compound. The proton NMR shows two peaks for the methylene protons adjacent to the mesyl group at 4.48 and 5.08 ppm, and two peaks for the corresponding amide proton at 10.54 and 10.65 ppm. In addition one of the pyrrole protons, presumably the C5 proton of the pyrrole unit at the amino terminus, is represented by two peaks at 7.22 and 7.26 ppm. This is indicative of two structural conformations -- the cis and trans of the N-terminus amide.

Cleavage Reactions: Comparisons of these compounds to N-bromoacetyldistamycin were made in two different experiments: a) N-hydroxyacetyldistamycin, N-chloroacetyldistamycin, N-bromoacetyldistamycin, and N-iodoacetyldistamycin; and b)

N-hydroxyacetyldistamycin, N-bromoacetyldistamycin, and N-mesylacetyldistamycin. (a) HOD, CD, BD, and ID at concentrations of 5 uM were each reacted with the 167 b.p. restriction fragment at 37° C under the same solvent conditions and carrier DNA concentrations as previously described for N-bromoacetyldistamycin. The workup procedure replaced the ethanol precipitation with phenol extraction following the reaction, but maintained the heat and heat/piperidine treatment. After 20 hours the hydroxyl and chloro show no sign of reactivity (Figure 11). The sites of cleavage for the iodo derivative are the same as those of the bromo, but the intensity or amount of cleavage is less. (b) HOD, BD, and MsD at concentrations of 5uM were each reacted with the 167 b.p. restriction fragment for 3 hours at 65° C under the same conditions and workup procedure. Again N-hydroxyacetyldistamycin is nonreactive. N-Mesylacetyldistamycin cleaves the DNA at the same sites as N-bromoacetyldistamycin, but at a slower rate.

Based on these results it appears that the leaving group does not contribute significantly to the exact placement of the electrophilic carbon. If this were so, we would have observed new and different sites of cleavage -- especially for the sulfonate, which clearly has different stereoelectronic properties from the halide series. Recall that analysis at a lower resolution, MPE footprinting, showed no alteration in the binding sites of N-bromoacetyldistamycin from distamycin A. Footprinting of HOD, CD, and ID shows these compounds have the same binding sites, as the natural product, distamycin A, and the analogous synthetic compound, N-bromoacetyldistamycin. The binding sites of N-Mesylacetyldistamycin were not analyzed.

The results of the hydroxyl and chloro derivatives, *i.e.*, no reaction, are not a surprise based on the relative leaving group ability. However the results for the iodo and mesyl compounds are unexpected. From this data it is not clear whether or not the decrease in reactivity is caused by an increase in the rate of hydrolysis (or degradation) of the iodo and mesyl compounds to the unreactive hydroxy species or because these molecules bind in a less favorable conformation for an S_N2 displacement (lower energy ground state or higher energy transiton state). These uncertainties will be addressed in the quantitative kinetic and thermodynamic studies of the reaction. To reach these levels of analysis, specifically kinetics, one must first isolate and characterize the reaction products and confirm the general mechanism of the cleavage reaction.

Figure 11: Autoradiogram of the Dependence of Cleavage on the Leaving Group. Determination of the Sites of Cleavage and Binding of N-Hydroxyacetyldistamycin (HOD), N-Chloroacetyldistamycin (CD), N-Bromoacetyldistamycin (BD), and N-Iodoacetyldistamycin (ID) on the 167 b.p. restriction fragment. Odd and even numbered lanes are DNA end labeled at the 5' and 3' positions, respectively. All reactions are 100 uM b.p. calf thymus DNA, 5 uM XD in 100 mM NaPhosphate pH 7.0 at 37° C. Cleavage reaction times were 20 hours.

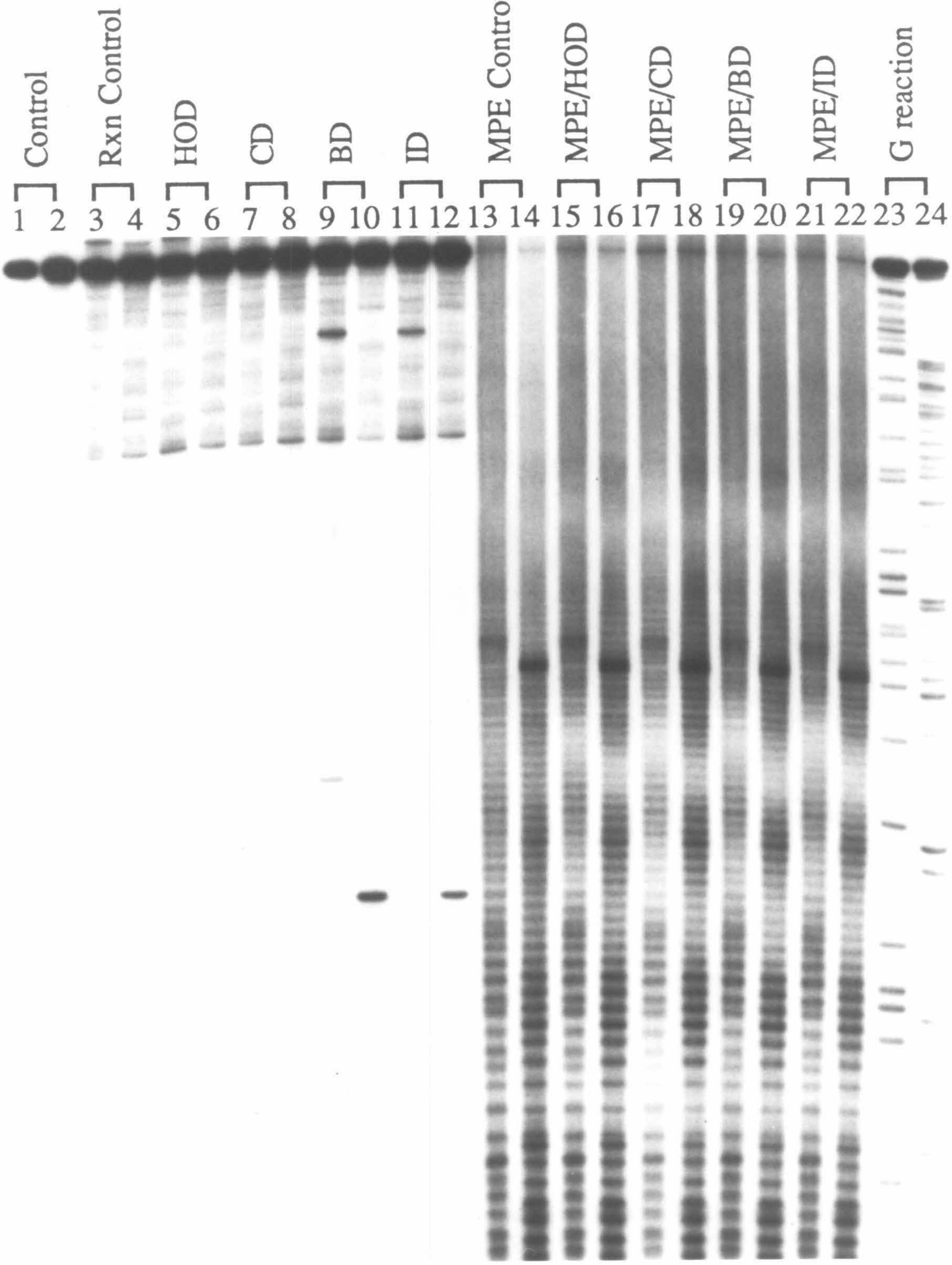
Control
Rxn Control
HOD
CD
BD
ID
MPE Control
MPE/HOD
MPE/CD
MPE/BD
MPE/ID
G reaction
1 2 3 4 5 6 7 8 9 10 11 12 13 14 15 16 17 18 19 20 21 22 23 24

E. N-Bromoacetyldistamycin Product Analysis: It is believed that cleavage of the DNA backbone by BD (and the other analogs) is dependent upon alkylation of adenine followed by depurination. If this is the mechanism it should be possible to detect and isolate the BD-adenine adduct. The following experimental route was taken in order to isolate the putative BD-adenine adduct. 1) ^{14}C labeled BD was synthesized for microscale reactions to analyze the BD-DNA products. 2) The products from the reaction of adenine free base and BD were compared with the released products from the reaction of DNA and BD by TLC/autoradiography of the labeled compounds and then reverse phase HPLC of the corresponding unlabeled compounds.

N-Bromo-[2-^{14}C]-acetyldistamycin **9** (B^{14}D) was synthesized by the same method as that used for the unlabeled compound. The compound was characterized by UV and NMR, two techniques which are relatively safe with regard to prevention of contamination and spillage of radioisotopic compounds.

There are five nucleophilic sites on adenine, N1, N3, N7, N9, and N6. Which site(s) are alkylated can be controlled by the solvent and pH.[73] Importantly it has been reported that reaction of the free base adenine (one equivalent) with 1-bromo-3-methyl-2-butene (one equivalent) in dimethylacetamide at 30° C for 7 hours results in alkylation at N3 (55-66% yield).[74] With this precedent in mind B^{14}D was mixed with eight equivalents of adenine in dimethylformamide at 75° C. A control reaction, B^{14}D in the absence of adenine, under identical solvent, concentration, and temperature conditions was done simultaneously. The reaction was monitored over 5 days by thin layer chromatography (Figure 12). After 8 hours two new products resulted from the reaction as shown by autoradiography of the TLC plate. By day 5 the slower migrating product completely decomposed to another product(s) which migrated in the solvent front.

Figure 12: Autoradiograms of the thin layer chromatographic plates utilized to monitor the reaction between ^{14}C-BD and Adenine. Lanes 1 are 4 mM ^{14}C-BD in DMF at 75° C and Lanes 2 are 4 mM ^{14}C-BD and 32 mM Adenine in DMF at 75° C, where A) 0 hours, B) 8 hours, C) 24 hours, and D) 5 days.

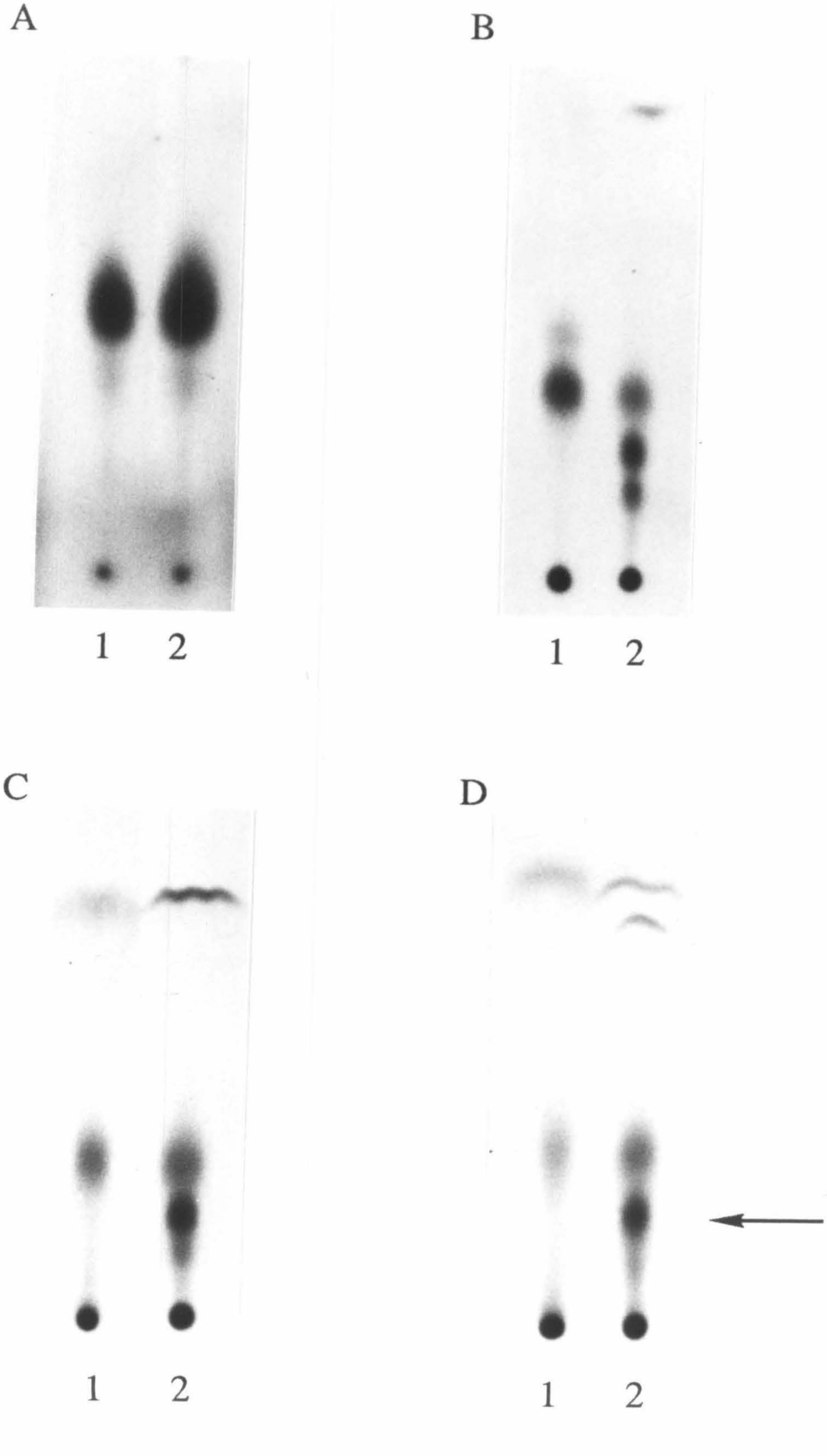
A
1
2
B
1
2
C
1
2
D
1
2

Product analysis of the reaction of BD with DNA was carried out on two DNA substrates, calf thymus DNA and a 15 base pair duplex, 5' CGGTAGTTTATCACA. The oligonucleotide duplex corresponds to the binding site and flanking sequences of the 167 b.p. restriction fragment in which the major cleavage site, basepair #48, is located. The oligonucleotide was utilized for the pilot carbon 14 DNA reactions. As mentioned these reactions were monitored by thin layer chromatography followed by autoradiography (Figure 13). After 96 hours at 37° C one new compound is produced (released) from a one to one mixture of the annealed 15mer and $B^{14}D$ (lane 5, arrow indicates new compound). *This product comigrates by TLC with the stable synthetic adenine adduct (lane 3) isolated previously from the reaction of adenine with BD.* At this time the reaction has not gone to completion, *i.e.,* a good portion of the starting material, BD, remains (lane 1, BD marker). Under the same conditions, but in the absence of DNA, BD decomposes to products which are immobile on silica (lane 4).

Additional verification of the common identity of the BD-oligonucleotide adduct and the BD-free base adenine adduct was obtained by reverse phase HPLC of the unlabeled compounds and reaction mixtures. Coinjection of the synthetic distamycin-adenine adduct with the BD-oligonucleotide reaction mixture resulted in coelution of the synthetic adduct with one of the peaks of the BD-oligonucleotide reaction mixture. Ultraviolet-visible spectra could be acquired of each compound following chromatography with a photodiode array detector. The spectra of the synthetic distamycin-adenine adduct and the BD-oligonucleotide product which coelutes with the synthetic compound are displayed in Figure 14. As shown, by UV-visible spectroscopy, these two compounds are *identical.*

In conclusion, a product from the reaction of adenine and BD corresponds to the major released product from the reaction of DNA with BD. This common product is believed to result from the reaction between the N3 of adenine and the methylene carbon of the BD acetyl group (Figure 15).

Figure 13: Determination of the ^{14}C-BD/Oligonucleotide (15mer) reaction products by thin layer chromatography. Lane 1) ^{14}C-BD, Lane 2) ^{14}C-HOD, Lane 3) ^{14}C-Distamycin-Adenine (DA), Lane 4 100 uM in 100 mM NaPhosphate pH 7.0 for 96 hours at 37° C, Lane 5) 100 uM ^{14}C-BD plus 100 uM 15mer in 100 mM NaPhosphate pH 7.0 for 96 hours at 37° C, and Lane 6) Cospot of the three synthetic compounds ^{14}C-BD, ^{14}C-HOD, and ^{14}C-DA.

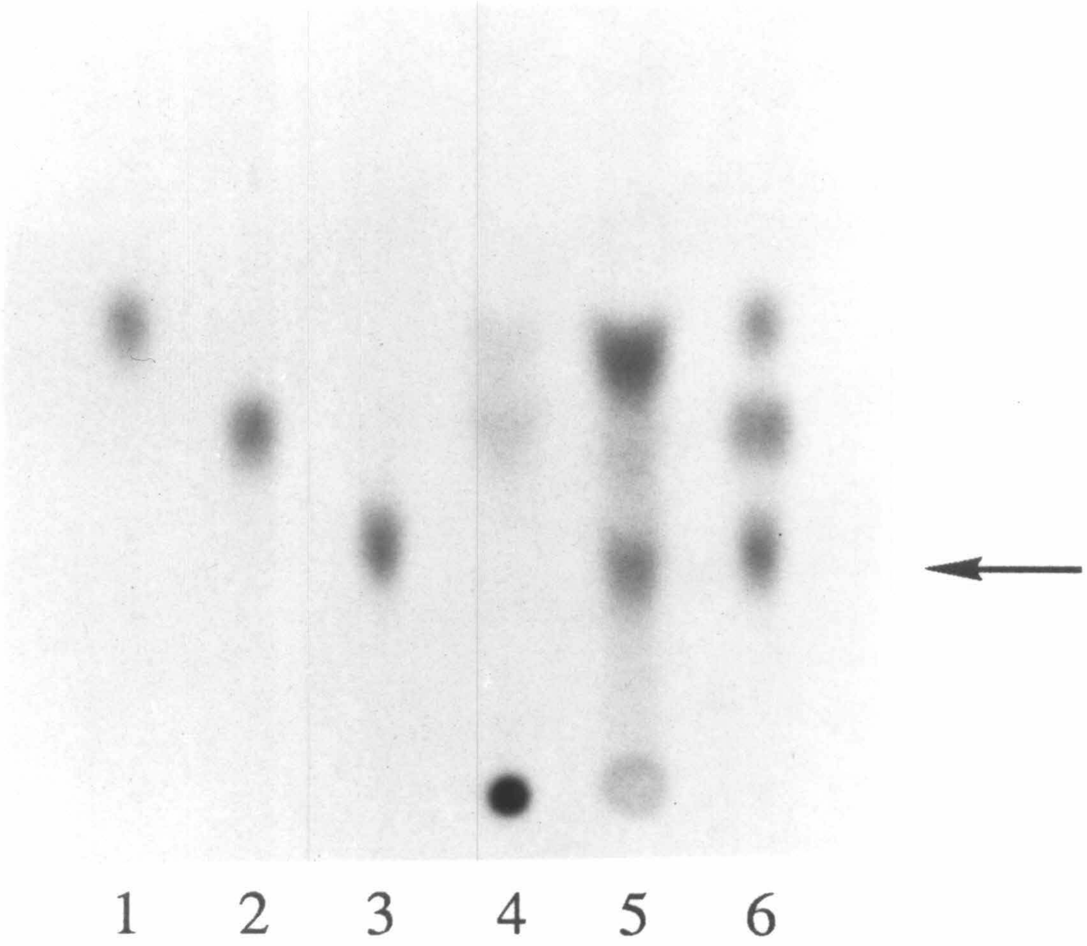
1
2
3
4
5
6

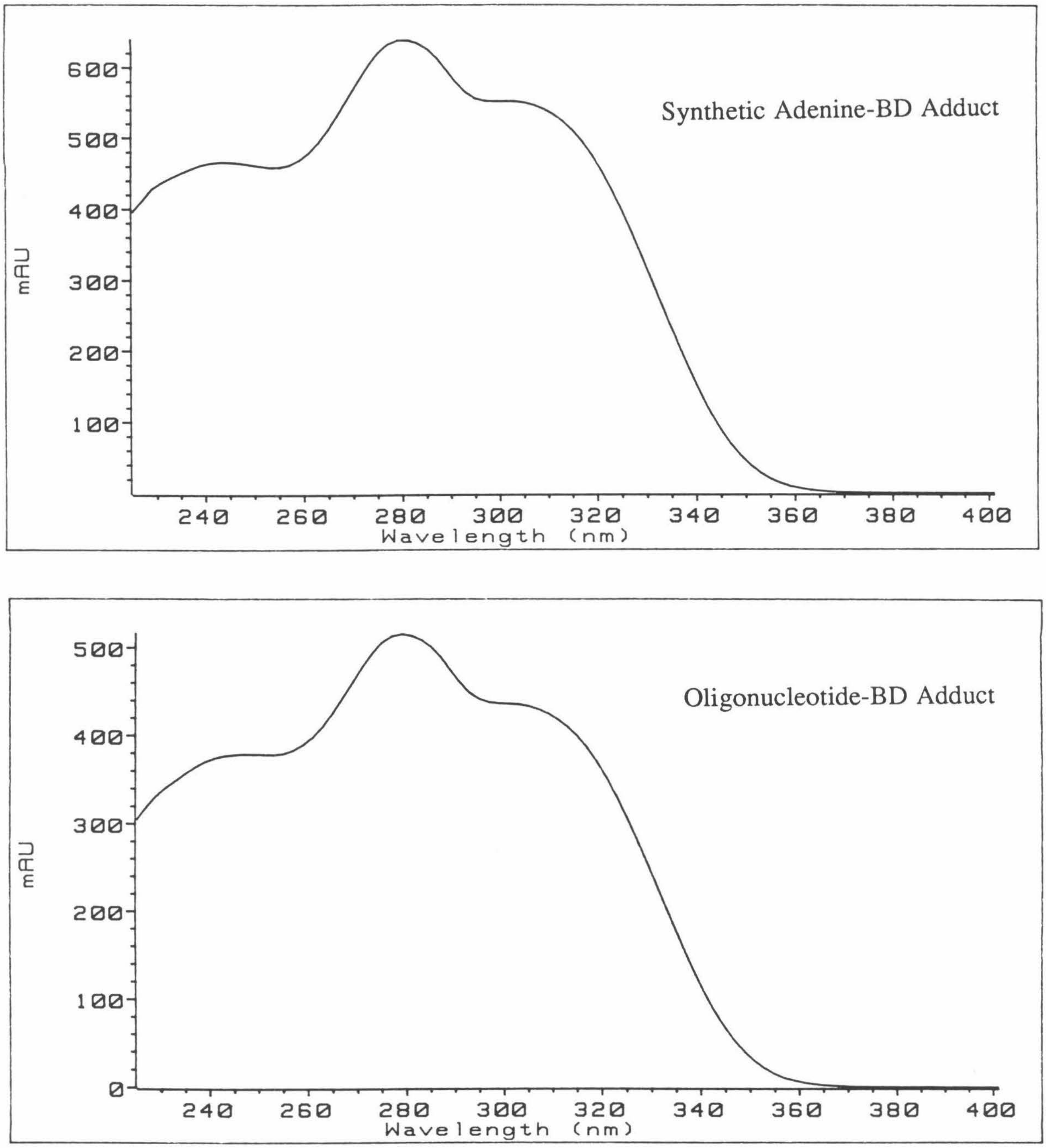

Figure 14: Ultraviolet-visible spectra from separate injections (225-400nm) of the synthetic BD-adenine adduct (top) and the 15 base pair oligonucleotide BD-adenine adduct (bottom) acquired by a photodiode array detector proceeding reverse phase high pressure chromatography. Solvent conditions were 11% acetonitrile/100 mM triethylammonium-formate pH 3.1.

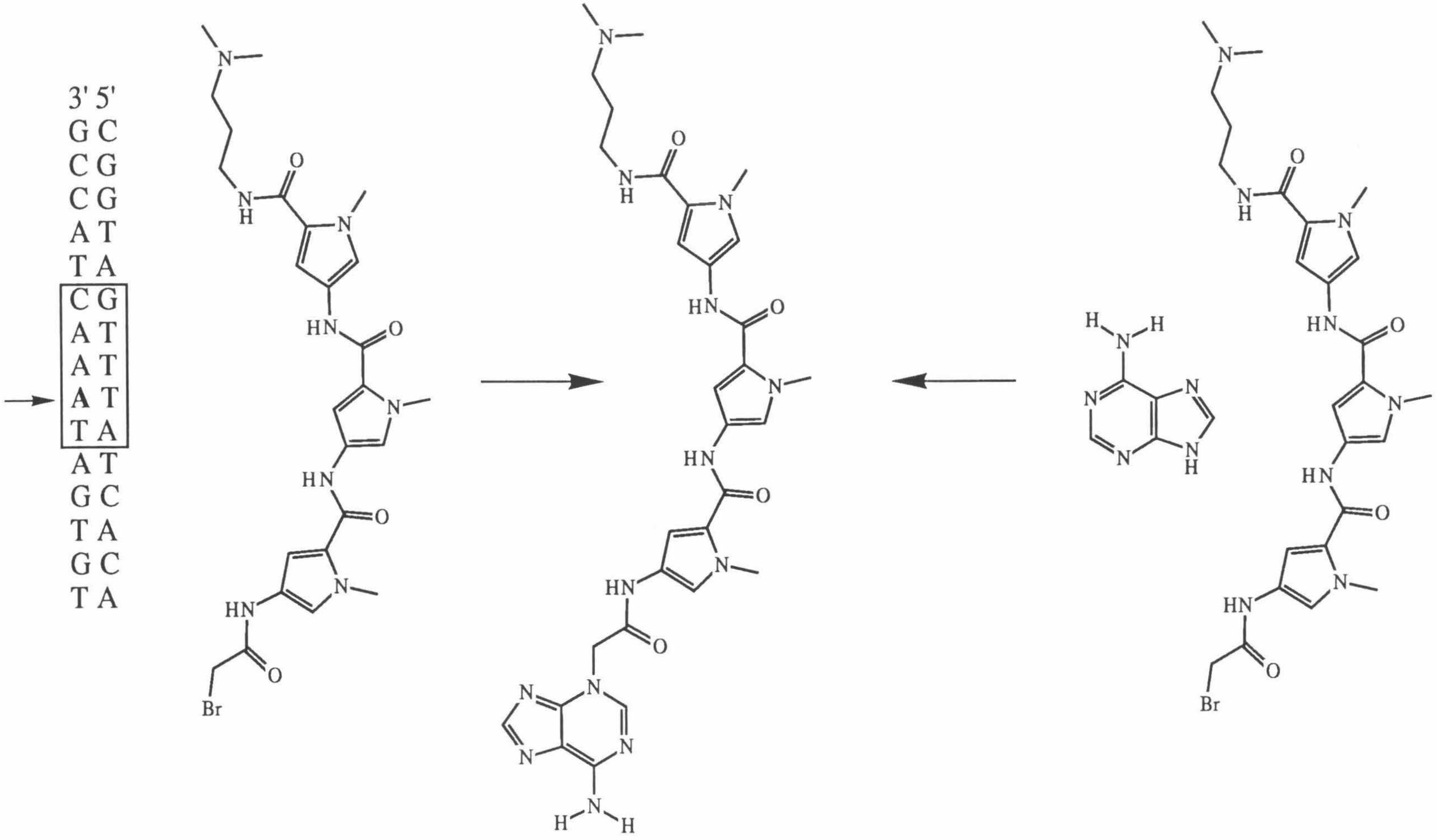
3' 5'
G C
C G
C G
A T
T A
C G
A T
A T
A T
T A
A T
G C
T A
G C
T A
Br
Br

Figure 15: Common Product from the free base adenine and oligonucleotide reaction with/BD.

Next, a very large scale DNA reaction was carried out, using sonicated calf thymus DNA, in order to isolate an *authentic* released DNA adduct for characterization by proton NMR. N-Bromoacetyldistamycin at 5.0 uM concentration was allowed to react with sonicated calf thymus DNA at 100 uM b.p. in 10 mM NaPhosphate (pH 7.0) for 56 hours at 48° C. The solution volume was 1380 milliliters. After purification by flash chromatography and reverse phase HPLC the following proton spectra was obtained for the isolated DNA product (Figure 16, upper spectrum). Enlargement and expansion of the aromatic region assured that both adenine and the three pyrroles are constituents of this molecule (Figure 16, lower spectrum). The NMR spectrum is identical to the synthetic adduct isolated from the reaction of BD with the free base adenine (compare Figure 16 and Figure 19). Additional verification of the common identity of the BD adduct was obtained by reverse phase HPLC, in which case upon coinjection the synthetic adenine adduct and the calf thymus adduct coeluted. Isotopic labeling schemes, ^{15}N at N3 of adenine and ^{13}C at the 2-acetyl of BD, will confirm by NMR the constitutional assignment of the structure of this common adduct.

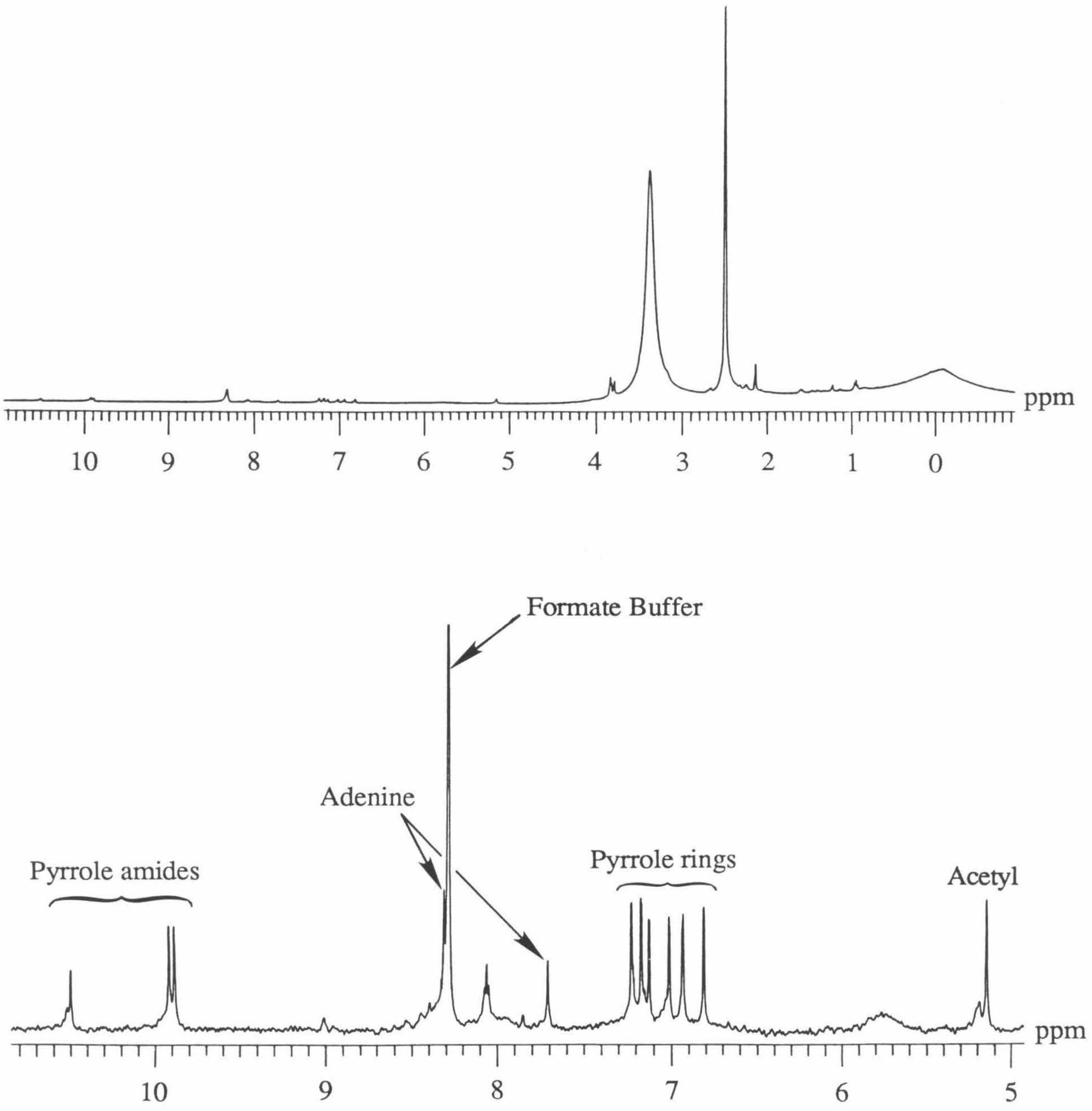

Figure 16: Proton Spectra of the authentic adenine adduct resulting from the reaction between sonicated calf thymus DNA and BD with tentative assignments. (Top) Full spectrum. (Bottom) Enlargement of the aromatic region.

F. Characterization of the Distamycin-Adenine Adduct: The synthetic distamycin-adenine adduct was characterized by ultraviolet, infrared, mass, and proton, carbon, and nitrogen nuclear magnetic resonance spectrometry.

The ultraviolet spectrum appears as a combination of the two reactants, DNA and BD, with an absorbance maximum at 280 nanometers in 11% acetonitrile/100 mM triethylammoniumformate pH 3.1 -- this is the solvent utilized for HPLC separation and verification of the purity of the compound (figure 17). The electronic properties of the adduct are solvent and pH dependent. In water (pH 5.5) the maximum absorbance occurs at 291 nm. This difference reflects changes either (or both) in the energy separation between the molecular orbitals in the ground and excited states and/or a reorientation of the transition electric dipole moments which lie in the plane of the adenine aromatic ring.[75] These changes can result from protonation of a specific nitrogen(s) or intermolecular interactions between the acetonitrile and TEA formate. With regard to protonation, a change of maxima is not observed for N3 adducts of adenine such as methyl, ethyl, and benzyl upon alteration of the pH. For example, the maxima for 3-benzyladenine are 275 nm at pH 1, 272 nm at pH 7, and 272 nm at pH 13.[76,77] Changes of absorbtion are observed though for the N1 adducts. 1-Benzyladenine displays a maxima at 259 nm at pH 3.0 and 270 at pH 13.0. In comparison (by pH) the results obtained for the distamycin adenine adduct imply that we can not rule out that nitrogen 1 is alkylated. To avoid the potential incongruenties displayed in the UV spectra due to differing alkylation groups (distamycin vs benzyl) nuclear magnetic resonance was pursued to *absolutely* define the site of covalent attachment in the distamycin-adenine adduct.

Figure 17: Three dimensional graphic of the Distamycin-Adenine Adduct acquired by a photodiode array detector during High Pressure Liquid Chromatography.
Time (min) *vs*. Wavelength (nm) *vs*. Absorbance (mA).

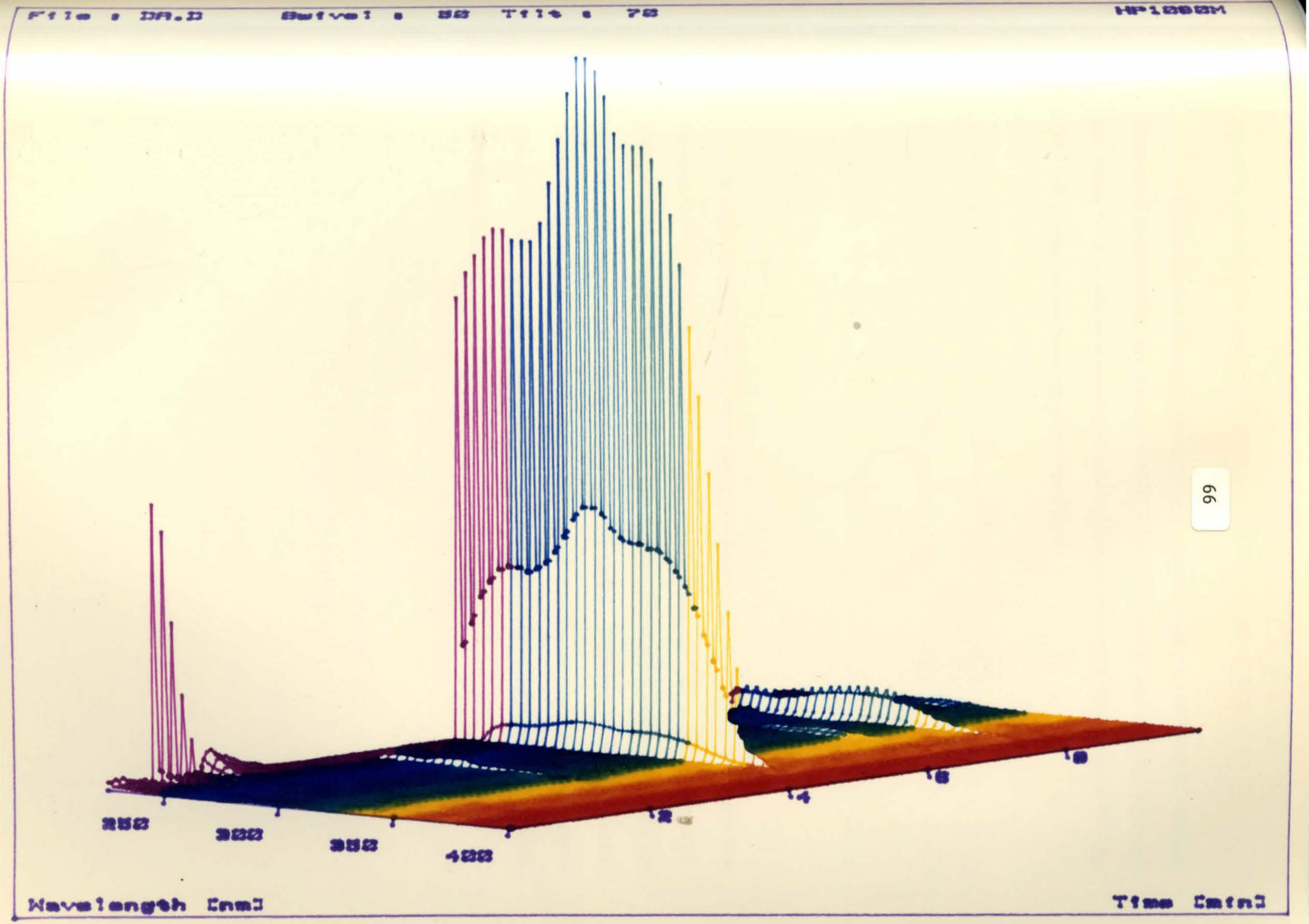
File : DA.D
Swivel : 50
Tilt : 70
HP1090M
250
300
350
400
2
4
6
8
Wavelength [nm]
Time [min]

1. Determination of the site of alkylation: At this stage we know that BD indeed does act as an electrophile and forms a covalent bond to adenine in duplex DNA. Although the proton NMR spectrum is consistent with covalent attachment at N3 of adenine,[78,79] the site of alkylation has not been rigorously elucidated.

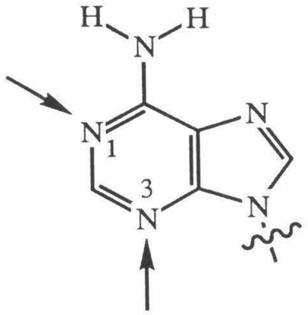

In order to unequivocally prove that the nucleophile of this reaction is nitrogen 3 of adenine, 3-[^{15}N]-adenine **19** (99% enriched) and N-bromo-[2-^{13}C]-acetyldistamycin **8** (99% enriched) were synthesized. If alkylation occurs at the N3 position we should see coupling through one ^{15}N-^{13}C bond, two spin 1/2 nuclei. Nitrogen 15 labeled adenine **19** was made in eight steps from imidazole by modification of established procedures (Scheme 2).[80-82] Carbon 13 labeled BD **8** was synthesized from the labeled TFA mixed anhydride **4**.

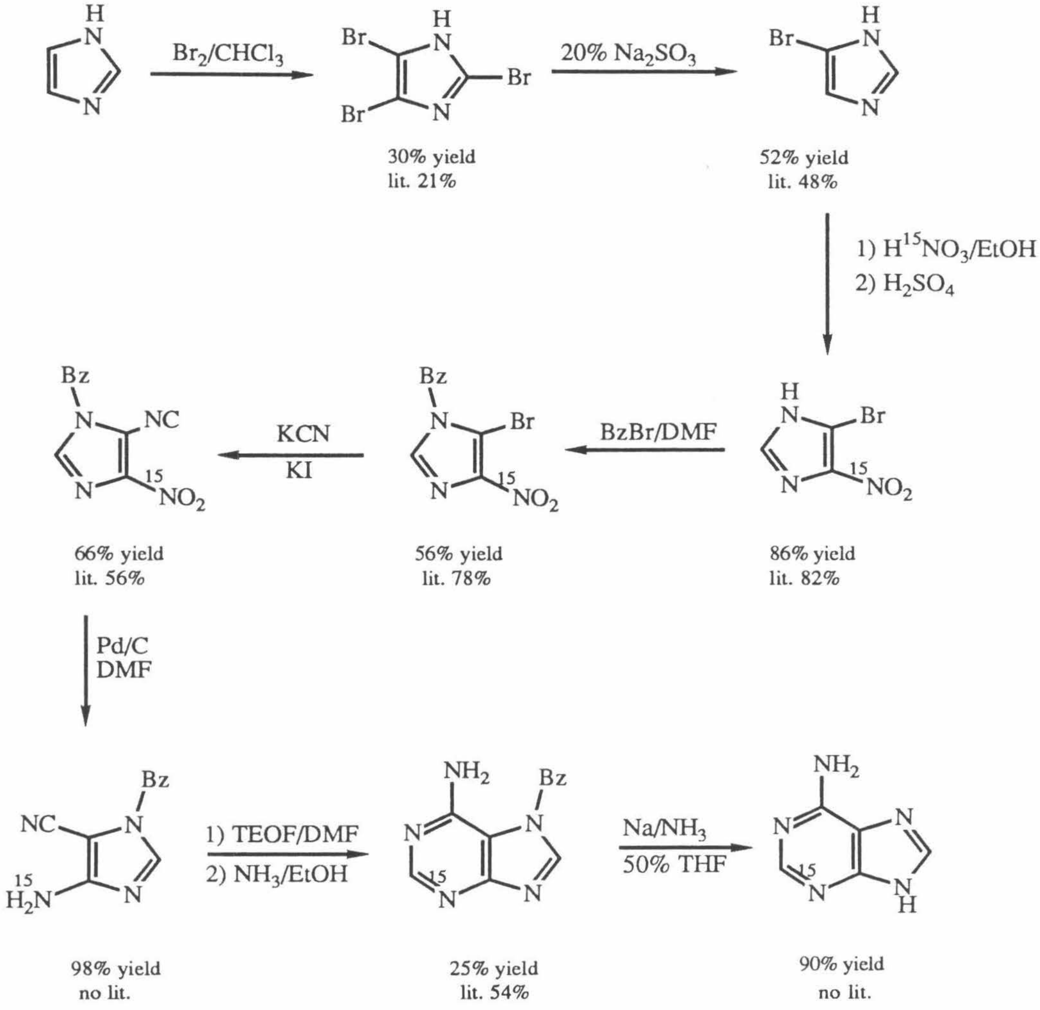
Br2/CHCl3
30% yield
lit. 21%
20% Na2SO3
52% yield
lit. 48%
1) H15NO3/EtOH
2) H2SO4
86% yield
lit. 82%
BzBr/DMF
56% yield
lit. 78%
KCN
KI
66% yield
lit. 56%
Pd/C
DMF
98% yield
no lit.
1) TEOF/DMF
2) NH3/EtOH
25% yield
lit. 54%
Na/NH3
50% THF
90% yield
no lit.

Scheme 2: Synthetic Scheme of [^{15}N3]-Adenine **19**.

Four isotopic combinations of distamycin-adenine **21** (DA) were synthesized, ^{12}C-^{14}N **21a**, ^{13}C-^{14}N **21b**, ^{12}C-^{15}N **21c**, and ^{13}C-^{15}N **21d** (Figure 18, proposed structure) and compared by proton, carbon, and nitrogen NMR. The proton spectra of the ^{15}N adducts provide the means to assign the C-2 and C-8 protons of the adenine (Figures 20 & 22). The C-2 proton appears at 8.31 ppm. A two bond coupling constant of 6.2 Hz is observed between it and the enriched nitrogen at position 3. This value is in good agreement with other two bond coupling constants observed for pyrrolic nitrogens and protons.[83,84] For example, the coupling constant of neat pyrrole measures as $^2J_{N\text{-}H} = 4.5$ Hz and that of N2 and H3 of 2-methylindazole measures as $^2J_{N\text{-}H} = 4.3$ Hz in dimethyl sulfoxide. These values are in contrast to two bond coupling constants of pyridinic nitrogens and protons. For example, the coupling constant for pyridine measures as $^2J_{N\text{-}H} = 11$ Hz in acetone,[83] that of N3-H2 of adenine measures as $^2J_{N\text{-}H} = 13$ Hz in D2O,[83] and that of N2-H3 of indazole as $^2J_{N\text{-}H} = 12.8$ Hz in dimethyl sulfoxide.[84] The C-8 proton of the distamycin-adenine adduct appears at 7.69 ppm. The difference between the two proton shifts of the alkylated adenine, C2 and C8, is 0.62 ppm. The acetyl methylene protons of the distamycin moiety shift downfield from 3.98 (BD) to 5.18 ppm upon alkylation. This assignment is verified by the proton spectra of the enriched ^{13}C compounds which show a splitting of the peak to a doublet, $^1J_{H\text{-}C}=142.8$ Hz (Figures 21 & 22). The characteristic peak assignments for the unlabeled adduct are given in Figure 23.

The nitrogen and carbon spectra of the three isotopically enriched compounds complement one another (Figures 24 & 25, respectively). The nitrogen spectra of the ^{12}C-^{15}N distamycin-adenine compound shows a singlet at -221.21 ppm. The double labelled compound shows a doublet at -221.51 with a one bond ^{15}N-^{13}C coupling constant of 11.0 Hz. In the ^{13}C spectra of the ^{13}C-^{14}N adduct we observe a singlet at 50.53 ppm. In the ^{13}C spectra of the ^{13}C-^{15}N adduct we observe a doublet at 50.55 ppm with $^1J_{C\text{-}N}=11.0$ Hz. These coupling constants are within the range of values observed for one bond coupling between carbon 13 and nitrogen 15.[84] For example, by carbon 13 NMR the coupling constant for 3-benzyladenine was measured as $^1J_{C\text{-}N} = 7.2$ Hz. These results firmly establish the site of alkylation of adenine by BD as N3.

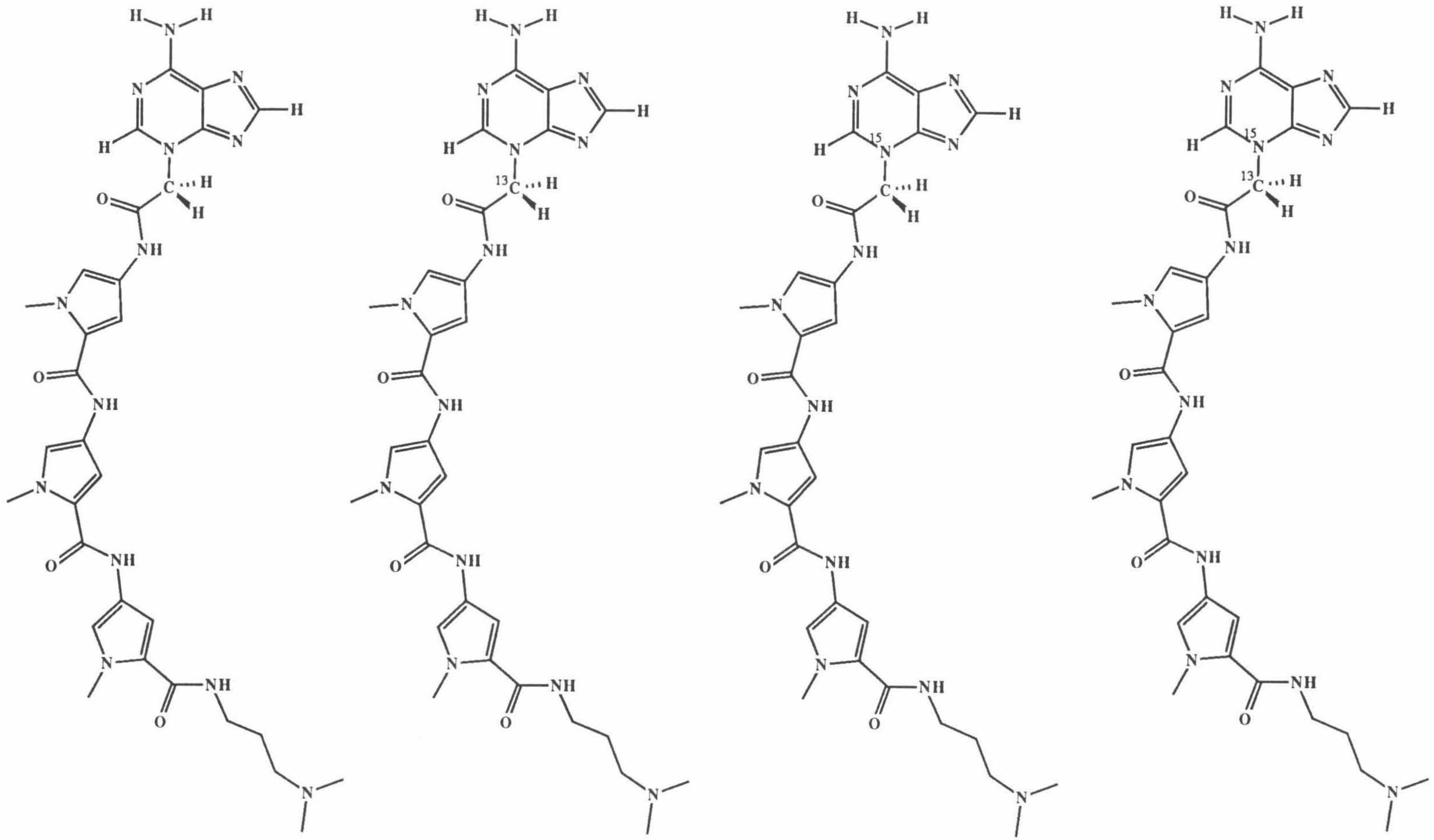

Figure 18: Synthetic Isotopically Labeled Distamycin-Adenine Adducts. Proposed Structures. (A) 3-(Acetyldistamycin)-adenine **21a**, (B) 3-([2-^{13}C]-Acetyldistamycin)-adenine **21b**, (C) 3-(Acetyldistamycin)-[^{15}N3]-adenine **21c**, and (D) 3-([2-^{13}C]-Acetyldistamycin)-[^{15}N3]-adenine **21d**.

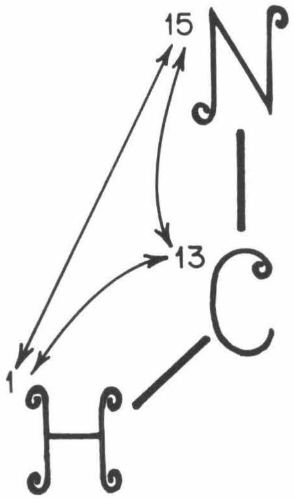
15
N
13
C
1
H

Proton Spectra of the Isotopically Labeled Adenine Adducts

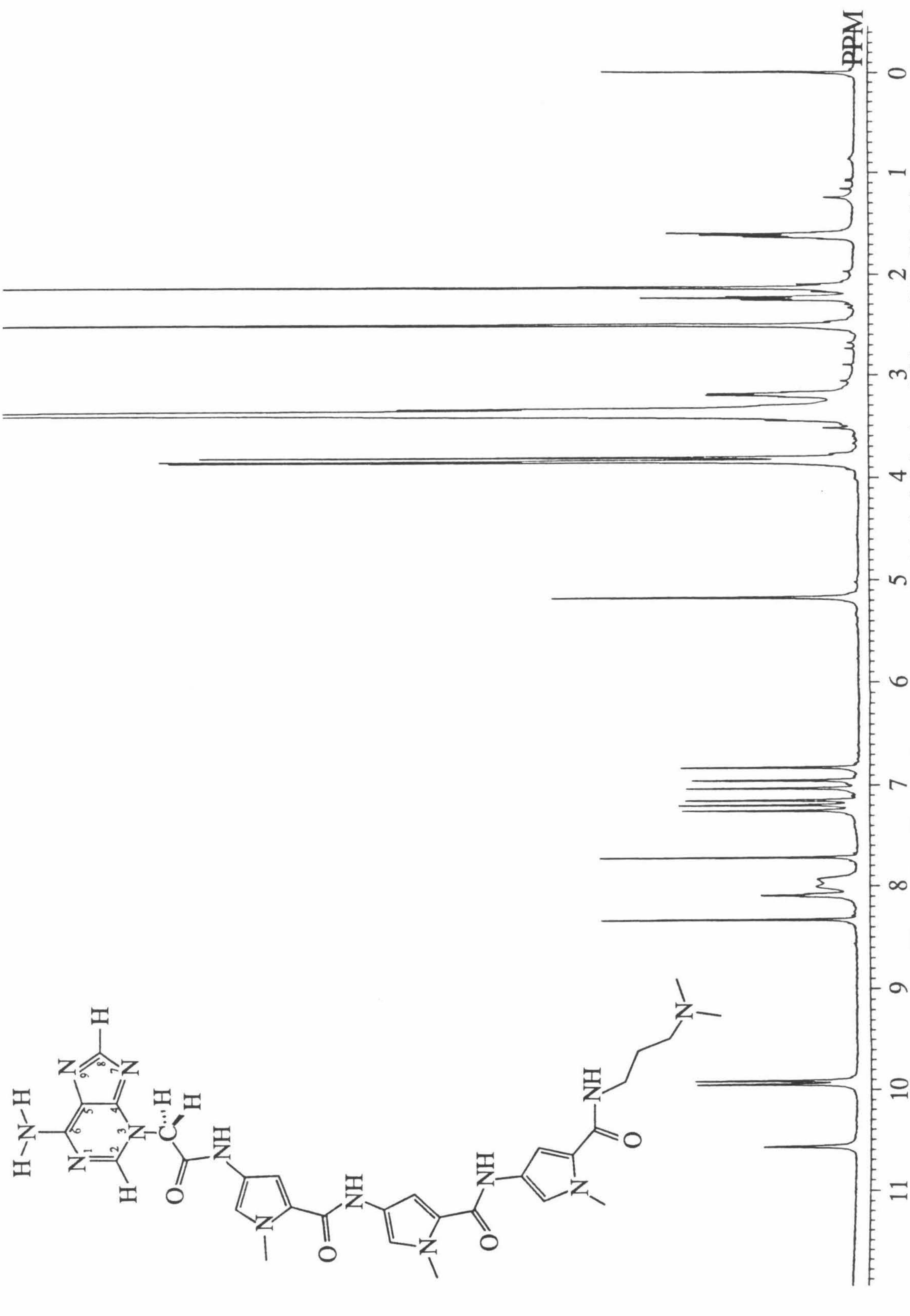

Figure 19: Proton Spectrum of the Unlabeled Adenine Adduct (Me$_2$SO-d$_6$).

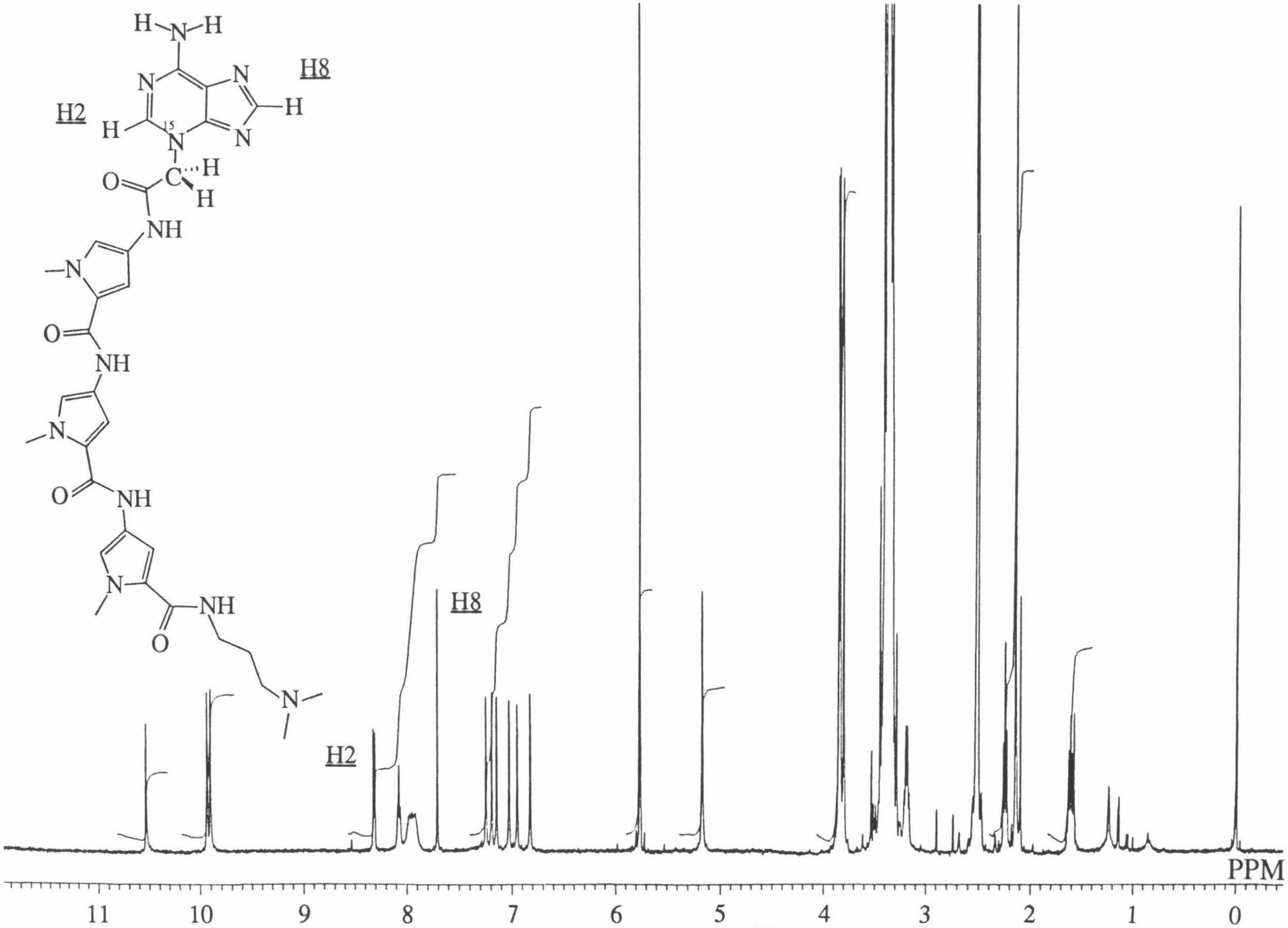

Figure 20: Proton Spectrum of the [^{12}C-^{15}N] Adenine Adduct (Me$_2$SO-d$_6$).

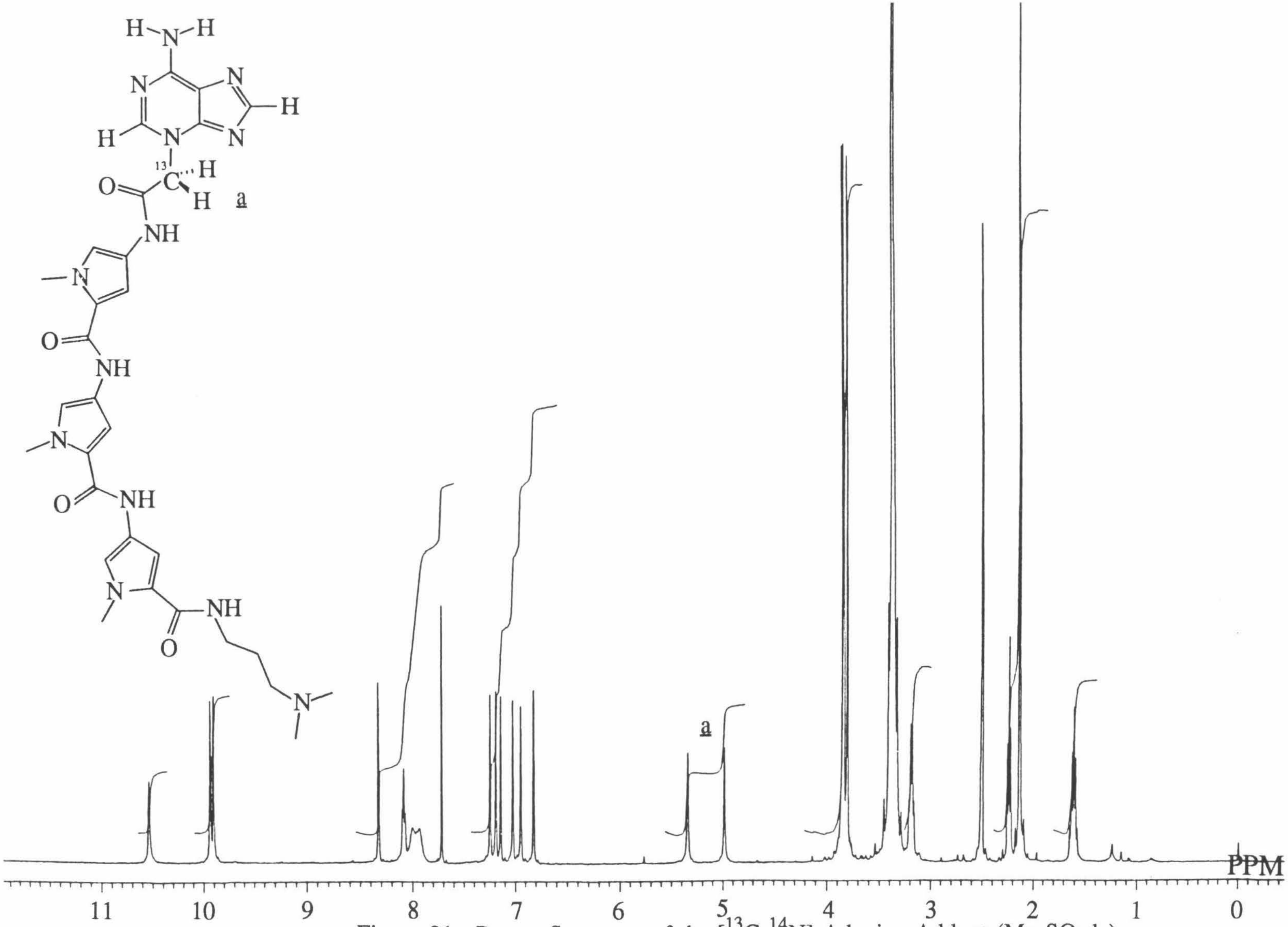

Figure 21: Proton Spectrum of the [^{13}C-^{14}N] Adenine Adduct (Me$_2$SO-d$_6$).

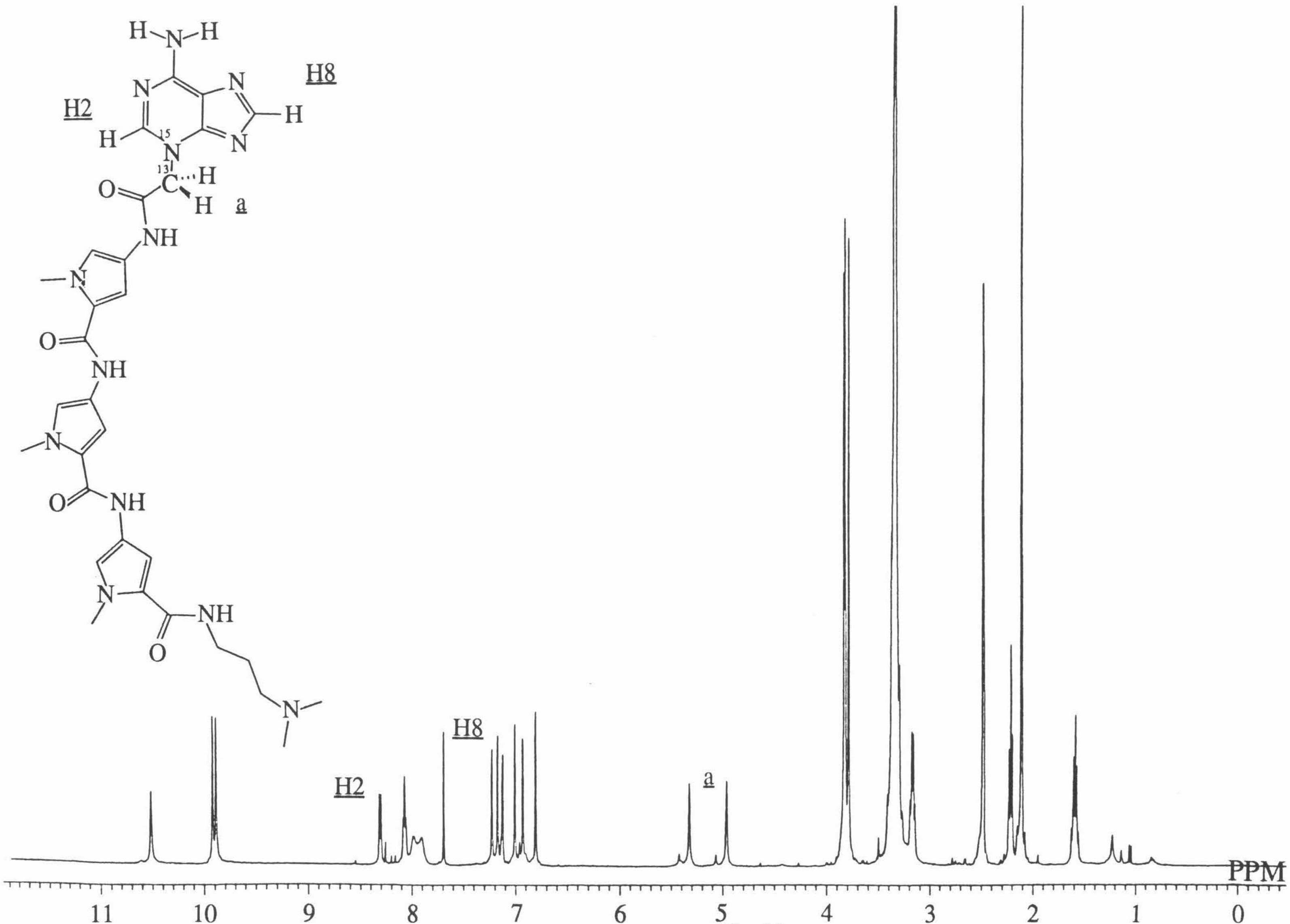

Figure 22: Proton Spectrum of the [^{13}C-^{15}N] Adenine Adduct (Me_2SO-d_6).

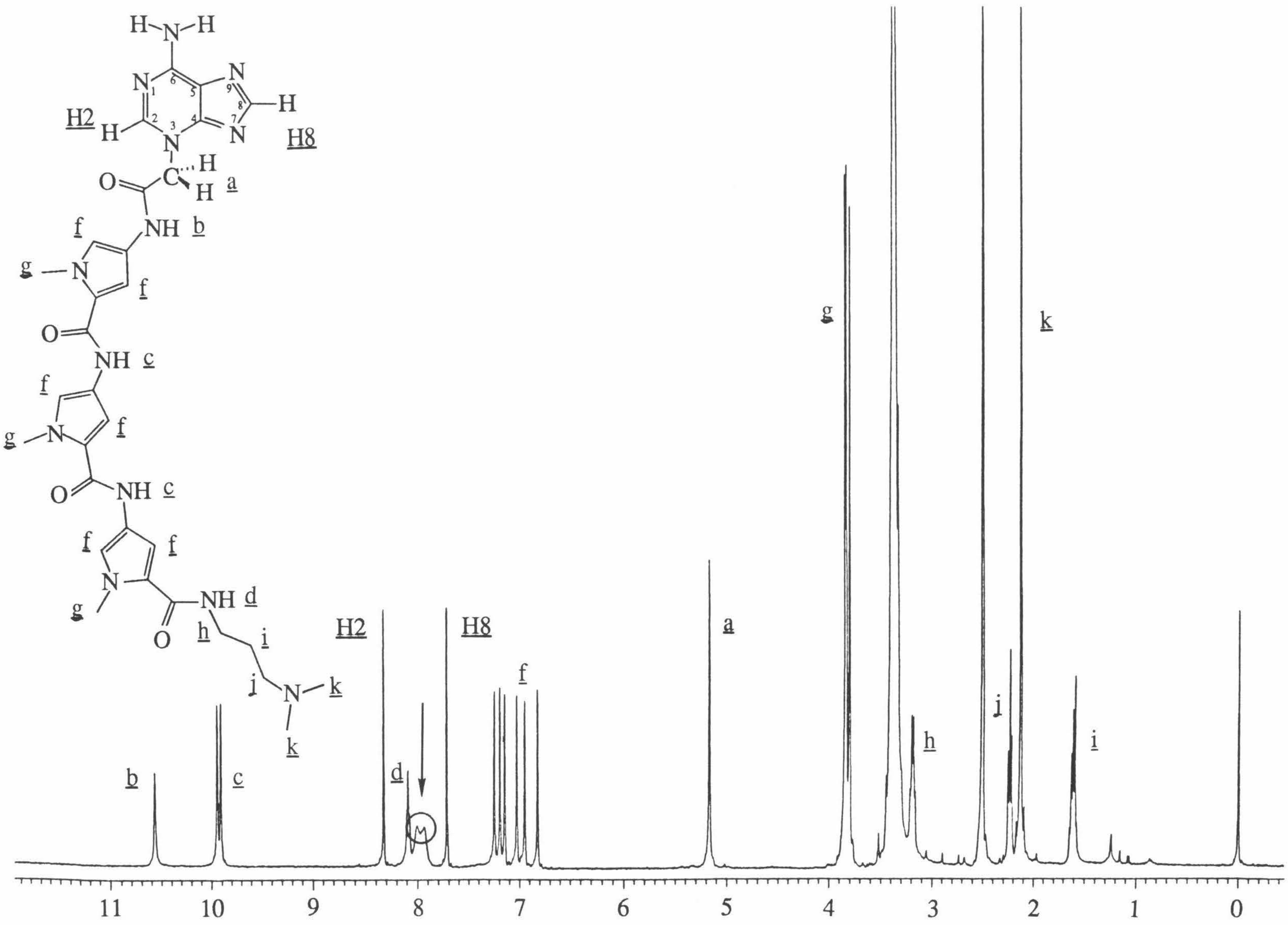

Figure 23: Proton Spectrum of the Unlabeled Adenine Adduct with the Pertinent Peak Assignmetns.

Nitrogen 15 Spectra
# of the
Isotopically
Labeled
Adenine Adducts

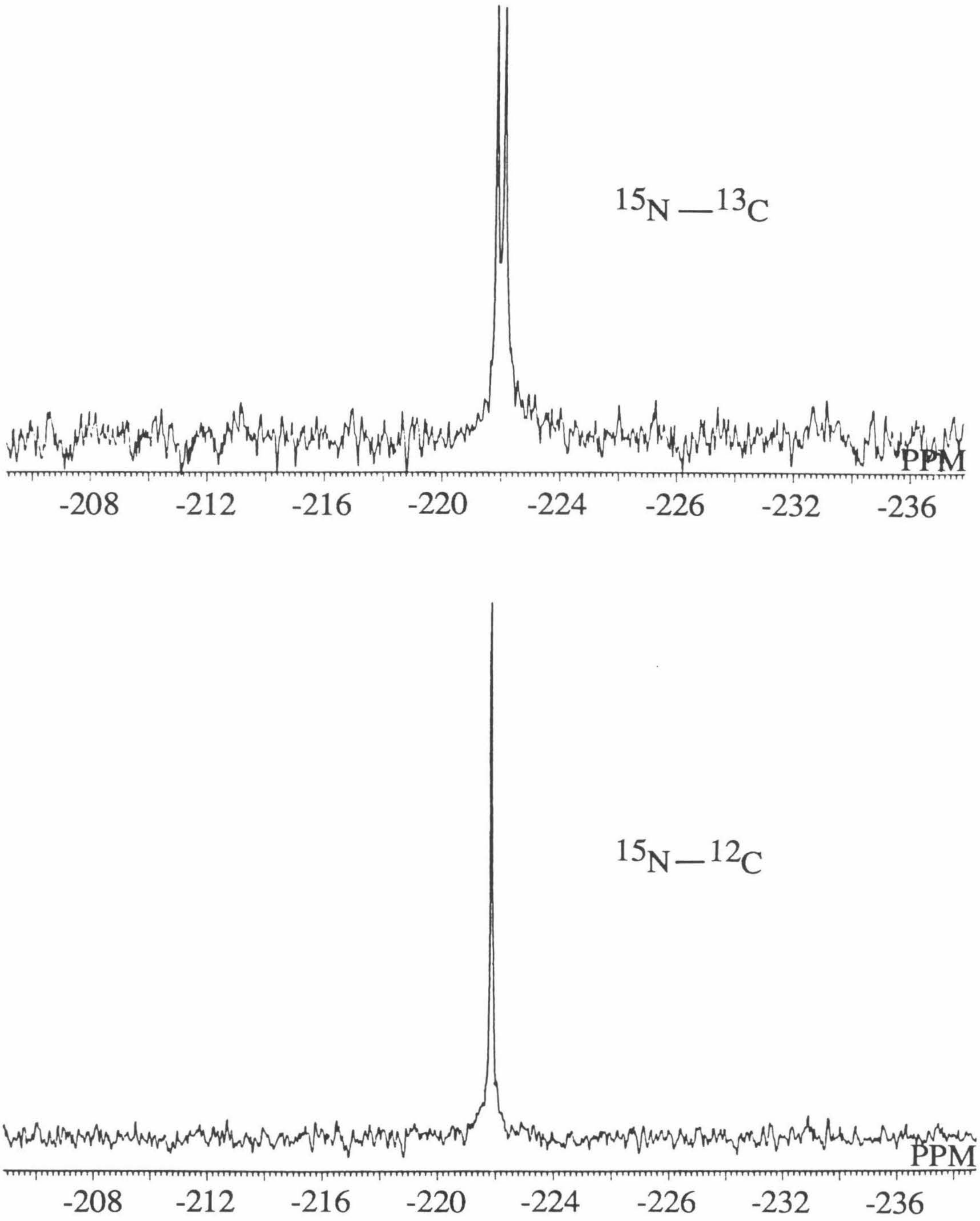

Figure 24: Nitrogen 15 Spectra of [^{13}C-^{15}N] and [^{12}C-^{15}N] 3-(Acetyldistamycin)-adenine.

Carbon 13 Spectra
# of the
Isotopically
Labeled
Adenine Adducts

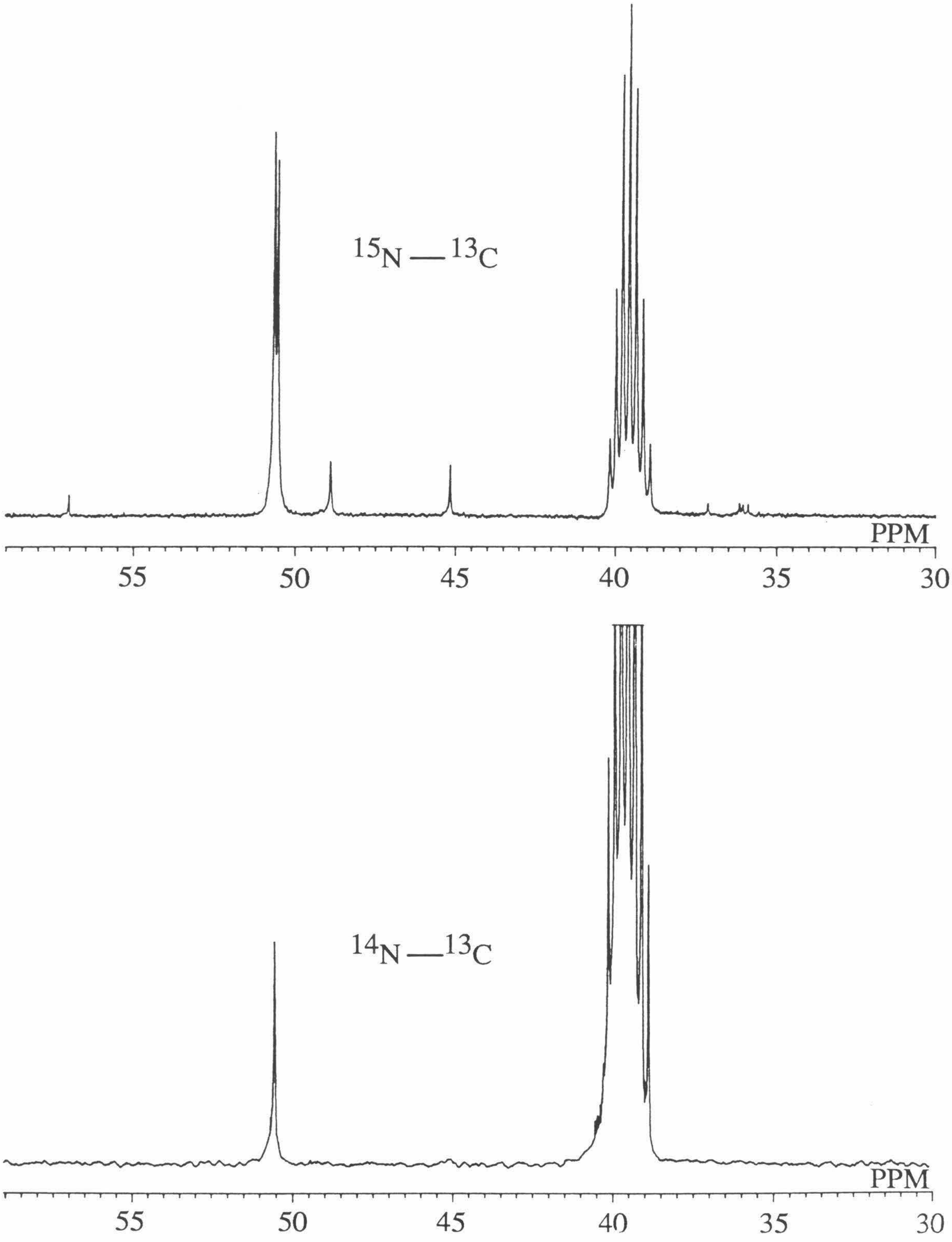

Figure 25: Carbon 13 Spectra of [^{13}C-^{14}N] and [13C-15N] 3-(Acetyldistamycin)-adenine.

2. Determination of the Tautomer of the Distamycin-Adenine Adduct (Amine *vs.* Imine): Two broad singlets, each equivalent to one proton at 8.02 and 7.95 ppm, appear in the proton spectra of 3-(Acetyldistamycin)-adenine (Figure 23). The basis of these signals are ambiguous and several inferences can be made about this result. Either (1) the spectrum represents the imino tautomer where the two protons are associated with different nitrogens, one with the exocyclic nitrogen, N6, and the other with the imidazole nitrogens, N7 or N9,[85-87] or (2) both protons are bonded to N6 as the amine, but they are nonequivalent and exist in two different chemical environments. This latter situation would be indicative of a barrier to rotation around the nitrogen carbon bond caused by resonance[88,89] or self base pairing.[90]

[6-^{15}N]Adenine **20** (99% enriched) was synthesized in order to unequivocally determine the number of protons attached to the exocyclic nitrogen (N6), *i.e.*, determine the tautomeric species of the adduct (Figure 26). By nitrogen 15 NMR, the imino form, which has one proton, will display a doublet (from ^{15}NH) and the amino form, which has two protons, will display a triplet (from $^{15}NH_2$). The labeled base was synthesized by nucleophilic aromatic substitution of the chloride substituent of 6-chloropurine with ^{15}N-benzylamine, followed by oxidative deprotection of the amine with ruthenium oxide and sodium periodate (Scheme 3).[91-93] With this compound in hand 3-(acetyldistamycin)-[^{15}N6]-adenine **21e** was synthesized by the method previously described (Figure 27).

The nitrogen 15 spectra of the labeled distamycin-adenine adduct displays a *triplet* at -282 ppm with a one bond coupling constant of 90.9 Hz (Figure 28). This signal is evidence for two protons bonded to the exocyclic nitrogen. The coupling constant is of the same magnitude as those of exocyclic amines of analogous heterocycles. For example, for adenine $^1J_{N\text{-}H}$ = 90 Hz (this thesis), for 1-methylcytosine $^1J_{N\text{-}H}$ = 90 Hz,[88,89] and for 5-azacytidine $^1J_{N\text{-}H}$ = 91 Hz.[89] Therefore, the adduct is in the amino form.

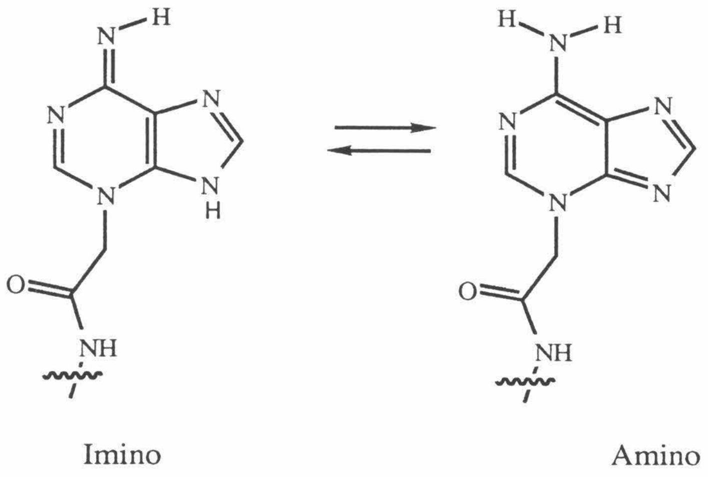
Imino
Amino

Figure 26: Tautomer: Imino *vs*. Amino.

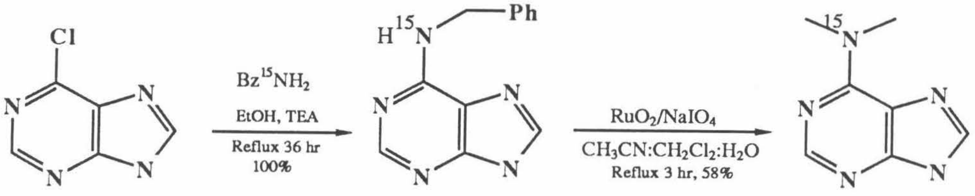
Cl
Bz^{15}NH$_2$
EtOH, TEA
Reflux 36 hr
100%
RuO$_2$/NaIO$_4$
CH$_3$CN:CH$_2$Cl$_2$:H$_2$O
Reflux 3 hr, 58%
Ph

Scheme 3: Synthetic Scheme of [^{15}N6]-Adenine **20**.

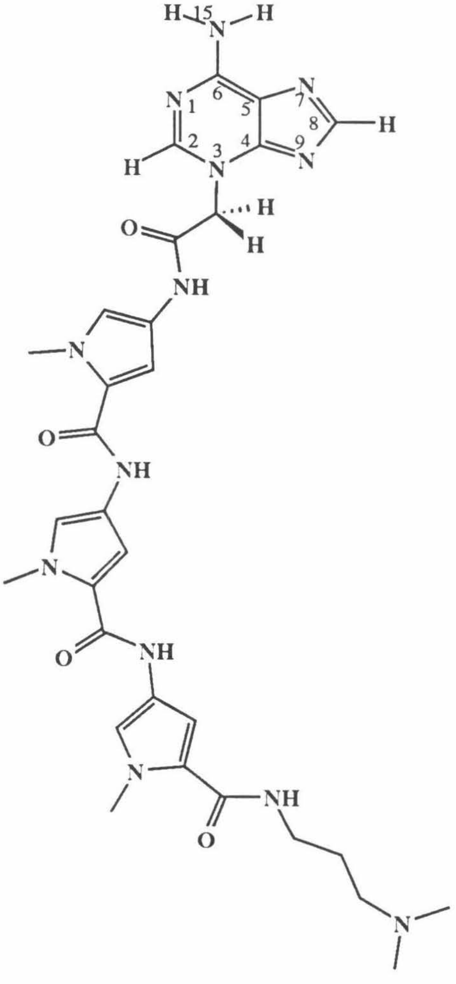

Figure 27: 3-(Acetyldistamycin)-[^{15}N6]-adenine **21e**.

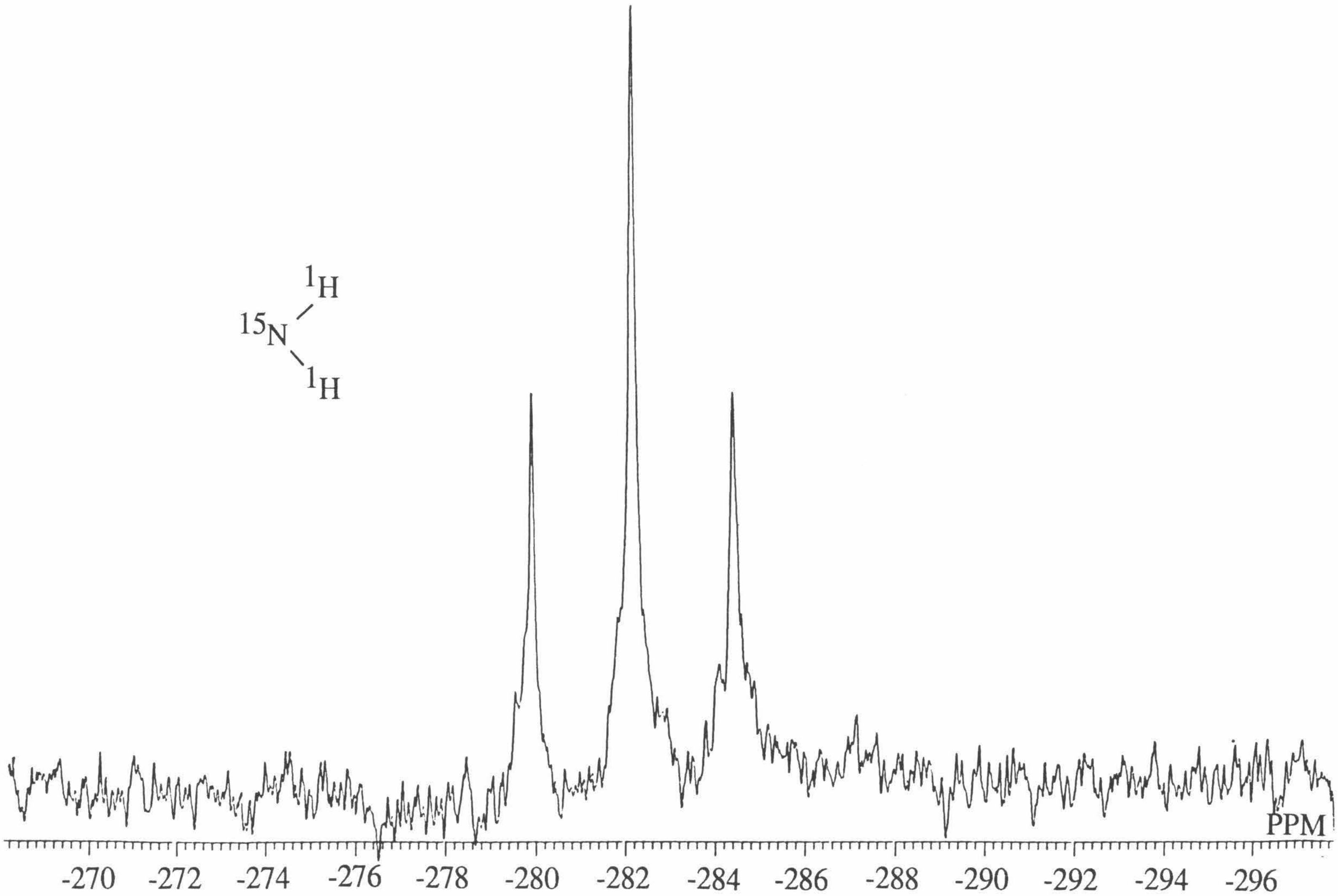

Figure 28: Nitrogen 15 Spectrum of 3-(Acetyldistamycin)-[^{15}N6]-adenine.

To unravel the mechanism of nonequivalence observed in the proton spectra, that is a barrier to bond rotation by resonance or self base pairing (Figure 29), the dependence of concentration on chemical shifts was examined (Figure 30). The proton spectra of the ^{15}N labeled adenine adduct at relatively high concentrations (130 mM) shows a pair of doublets or quartet. As the concentration is decreased the peaks coalesce. At 2.5 mM a single doublet with a N-H coupling constant of 90.2 Hz is observed indicating that the protons are equivalent. The results at low concentrations demonstrate that alkylation at the N3 site of adenine by BD does not create a barrier of rotation around the C-N exocyclic bond. The protons are nonequivalent at high concentrations not because of base stacking (this would alter the chemical shifts of H2 and H8), but because of self base pairing as observed in crystal structures of similar compounds, adenine, 9-methyladenine, and deoxyadenosine.[90]

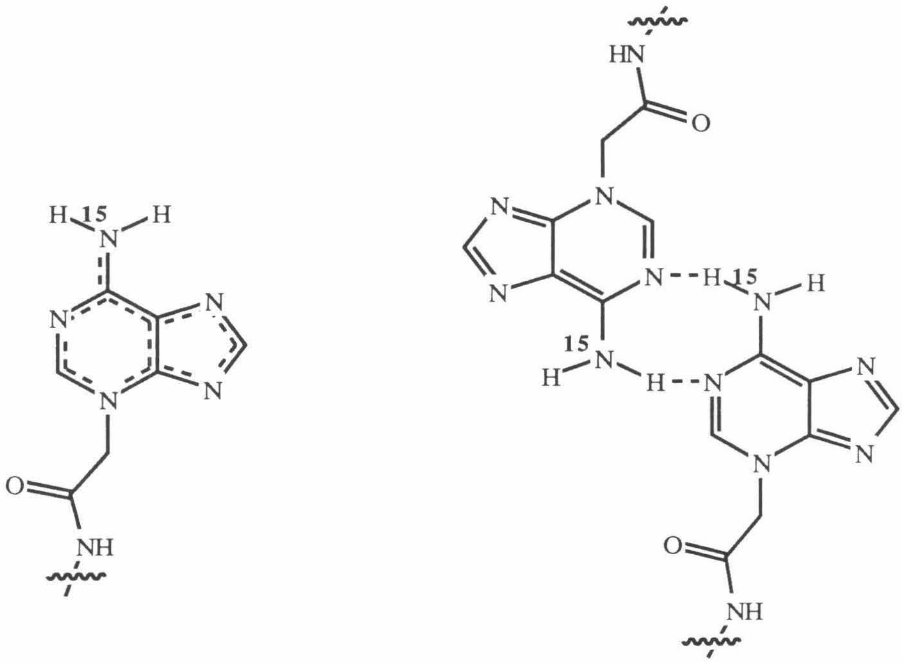

Figure 29: Resonance *vs*. Self Base Pairing.

Figure 30: Proton Spectra of 3-(Acetyldistamycin)-[^{15}N6]-adenine from 130 mM (self base pairing) to 2.5 mM (free rotation).

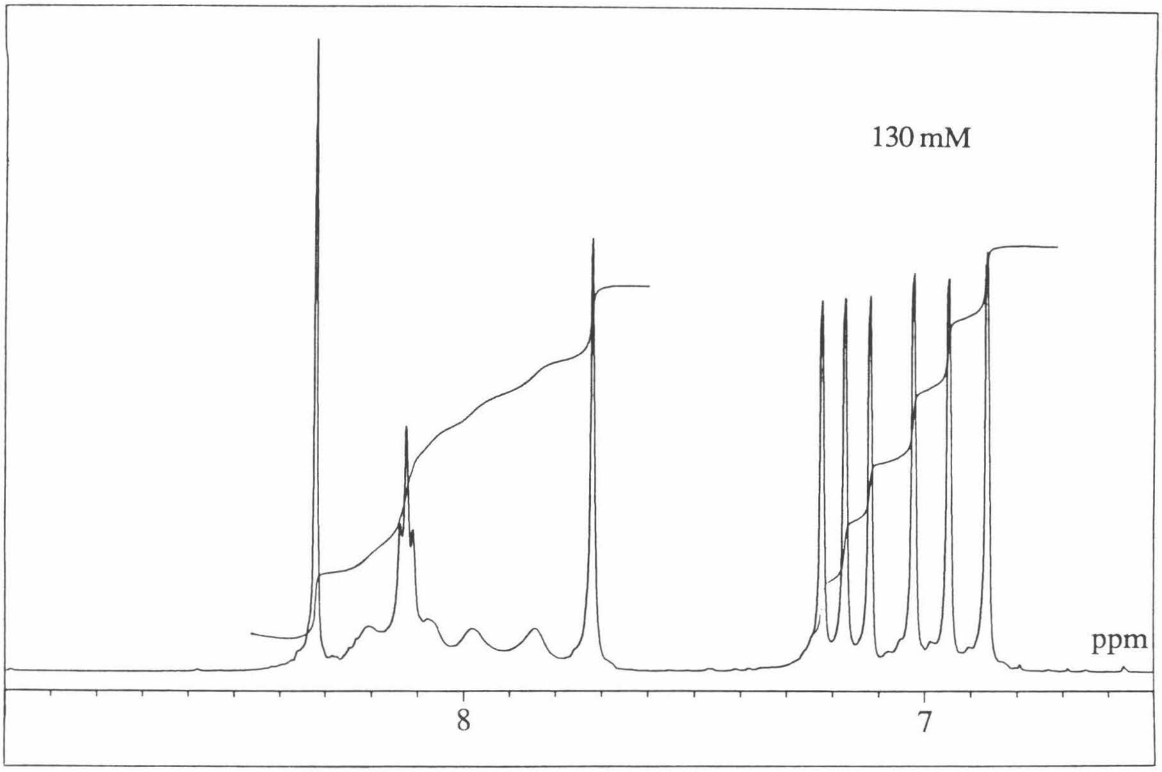
130 mM
ppm
8
7

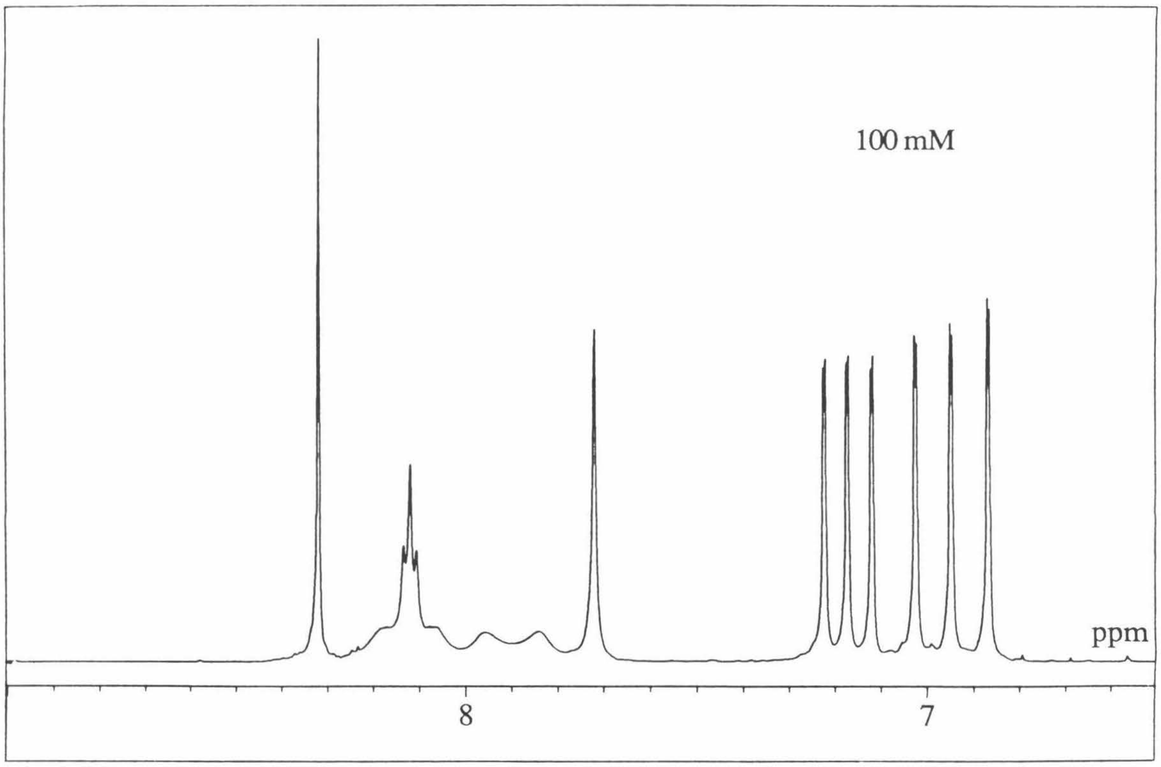
100 mM
ppm
8
7

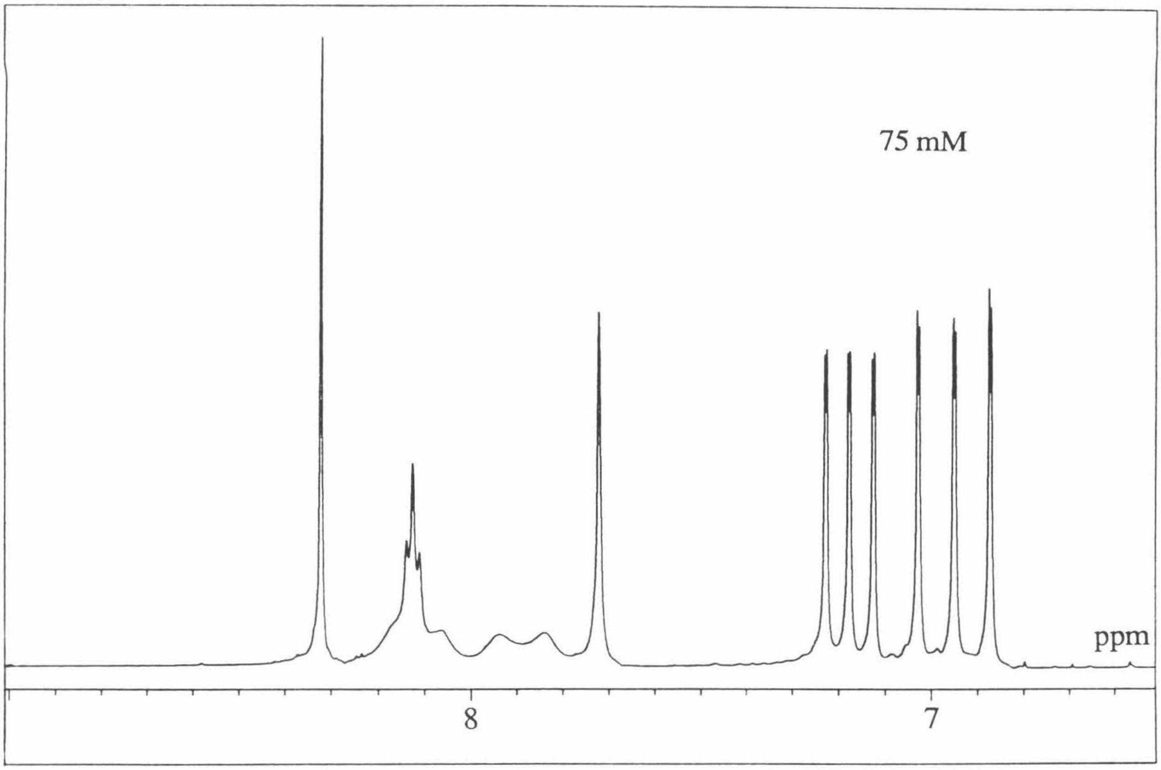
75 mM
ppm
8
7

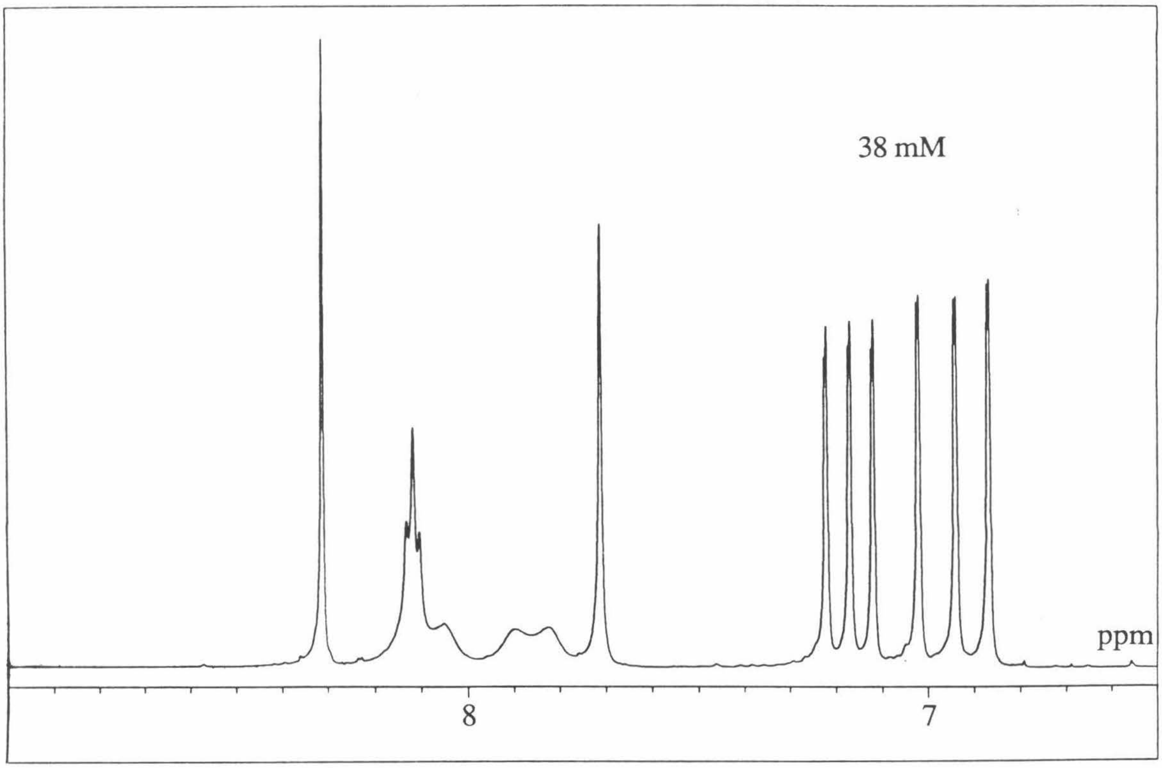
38 mM
ppm
8
7

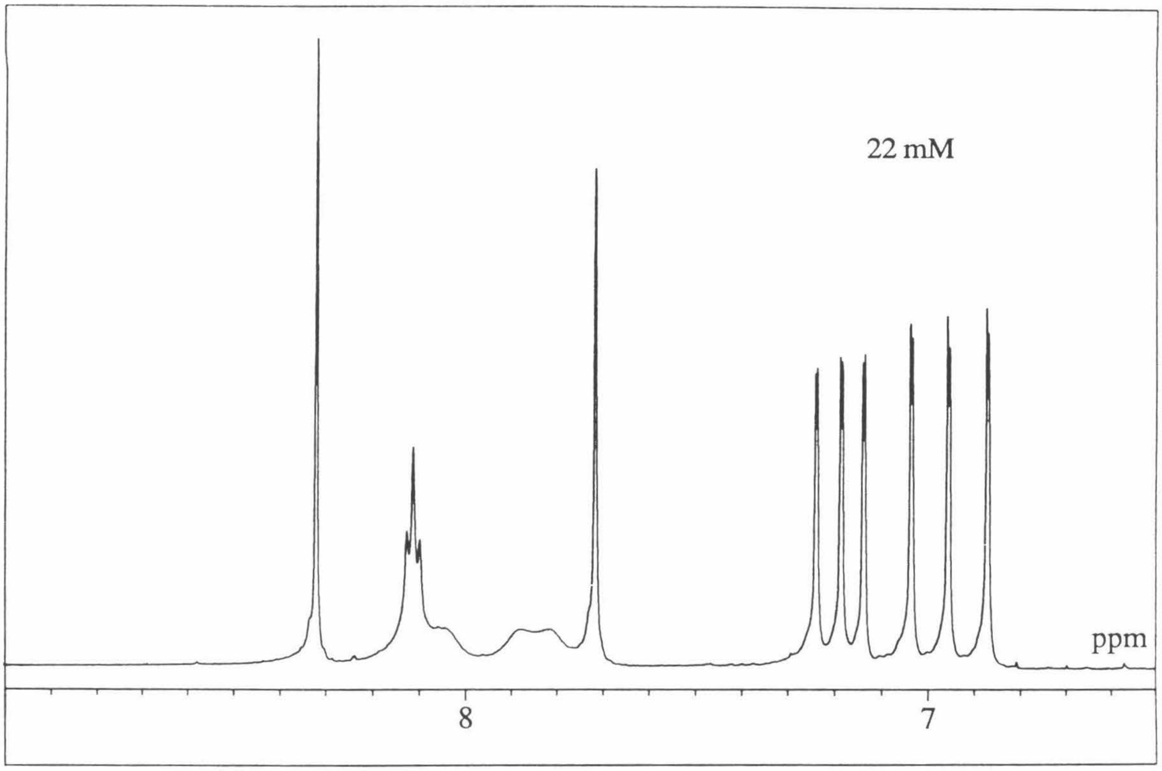
22 mM
ppm
8
7

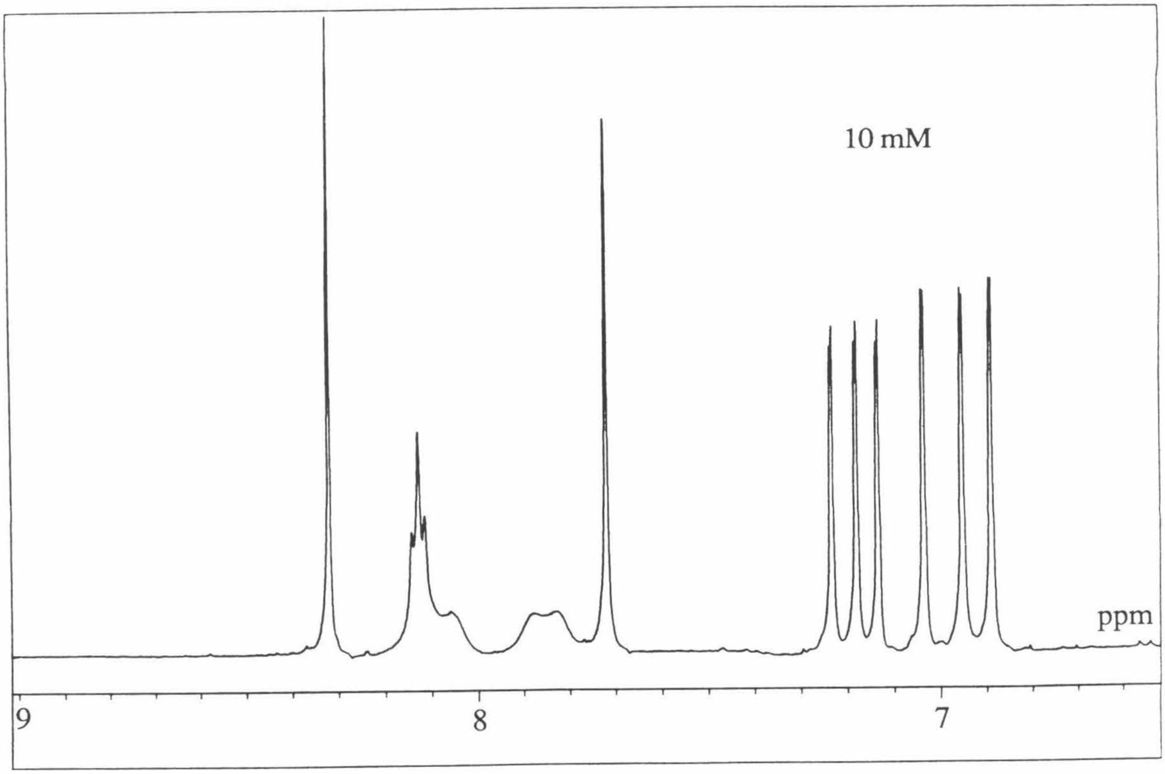
10 mM
ppm
9
8
7

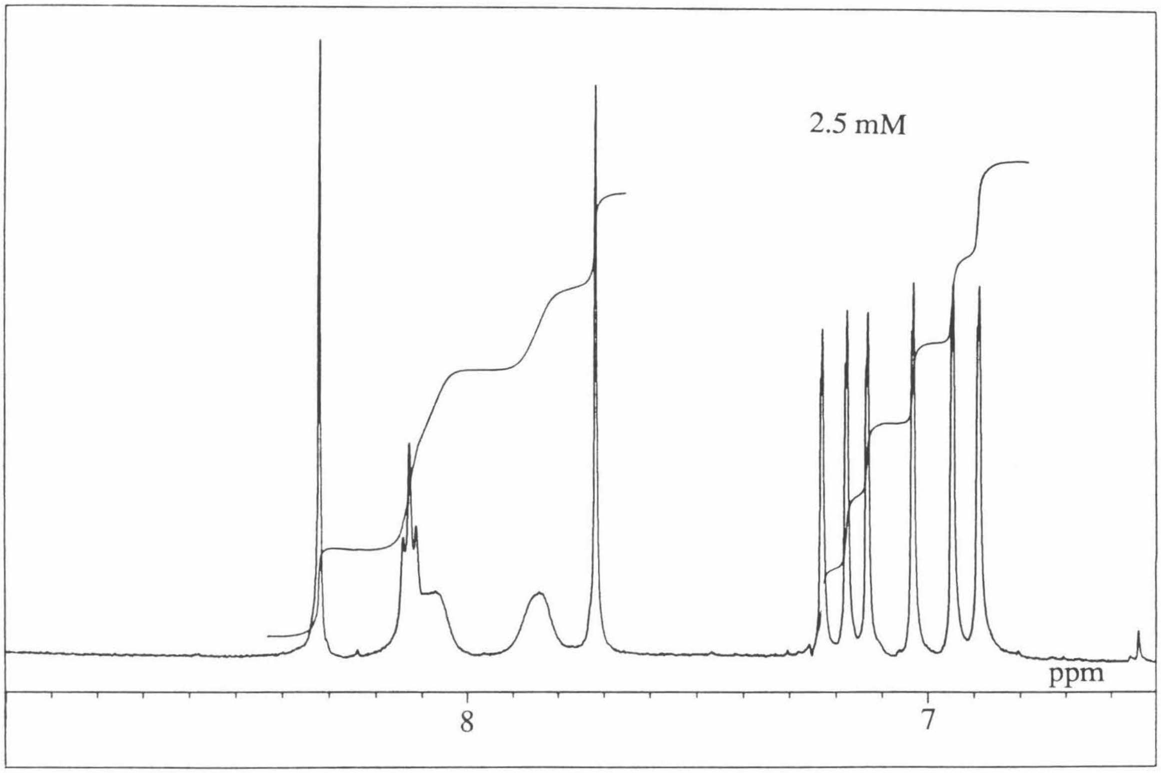

FREE ROTATION

Peak Assignment of the Carbon 13 Spectrum: A common point of reference for product characterization of alkylated purines is the carbon 13 spectrum, specifically the peaks corresponding to the five aromatic ring carbons. This method was utilized by Hurley and coworkers to establish the site of alkylation for CC1065 on adenine.[38] For comparative purposes and attainment of a complete picture the same has been done for the BD adduct. However, due to the complexity of the spectrum of 3-(acetyldistamycin)-adenine, a simplified model adduct (Figure 31) was synthesized. The purpose was to exclude the aromatic pyrrole carbons which overlap with those of the purine. Verification that the model compound 3-(N-acetyl-N'N'-dimethyl-1,3-propane diamine)-adenine **23** (or the acronym DOA) is an N3 adenine adduct lies in its proton spectrum, specifically in the difference of chemical shift for the protons at the 2 and 8 positions of the adenine moiety, $\Delta\delta = 0.51$.[78,79,84]

Assignment of the alkyl substituent carbons is relatively straightforward, through analysis of the splitting patterns (number of attached protons) and chemical shifts (adjacent atoms) which are given in the proton coupled spectrum (Figure 32).

Also, in the coupled spectrum, the C2 and C8 carbons of the purine are distinguishable as doublets. There are discrepencies in the literature, though, as to the peak assignment for these two, specifically between those given for CC1065 and those given for 3-butyladenine.[78] To differentiate the two carbons of the model adduct, DOA, their respective protons were selectively decoupled (Figure 33).[95] This technique was feasible because of the previous peak assignments made for these protons in the N15 experiments (recall the two bond coupling between H2 and N3). Selective irradiation at the resonance frequency corresponding to H2 causes a collapse of the C2 doublet to a singlet in the otherwise proton coupled spectrum. This transformation occurs at 144.4 ppm. Irradiation at the H8 frequency does the same at 151.8 ppm. Therefore, the shift for C2 is 144.4 and that for C8 is 151.8. The chemical shifts for CC1065 are reported as 153.6 ppm for C2 and 144.4 for C8 (Table 2).[38] Thus there appears to be a misassignment of C2 and C8 in the CC1065-adenine adduct as reported in the literature. Their method of assignment was limited to the INEPT and DEPT pulse sequences which will not differentiate between C2 and C8. It is curious that the chemical shifts of the proton spectrum of CC1065, which were sent to us by Hurley in a preprint, do not correspond to those of an N3 adduct (Figure 34, Table 3). Proton shifts are relatively insensitive to solvent, especially between similar aprotic solvents, such as DMF and DMSO. There are routes to rearrangement of adenine benzylated at the 3 position to one benzylated at the 6 position under autoclaving conditions,[96] and thus potentially under inappropriate storage conditions. However, misassignments have occurred before, such as with Mitomycin C,[70] and can make a significant impact on our understanding of the mechanism of action of these compounds with DNA. In this case (as with BD) nitrogen 15 NMR would elucidate the absolute configuration of the CC1065 adenine adduct.

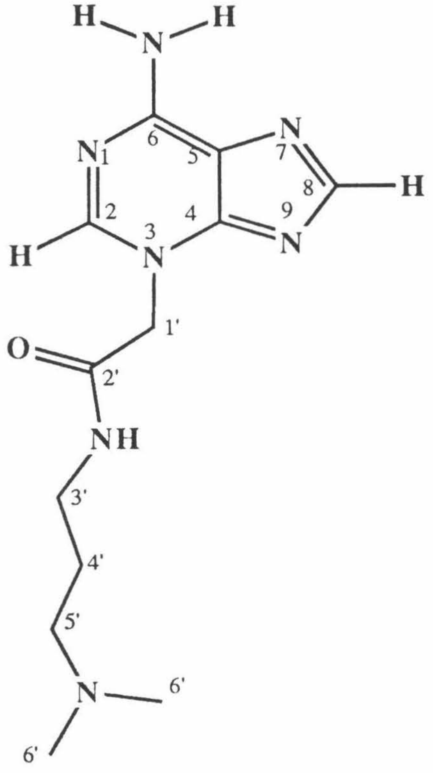

Figure 31: 3-(N-Acetyl-N'N'-dimethyl-1,3-propane diamine)-adenine **23** (DOA).

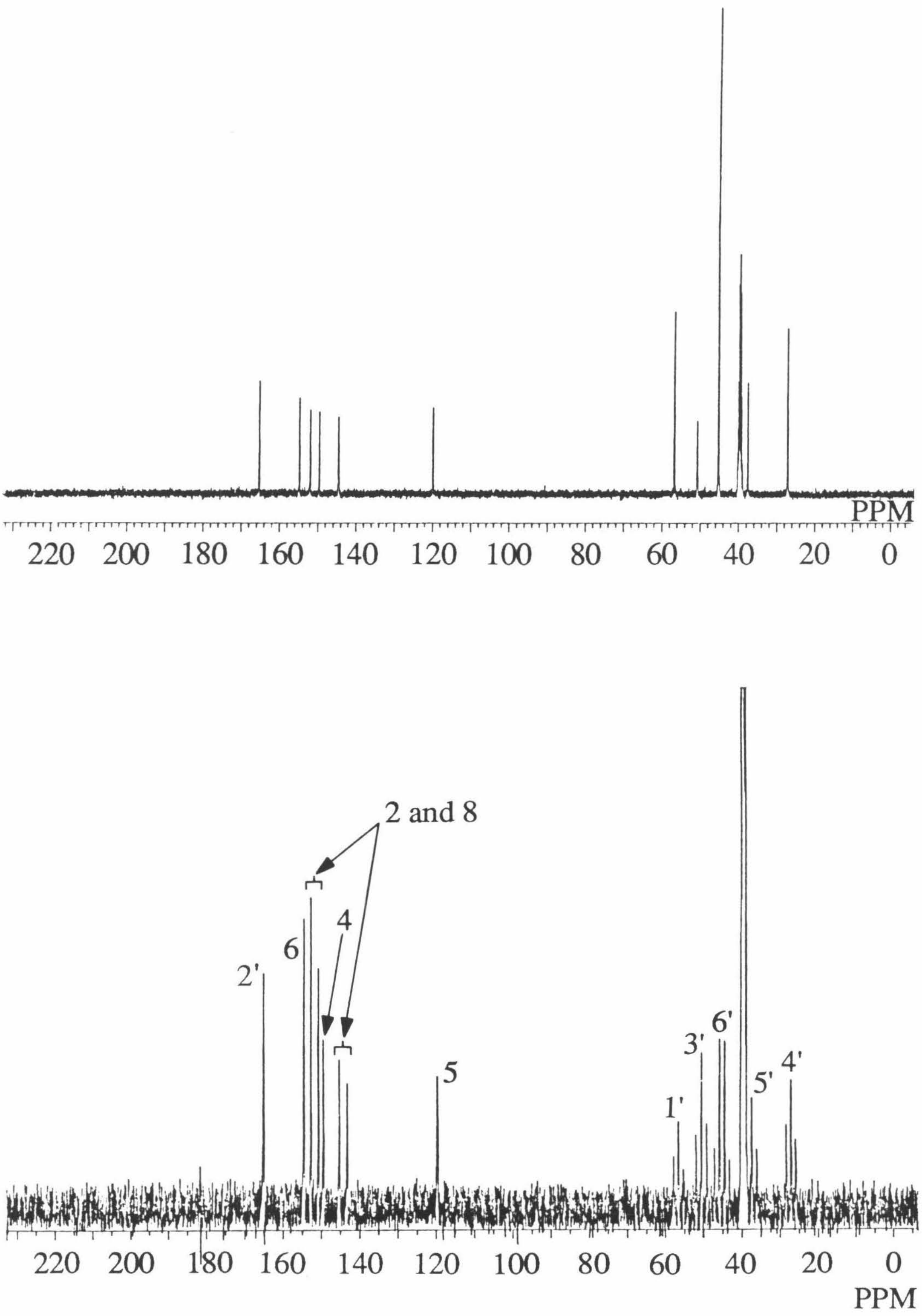

Figure 32: Proton decoupled carbon 13 spectrum of DOA (top). Proton coupled carbon 13 spectrum of DOA (bottom).

Figure 33: Proton Selective Decoupling to assign the Carbon 13 peaks of C2 and C8 in the Adenine Moiety of DOA. Panel A) Control, uncoupled spectra, Panel B) Selective decoupling of the proton at the 8 position, and Panel C) Selective decoupling of the proton at the 2 position.

A

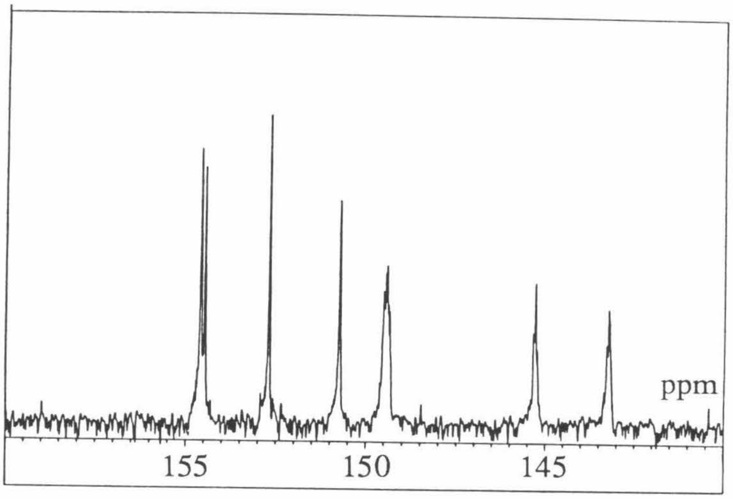

B

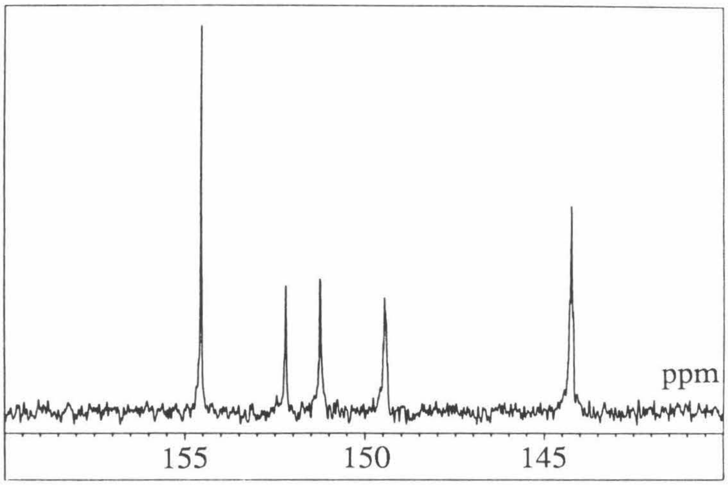

C

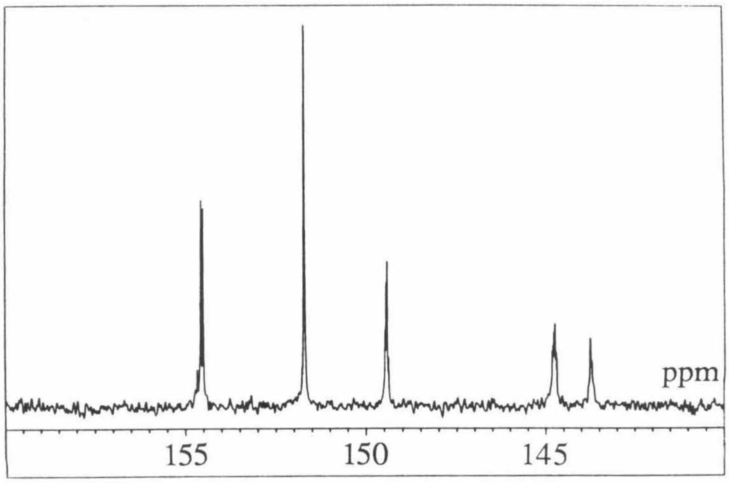

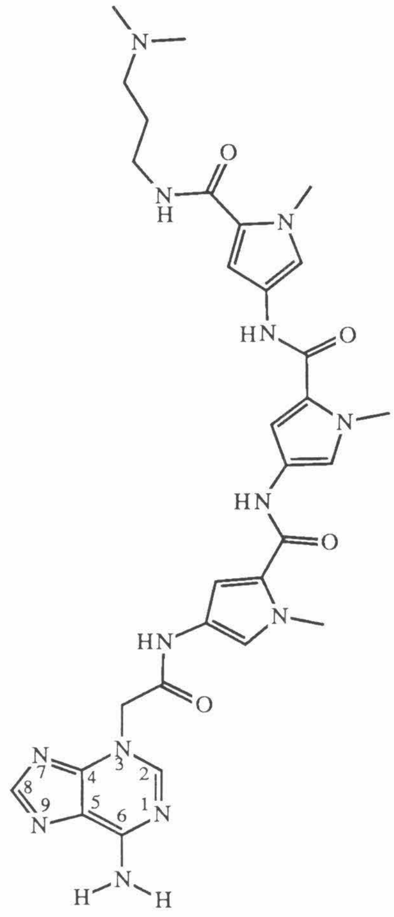

I

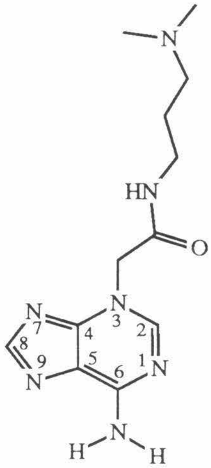

II

Figure 34a: Assigned N3 adenine adducts of I) N-Bromoacetyldistamycin and II) N-(Bromoacetyl)-N'N'-dimethyl-1,3-propanediamine.

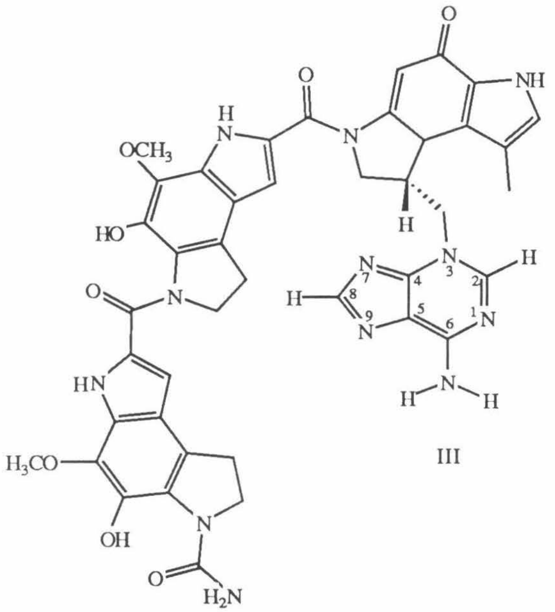

III

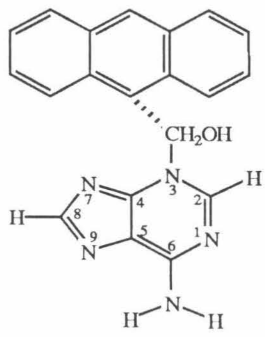

IV

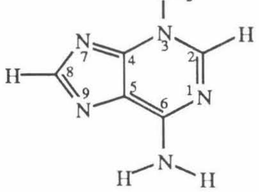

V

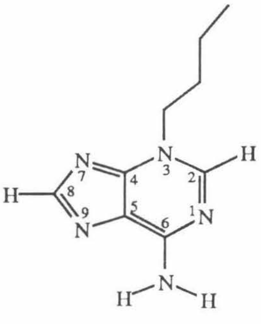

VI

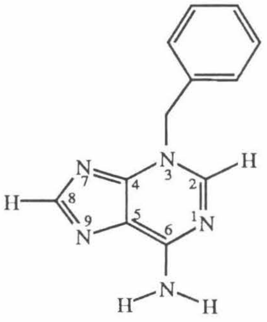

VII

Figure 34b: Assigned N3 adenine adducts of III) CC1065,[38] IV) 9-anthryloxirane,[79] V) methyltoluenesulfonate,[78] VI) butylbromide,[78] VII) benzylbromide.[78]

Table 2: Carbon 13 Spectral Assignments for Adenine derivatives and N3 adducts.

Compound	C2	C4	C5	C6	C8	Solvent	Method	Ref.
Adenine	152.4	151.3	117.5	155.3	139.3	DMSO		86
Adenosine	152.2	149.0	119.0	156.0	139.8	DMSO		97
II	144.4	149.5	119.7	154.6	151.8	DMSO	a	d
III	153.6	151.5	121.5	155.9	144.4	DMF	b	38
VI	143.7	150.0	120.8	155.3	152.8	DMSO	c	78

(a) H1 Selective Decoupling, (b) INEPT and DEPT, (c) H1 Selective Decoupling, Br-C8, (d) this thesis.

Table 3: Proton (H2 and H8) Spectral Assignments for N3 Adenine Adducts.

Adduct	H2	H8	Solvent	Ref.
I	8.31	7.69	DMSO	a
II	8.25	7.73	DMSO	a
III	7.80	8.06	DMF	98
IV	8.44	7.82	$CDCl_3$	79
V	8.27	7.77	DMSO	78
VI	8.37	7.78	DMSO	78
VII	8.60	7.80	DMSO	78

(a) this thesis

G. DNA Product Analysis: To complete the elucidation of the type of mechanism by which BD cleaves the phosphodiester backbone the DNA products *at each stage of the reaction and workup procedure* were monitored and characterized by their gel electrophoretic mobilities. Analysis was carried out on the 15 base pair duplex, 5'-CGGTAGTTTATCACA-3'. Recall, this sequence corresponds to the binding site and flanking sequences of the 167 b.p. restriction fragment in which the major cleavage site, base pair #48, is located. Only products of the cleaved strand were monitored. This strand, labeled either at the 3' or 5' end, was analyzed by 20% polyacrylamide gel electrophoresis (Figure 35, Panel A -- 3' Label, Panel B -- 5' Label).

A one to one mixture of the 15mer and BD (10 uM each) in 100 mM Na Phosphate buffer (pH 7.0) was incubated at 37° C for zero (lanes 1-5) and twenty-four hours (lanes 6-10). Aliquots for gel analysis were removed at each of the following consecutive steps, 1) incubation, lanes 1 and 6, 2) heat, 15 minutes at 90° C, lanes 2 and 7, 3) 1M piperidine, 5 minutes at room temperature, lanes 3 and 8, 4) 1M piperidine, 15 minutes at 90° C, lanes 4 and 9, and 5)1M piperidine, 30 minutes at 90° C, lanes 5 and 10. In so doing many of the intermediate DNA products that preceed and lead to the final 3' and 5' phosphate functional groups at the termini of the two new fragments where cleavage of the backbone occurs were trapped and visualized.

Two products are distinguishable from the 3' labeled oligo (analysis of the 5' termini) immediately following the 24 hour time period at 37° C (Panel A, lane 6). The slow migrating band corresponds to the strand with the acetyldistamycin covalently attached to it. The additional molecular weight, change of shape, and/or more electropositive character slows the migration rate of the macromolecule. This assignment has been verified by detection of carbon 14 in the band after reacting the 15mer with C14 labeled BD. The middle band migrates at a rate corresponding to 15 base pairs. This band might also include depurinated oligonucleotide. The fastest migrating band is a 6mer, the cleaved product. Heating the reaction at 90° C for 15 minutes almost completes depurination and cleavage of the strand by β-elimination (lane 7). Completion of cleavage requires piperidine and heat (lanes 9,10).

The 5' labeled strand (analysis of the 3' termini) shows three distinct products following a 24 hour reaction time (Panel B, lane 6). Again the slowest moving band corresponds to the 15mer plus acetyldistamycin. The strong band is the 15mer. The first, *i.e.,* slowest, faint band is believed to be an eight base strand plus the sugar remaining after the β-elimination step. And, the final band is the 8mer following removal of the sugar residue. Piperidine and heat complete depurination and removal of the sugar yielding a single product, an 8mer. The control lanes, (1-5, BD + 15mer, t=0 hr) demonstrate that the cleaved DNA and the preceeding products are not a result of the addition and presence of BD prior to the heat and base workup procedure. Product assignments for each band are summarized in Figure 36.

Figure 35: Autoradiogram of the Sequential Analysis of the Oligonucleotide Products by Gel Electrophoresis (20% polyacrylamide). 10 uM BD in 100 mM NaPhosphate pH 7.0. Panel A) incubation time of 0 hours and Panel B) incubation time of 24 hours. Lane 1) incubation at 37° C, Lane 2) heat for 15 minutes at 90° C, Lane 3: 1M piperidine wash, Lane 4) Heat in 1M piperidine for 15 minutes at 90° C, and Lane 5) Heat in 1M piperidine for 30 minutes at 90° C.

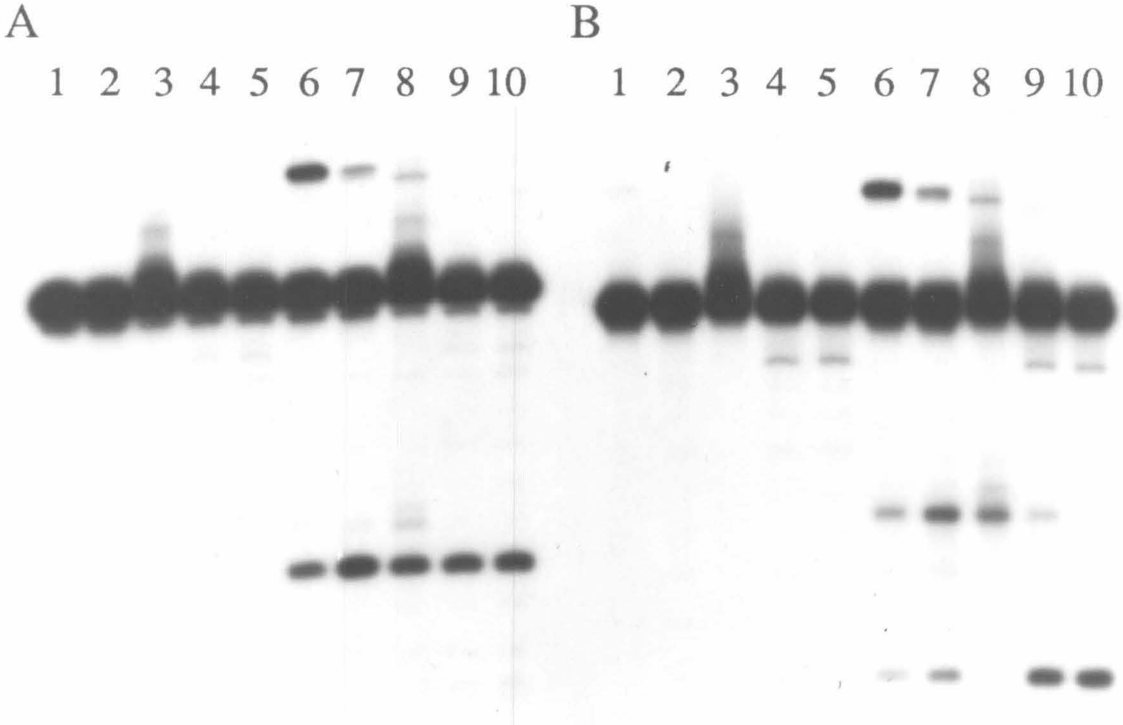
A
1 2 3 4 5 6 7 8 9 10
B
1 2 3 4 5 6 7 8 9 10

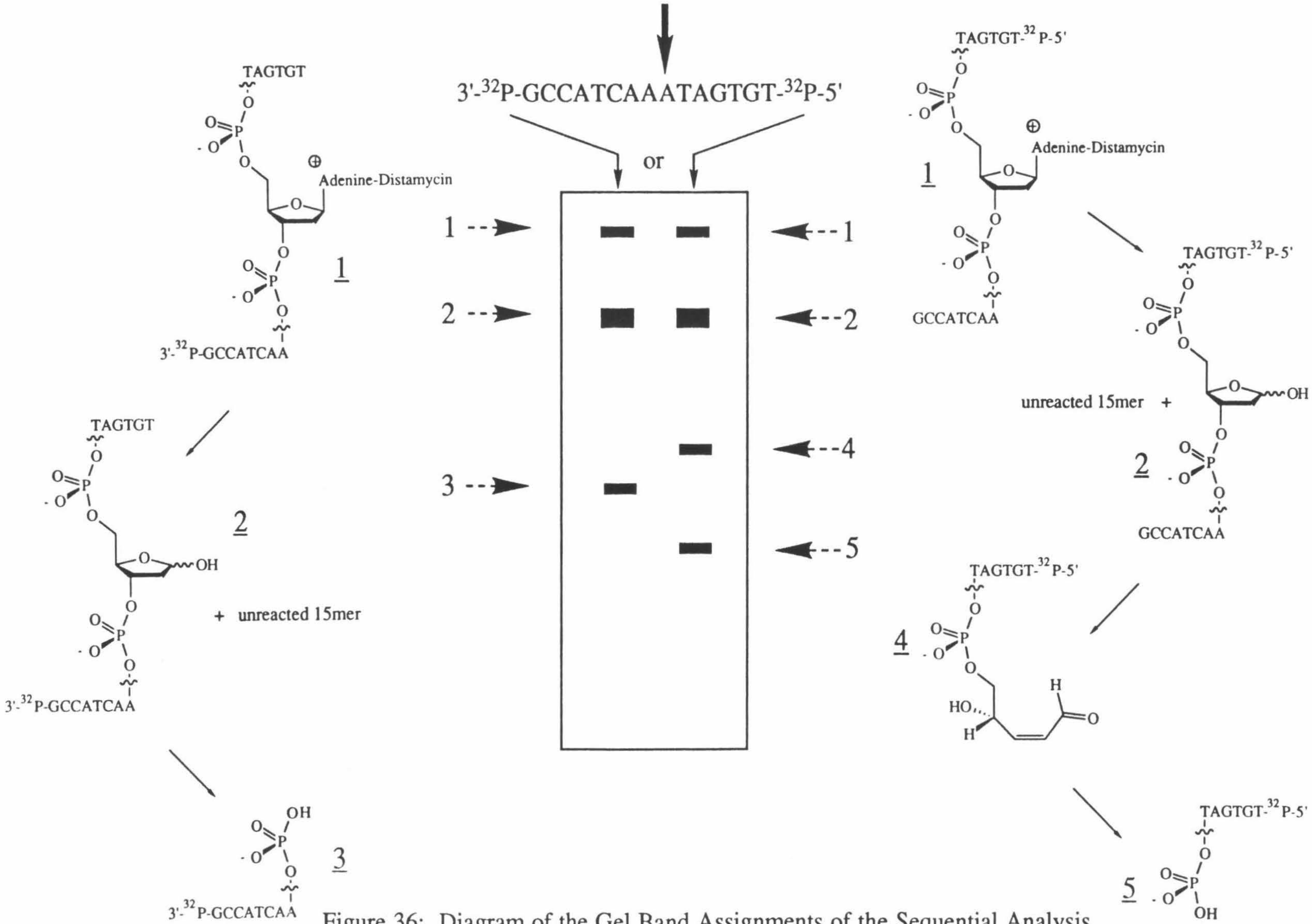
3'-^{32}P-GCCATCAAATAGTGT-^{32}P-5'
or
1
2
3
1
2
4
5
TAGTGT
Adenine-Distamycin
1
3'-^{32}P-GCCATCAA
TAGTGT
2
+ unreacted 15mer
3'-^{32}P-GCCATCAA
3
3'-^{32}P-GCCATCAA
TAGTGT-^{32}P-5'
Adenine-Distamycin
1
GCCATCAA
TAGTGT-^{32}P-5'
unreacted 15mer +
2
GCCATCAA
TAGTGT-^{32}P-5'
4
TAGTGT-^{32}P-5'
5

Figure 36: Diagram of the Gel Band Assignments of the Sequential Analysis of the Oligonucleotide Products.

The 3' and 5' termini of the DNA substrate at the site of cleavage after piperidine treatment are phosphate groups. The presence of a phosphate functional group was detected by reacting each labeled cleaved oligonucleotide fragment with the appropriate phosphatase. T4 Polynucleotide Kinase hydrolyzes a 3' phosphate to a hydroxyl group and Calf Intestinal Phosphatase hydrolyzes a 5' phosphate (Figure 37). Removal of the phosphate group decreases the electrophoretic mobility of the fragment. The two types of termini, hydroxyl and phosphoryl, are resolved by gel electrophoresis using 20% polyacrylamide. Comparison of reactants (lanes 2) and products (lanes 3) are shown in Figure 38. Both the 5' and 3' termini are phoshpate groups after the complete workup procedure of the BD cleavage reaction. Lanes 1 and 4 are the corresponding G + A reactions for the labeled 15mer. Cleavage of the backbone at all guanines and adenines results from heating the strand in the presence of formic acid followed by the traditional 30 minute piperidine workup procedure. This reaction also yields phosphates for both the 3' and 5' termini at the sites of cleavage.

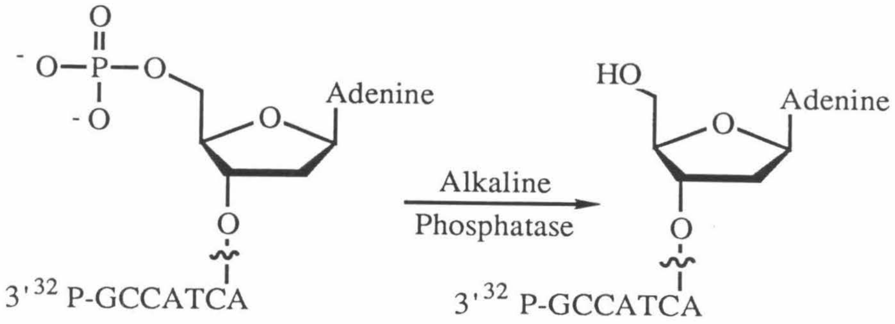
Adenine
Alkaline
Phosphatase
HO
Adenine
3'32 P-GCCATCA
3'32 P-GCCATCA

5' Terminus

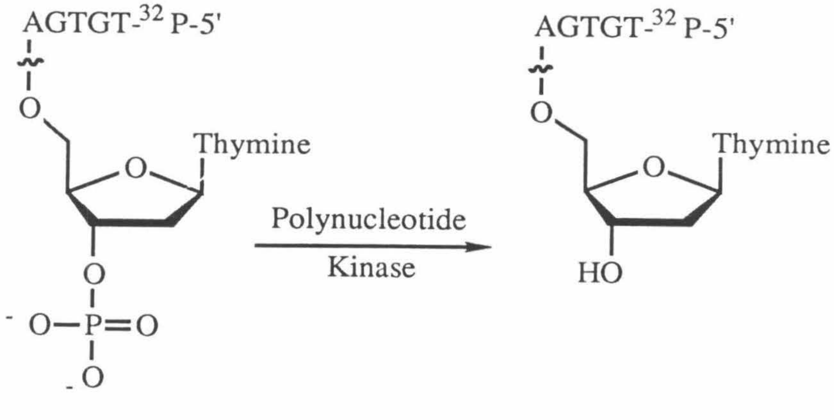
AGTGT-32 P-5'
Thymine
Polynucleotide
Kinase
AGTGT-32 P-5'
Thymine
HO

3' Terminus

Figure 37: Diagram of the Enzymatic Characterization of the Cleaved Oligonucleotide Products.

Figure 38: Autoradiogram of the Enzymatic Characterization of the Cleaved Oligonucleotide (15mer) Terminal Functional Groups. Panel (A) 5' Terminus: Lane 1) G + A reaction, Lane 2) BD cleavage reaction (48 hours, 37° C), Lane 3) BD cleavage reaction followed by treatment with Alkaline Phosphatase, and Lane 4) G + A reaction followed by treatment with Alkaline Phosphatase. Panel (B) 3' Terminus: Lane 1) G + A reaction, Lane 2) BD cleavage reaction (48 hours, 37° C), Lane 3) BD cleavage reaction followed by treatment with Polynucleotide Kinase, and Lane 4) G + A reaction followed by treatment with Polynucleotide Kinase.

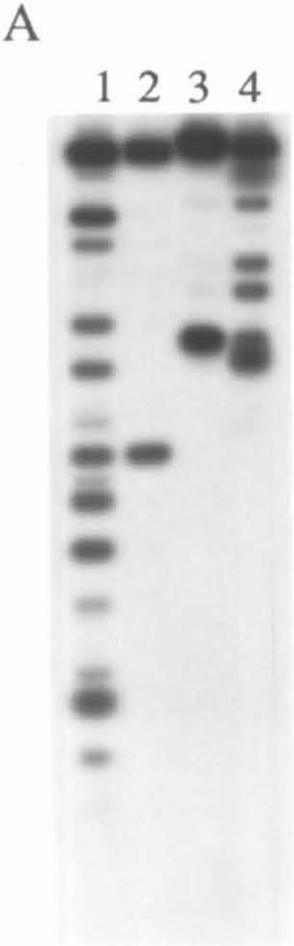
A
1 2 3 4

B
1 2 3 4

In the presence of DNA we detect only one BD product, 3-(acetyldistamycin)-adenine, following a 96 hour reaction time. In order to detect any other BD products and account for other reaction pathways (which might have gone undetected because of the time frame and relatively slow rates, such as hydrolysis or polymerization) the reaction between carbon 14 labeled BD and the 15mer was monitored by TLC/autoradiography over three half lives or until 12% of the starting material remained (Figure 39). Observations and analyses were done at reaction times of 2 days (A), 4 days (B), 10 days (C) and 14 days (D). With time there is a progressive increase in the amount of the adenine adduct and decrease in the BD reactant. The amount of the hydroxy derivative and baseline products stays constant throughout the experiment as measured by scintillation counting. The small amounts of these compounds detected are likely a result of the workup process. After 14 days at 37° C in 100 mM NaPhosphate (pH 7.0) the *sole released product* is 3-(acetyldistamycin)-adenine. In the presence of DNA then, the degradation pathways taken by BD when alone in solution are prevented. Therefore, with DNA as the host, the BD guest is protected and preferentially affords one specific intracomplex reaction.

Figure 39: Autoradiogram of the Moderation of the Oligonucleotide/BD Reaction Pathway by Thin Layer Chromatography. 100 uM 15mer and 100 uM ^{14}C-BD in 100 mM NaPhosphate pH 7.0 at 37°C after A) 2 days, B) 4 days, C) 10 days, and D) 14 days.

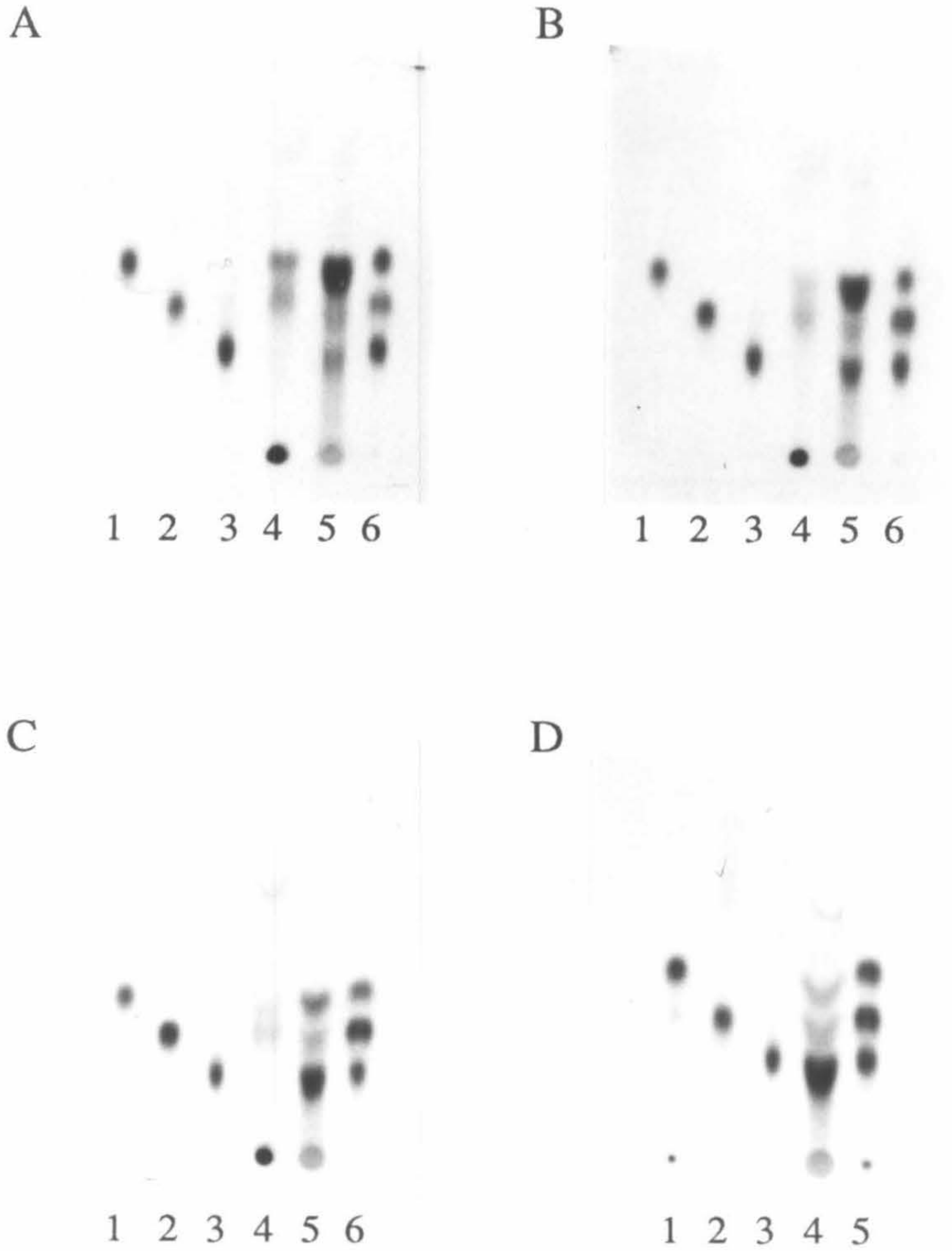
A
B
1 2 3 4 5 6
1 2 3 4 5 6
C
D
1 2 3 4 5 6
1 2 3 4 5

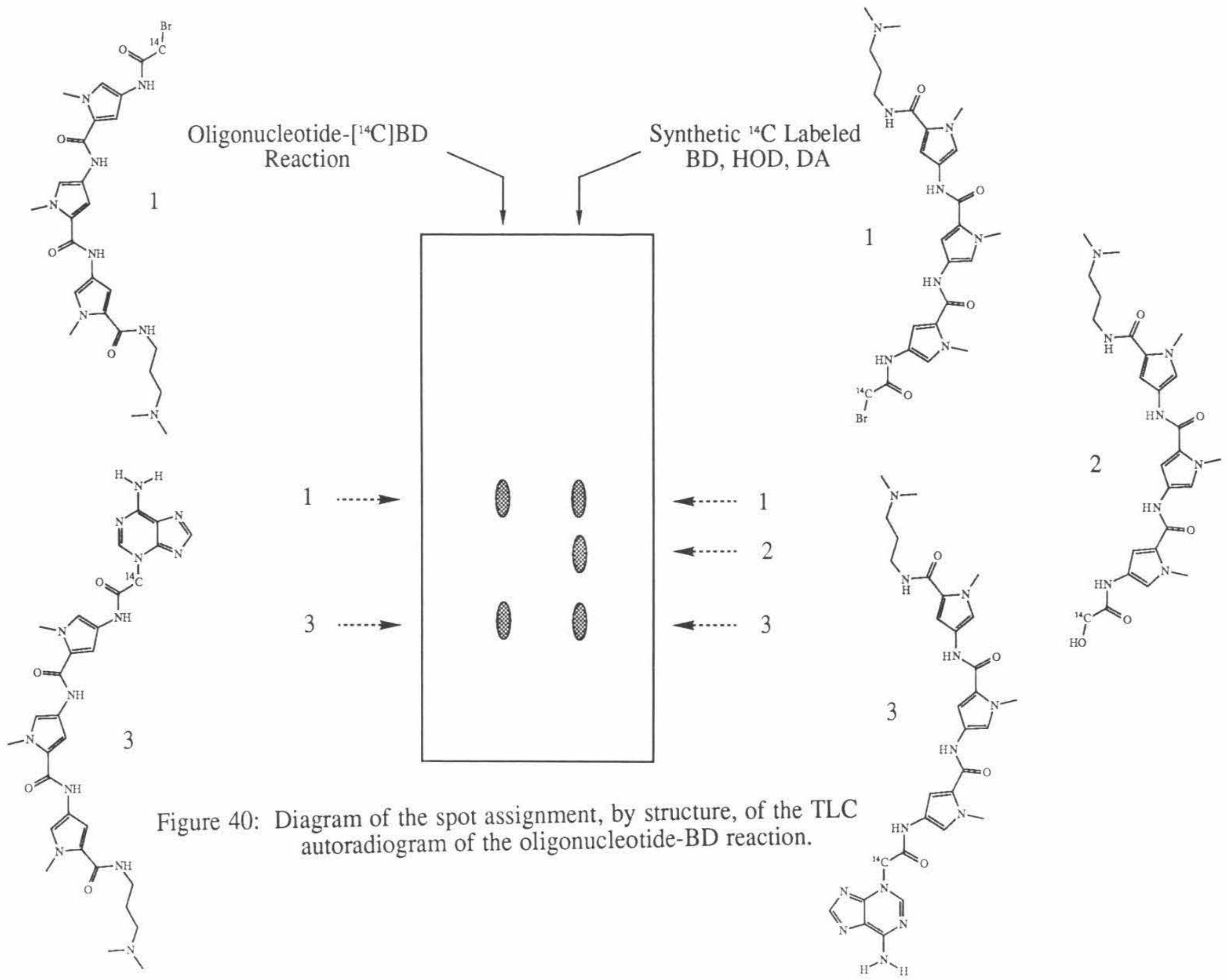
Oligonucleotide-[^{14}C]BD
Reaction
Synthetic ^{14}C Labeled
BD, HOD, DA
1
2
3
1
3
1
2
3
1
3

Figure 40: Diagram of the spot assignment, by structure, of the TLC autoradiogram of the oligonucleotide-BD reaction.

H. Kinetic Analysis: The reaction of the N-haloacetyldistamycins (Cl, Br, and I) with double helical DNA which results in sequence specific strand cleavage of duplex DNA has four experimentally distinguishable steps: (1) binding to the double helical DNA, (2) akylation/covalent attachment to adenine, (3) depurination of adduct, and (4) strand cleavage. Two oligonucleotide duplexes, a 15mer, 5'-CGGTA**GTTTA**TCACA-3', and a 21mer, 5'-TCACAGTT**AAATT**GCTAACGC-3', were utilized as the DNA substrates for kinetic analysis of the cleavage reaction. Each oligonucleotide contains only one of the five base pair binding sites from the 167 base pair restriction fragment (Figure 41). These binding sites are assigned as site #2, within which cleavage occurs at adenine 48, and site #3 within which cleavage occurs at adenines 58 and 59.

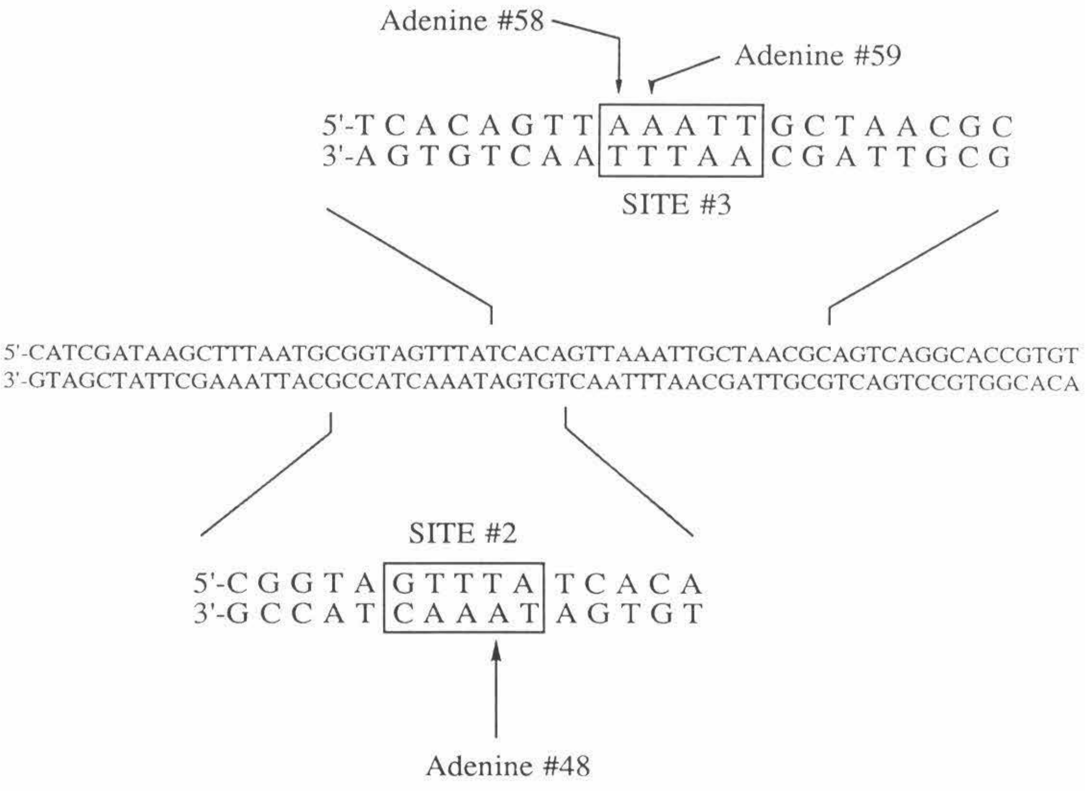
Adenine #58
Adenine #59
5'-T C A C A G T T A A A T T G C T A A C G C
3'-A G T G T C A A T T T A A C G A T T G C G
SITE #3
5'-CATCGATAAGCTTTAATGCGGTAGTTTATCACAGTTAAATTGCTAACGCAGTCAGGCACCGTGT
3'-GTAGCTATTCGAAATTACGCCATCAAATAGTGTCAATTTAACGATTGCGTCAGTCCGTGGCACA
SITE #2
5'-C G G T A G T T T A T C A C A
3'-G C C A T C A A A T A G T G T
Adenine #48

Figure 41: Oligonucleotide sequences abstracted from the 167 b.p. restriction fragment for kinetic analysis

1. Binding/Complexation: The percentage of ligand bound to the 15mer, binding site #2, was quantitated by equilibrium dialysis in conjunction with scintillation counting. Two compounds were studied, N-acetyldistamycin (AcD) and N-bromoacetyldistamycin, both labeled with carbon 14. The N-acetydistamycin was utilized as a control, first to determine, the time required for diffusion and equilibration across the dialysis membrane and second, to see if there was a detectable difference in binding affinities for a ligand with N-acetyl *vs.* N-bromoacetyl on the tripeptide.

The apparatus utilized was acquired from a commercial source (Spectrum Medical Industries, Inc.). It has a five cell carrier which rotates at 5, 10 or 20 revolutions per minute and can be placed inside of a temperature controlled water bath. Each cell is comprised of two Teflon parts precision machined to seal a semipermeable membrane (molecular weight cut off of 3500) between the two halves. This configuration creates a cell with two compartments each with an effective volume of one milliliter. Each compartment has three ports for introducing and removing samples. Cells are rotated about the axis perpendicular to the membrane.

For our purposes all experiments were conducted at 37° C at a rotation rate of 10 rpm. The time required for equilibration to occur was determined to be six hours at 10 uM AcD, 100 mM NaPhosphate (Figure 42). In order to measure the amounts of ligand bound (L_B) and ligand free (L_F) in solution with the 15mer, premixed samples (ligand + oligonucleotide) were introduced in one compartment and complementary buffer in the other (Figure 43). After an equilibration time of 8 hours samples on each side were removed, and both compartments were washed two times with 1 ml of the reaction buffer. The amount of compound in each compartment was then measured by scintillation counting.

The results obtained for both AcD and BD are listed in Table 4 (scintillation data) and Table 5 (derived results). From this data the binding constants for binding site #2, GTTTA, within the 15 base pair oligonucleotide were calculated from the following equation, $K = L_B / L_F (DNA_F)$, where L_B is the concentration of BD bound to DNA, L_F is the concentration of unbound BD and DNA_F is the concentration of unbound DNA. From Table 4 we find that at 100 uM DNA to 10 uM BD (2 runs) $L_B = 7.60$ uM, $L_F = 0.15$ uM and $DNA_F = 92.4$ uM from which the binding constant for N-bromooacetyldistamycin is calculated to be $K_{BD} = 5.5 \times 10^5 (\pm 0.1)\ M^{-1}$. At 100 uM DNA to 10 uM AcD (2 runs) $L_B = 7.73$ uM, $L_F = 0.09$ uM, and $DNA_F = 92.3$ uM from which the binding constant for N-acetyldistamycin is calculated to be $K_{AcD} = 8.8 \times 10^5 (\pm 0.4)\ M^{-1}$. The higher affinity of N-acetyldistamycin for this binding site $K_{AcD} = 1.6\ K_{BD}$, might be due to differences in the hydrophobic nature of the two molecules (solvent *vs.* minor groove solubility) or the steric fit within the minor groove -- both of which can originate from the electronegative and atomically larger halogen atom.

The melting temperatures for the 15mer were determined in order to assess the percentage of the oligonucleotide in the single stranded state at any given temperature, at different ionic strengths, and with or without the ligand, BD. This transition is easily observed by ultraviolet spectroscopy at 260 nm. Upon dissociation, from the double to the single stranded state one observes an increase in absorbance, since the single stranded form has a larger extinction coefficient due to the unstacking and randomization of the bases. The only limitation with this technique is the allowed concentration range (Beer's Law). The concentration of the 15mer utilized was 2.5 uM with respect to the strand or binding site (30 uM b.p.). This concentration places the absorbance in the range of 0.70 to 0.97. The melting curves for the oligomer in 10 and 100 mM NaPhosphate (pH 7.0) with and without one equivalent of BD are shown in Figure 44 and 45, respectively. The concentration of the buffer refers to the concentration of the sodium cation. The most significant affect on the helix to coil transition of the oligonucleotide is observed with a change in sodium ion concentration. In the absence of BD an increase in the melting temperature by 17° C is observed with an increase in the concentration of salt by one order of magnitude, 10 mM to 100 mM. In the presence of BD (one equivalent, 2.5 uM) the same change in buffer concentration results in an increase of 14.5° C. These results are to be expected based on the polyelectrolyte theory, which predicts an increase in the melting temperature and also the rate of renaturation with an increase in the ionic strength.

BD increases the melting temperature of the oligo by 4° C and 1.5° C, at 10 and 100 mM NaPhosphate, respectively. Therefore the ligand does not significantly stabilize the duplex upon binding. These results are contrary to what has been reported in the literature for netropsin and distamycin A.[45,54,99] Both of these compounds are considered helix stabilizers. Increases in melting temperatures have ranged from 23 to 46° C upon binding, depending on the sequence and ion concentration. However, these experiments were conducted on polymers, not oligomers, and primarily homopolymers (*e.g.*, poly d(A)-d(T) and poly d(A-T)), not heterooligomers. The fact that BD does not stabilize this 15 base pair duplex might reflect that the activation energy required to melt the flanking sequences is equal to or greater than the energy of dissociation of the ligand.

The primary objective of the melting temperature experiments was to determine the optimal conditions for formation and maintenance of the duplex, since this is the reactive state for the next step, alkylation. Relevant temperatures to the alkylation experiments are 37° and 45° C, for which the percentage of DNA in the single stranded state is listed in Table 6. Based on these results kinetic analysis of the alkylation step was conducted at a sodium concentration of 100 mM (pH 7.0), under which there is 1.0% and 7.9% in the single stranded state in the presence of BD at 37° C and 45° C, respectively.

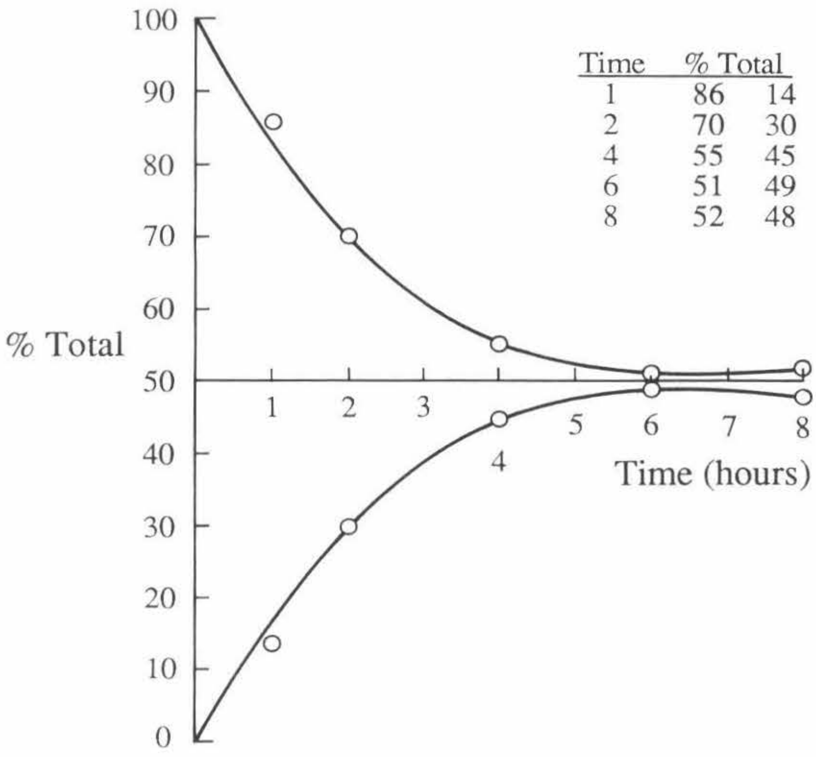

Time	% Total	
1	86	14
2	70	30
4	55	45
6	51	49
8	52	48

Figure 42: Equilibration Time of N-acetyldistamycin. 10 uM AcD in 100 mM Na Phosphate pH 7.0 at 37°C.

Figure 43: Diagram of Equilibrium Dialysis System and Technique. Boxed is the equation utilized for determination of the amont of ligand bound to the oligonucleotide, where L_B is the ligand bound and L_F is the ligand free. A corresponds to the measured counts per minute of the solution in Compartment A, and B is the measured cpm of the solution in Compartment B after equilibration.

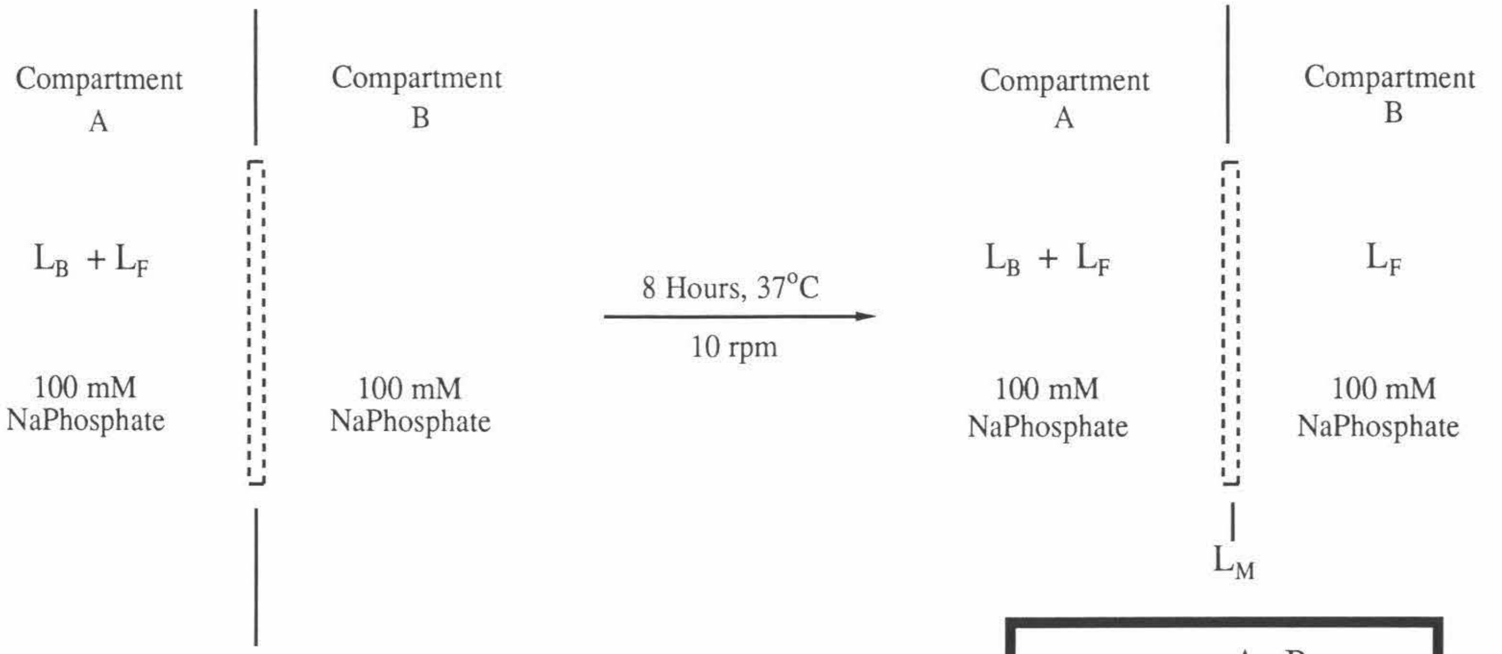
Compartment A
Compartment B
$L_B + L_F$
100 mM NaPhosphate
100 mM NaPhosphate
8 Hours, 37°C
10 rpm
Compartment A
Compartment B
$L_B + L_F$
L_F
100 mM NaPhosphate
100 mM NaPhosphate
L_M

$$\% \text{ Bound} = \frac{A - B}{A}$$

where $A = L_B + L_F$ and $B = L_F$

$$\% \text{ Free} = 100 - \% \text{Bound}$$

Table 4: Equilibrium Dialysis: Scintillation Data in Counts per Minute.[a]

a) values are corrected for background counts (30 cpm).

Ligand	L_{Total}	Compartment A $L_B + L_F$	Compartment B L_F	Membrane L_M
AcD	138 527 ± 1386	106 840 ± 1037	1 278 ± 16	30 349
	138 527 ± 1386	107 310 ± 1041	1 265 ± 18	29 892
BD	7 717 ± 77	5 789 ± 58	112 ± 5	1 756
	7 717 ± 77	5 953 ± 60	110 ± 5	1 594

L_B = Ligand Bound L_F = Ligand Free L_M = Ligand in Membrane

Table 5: Equilibrium Dialysis: % Bound and % Free

Ligand	Starting Concentration (uM) DNA	Starting Concentration (uM) Ligand	Equilibrium Concentration (uM) $\text{Ligand}_{EqT}\left(\frac{A+B}{L_{Total}} \times 10\right)$	Equilibrium Ratio DNA:Ligand	% Bound	% Free
AcD	100.0	10.0	7.80	12.8 : 1.0	98.8 ± 0.0	1.2 ± 0.0
	100.0	10.0	7.84	12.8 : 1.0	98.8 ± 0.0	1.2 ± 0.0
BD	100.0	10.0	7.65	13.0 : 1.0	98.0 ± 0.2	2.0 ± 0.2
	100.0	10.0	7.85	12.7 : 1.0	98.1 ± 0.1	1.9 ± 0.1

A = counts/minute in compartment A B = counts/minute in compartment B

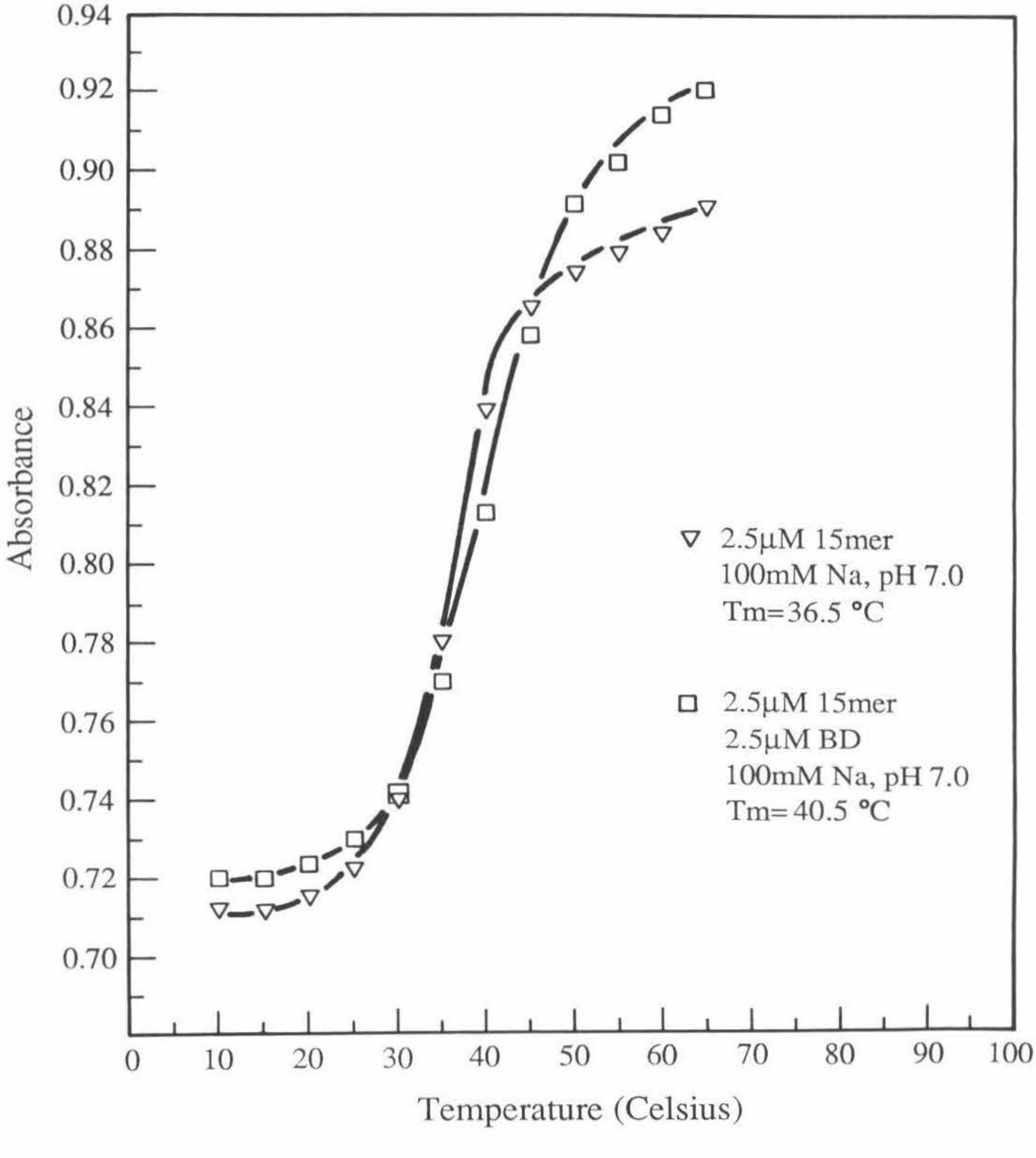

Figure 44: Graph of the Melting Temperature of the 15 base pair Oligonucleotide at 10 mM NaPhosphate pH 7.0.

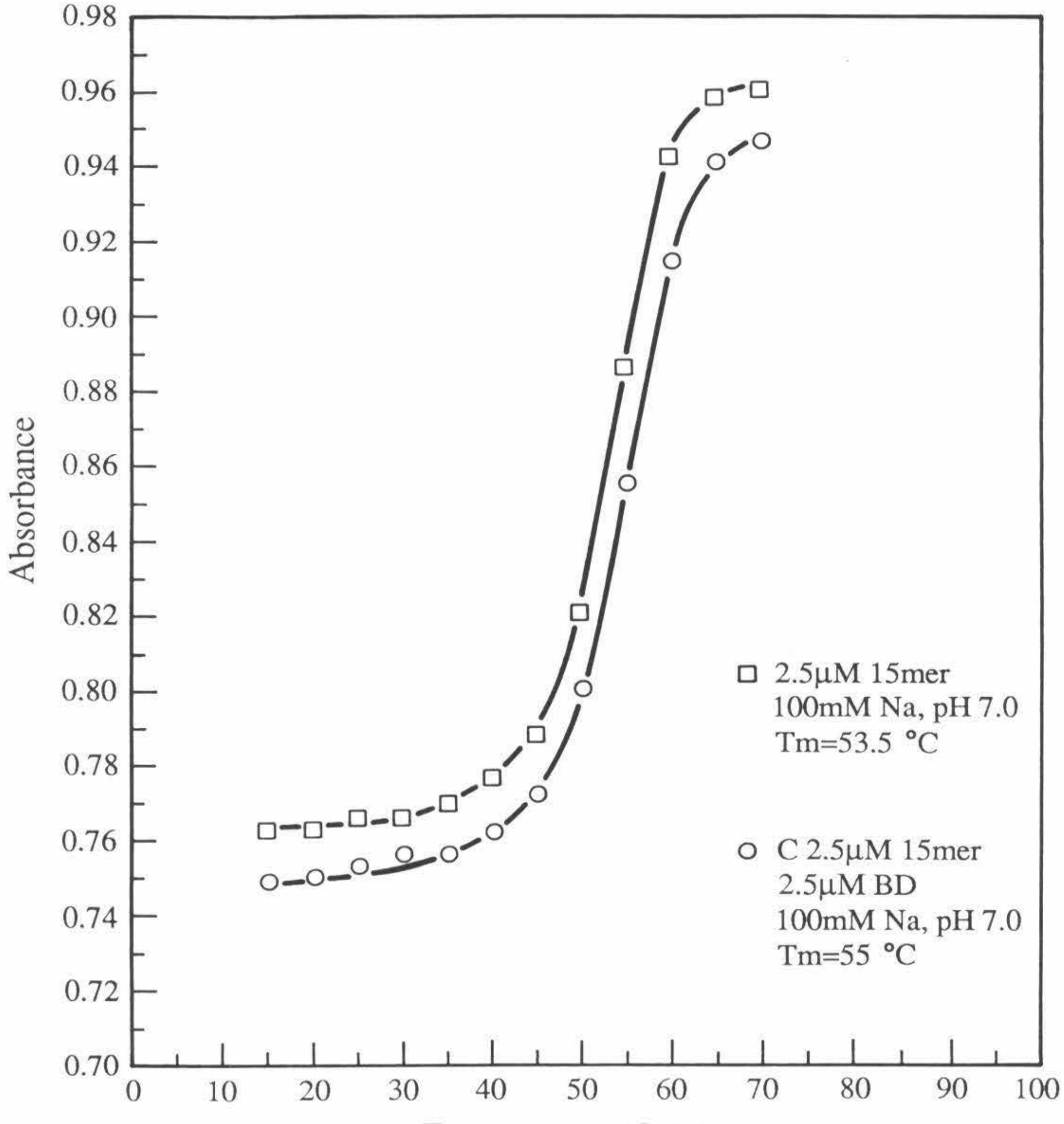

Figure 45: Graph of the Melting Temperature of the 15 base pair Oligonucleotide at 100 mM NaPhosphate pH 7.0.

Table 6: Percentage of the 15 b.p. oligonucleotide in the single stranded state at different temperatures.

Temperature	10 mM NaPhosphate		100 mM NaPhosphate	
	w/o BD	w/BD	w/o BD	w/BD
33° C	25	15	1.0	0.0
37° C	50	31	3.1	1.0
41° C	82	50	6.2	3.7
45° C	94	74	11	7.9
49° C	100	90	25	19
53° C	100	98	50	37
57° C	100	100	75	63
61° C	100	100	93	85
T_m	36.5° C	40.5° C	53.5° C	55.0° C

2. Alkylation/Covalent Attachment: The alkylation rate was determined by monitoring the reaction by reverse phase HPLC, an example of which is shown in Figure 46 for N-bromoacetyldistamycin and the 15mer. This method provides a means to simultaneously observe the disappearance of the reactant, BD (1) and the appearance of the product, 3-(acetyldistamycin)-adenine (5). Verification of the peak assignments was possible by real time acquisition of the ultraviolet spectra of each compound as it eluted off the column (Figure 46, Boxes E and F). In addition, we compared individual and coinjections of the synthetic compounds (BD, HOD, DA) to that of the oligonucleotide reactions. Changes in concentrations through time were quantitatively determined by peak area and with reference to an internal standard, 3-nitrobenzene sulfonic acid (4). It will be assumed that under the given chromatographic conditions all of the ligand noncovalently associated with the DNA is consistently separated and accounted for, thus the rate of disappearance of N-bromoacetyldistamycin is equivalent to the rate of its covalent attachment to the DNA. Hydrolysis of the compound does not occur. The amount of N-hydroxyacetyldistamycin stays constant throughout the entirety of the reaction. In addition to N-bromoacetyldistamycin, the rates of alkylation for N-chloro and N-iodoacetyldistamycin were determined.

Figure 46: HPLC chromatograms of the BD/15mer reaction. 250 uM 15mer, 50 uM BD, 70 uM 3-Nitrobenzene sulfonic acid in 100 mM NaPhosphate pH 7.0 at 37^{o} C. Panel A) 0 hours, B) 48 hours, C) 72 hours, D) 120 hours, E) UV spectra of 15mer and BD and, F) UV spectrum of 3-(Acetyldistamycin)-adenine. Peak assignments (1) N-Bromoacetyldistamycin, (2) N-Hydroxyacetyldistamycin, (3) 15 b.p. oligonucleotide, (4) 3-Nitrobenzenesulfonic acid, and (5) 3-(Acetyldistamycin)-adenine.

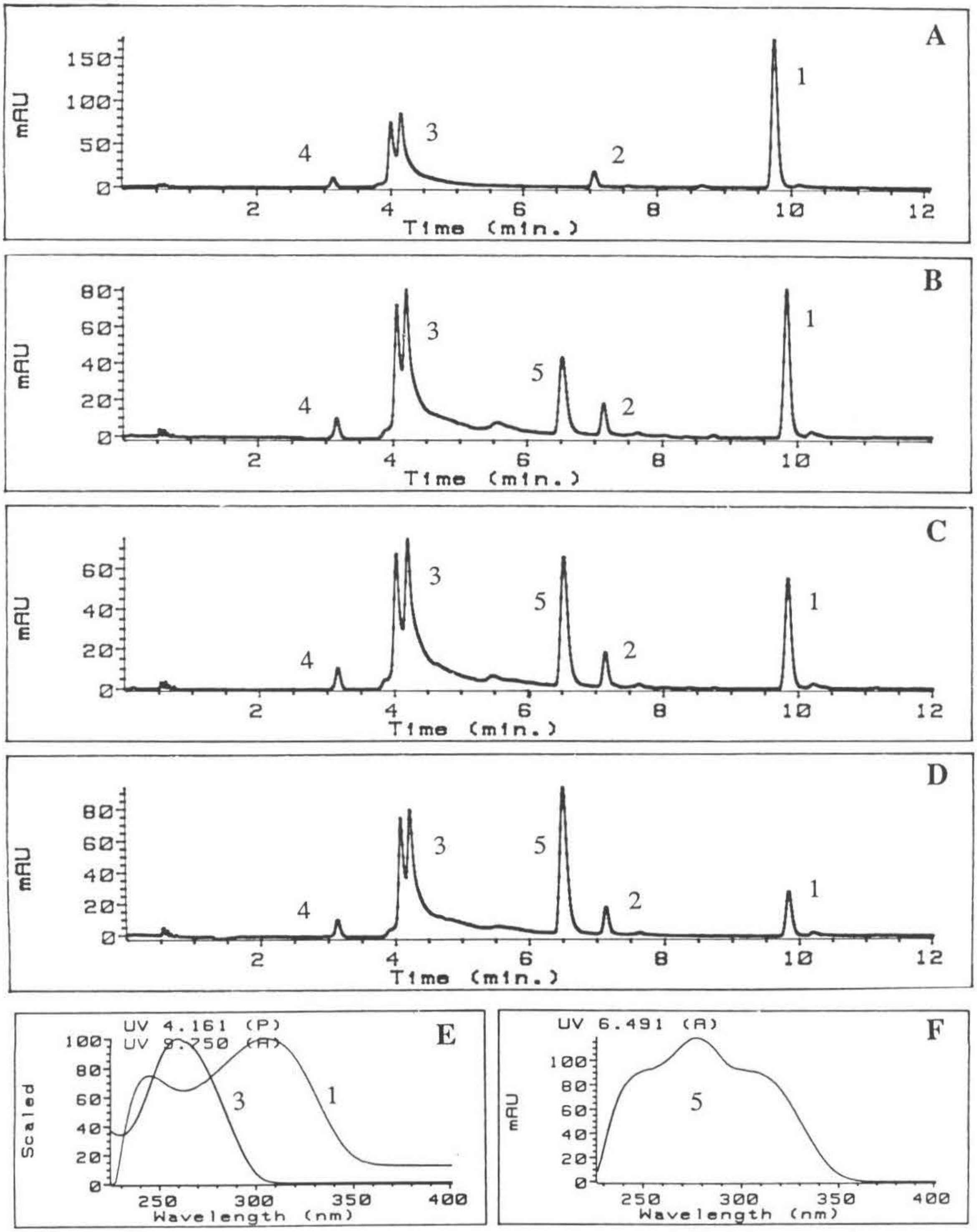
A
B
C
D
E
F
mAU
Time (min.)
0
2
4
6
8
10
12
150
100
50
80
60
40
20
1
2
3
4
5
UV 4.161 (P)
UV 9.750 (A)
Scaled
Wavelength (nm)
250
300
350
400
UV 6.491 (A)

Rate of Alkylation of Adenine 48 / Binding Site #2 / 15mer:

N-Bromoacetyldistamycin: The rate of disappearance of BD is described by the first order rate expression, $-\ln [\mathrm{BD}]/[\mathrm{BD}]_0 = kt$. Based on this description, one may consider a minimal mechanistic scheme of prior complexation of BD with duplex DNA followed by a first order reaction within the complex to afford the covalently bound distamycin to adenine. This type of reaction is analogous to that of an enzyme with a site specific irreversible inhibitor.[100]

$$\mathrm{DNA} \quad + \quad \mathrm{BD} \underset{k_{-1}}{\overset{k_1}{\rightleftharpoons}} \mathrm{DNA}\cdot\mathrm{BD} \xrightarrow{k_2} \mathrm{DNA\text{-}D}$$

Initial studies found that the rate of disappearance of BD and the apparent rate constant varies when the ligand and DNA concentration ratio is changed (Figure 47, Table 7). At a 1:1 ratio (50 uM 15mer : 50 uM BD) the rate constant measures as $k = 9.84 \times 10^{-3}\ h^{-1}$, at a 2:1 ratio (100 uM 15mer : 50 uM BD) the rate constant measures as $1.47 \times 10^{-2}\ h^{-1}$, and at a 5:1 ratio (250 uM 15mer : 50 uM BD) the rate constant measures as $k = 1.56 \times 10^{-2}\ h^{-1}$ at 37° C. Again, these results indicate that the kinetics of the BD/DNA system are analogous to those of an enzyme and other designed biomimetic systems, such as the cyclodextrins.[100,101] In these analogous systems the rate and the rate constant of the reaction is variant to the substrate, enzyme, or host concentrations as described by the Michaelis-Menten and Lineweaver-Burke equations and plots. The results of the BD-oligonucleotide reactions then are a reflection of the different percentages of the amount of ligand complexed with the oligonucleotide. As the DNA:BD ratio increases so does the percentage of ligand bound. Therefore, the maximum rate and absolute rate constant of the alkylation step should become evident by saturation of one reactant with the other, or 100 % complexation of BD and the 15mer.

In order to determine the absolute or maximum rate of alkylation, *based on the rate of disappearance of BD,* a fixed concentration of the ligand was chosen, 10 uM. Then, the rate of disappearance was maximized by *saturation of the ligand with the* *oligonucleotide.* The purpose was to achieve the condition where $[BD]_T = [BD{\cdot}DNA]$ or >99% of the ligand is bound. At 37° C this equivalence is attained at 100 uM 15mer to 10 uM BD, which are those conditions utilized for measurement of the binding constant by equilibrium dialysis. A verification that saturation kinetics is achieved under these conditions was conducted by increasing the ratio to 25:1 and comparing this rate to the 10:1 rate (Table 8, Figure 48). The rate of disappearance of BD at 25:1 (15mer:BD) is equivalent to the rate measured at 10:1. Therefore, at 100 uM 15mer : 10 uM BD and 37° C, the rate of disappearance has been maximized. This result implies that 100 % of the ligand is bound to the DNA under these conditions and saturation kinetics have been attained. Equilibrium dialysis measurements indicated that 98.0 % of BD is bound to the binding site under similar conditions.

In a separate experiment, 3 unique samples under the established reaction conditions (100 uM 15mer, 10 uM BD) were analyzed for measurement of the rate of alkylation at adenine 48 by N-bromoacetyldistamycin at 37° C (Table 9, Figure 49). From $-\ln [BD]/[BD]_o = -kt$ we find that $k_{BD} = 1.94 \times 10^{-2}\ h^{-1}$ ($\pm$ 0.03, $\sigma = 0.9976$), $t_{1/2} = 35.8$ hours.

N-Iodoacetyldistamycin: The overview of the dependence of strand cleavage on the leaving group indicated that within the series OH, Cl, Br, I, and Ms, the leaving group does not determine the site of cleavage or placement of the electrophile. However, the rate of cleavage is determined by this group. Of special interest is the observation that the iodo appeared slower than the bromo on the 167 restriction fragment. To determine whether the decrease in reactivity is caused by an increase in the rate of hydrolysis (thus competitive binding by HOD and inhibition of alkylation) or degradation, the reaction was analyzed over time by HPLC (Figure 50). These chromatograms indicate that the DNA prevents hydrolysis and degradation and directs the reaction down the intended pathway. Further insight was searched for in the quantitative kinetic analysis, specifically the relative rates of ID and BD.

The apparent rate of alkylation of ID is slow compared to BD at 45°C. The verification of saturation kinetics was not obtained at this temperature. But, under the reaction conditions chosen (100 uM DNA, 10 uM ID) it will be assumed that [ID•DNA] = [BD•DNA]. Again the rates of disappearance of the reactants, BD and ID, are described by the first order rate equation, $-\ln [XD]/[XD]_0 = kt$. As derived from the data (Table 10 and Figure 51 (ID), Table 11 and Figure 52 (BD)) $k_{ID} = 3.20 \times 10^{-2}\ h^{-1}$ ($\pm$ 0.10, σ = 0.995), $t_{1/2}$ = 13.4 hours and $k_{BD} = 5.25 \times 10^{-2}\ h^{-1}$ ($\pm$ 0.02, σ = 0.998), $t_{1/2}$ = 22.3 hours at 45°C. The relative rate of alkylation, k_{ID}/k_{BD}, is 0.6. Further studies were conducted on binding site #3, adenines 58 and 59, which will be presented in the next section.

N-Chloroacetyldistamycin: The relative rate of disappearance of N-chloroacetyldistamycin was also measured on the 15mer at 45°C (100 uM 15mer, 10 uM CD). This system is not well behaved. Beyond a reaction time of 48 hours competing peaks elute near or with the internal reference. These peaks are probably nucleotides or shorter DNA fragments. The data set is limited then, with regard to moderation of the reaction over time, because the rate of alkylation is so slow for this compound. Therefore, the derived rate constant is an *estimate* based on the initial rate of disappearance of N-chloroacetyldistamycin.

Four separate samples were examined at 48 hours from which initial rates were determined. Assuming that the chloro reaction adheres to first order kinetics and complies with the rate equation which describes this order, $k_{CD} \sim 2.9 \times 10^{-3}\ h^{-1}$, $t_{1/2}$ = 238 days, and k_{CD}/k_{BD} = 0.06 at 45°C.

Compound	Temperature °C	$10^2 k\ (hr^{-1})$	k_{rel}
BD	37	1.94	0.37
BD	45	5.25	1.00
ID	45	3.20	0.61
CD	45	0.29	0.06

Kinetic Analysis: Adenine 48 / Site #2 / 15mer

Standard Conditions: 100 mM NaPhosphate pH 7.0, 37°C
14 uM 3-Nitrobenzenesulfonic acid

Table 7: Concentration and the Rate of Alkylation.

Time hours	-ln ([BD] / [BD]$_o$) Sample 1	 Sample 2	 Sample 3
0	0.00	0.00	0.00
24	0.29	0.30	0.38
48	0.48	0.69	0.77
72	0.73	1.04	1.16
96	0.98	1.39	1.47
120	1.19	1.75	1.89

Figure 47: Concentration and the Rate of Alkylation.

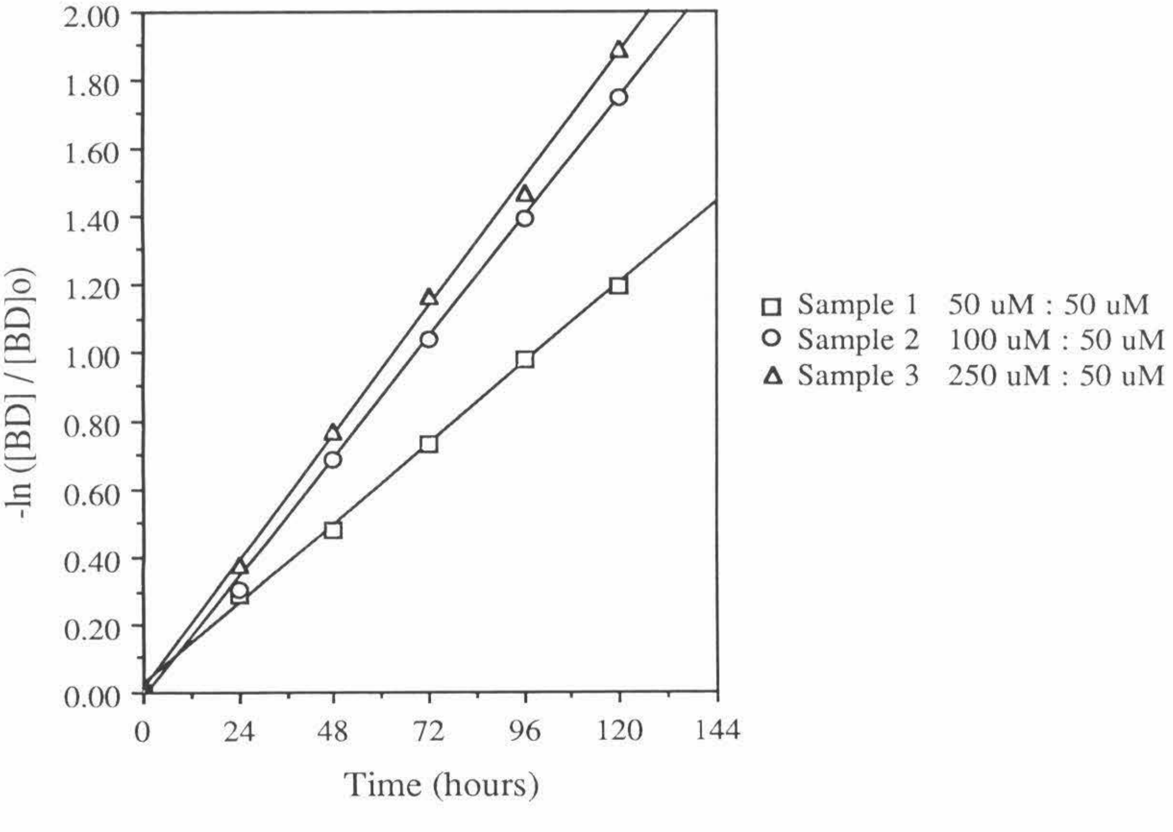

Kinetic Analysis: Adenine 48 / Site #2 / 15mer

Table 8: Verification of the Maximization of the Rate of Alkylation.

Standard Conditions: 10 uM BD, 37°C
100 mM NaPhosphate pH 7.0, 14 uM 3-Nitrobenzenesulfonic acid

Time hours	-ln ([BD] / [BD$_o$]) Sample1	 Sample 2	 Sample 3
0	0.00	0.00	0.00
24	0.44	0.42	0.42
48	0.91	0.90	0.84
72	1.40	1.37	1.37
96	1.88	1.90	1.86

Figure 48: Verification of the Maximization of the Rate of Alkylation.

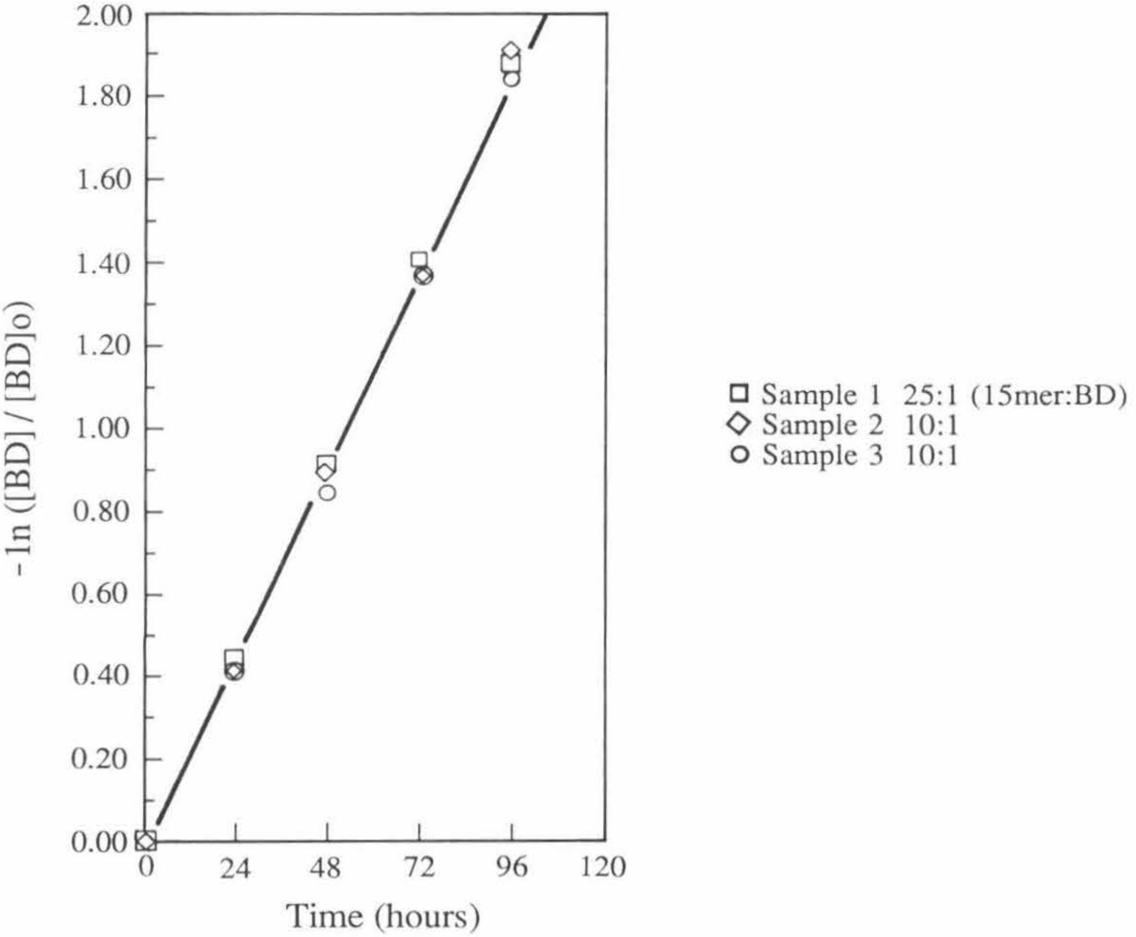

Kinetic Analysis: Adenine 48 / Site #2 / 15mer

Standard Conditions: 100 um 15mer, 10 uM BD
100 mM NaPhosphate pH 7.0, 14 uM 3-Nitrobenzenesulfonic acid

Table 9: The Absolute Rate of Alkylation: N-Bromoacetyldistamycin, 37°C.

Time hours	$-\ln([BD]/[BD]_o)$ Sample 1	Sample 2	Sample 3
0	0.00	0.00	0.00
12	---	0.16	0.23
24	0.41	0.35	0.47
36	0.67	0.63	0.61
48	0.90	0.90	0.93
60	1.08	1.08	1.15
72	---	1.33	1.41
84	1.59	1.59	1.62

Figure 49: The Absolute Rate of Alkylation.

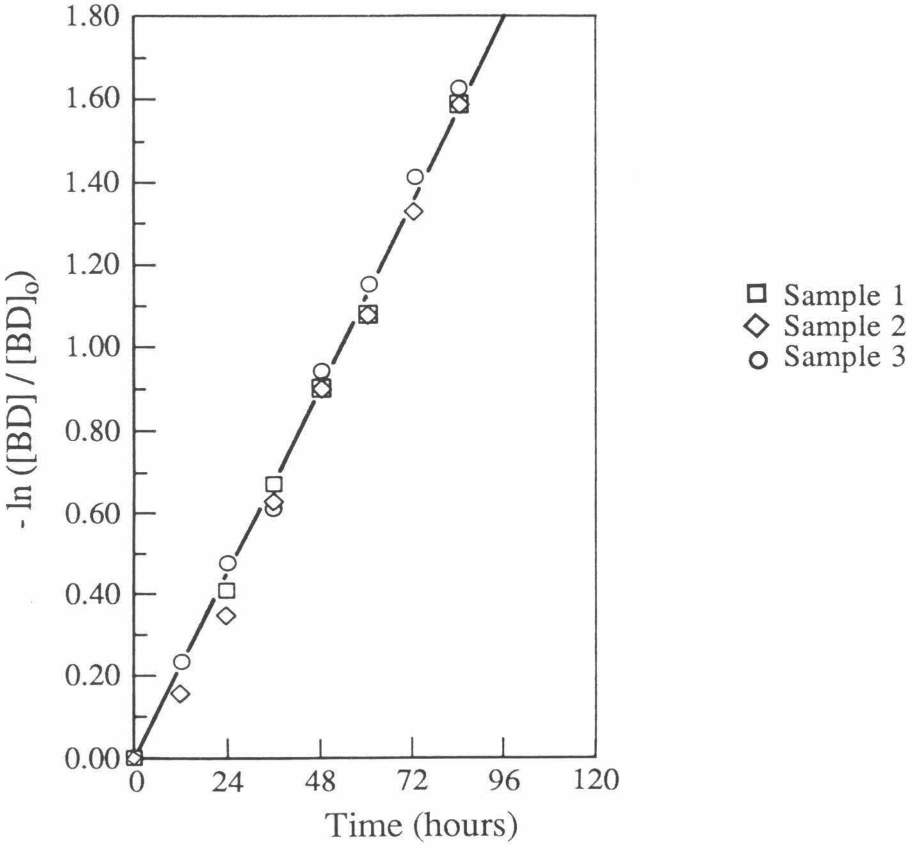

Figure 50: HPLC Chromatograms of the ID/15mer reaction. 100 uM 15mer, 10 uM ID, and 14 uM 3-Nitrobenzenesulfonic acid in 100 mM NaPhosphate pH 7.0 at 45° C. Panel A) 0 hours, B) 12 hours, C) 24 hours, D) 36 hours, and E) 54 hours. Peak assignments (1) N-iodoacetyldistamycin, (2) 15 b.p. oligonucleotide, (3) 3-nitrobenzenesulfonic acid, and (4) 3-(acetyldistamycin)-adenine.

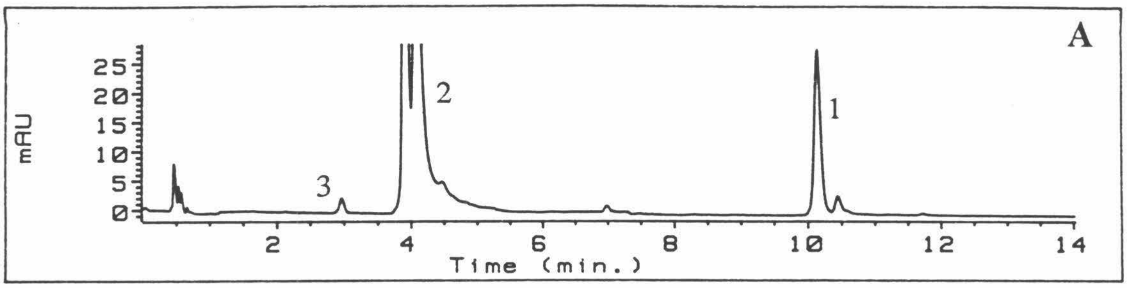
A
mAU
0
5
10
15
20
25
3
2
1
2
4
6
8
10
12
14
Time (min.)

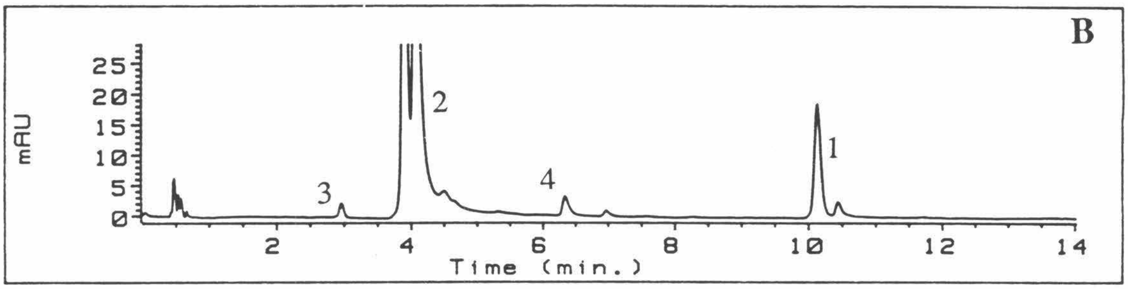
B
mAU
0
5
10
15
20
25
3
2
4
1
2
4
6
8
10
12
14
Time (min.)

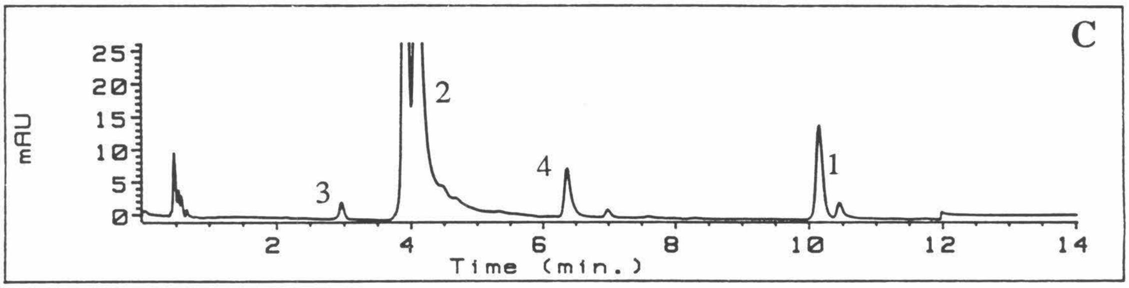
C
mAU
0
5
10
15
20
25
3
2
4
1
2
4
6
8
10
12
14
Time (min.)

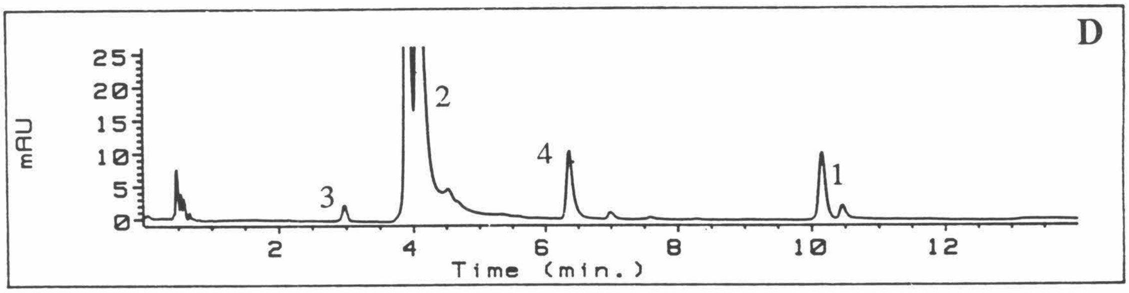
D
mAU
0
5
10
15
20
25
3
2
4
1
2
4
6
8
10
12
Time (min.)

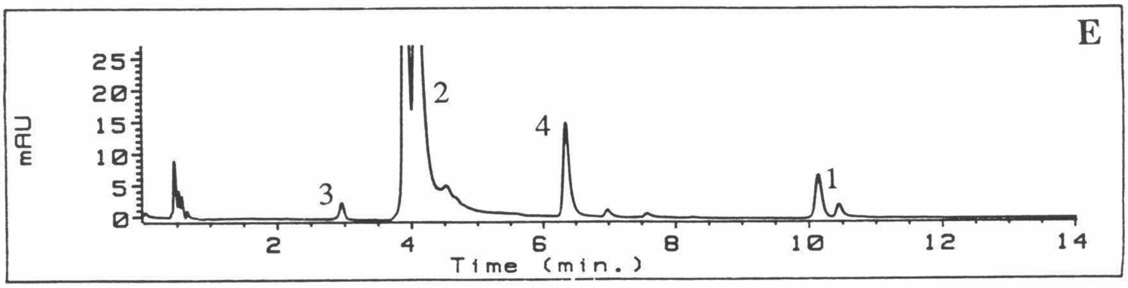
E
mAU
0
5
10
15
20
25
3
2
4
1
2
4
6
8
10
12
14
Time (min.)

Kinetic Analysis: Adenine 48 / Site #2 / 15mer

Relative Rates: N-Iodoacetyldistamycin *vs.* N-Bromoacetyldistamycin.

Standard Conditions: 100 uM 15mer, 10 uM XD, 45°C
100 mM NaPhosphate pH 7.0, 14 uM 3-Nitrobenzenesulfonic acid

Table 10: N-Iodoacetyldistamycin.

Time hours	$-\ln([ID]/[ID]_o)$ Sample 1	Sample 2
0	0.00	0.00
6	0.17	0.14
12	0.36	0.32
18	0.53	0.50
24	0.68	0.70
30	0.90	0.92
36	1.13	1.10
45	1.36	1.42
54	1.70	1.64
60	1.82	2.03

Table 11: N-Bromoacetyldistamycin.

Time hours	$-\ln([BD]/[BD]_o)$ Sample 1	Sample 2
0	0.00	0.00
2	0.08	0.08
4	0.21	0.22
6	0.29	0.32
8	0.40	0.41
10	0.52	0.52
12	0.64	0.63
14	0.71	0.71
16	0.85	0.82
18	0.93	0.98
20	1.02	1.04

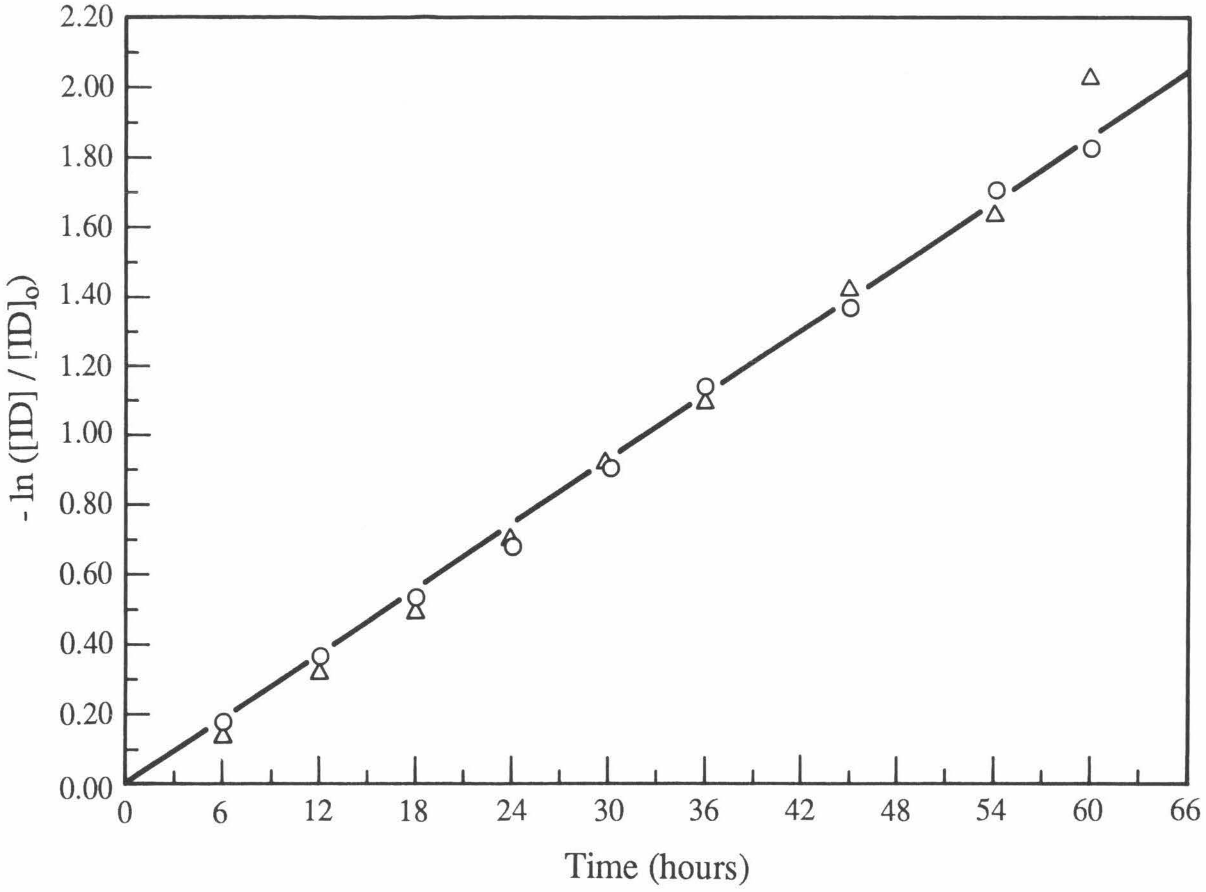

Figure 51: Rate of Alkylation of ID/15mer at 45° C. Graph of Time *vs.* -ln ([ID] / [ID]$_o$).

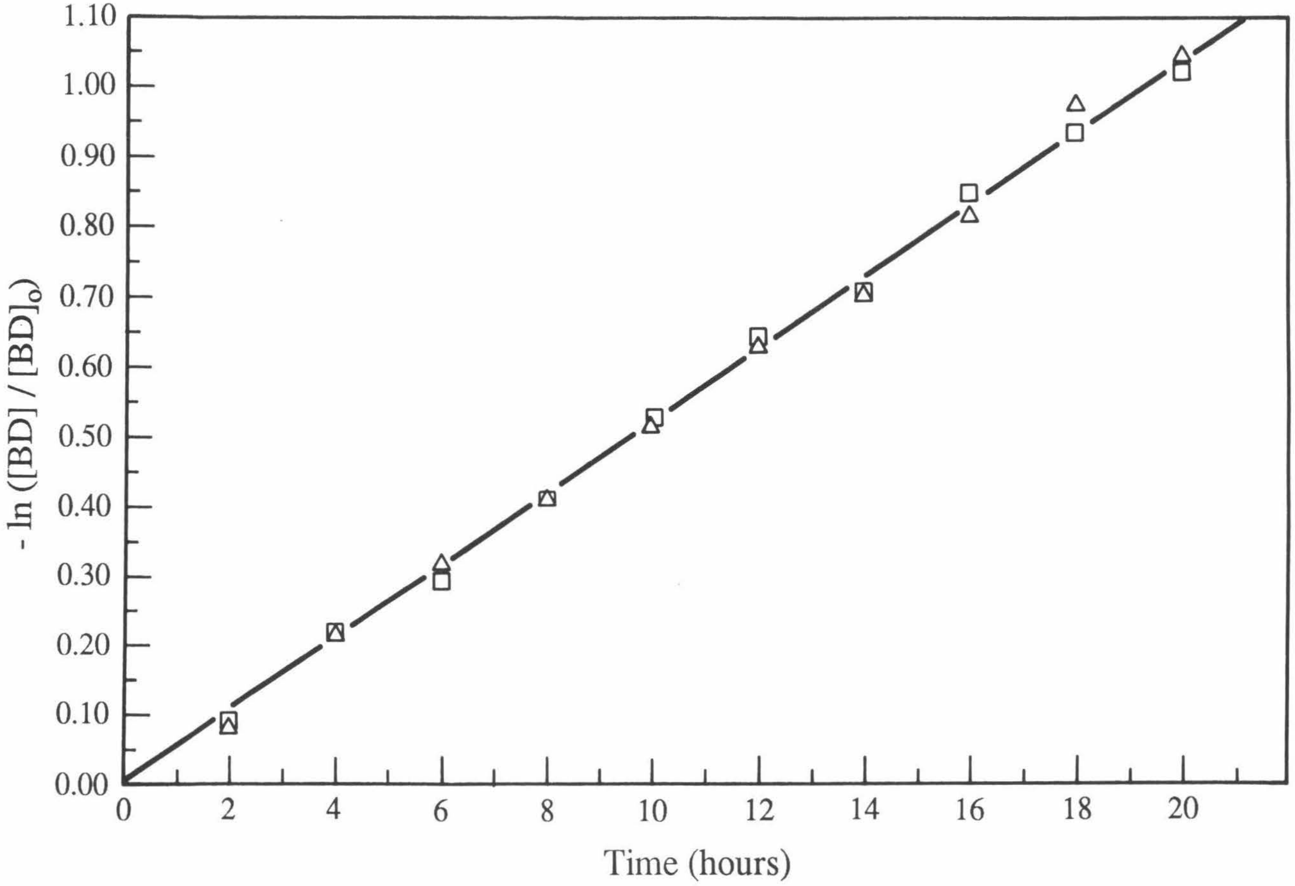

Figure 52: Rate of Alkylation of BD/15mer at 45° C. Graph of Time *vs*. -ln ([BD] / [BD]$_o$).

Rate of Alkylation of Adenine 58 and 59 / Binding Site #3 / 21mer:

The 21 base pair oligonucleotide, 5'-TCACAGTT**AAATT**GCTAACGC, was utilized to determine the rates of alkylation of adenines 58 and 59 within binding site #3 of the 167 base pair restriction fragment.

N-Bromoacetyldistamycin: The rate of disappearance of BD upon reaction with the 21mer (100 uM DNA, 10 uM BD) at 45° C was measured by HPLC (Table 12, Figure 53). Again following first order kinetics, the rate constant measures as 5.61 x 10^{-3} h^{-1} ($\pm$0.17, $\sigma = 0.989$), $t_{1/2}$ = 130 hours.

Recall from the temperature studies on the 167 base pair fragment that at 45° C both adenine 58 and 59 are alkylated. To assess the relative contributions of adenines 58 and 59 to the rate of disappearance of BD, as measured by HPLC, the respective amounts of cleavage at each base site was determined by gel electrophoresis and scintillation counting of the 5' labeled oligonucleotide (Figure 54, Table 13). We now know that the values obtained by this technique reflect the rate of alkylation. However, this technique is not as precise as HPLC. The process by which the polyacrylamide is sliced and transferred to the scintillation vials is susceptable to error. From the scintillation data the rate of alkylation of adenine 58 measures as four times faster than that of adenine 59.

Measurement of the relative amounts of cleavage of these two sites was also done by laser densitometric analysis of the gel autoradiogram obtained for the cleavage reaction after two days. The amounts of cleavage at each base site were quantitated from the gel scan by weight. By this technique the rate of alkylation of adenine 58 measures as 6.6 times faster than that at adenine 59. Note, that the x-ray film was not preflashed prior to exposure, which could be the basis of this discrepancy.

Based on the following equation, $-\ln([BD] / [BD]_o) = (k_{58} + k_{59})t$, the rate constants are calculated to be $k_{58} = 4.50 \times 10^{-3}\ h^{-1}$ ($\pm$0.05) and $k_{59} = 1.11 \times 10^{-3}\ h^{-1}$ ($\pm$ 0.05), where $k_{58} + k_{59} = 5.61 \times 10^{-3}\ h^{-1}$ (as derived from the HPLC and scintillation data).

N-Iodoacetyldistamycin (a continuation of the relative rate): The unexpected slow alkylation rate of ID with respect to BD might be a reflection of the groove width or helical twist. One of the aims of examining binding site #3, was to elucidate the importance of the DNA sequence and consequently geometry and conformation on the relative rates of alkylation with regard to the leaving group. The comparison was done at 65° C, 100 uM DNA, 10 uM ID. Two data points were collected for each compound at 3 and 6 hours, from which initial rates were calculated as $k_{ID} = 4.0 \times 10^{-2}\ h^{-1}$, $t_{1/2} = 17.2$ hours and $k_{BD} = 6.7 \times 10^{-2}\ h^{-1}$, $t_{1/2} = 10.4$ hours. Again the relative rate $k_{ID}/k_{BD} = 0.60$.

Further analysis of the relative rate phenomenon was conducted now at 45° C on site 59 by gel slicing and scintillation counting, see Figure 54. Again for both adenine 59 and 58 the relative rate of k_{ID}/k_{BD} averages to 0.60 from two different reaction times, two and three days, and at two different concentration ratios (21mer:XD), 5:1 and 10:1, see Table 14. Analyzed by laser densitometry, the relative rate measures as $k_{ID}/k_{BD} = 0.42$ after a reaction time of 2 days and DNA:XD ratio of 10:1. A comparison of the ratios of the more intense peak to the weaker peak obtained from the two techniques, scintillation counting *vs.* laser densitometric analysis, shows that (in all cases) those determined by laser densitometry are consistently greater (approximately 1.4 times) than those gathered by scintillation counting. Since the HPLC data and scintillation counting data (*e.g.*, k_{ID}/k_{BD}) are identical, scintillation counting is considered the preferred technique for obtainment of quantitative data from the cleavage experiments.

Based on the data collected, the relative rate of reactivity of the iodo compound is fixed regardless of temperature, sequence (binding site) and base at which cleavage occurs. Therefore, it appears that the source of discrimination resides within the DNA cleaving molecule itself, not the DNA. The optimal position for displacement of the halogen in solution (unconstrained) of the halogen might be different from that achievable in the minor groove given the fixed geometry of the incoming nitrogen nucleophile. Therefore, this result may be a reflection of the optimal conformation and geometry of the cleavage moiety in the transition state.

The covalent radius of the iodine atom is 1.33 å and the Van der Waal radius is 2.20 å. In contrast, the covalent radius of bromine is 1.14 å and the Van der Waal radius is 2.00 å. The larger values of both radii might prevent the iodine from achieving the optimal conformation or position for displacement by the nucleophile.

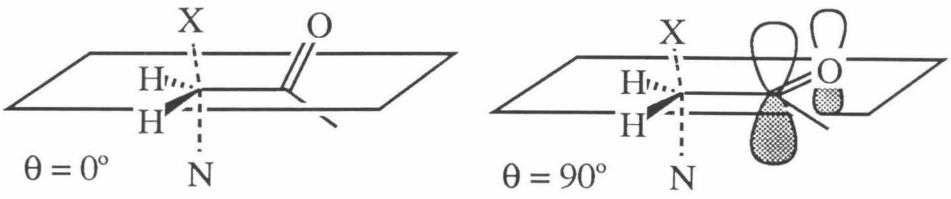

Supportive evidence of this transition state model exists in the infrared[102] and NMR[103] studies of the rotational isomerism of 2-bromo and 2-chloroacetophenone. (The covalent radius of chlorine is 0.99 å and the Van der Waal radius is 1.81 å.) Both studies indicate that the ratio of the eclipsed isomer, ($\theta = 0^{o}$) to the gauche ($\theta = 45^{o}$), is higher for the chloro over the bromo regardless of solvent and dielectric effects. Based on these results we expect the ratio of the eclipsed isomer to the gauche isomer for N-iodoacetyldistamycin to be smaller than that of N-bromoacetyldistamycin.

Finally, product analysis of the chromatograms acquired for the 21mer and BD at 45° C revealed that instead of one product, two products are observed, which elute at about the same time (Figure 55 and 56, peak label 5). Previous experience with separation of the synthetic 3-(acetyldistamycin)-adenine from the other synthetic adenine adduct had shown that by reverse phase HPLC under these solvent conditions the elution times of the compounds are within seconds to one minute of each other on a column 1.7x the length of the column used for these experiments. Therefore, it is not unreasonable to set a hypothesis that this could be another adenine adduct, such as the N1. Alternatively, it might be a product from degradation of the adduct. Unfortunately, at the concentrations utilized it is impossible to retrieve a meaningful spectra from the data generated by the photodiode array detector.

Kinetic Analysis: Adenine 58,59 / Site #3 / 21mer

Standard Conditions: 100 uM 21mer, 10 uM XD
100 mM NaPhosphate pH 7.0,14 uM 3-Nitrobenzenesulfonic acid

Table 12: Rate of Alkylation of Adenines 58 and 59 by BD at 45° C.

Time hours	-ln ([BD] / [BD]$_o$) Sample 1	 Sample 2
0	0.00	0.00
24	0.16	0.15
48	0.27	0.29
84	0.44	0.41
108	0.61	0.62
120	0.70	0.72
144	0.77	0.84

Figure 53: Rate of Alkylation of Adenines 58 and 59 by BD at 45° C.

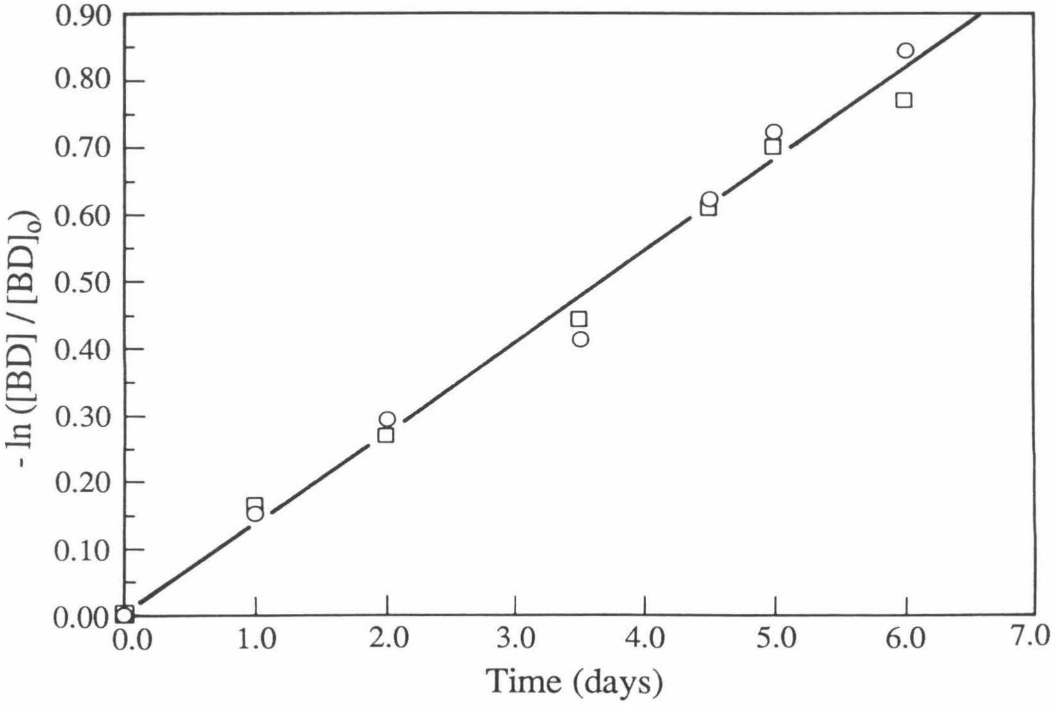

Figure 54: Measurement of the Relative Rates at Adenines 58 and 59 (Site #3/21mer) for N-Bromoacetyldistamycin and N-Iodoacetyldistamycin after 2 days at 45^{o} C. Lanes 1 and 2) 50 uM 21mer and 10 uM ID, Lanes 3 and 4) 50 uM 21mer and 10 uM BD, Lanes 5 and 6) 100 uM 21mer and 10 uM ID, and Lanes 7 and 8) 100 uM 21mer and 10 uM BD. All reactions were in 100 mM NaPhosphate pH 7.0.

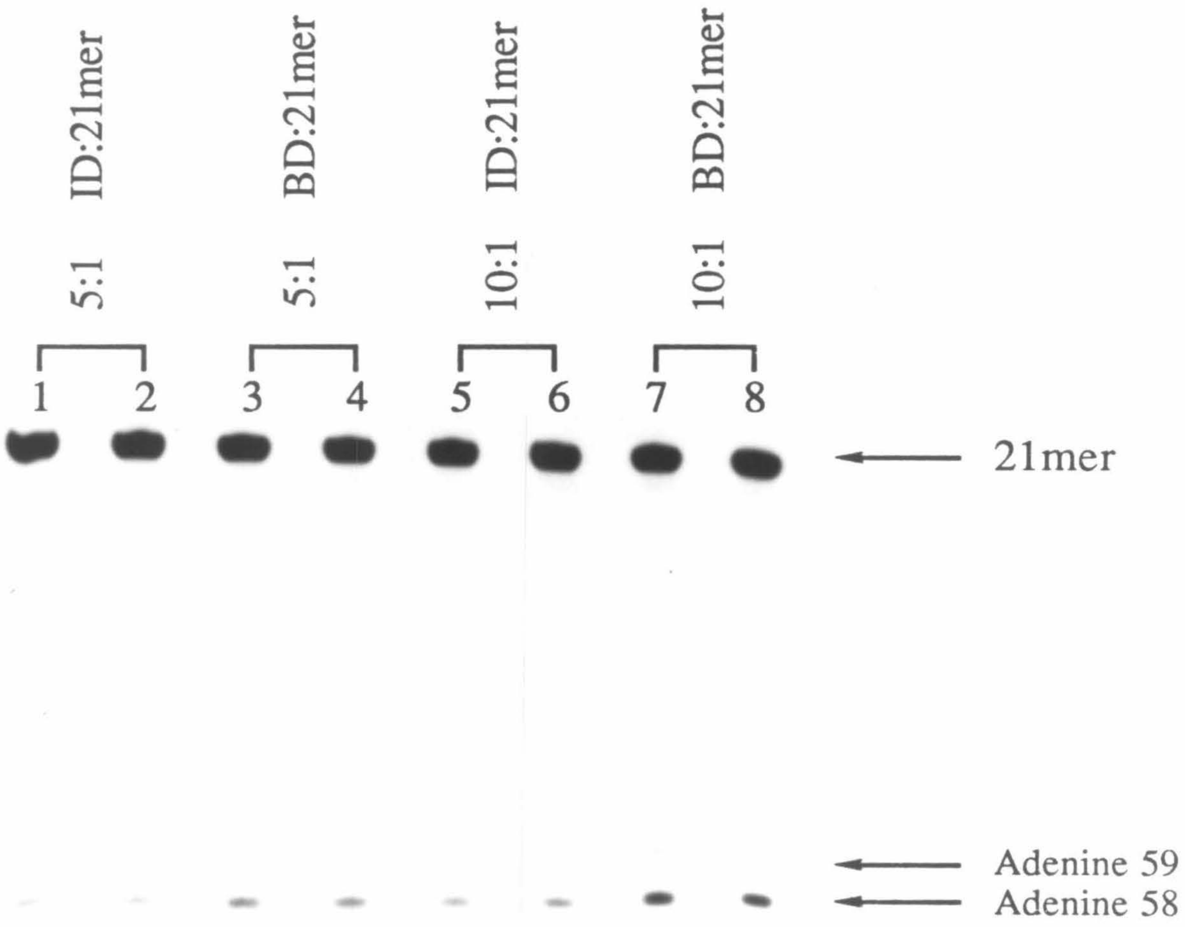
5:1 ID:21mer
5:1 BD:21mer
10:1 ID:21mer
10:1 BD:21mer
1
2
3
4
5
6
7
8
21mer
Adenine 59
Adenine 58

Table 13: Relative Rate of Alkylation by BD: Adenine 58 *vs*. 59.

Ratio	Time	Sample	Adenine		Ratio
DNA:BD	day		58	59	58/59
10:1	2	1	7.59	1.80	4.22
		2	7.45	1.87	3.98
	3	1	10.1	2.34	4.32
		2	10.3	2.45	4.20
5:1	2	1	4.55	1.19	3.82
		2	4.34	1.13	3.84
	3	1	5.97	1.39	4.29
		2	5.99	1.43	4.19

Values represent the % of cleavage at each adenine with respect to the total amount of oligonucleotide (21mer).

Table 14: Relative Rate of Alkylation, ID/BD: Adenines 58 and 59.

Ratio DNA:XD	Time days	Adenine	N-Bromoacetyldistamycin Sample 1	N-Bromoacetyldistamycin Sample 2	N-Bromoacetyldistamycin Average	N-Iodoacetyldistamycin Sample 1	N-Iodoacetyldistamycin Sample 2	N-Iodoacetyldistamycin Average	ID/BD Average
10:1	2	59	1.80	1.87	1.84	1.12	1.08	1.10	0.60
		58	7.59	7.45	7.52	4.04	4.16	4.10	0.54
	3	59	2.34	2.45	2.40	1.66	1.52	1.59	0.66
		58	10.1	10.3	10.2	6.73	6.22	6.48	0.63
5:1	2	59	1.19	1.13	1.16	0.64	----	0.64	0.55
		58	4.55	4.34	4.44	2.50	----	2.50	0.56
	3	59	1.39	1.43	1.41	0.87	0.94	0.90	0.64
		58	5.97	5.99	5.98	3.66	4.06	3.86	0.64

Values represent the % of cleavage at each adenine with respect to the total amount of oligonucleotide (21mer).

Figure 55: HPLC Chromatograms of the BD/21mer reaction. 100 uM 21mer, 10 uM BD, and 14 uM 3-Nitrobenzenesulfonic acid in 100 mM NaPhosphate pH 7.0 at 45° C. Panel A) 0 hours, Panel B) 24 hours, Panel C) 72 hours, and Panel D) 120 hours. Peak assignments 1) BD, 2) DOH, 3) 21mer, 4) internal standard, and 5) ?.

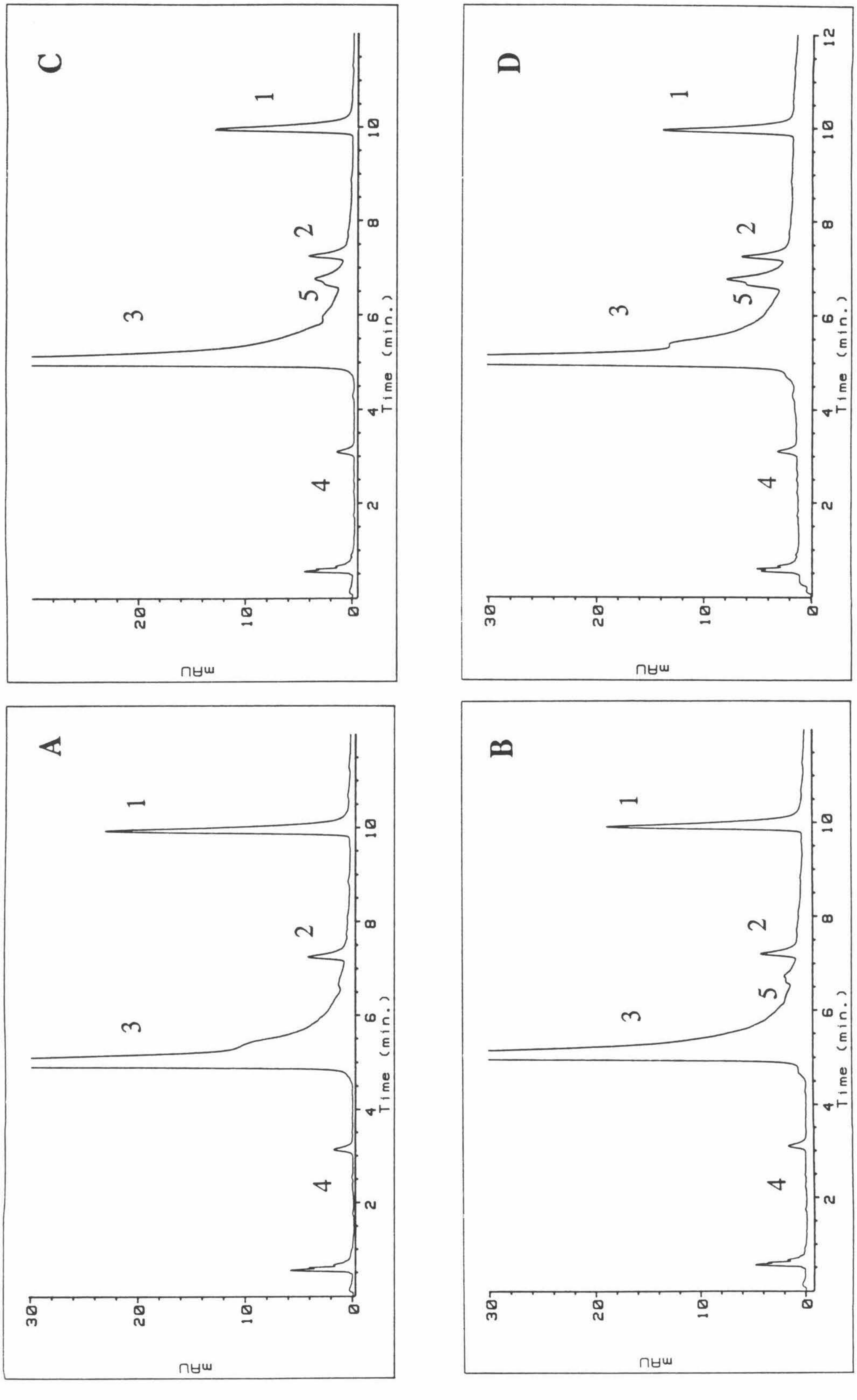
A
B
C
D
mAU
30
20
10
0
Time (min.)
0
2
4
6
8
10
12
1
2
3
4
5

Figure 56: HPLC Chromatogram of the BD/21mer reaction after 168 hours under the conditions described for the previous figure (55). The circled peaks are not characterized.

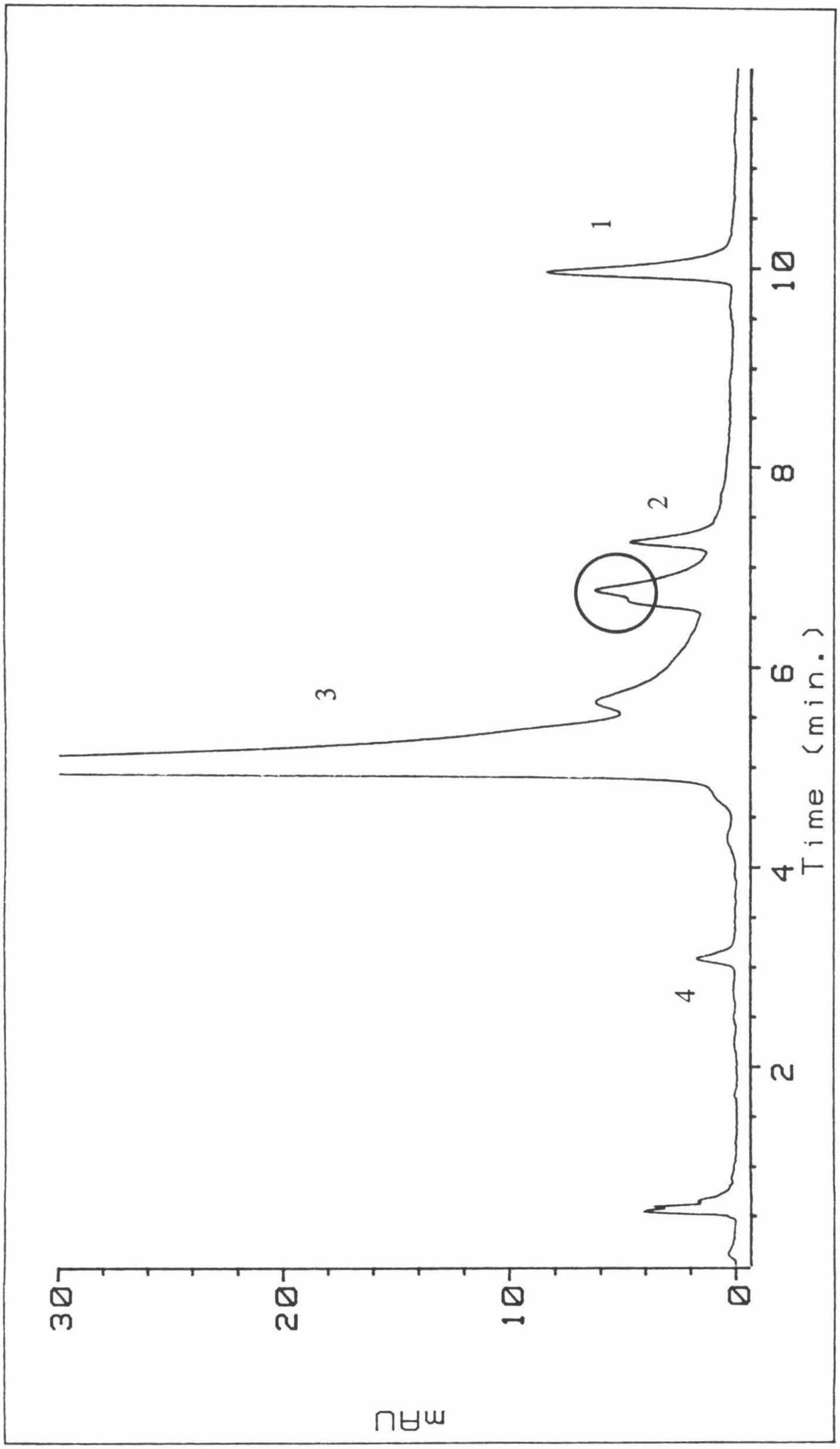
mAU
30
20
10
0
2
4
6
8
10
Time (min.)
1
2
3
4

3. Depurination/Base Release: Alkylation at nitrogen 3 of adenine disrupts the electronic integrity of the DNA base, which leads to labilization and hydrolysis of the N-glycosidic bond.[104-106] The rate at which this bond breaks to release the 3-(Acetyldistamycin)-adenine adduct is dependent on the rate of alkylation and the concentration of the covalent DNA-Distamycin intermediate. Determination of the rate of depurination then requires a cohesive analysis of both steps.

It is proposed that the reaction through depurination involves two consecutive first order rate processes.[107]

$$\mathrm{DNA{\bullet}BD} \xrightarrow{k_1} \mathrm{DNA{-}D} \xrightarrow{k_2} \mathrm{DNA + DA}$$

The characteristics of this type of reaction can be obtained by formulating the rate equations for the appearance and disappearance of the three distamycin reaction species.

$$-d[BD]/dt = k_1[DNA{\bullet}BD]$$

$$d[DNA{-}D]/dt = k_1[DNA{\bullet}BD] - k_2[DNA{-}D]$$

$$d[DA]/dt = k_2[DNA{-}D]$$

Integration of these equations yields the concentrations of each species at any given time.

$$[DNA{\bullet}BD] = [DNA{\bullet}BD]_0\, e^{-k_1 t}$$

$$[DNA{-}D] = [DNA{\bullet}BD]_0 \left\{ \frac{k_1}{k_2 - k_1} \right\} (e^{-k_1 t} + e^{-k_2 t})$$

$$[DA] = [DNA{\bullet}BD]_0 \left\{ 1 + \left(\frac{1}{k_1 - k_2} \right) \left(k_2 e^{-k_1 t} - k_1 e^{-k_2 t} \right) \right\}$$

Iterative fitting of these formulas to the experimental HPLC data was utilized to determine if indeed the reaction is of this type and if so to determine k_2, the rate constant for depurination. To achieve this goal required determination of the concentration of each reaction species at each recorded time point. For the sake of precision, the extinction coefficients for both the reactant, N-bromoacetyldistamycin and product, 3-(acetyldistamycin)-adenine, were determined under the HPLC buffer conditions at which they each eluted (Tables 15 & 16, respectively). This information is critical because the spectra of DA is solvent and pH dependent. At 304 nM the extinction coefficient for BD is 36,500 and for DA it is 26,800. The ratio of the extinction coefficients for DA:BD is 0.73 at this wavelength.

The concentrations of product (DA) and reactant (BD) with respect to the internal standard were determined by the area of the peaks recorded at 304 nm on the HPLC chromatograms. Four unique reactions conducted at initial concentrations of 100 uM 15mer and 10 uM BD in 100 mM NaPhosphate pH 7.0 at 37° C were analyzed. The amounts of each species normalized to the initial concentration of BD (t = 0) are listed in Table 17. The consistent total quantity of DA and BD in solution at any given time supports the earlier conclusion drawn from the carbon 14 labeling experiments that alkylation occurs only at the N3 of adenine in this system (15mer, 37° C). The final product was not detected until after 24 hours. The existence of such an induction period is an indication that the product is not formed directly in the reaction but via some intermediate. The amount of the presumed DNA-distamycin intermediate was determined by subtraction of the relative amounts of reactant, BD, and product, DA, from 1.0. A plot of the average concentration (Table 18) of each compound over time is displayed in Figure 57.

The equation-derived values after iterative fitting, where $k_1 = 1.94 \times 10^{-2}\ h^{-1}$ and k_2

$= 7.76 \times 10^{-2}\ h^{-1}$, are listed in Table 19 and the corresponding graph is displayed in Figure 58. An overlay of the derived and real data points is shown in Figure 59. From these graphical representations it is clear that the equations are obeyed. Therefore the reaction consists of two consecutive first order processes -- first alkylation and then depurination. The derived rate constants indicate that alkylation is the rate determining step of this portion of the cleavage reaction. The balance between the two events reveals the stability of the covalent intermediate. Since the rate constants are relatively close and that of depurination is the greater only a small accumulation of the covalent complex is expected and observed. The amount of the intermediate is initially zero, passes through a maximum at 24 hours and then slowly diminishes. The rate of formation of the adenine adduct is always proportional to the concentration of the intermediate. Therefore, the maximum rate at which the product appears occurs at 24 hours. Thereafter the rate gradually diminishes to zero as the reaction approaches completion.

Table 15: Determination of the Extinction Coefficients of BD Under HPLC Conditions.

Sample	Absorbance (nm) 304	 270	 260
1	0.728	0.443	0.430
2	0.730	0.445	0.433
3	0.732	0.451	0.436
4	0.734	0.445	0.437
Avg	0.731	0.446	0.434
ε	36,500	22,300	21,700

Solvent: 17% Acetonitrile/100 mM Triethyl-ammonium Formate pH 3.1

Table 16: Determination of the Extinction Coefficients of DA Under HPLC Conditions.

Sample	Absorbance (nm) 304	 270	 260	λ_{max}, Ab
1	0.546	0.582	0.485	280, 0.647
2	0.532	0.562	0.467	280, 0.635
3	0.537	0.567	0.474	280, 0.635
4	0.524	0.565	0.474	280, 0.625
Avg	0.535	0.569	0.475	280, 0.636
ε	26,800	28,400	23,800	31,800

Solvent: 11% Acetonitrile/100 mM Triethyl-ammomnium Formate pH 3.1

Table 17: Relative Amounts of Product (DA) and Reactant (BD) over Time.

Time	[BD]	[DA]	[DA] + [BD]
0	1.00	0.00	1.00
12	0.85	--	--
24	0.64	0.22	0.86
36	0.53	0.32	0.85
48	0.42	0.47	0.89
60	0.33	0.54	0.87
72	0.26	0.62	0.88
0	1.00	0.00	1.00
12	0.79	--	--
24	0.69	0.20	0.89
36	0.54	0.33	0.87
48	0.43	0.47	0.90
60	0.33	0.58	0.91
72	0.26	0.64	0.90
0	1.00	0.00	1.00
12	0.79	--	--
24	0.69	0.21	0.90
36	0.53	0.38	0.91
48	0.42	0.48	0.90
60	0.34	0.60	0.94
72	0.27	0.66	0.93
84	0.21	0.73	0.94
0	1.00	0.00	1.00
12	0.79	--	--
24	0.63	0.21	0.84
36	0.50	0.34	0.84
48	0.39	0.44	0.83
60	0.33	0.56	0.89
72	0.26	0.65	0.91

The relative amounts of product (DA) and (BD) were determined by area of the absorbance peak at 304 nm on the HPLC chromatograms. The extinction coefficient of DA = 0.73BD.

Table 18: Relative Amounts of the Reaction Species over Time.

Time hours	[BD]	[DA]	$[BD]_0$ - [BD + DA]
0	1.00	0.00	0.00
12	0.80	---	---
24	0.66	0.21	0.13
36	0.53	0.34	0.13
48	0.42	0.46	0.12
60	0.33	0.57	0.10
72	0.26	0.64	0.10

These are the averaged values of the previous page.

Figure 57: Graph of Relative Amounts of the Reacion Species through Time.

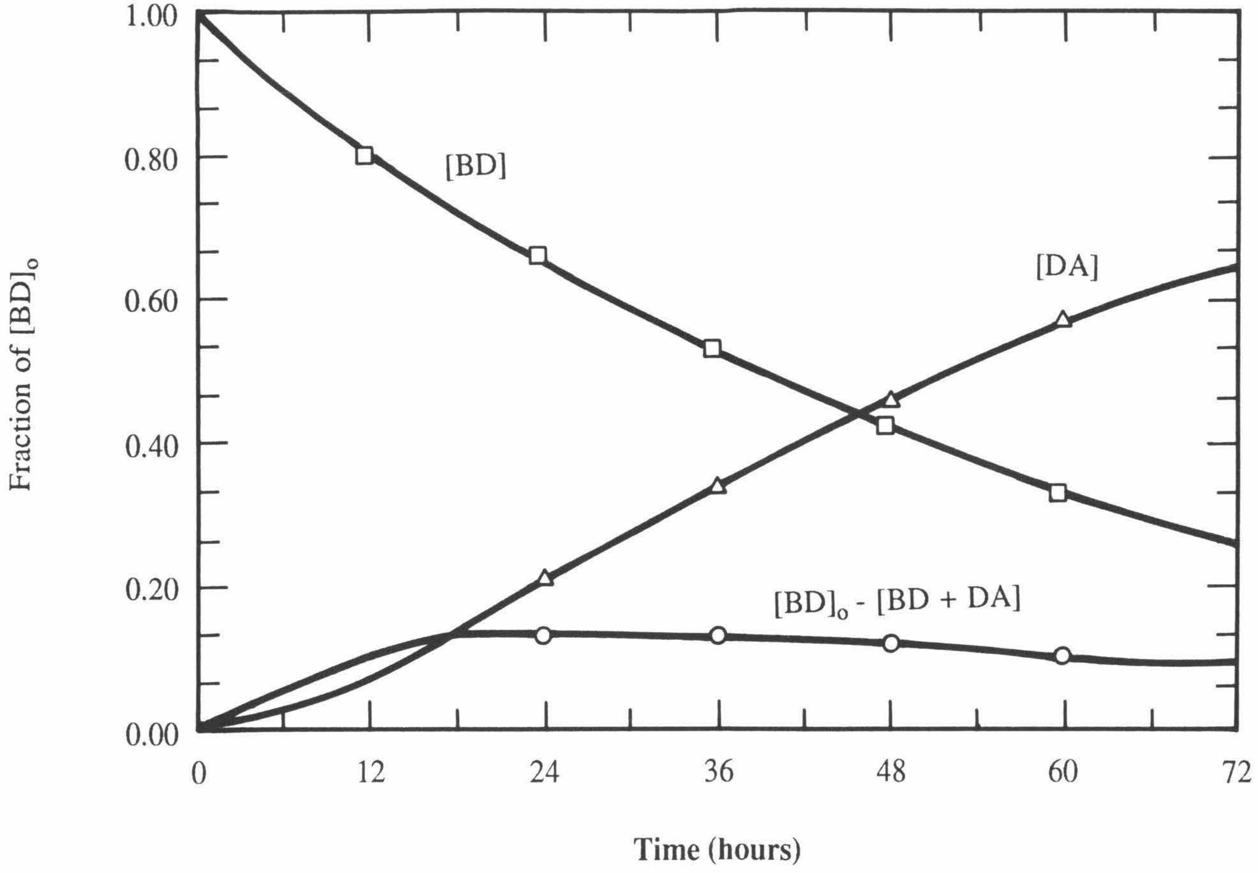

Figure 58: Equation-Derived Graph of the Relative Amounts of the Reaction Species through Time.

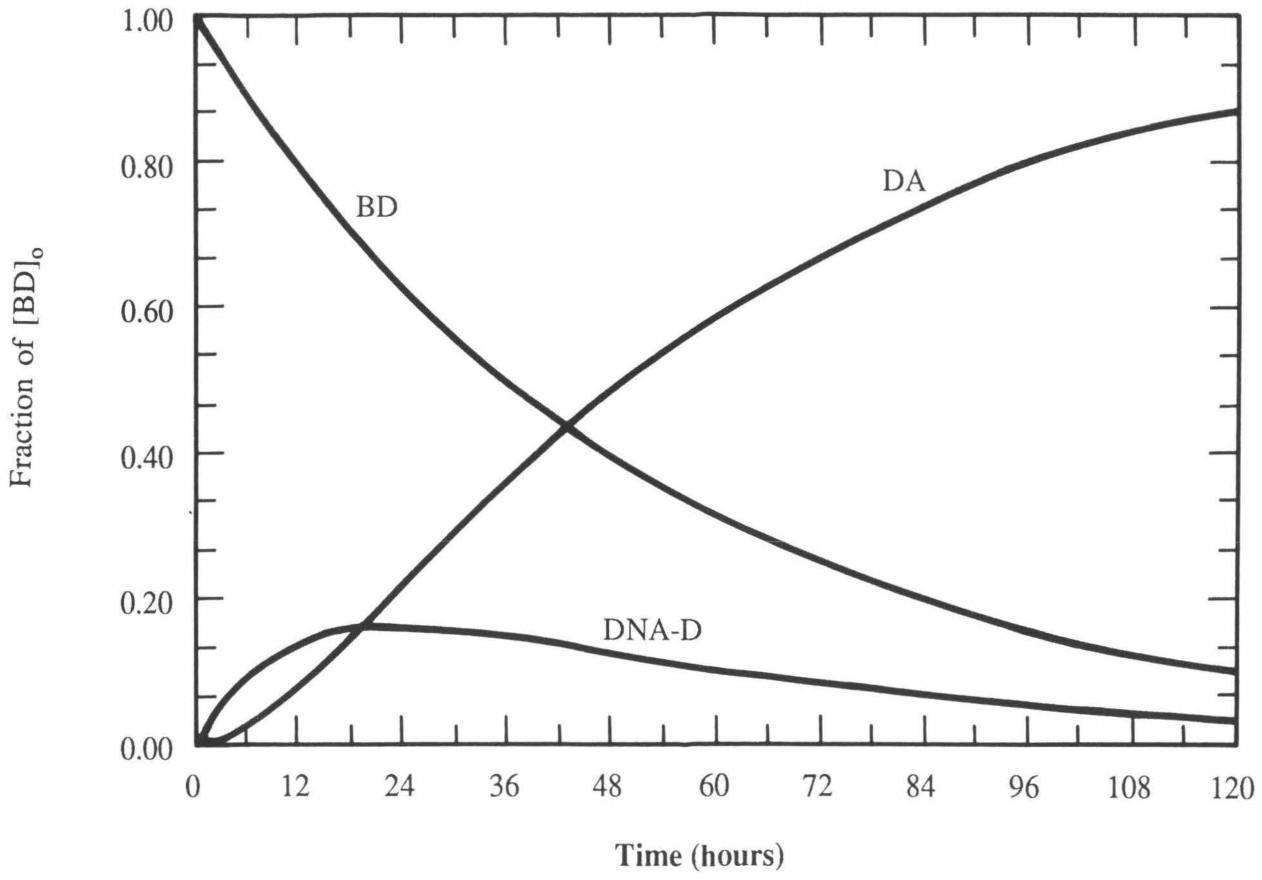

Figure 59: Graph Overlay of Real and Derived Data.

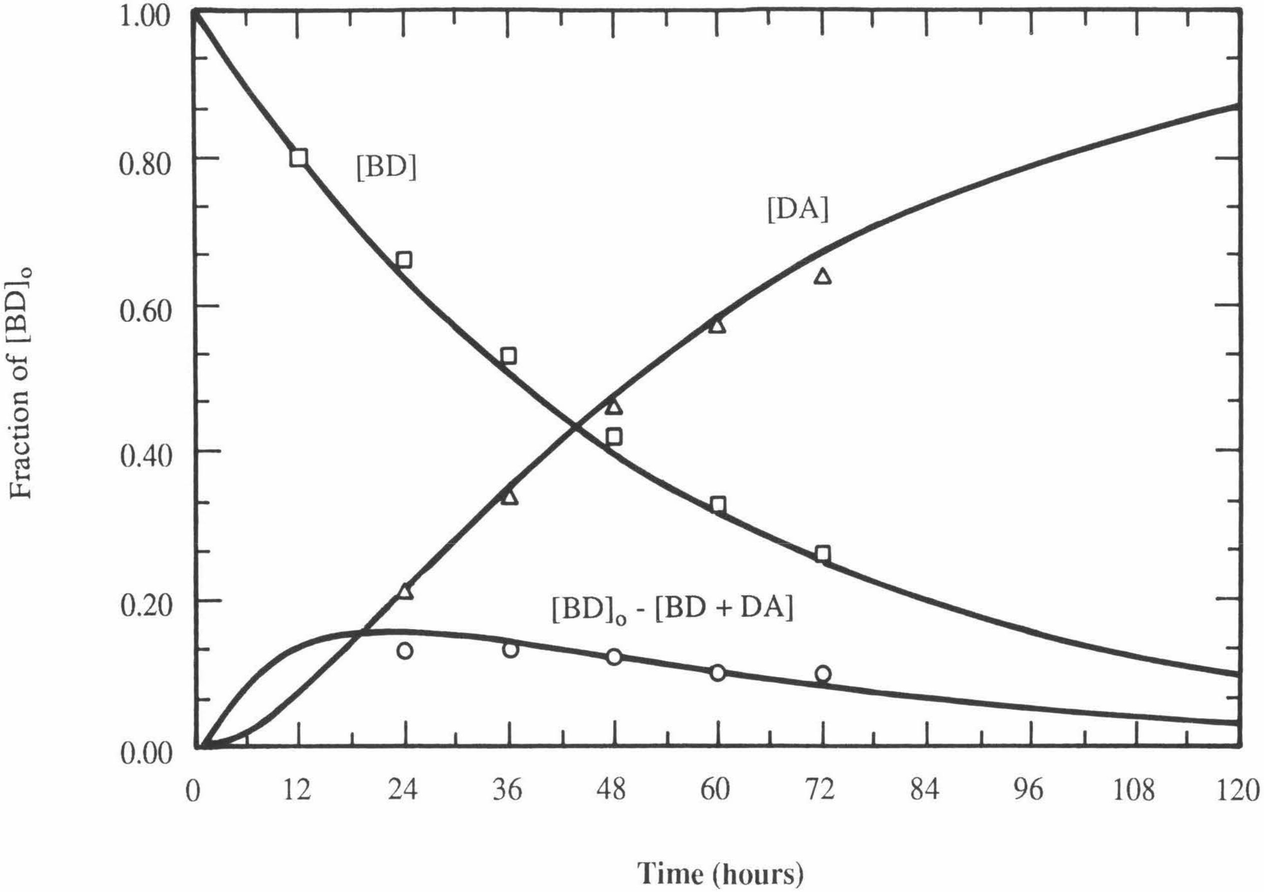

I. A Comparison to CC1065: The cleavage specificities of the synthetic molecule, N-bromoacetyldistamycin, and the natural product, CC1065, were compared on the 167 b.p. restriction fragment. Each compound was allowed to react with the labeled fragment (3' and 5') at 37° C under the same solvent conditions and carrier DNA concentrations as previously described for all other reactions with this restriction fragment (10 mM NaPhosphate pH 7.0, 100 uM b.p. calf thymus DNA). After the specified incubation times , BD (one and 10 hours) and CC1065 (one hour), each reaction mixture was heated for 15 minutes at 90° C in the reaction buffer and then again for 15 minutes at 90° C in 1M piperidine.

Sites of cleavage were determined by high resolution denaturing gel electrophoresis (Figure 60). After one hour we observe a minute amount of cleavage at adenine, base pair #48, by BD. On the other hand, after one hour under the same reaction conditions and workup procedure, CC1065 cleaves the DNA in high yields at 8 adenines and relatively low yields at 13 adenines (Histogram, Figure 61). After ten hours BD approaches the same degree of cleavage at only one adenine as observed with CC1065 after a one hour reaction time (at a multitude of adenines).

Relative to BD, CC1065 is a highly reactive and nonselective DNA cleaving molecule. Though different in chemical structure, BD and CC1065 have similar recognition properties. As evident in the histogram all of the sites of cleavage and thus covalent binding sites of CC1065 lie within or overlap the binding sites mapped out on this restriction fragment for BD by MPE footprinting studies. Therefore the reactivity and cleavage specificity differences are not a consequence of the general type (AT rich regions) of the DNA sequence recognized.

Differences in recognition and reaction exist at the next level of the DNA complexity (the geometry of the base pairs within and around the the site of alkylation) and the small molecule complexity (the spatial positioning of the electrophile relative to the binding moiety and the electrophilic nature of the methylene group).

With regard to the small molecule, if the cyclopropyl group of CC1065 is inherently closer to the floor of the minor groove than the electrophilic methylene of BD, then one would expect a higher degree of reactivity of CC1065 based on the proximity effect. For CC1065 the orientation requirement of the nucleophile and leaving group (colinearity) maybe more attainable based on the configuration of the two reactants upon complexation. We found this to be restricted for BD based on the results obtained for the other halogens in the series. CC1065 has strain energy to destabilize the reactant and resonance to stabilize the product, whereas BD has only the inductive effects of the electronegative atom to activate the methylene group.

Any difference in the binding affinity for different sites is not reasonably accounted for by the sites and efficiency of cleavage via alkylation by BD or CC1065. For example, if we compare DE (Distamycin-EDTA) and BD, we find that the cleavage pattern of DE is more intense at binding site #3, 5' AAATT, than the one where BD executes its preferential cleavage, binding site #2, 5' GTTTA. DE's ability to cleave the DNA is not dependent upon the correct juxtapositioning of a specific base or atom of the DNA with the cleaving moiety, a nonsequence specific diffusable oxidant. Therefore, it seems that the binding affinity for site #3 is greater, but the difference from site #2 is not significant enough to counter the relative rates of alkylation at adenine 48 and 58 by BD. Also, recall from the introduction of CC1065 that Hurley and coworkers have been unable to footprint the nonreactive analog of this natural product, which implies a lower binding constant than MPE (10^5). The apparently lower binding constant of CC1065 might also contribute to its lack of cleavage specificity relative to BD.

Figure 60: Comparison of the cleavage sites of CC1065 to BD on the 167 b.p. restriction fragment. Odd and even numbered lanes are DNA end labeled with ^{32}P at the 5' and 3' positions respectively. All reactions are 100 uM b.p. calf thymus DNA, 5 uM cleaving reagent in 10 mM NaPhosphate pH 7.0.

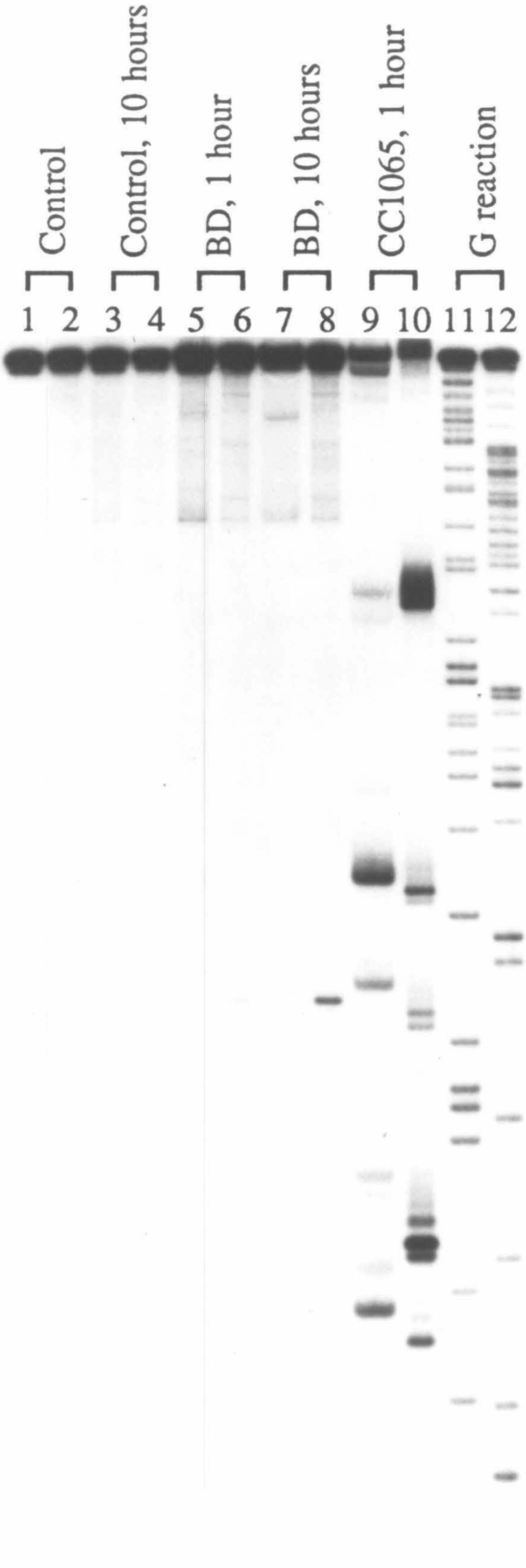
Control
Control, 10 hours
BD, 1 hour
BD, 10 hours
CC1065, 1 hour
G reaction
1
2
3
4
5
6
7
8
9
10
11
12

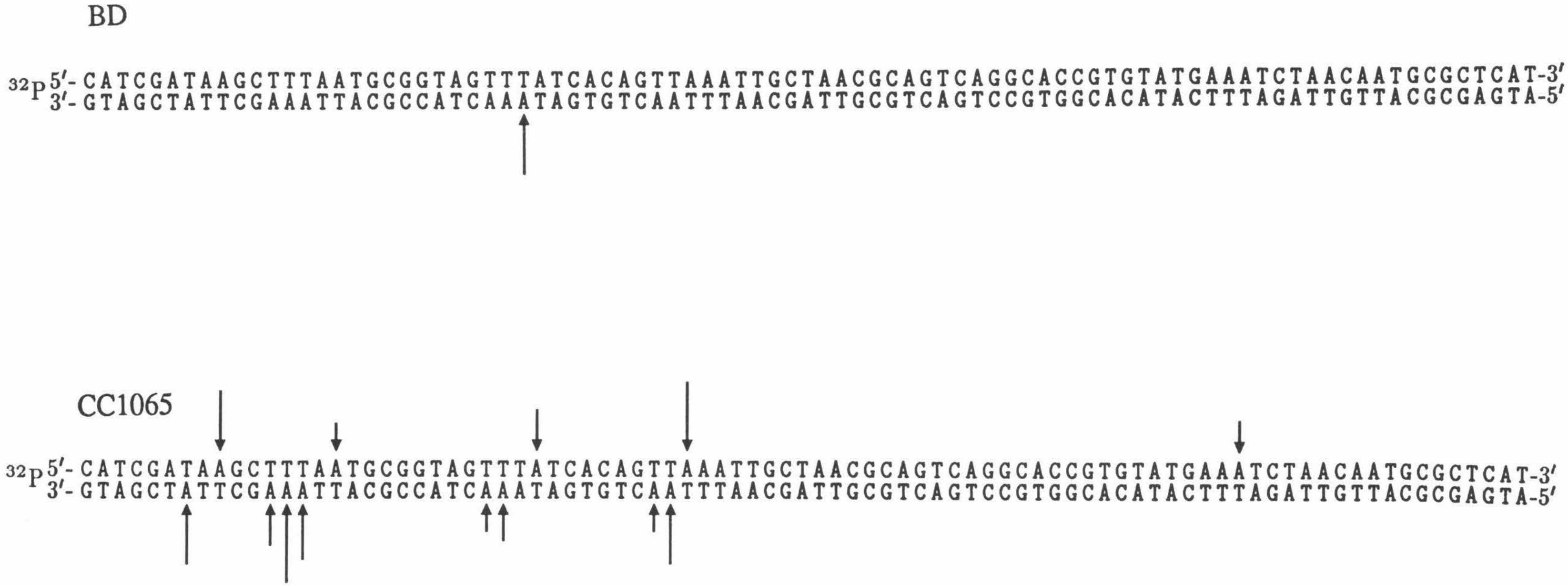
BD
^{32}P 5′- CATCGATAAGCTTTAATGCGGTAGTTTATCACAGTTAAATTGCTAACGCAGTCAGGCACCGTGTATGAAATCTAACAATGCGCTCAT-3′
3′- GTAGCTATTCGAAATTACGCCATCAAATAGTGTCAATTTAACGATTGCGTCAGTCCGTGGCACATACTTTAGATTGTTACGCGAGTA-5′
CC1065
^{32}P 5′- CATCGATAAGCTTTAATGCGGTAGTTTATCACAGTTAAATTGCTAACGCAGTCAGGCACCGTGTATGAAATCTAACAATGCGCTCAT-3′
3′- GTAGCTATTCGAAATTACGCCATCAAATAGTGTCAATTTAACGATTGCGTCAGTCCGTGGCACATACTTTAGATTGTTACGCGAGTA-5′

Figure 61: Histogram of sites of cleavage of CC1065 and BD between base pairs 22 and 108 of the pBR322 plasmid. Arrows indicate sites of DNA cleavage resulting from the reaction of BD (10 hours at 37° C) and CC1065 (1 hour at 37° C) on the 167 b.p. restriction fragment.

Conclusion

In conclusion, the attachment of a cleaving moiety to a DNA binding unit creates a synthetic DNA cleaving reagent. The cleavage specificity is determined by both the binding unit and the cleaving moiety. The first generation of this family of double helical DNA cleaving reagents was methidiumpropyl-EDTA(Fe-II), (MPE), Figure 62. This synthetic molecule displayed low cleavage specificity since both the binding unit (an intercalator with low sequence specificity) and the cleaving moiety (a diffusible oxidant) are nonspecific. For this reason MPE is useful for DNA footprinting, a technique which determines the binding sites of small molecules and proteins on double helical DNA.

In the next generation of synthetic compounds, a higher degree of DNA cleavage specificity was achieved by attachment of the nonspecific EDTA cleaving moiety to a sequence specific binding unit, tri-N-methylpyrrolecarboxamide, to give distamycin-EDTA (Fe-II), (DE), Figure 62. This type of design is useful for determining the sequence specificity and recognition elements of the DNA binding unit.

In the third generation, this thesis, an even higher degree of DNA cleavage specificity was achieved by attachment of a nondiffusible cleaving moiety, an electrophile, to the sequence specific binding unit, tri-N-methylpyrrolecarboxamide, to yield N-bromoacetyl- distamycin, (BD), Figure 62. From the point of view of designing a highly specific DNA cleaving molecule, this combination of a nondiffusible sequence-specific DNA cleaving element with a sequence-specific DNA binding element affords a highly discriminating DNA cleaving molecule.

The difference in the DNA cleavage specificity of DE and BD and the MPE footprints of distamycin A and BD on the 167 base pair restriction fragment are shown in the form of a histogram in Figure 63.

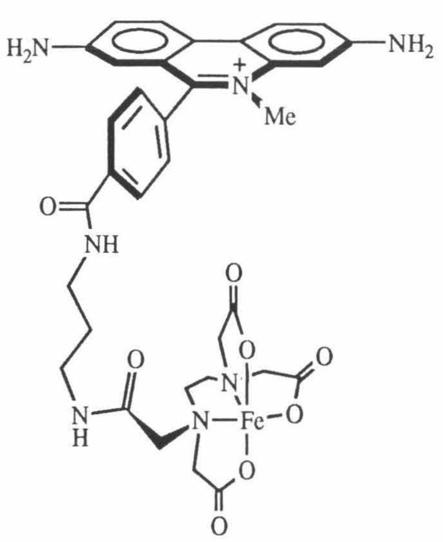

Methidiumpropyl EDTA-Fe(II)

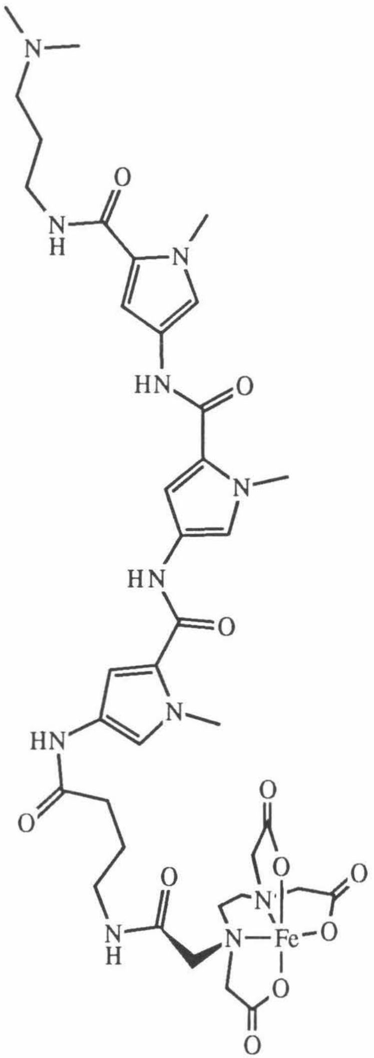

Distamycin EDTA-Fe(II)

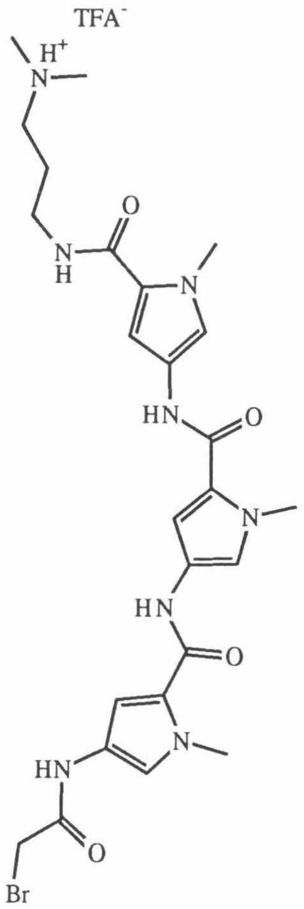

N-Bromoacetyldistamycin

Figure 62

Figure 63: Base pairs 22-108 on the 167 b.p. restriction fragment (Eco RI/Rsa I) from pBR322 plasmid. *Top row*, MPE-Fe(II) footprints of distamycin A at 5 uM concentration (37°C). Histograms on each strand represent region on the 5' and 3' ^{32}P end labeled DNA restriction fragment protected by distamycin A (D) from cleavage by MPE-Fe(II). *Second row*, Cleavage of the same DNA fragment by DE-Fe(II) at 5 uM concentraiton (37°C). *Third row*, Major sites of DNA cleavage resulting from the reaction with BD at 5 uM concentration after 10 h at 37°C. *Fourth row*, MPE-Fe(II) footprints of BD at 5 uM concentration (37°C). Asymmetric histograms on each strand represent regions on the 5' and 3' ^{32}P end labeled DNA restriction fragment protected by BD from cleavage by MPE-Fe(II). Boxes in all rows are equilibrium binding sites of the tripeptide (D, DE, BD) whose assignment is based on the MPE-Fe(II) footprinting and affinity cleaving models.

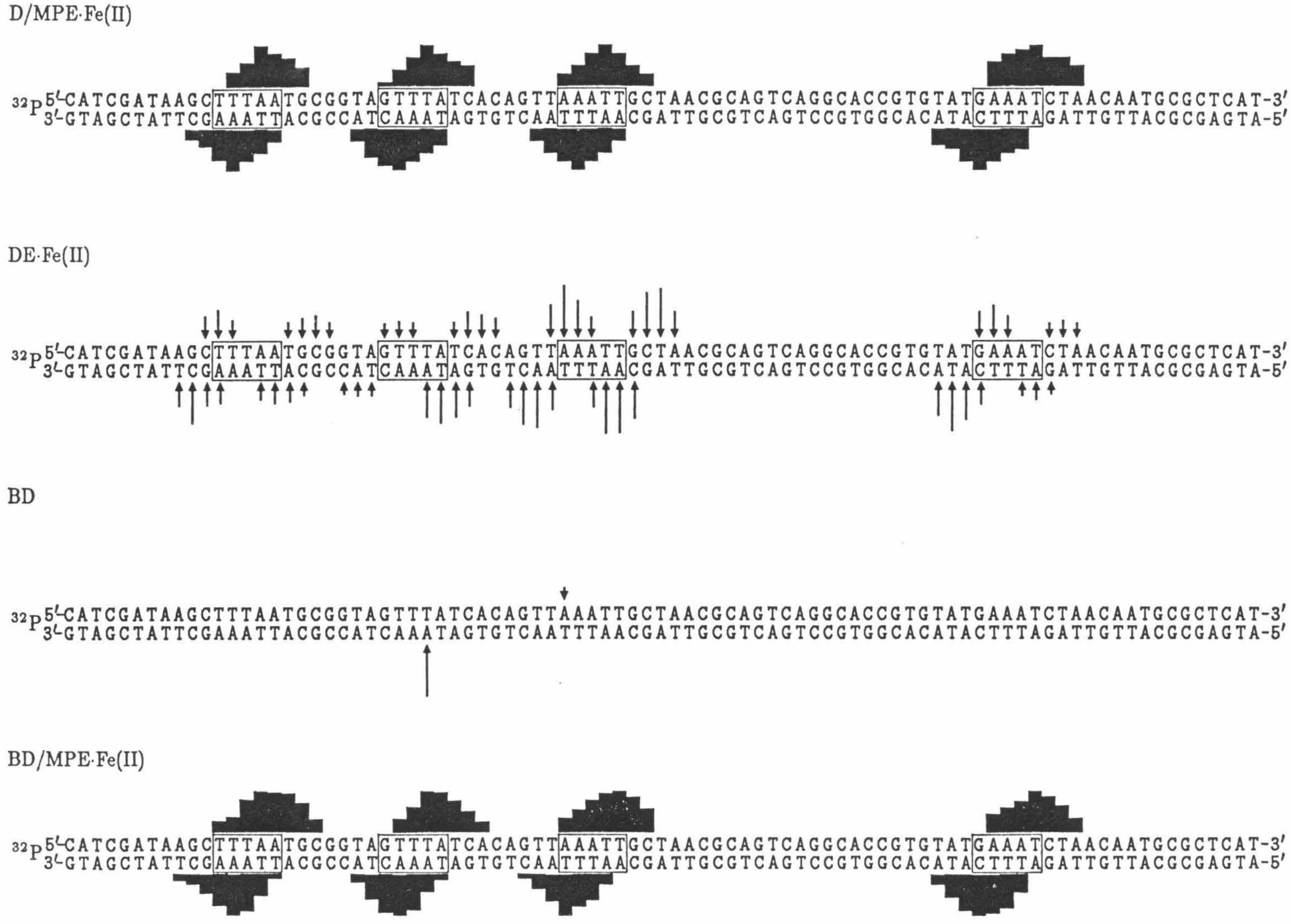
D/MPE·Fe(II)
32P 5′-CATCGATAAGCTTTAATGCGGTAGTTTATCACAGTTAAATTGCTAACGCAGTCAGGCACCGTGTATGAAATCTAACAATGCGCTCAT-3′
3′-GTAGCTATTCGAAATTACGCCATCAAATAGTGTCAATTTAACGATTGCGTCAGTCCGTGGCACATACTTTAGATTGTTACGCGAGTA-5′
DE·Fe(II)
32P 5′-CATCGATAAGCTTTAATGCGGTAGTTTATCACAGTTAAATTGCTAACGCAGTCAGGCACCGTGTATGAAATCTAACAATGCGCTCAT-3′
3′-GTAGCTATTCGAAATTACGCCATCAAATAGTGTCAATTTAACGATTGCGTCAGTCCGTGGCACATACTTTAGATTGTTACGCGAGTA-5′
BD
32P 5′-CATCGATAAGCTTTAATGCGGTAGTTTATCACAGTTAAATTGCTAACGCAGTCAGGCACCGTGTATGAAATCTAACAATGCGCTCAT-3′
3′-GTAGCTATTCGAAATTACGCCATCAAATAGTGTCAATTTAACGATTGCGTCAGTCCGTGGCACATACTTTAGATTGTTACGCGAGTA-5′
BD/MPE·Fe(II)
32P 5′-CATCGATAAGCTTTAATGCGGTAGTTTATCACAGTTAAATTGCTAACGCAGTCAGGCACCGTGTATGAAATCTAACAATGCGCTCAT-3′
3′-GTAGCTATTCGAAATTACGCCATCAAATAGTGTCAATTTAACGATTGCGTCAGTCCGTGGCACATACTTTAGATTGTTACGCGAGTA-5′

Experimental

Reagents and Materials. Silica gel 60 (230-400 mesh) was from EM Science. Dimethylformamide was HPLC grade from Burdick and Jackson and dried over 3 å molecular sieves. Adenine was from Sigma. Bromoacetic-[2-^{13}C]-acid (99.8% ^{13}C) was from MSD Isotopes. Bromo-[2-^{14}C]-acetic acid (Code CFA.18, Batch 51, 52mCi/mmol), [1-^{14}C]-glycolic acid, sodium salt (Code CFA.167, Batch 32, 8.8 mCi/mmol), [1-^{14}C]-acetic anhydride (CFA.86, Batch 212, Specific Activity 30 uCi/umole) were from Amersham. $H^{15}NO_3$ (99.9% enriched) was from Merck Sharpe and Dohme. Calf thymus DNA (Sigma: Type 1, Sodium Salt, "Highly Polymerized"). Enzymes were from Boehringer Mannheim. CC1065 was a gift from the UpJohn Company (Dr. Wendell Wierenga). Reagents for oligonucleotide synthesis were from Beckman. All other reagents were from Aldrich.

Instrumentation. Infrared spectra were recorded on a Shimadzu model IR-435 infrared spectrometer. Mass spectra (high resolution positive ion fast atom bombardment) were done at the Midwest Center for Mass Spectrometry at the University of Nebraska. UV-vis spectra were obtained on a Beckman Model 25 UV-Vis spectrophotometer and a Perkin-Elmer Lambda 4C UV/Vis spectrophotometer. Proton, carbon, and nitrogen NMR spectra were acquired from a JEOL GX400 and are recorded in parts per million internally from tetramethylsilane (proton), dimethyl sulfoxide (carbon), and externally from 1M $Na^{15}NO_3$ (nitrogen). The ^{15}N3 adenine adduct experiments utilized the G40T10 probe, a pulse delay of 5 sec, a pulse width of 45 usec, and were proton decoupled w/o NOE. The ^{15}N6 adduct experiments utilized the G40MU probe, a pulse delay of 1.0 sec, pulse width of 135 usec, and were proton coupled w/o NOE.

A Beckman System 1 Plus DNA Synthesizer was utilized for synthesis of oligonucleotides.

Semipreparative high pressure liquid chromatography was performed with two Altex 110A pumps, an Altex model 420 controller, a Beckman model 165 variable wavelength two channel detector and a Spectra Physics two channel integrator. Fast protein liquid chromatography (FPLC) of synthetic oligonucleotides was performed with two Pharmacia P-500 pumps, an LCC-500 controller, UV-2 dual path monitor and Frac-100 fraction collector.

Kinetics and Thermodynamics: Temperature was controlled and maintained in an aluminum alloy box (6 cm x 6 cm) within a Forma Scientific Model 2006 temperature bath. Weight measurements were done on a Sartorious Microbalance, Model 4504MP8, which reads down to 0.1 ug and is accurate and stable at 1 ug. UV absorbances were obtained on a Perkin Elmer Lambda 4C UV/Vis spectrophotometer. Equilibrium dialysis was done with a 5 Cell Equilibrium Dialyzer obtained from Spectrum. Scintillation counting was conducted on the Beckman 3801 system, for which samples were dissolved in Beckman Ready-Solv MP aqueous scintillation cocktail. The Hewlett Packard HP1090M work station was utilized for high pressure liquid chromatography (ternary solvent capabilities), peak detection (photodiode array dector) and data storage and analysis (peak area and height). Densitometry was performed by an LKB Ultroscan XL laser densitometer.

Synthesis of P3 Amine (2). A solution of 0.5 grams of **1** in 250 ml of dimethyl formamide was hydrogenated over 100 mg of 5% Pd/C at atmospheric pressure for 12 hours. The mixture was filtered through Celite.[1] Solvent was removed under vacuo and the amine **2** was flash chromatographed using 35% $MeOH/CH_2Cl_2$ saturated with ammonia: ^1H NMR ($MeSO_2$-d_6) δ 1.64 (m,2), 2.20 (s,6), 2.32 (t,2), 3.19 (m,2), 3.74 (s,3), 3.81 (s,3), 3.84 (s,3), 6.28 (d,1), 6.39 (d,1), 6.84 (d,1), 7.02 (d,1), 7.20 (d,1), 7.22 (d,1), 8.10 (t,1), 9.64 (s,1), 9.90 (s,1); IR (KBr) 3300, 3100, 1640, 1580, 1520, 1462, 1430, 1400, 1345, 1258, 1200, 1100, 1050; m/z 469.267.

Synthesis of the TFA mixed anhydride[2] (4). Bromoacetic acid is recrystallized with ether/hexane (1:10), the triflouroacetic anhydride is distilled, and the diethyl ether is freshly distilled from $LiAlH_4$. A one to one mixture (10 mM) of the anhydride and the acid is stirred at room temperature in diethyl ether for one hour. The solvent is removed. The syrup is redissolved in ether/pet ether (1:1) and reconcentrated several times. The mixed anhydride is crystallized by adding first diethyl ether, then petroleum ether (1:1), followed by cooling in dry ice for one to five minutes. Solvent is poured off and the needles are recrystallized with the same solvents. The crystals are dried under vacuum and stored at -20°C: H1 NMR ($CDCl_3$) **4a** δ 4.03 (s,2); **4b** δ 4.24 (s,2); **4c** δ 3.77 (s,2).

Synthesis of N-Haloacetyldistamycin (3). To a stirring solution of the trifluoroacetic mixed anhydride **4** (5mM in CH_2Cl_2 at 0° C under argon) 0.83 equivalents of the amine **2** (100mM in CH_2Cl_2) was added. The reaction was stirred for five minutes. One equivalent of triflouroacetic acid was added. After five minutes the reaction was quantitative by TLC (1.5% NH_4OH/MeOH). The product was precipitated from solution with diethyl ether then washed several times with ether by centrifugation. Complete removal of ether was done under vacuum. The white solid is stored at -20 degrees or less. Yield 60%.

N-Bromoacetyldistamycin (3a). ^{1}H NMR (MeSO$_2$-d$_6$) δ 1.84 (m,2), 2.80 (s,6), 3.08 (m,2), 3.25 (m,2), 3.82 (s,3), 3.85 (s,6), 3.98 (s, 2), 6.94 (s,2), 7.06 (d,1), 7.18 (d,1), 7.20 (d,1), 7.24 (d,1), 8.17 (t,1), 9.40 (br s,1), 9.92 (s,1), 9.95 (s,1), 10.36 (s,1); UV max (H$_2$O) 242, 303 (ε 35000); IR (KBr) 3300, 1640, 1580, 1530, 1460, 1430, 1400, 1260, 1200, 1170, 1130, 1105; m/z 591.187.

N-Chloroacetyldistamycin (3b). ^{1}H NMR (MeSO$_2$-d$_6$) δ 1.84 (m,2), 2.79 (s,6), 3.07 (m,2), 3.25 (m, 2), 3.82 (s,3), 3.85 (s,6), 4.19 (s,2), 6.94 (d,1), 6.95 (d,1), 7.06 (d,1), 7.18 (s,1), 7.20 (s,1), 7.24 (s,1), 8.17 (t,1), 9.45 (br s,1), 9.92 (s,1), 9.95 (s,1H), 10.29 (s,1); H1 NMR (D$_2$O) δ 1.76 (m,2), 2.61 (s,6), 2.86 (m,2), 3.14 (m,2), 3.44 (s,3), 3.47 (s,3), 3.48 (s,3) 3.85 (s,2), 6.32 (s,1), 6.36 (s,1), 6.40 (s,1), 6.67 (s,1), 6.70 (s,1), 6.72 (s,1); ^{13}C NMR - peak assignments and coupling constants were determined by analysis of the INEPT multipulse sequence spectrum (Me$_2$SO$_2$-d$_6$) δ 24.72 (1, acetyl, $^1J_{C\text{-}H}$=129 Hz), 35.52 (1, aliphatic chain, $^1J_{C\text{-}H}$=140 Hz), 35.98, 36.06, 36.14 (3, N-methyl, pyrrole, $^1J_{C\text{-}H}$=132 Hz), 42.18 (2, N,N-dimethyl, aliphatic chain, $^1J_{C\text{-}H}$=142 Hz), 42.95, 54.71 (2, aliphatic chain, adjacent to nitrogens, $^1J_{C\text{-}H}$=151,142 Hz), 103.87, 104.18, 104.45, 117.69, 118.03, 118.11 (6, tertiary, pyrrole,$^1J_{C\text{-}H}$=176,191 Hz), 120.80, 121.64, 121.82, 122.15, 122.35, 122.67 (6, quaternary, pyrrole), 157.73, 157.90, 161.01, 162.40 (4C, amide); UV max (H2O) 240, 302 (ε 35000); IR (KBr) 3300, 1680, 1640, 1580, 1530, 1460, 1430, 1400, 1260, 1200, 1170, 1130, 1105; m/z 545.24.

N-Iodoacetyldistamycin (3c). ^{1}H NMR (MeSO$_2$-d$_6$) δ 1.84 (m,2), 2.79 (s,6), 3.08 (m,2), 3.25 (m,2), 3.79 (s,2), 3.82 (s,3), 3.85 (s,6), 6.92 (d,1), 6.95 (d,1), 7.06 (d,1), 7.17 (s,1), 7.18 (s,1), 7.23 (s,1), 8.16 (t,1), 9.34 (br s,1), 9.91 (s,1),9.94 (s,1), 10.29 (s,1); UV max (H$_2$O) 240, 304 (ε 35000); IR (KBr) 3300,1640, 1580, 1540, 1465, 1435, 1405, 1260, 1200, 1175, 1130, 1105; m/z 637.173.

Synthesis of N-Hydroxydistamycin (5). 7.5 mg of glycolic acid and 13 mg of N-hydroxytriazole were mixed in 1 ml of DMF for five minutes. 45 mg in 0.75 ml of DMF of the amine **2** was added followed by 24 mg of of dicyclohexylcarbodiimide. The reaction was stirred at room temperature for six hours. The DMF was removed under vacuum. The product was purified by flash chromatography with 15%MeOH/CH$_2$Cl$_2$ saturated with ammonia to yield 43 mg of **5** (86%): ^{1}H NMR (Me$_2$SO-d$_6$) δ *1.65* (q,2), 2.24 (s,6), 2.38 (t,2), 3.19 (quartet,2), 3.80 (s,3), 3.83 (s,3), 3.84 (s,3), 3.95 (d,2), 5.59 (t,1), 6.84 (d,1), 7.04 (s,2), 7.18 (d,1), 7.20 (d,1), 7.24 (d,1), 8.09 (t,1), 9.66 (s,1), 9.89 (s,1), 9.92 (s, 1); UV max (H$_2$O) 235, 303 nm; m/z 527.23.

Synthesis of N-Mesylacetyldistamycin (6). 3 mg of N-hydroxydistamycin **5** was dissolved in 2 ml of acetonitrile/pyridine (1:1). The solution was cooled to 0°C then 200 uL of methane sulfonyl chloride (450 equivalents) was added. The reaction was complete within a few minutes. Product was precipitated by addition of diethyl ether. Solvent was removed and the compound dried under vacuo. ^{1}H NMR (Me_2SO-d_6) δ 2.15 (m,2), 3.02 (d,6), 3.33 (m,2), 3.54 (m,2), 4.07 (s,3), 4.14 (s,6), 4.48 (s,1), 5.08 (s,1), 7.20 (s,1), 7.22, 7.26 (d,1), 7.33 (s,1), 7.46 (s,1), 7.48 (s,1), 7.52 (s,1), 10.16 (br s,1), 10.20 (s,1), 10.25 (s,1), 10.54, 10.65 (d,1).

Synthesis of N-[2-Bromoacetamido]-N'N'-dimethyl-1,3-propane diamine (7). 2.5 ml of N'N'-Dimethyl-1,3-propane diamine and 1.7 ml of Bromoacetylbromide (20:20 mmoles) were added simultaneously to 40 ml of acetonitrile at 0°C over a ten minute time period via two addition funnels. To crystallize, one equivalent (with respect to solvent) of diethyl ether was added. The solution was kept at room temperature until the emulsion had dissipated and then placed in the refrigerator overnight. The solvent was poured off and the needles were washed with dry diethyl ether and dried under vacuo: ^{1}H NMR (Me_2SO-d_6) δ 1.80 (m,2), 2.78 (d,6), 3.06 (q,2), 3.15 (q,2), 3.90 (s,2), 8.52 (t,1), 9.53 (br s,1); IR (KBr) 3250, 3060, 2940, 2690, 2470, 1650, 1562, 1315, 1210, 980; m/z 223.04.

Synthesis of N-Bromo-[2-^{13}C]-acetyldistamycin (8). The same procedure as for **3** was utilized, except the mixed anhydride **3** was 99.8 % enriched at carbon 2 of the bromoacetyl fragment: ^{1}H NMR (Me_2SO-d_6) δ 1.82 (m,2), 2.78 (d,6), 3.06 (br s,2), 3.24 (m,2), 3.77:4.16 (d,2, $^1J_{H\text{-}C}$=153.9 Hz), 3.80 (s,3), 3.84 (s,6), 6.93 (s,2), 7.04 (s,1), 7.16 (s,1), 7.18 (s,1), 7.22 (s,1), 8.16 (t,1),9.25 (br s,1), 9.90 (s,1), 9.93 (s,1), 10.34 (s,1); ^{13}C NMR (Me_2SO-d_6) δ 29.78; m/z 590.191.

Synthesis of N-Bromo-[2-^{14}C]-acetyldistamycin (9). 60 umoles of bromo-[2-^{14}C]-acetyltrifluoroacetic mixed anhydride **4** (0.5 uCi/umole synthesized from Bromo-[2-^{14}C]-Acetic Acid) in 0.5 ml in CH_2Cl_2 was added to 50 umoles of the amine **2** in 5 mLof CH_2Cl_2 at 0° C under argon. After two minutes 100 uL of triflouroacetic acid was added. Solvent was removed. The residue was taken up into 0.5 mL of methanol and 0.5 mL of dichloromethane. 10 mL of diethyl ether was quickly added. 28 mg of the white precipitate was collected and washed with ether by centrifugation Yield 80%: ^{1}H NMR (Me_2SO-d_6) δ 1.84 (m, 2), 2.78 (s, 6), 3.06 (m, 2), 3.23 (m, 2), 3.80 (s,3), 3.84 (s, 6), 3.97 (s,2), 6.94 (s,2), 7.04 (d,1), 7.16 (d,1), 7.19 (d,1), 7.22 (d,1), 8.17 (t, 1), 9.23 (br s, 1), 9.91 (s, 1), 9.94 (s, 1), 10.34 (s, 1).

Synthesis of N-Hydroxy-[1-^{14}C]-acetyldistamycin (10). 5.68 umoles of the [1-^{14}C]-glycolic acid, sodium salt was transferred in water to a three mL reaction vial. The water was removed by lyopholization. One equivalent each (5.68 umoles) of the amine **2**, n-Hydroxybenzotriazole, and dicyclohexylcarbodiimide in dichloromethane was added to the vial giving a total volume of 400 uL. Approximately one mg of 18-Crown-6 ether was added. After five hours an additional 6 umoles of both DCC and nHBT was added. After 20 hours the solvent was removed and the reaction mixture was flash chromatographed through a pipette using 15% MeOH/CH_2Cl_2 saturated with ammonia to yield 2.5 mg (84%) of **10** (8.8 uCi/umole).

Synthesis of [1-^{14}C]-Acetyldistamycin (11). 9 umoles of the amine **2** and 80 umoles of triethylamine in approximately 2 mL of dichloromethane was placed inside and at the sealed end of the enclosed ampoule containing 8.3 umoles of [1-^{14}C]-acetic anhydride. The seal was broken with a glass rod and the solution poured into the previously evacuated ampoule. An additional eight umoles of the tripeptide amine was added. The reaction mixture was removed by pipette, the solvent was carefully removed and the product was isolated by preparative thin layer chromatography, 1% NH_4OH/MeOH. Verification of the product was determined by cospotting on TLC the characterized unlabeled N-acetyldistamycin.

Synthesis of 2,4,5-Tribromoimidazole (12).[65] In a two liter three neck round bottom flask 120 grams of imidazole is suspended into 720 mL of chloroform. The imidazole does not dissolve completely. The solution is then cooled to 0°C, stirred, and continuously flushed with argon (the argon exits through a 1M NaOH base bath before exposure to the atmosphere). 84 mL of bromine in 320 mL of chloroform is added dropwise by an addition funnel over a period of one hour. Upon addition of the bromine the imidazole completely goes into solution. After 10 minutes an orange precipitate appears. After completion of addition the precipitate is collected by filtration through a Büchner funnel. The solid is then washed and soaked with water to remove the excess Br_2. The collected product is recrystallized with glacial acetic acid and washed with cold glacial acetic acid. Addition of water to the acid supernatant from the initial crop yields more of the 2,4,5-Tribromoimidazole. Overall yield is 86.5 grams (30%): mp 218° C.

Synthesis of 4-Bromoimidazole (13).[65] 100 grams of **12** and 250 grams of Na_2SO_3 are refluxed in 900 mL of water for two hours. At this time another 100 grams of Na_2SO_3 is added. The mixture is refluxed for an additional two hours. The solution is cooled and transferred to a four liter separatory funnel. A precipitate may form at this step which is the product and should be removed by filtration. The remaining product is extracted from the aqueous solution with ether. Overall yield is 25 grams (52%): mp

131-132°C; ^{1}H NMR (Me_2SO-d_6) δ 7.28 (s,1), 7.67 (s,1).

Synthesis of 4-Bromo-5-[^{15}N]-nitroimidazole (14)[66] 2.33 grams of **13** is dissolved into 12 mL of ethanol. The solution is cooled to 0°C. One gram of $H^{15}NO_3$ is carefully added dropwise with a disposable pasteur pipette. A white precipitate forms. The solvent is removed. The white precipitate is carefully redissolved into 12 mL of concentrated H_2SO_4 and heated at 90° C for one hour. The reaction is then cooled to 0° C. Upon dilution with ice water, an off-white precipitate forms, which is collected and washed with water by filtration. The product is dried under vacuum to yield 2.6 grams (85%). Another batch of this compound was synthesized under the same procedure with 11.41 gram of **13** and 5 grams of $H^{15}NO_3$. Yield 12.9 grams (86%): mp 279° C. ^{1}H NMR (Me_2SO) δ 8.00 (s, 1).

Synthesis of 1-Benzyl-4-bromo-5-[^{15}N]-nitroimidazole (15).[67] 15.5 grams of **14** is dissolved into 160 ml of dimethyl formamide (dried over 3å molecular sieves). 16 mL of benzyl bromide is added. The reaction mixture is refluxed for three hours. It is then cooled to 125° C for seven hours. The solvent is removed by rotovap under vacuum. The residue is washed with water and recrystallized from ethanol. Filtration glassware must be hot to execute an effective transfer. Yield 16 grams (56%): mp 141-142° C. ^{1}H NMR (Me_2SO-d_6) δ 5.49 (s,2), 7.20-7.41 (m, 5), 8.25 (s, 1).

Synthesis of 1-Benzyl-4-[^{15}N]-nitro-5-cyanoimidazole (16)[67] 14.65 grams of **15** is dissolved into 300 mL of methanol. 6.63 grams of potassium cyanide and 0.85 gram of postassium iodide is added. The reaction mixture is refluxed for five hours. The solution is cooled to room temperature and the solvent is removed. The remaining residue is redissolved in chloroform from which salts are removed by extraction with water. The organic layer is dried ($MgSO_4$) and the solvent is removed. The product is recrystallized from ethanol. Additional product may be cleanly precipitated from the ethanol supernatant by dilution with water. TLC conditions, 2% MeOH/CH_2Cl_2, reactant $R_f = 0.48$, product $R_f = 0.56$. Yield 7.69 grams (66%): ^{1}H NMR (Me_2SO-d_6) 5.50 (s, 2), 7.32-7.44 (m, 5), 8.45 (s, 1).

Synthesis of 1-Benzyl-4-[^{15}N]-amino-5-cyanoimidazole (17). A solution of 0.3 grams of **16** in 125 mL of DMF was hydrogenated over 30 mg Pd/C at room temperature under atmospheric pressure for three hours. The mixture was filtered *through celite*. The DMF was removed under vacuo at 35° C. The resulting pale yellow solid was washed three times with diethyl ether. The amine **17** was flash chromatographed using 5% MeOH/CH_2Cl_2 giving white crystals, yield 98%: ^{1}H NMR ($MeSO_2$-d_6) δ 5.20 (s,2), 7.20-7.43 (m,5), 7.83 (s,1), 8.80 (t, 2, $^1J_{H\text{-}N} = 92$ Hz); IR (nujol) N-H 3250, CN 2200, others 2900, 1580, 1460, 1379, 1250, 1020, and 860; m/z 200.

Synthesis of 7-Benzyl-[3-^{15}N]-adenine (18).[67] 140 mg of **17** is added to a solution of 1.7 mL of triethylorthoformate in 10 mL of DMF. The triethylorthoformate has been distilled. The solution is dilute to prevent dimerization of the imidazole by reaction of the amine with the imidate. The reaction mixture is refluxed for one hour. The solvent is removed by rotovap under vacuum at a temperature below 40^{o} C. The imidate product (Rf = 0.9, 10% MeOH/CH_2Cl_2) is extracted with diethyl ether. The solvent is removed from the extract and the residue is resuspended in absolute ethanol saturated with anhydrous ammonia in order to complete the ring closure. The solution is a set at room temperature for two hours and the solvent is removed. The product is purified by flash chromatography, 10% MeOH/CH_2Cl_2, Rf = 0.4. Yield 40 mg (25%).

Synthesis of [3-^{15}N]-Adenine (19). 70 mg of **18** in liquid ammonia/THF (1:1, 50 mL) was debenzylated by addition of sodium under refluxing conditions for 10 minutes, then quenched with isoprene. The product was flash chromatographed using 20% MeOH/CH_2Cl_2 saturated with ammonia. Yield 90%: ^{1}H NMR (Me_2SO-d_6) δ 7.09 (s,2), 8.08 (d,1, $^2J_{H\text{-}N}$=3 Hz), 8.12 (s,1); ^{15}N NMR (Me_2SO) δ -146; m/z 137.

Synthesis of [6-^{15}N]Adenine (20). ^{15}N-Benzamide was reduced to ^{15}N-benzylamine using $LiAlH_4$ in dry diethyl ether. 1.23 grams (8 mmoles) of 6-chloropurine, 9 mmoles of ^{15}N-benzylamine, and 3.34 ml (24 mmoles) of triethylamine was refluxed for 36 hours in 100 mL of absolute ethanol. The product was preabsorbed onto silica and flash chromatographed with 1.5% MeOH/$CHCl_3$. 1.8 grams of the [6-^{15}N]benzyladenine was recovered (100% yield). Debenzylation to **20** was accomplished by oxidative cleavage as described in the synthesis of [6-^{15}N]-deoxyadenosine. 1.8 grams (8 mmoles) of [6-^{15}N]benzyladenine was added to a 2:2:3 mixture of CH_2Cl_2/CH_3CN/H_2O (180:180:280 ml) in a one liter flask, followed by 6.84 grams (4 eqv.) of $NaIO_4$ and then 55 mg of ruthenium oxide (RuO_2/H_2O). The heterogeneous mixture was refluxed for three hours. Flash silica was added and the solvent removed under vacuo. The absorbed material was flashed over 2" of silica with 1.5% NH_4OH/MeOH to remove the ruthenium. Remaining salts were filtered away. Solvent was removed. Benzyl derivatives were extracted with diethyl ether. The product **20** was flash chromatographed using 1.5:1.5:7.0 EtOH/MeOH/$CHCl_3$. Alternatively a solvent elution gradient from 10 to 30% MeOH/CH_2Cl_2 saturated with ammonia may also be utilized. 0.62 grams of **20** was recovered after purification. 58% yield. Note: The TLC reaction monitor indicated complete oxidation of the starting material. Low yield may indicate oxidation of adenine and/or loss of compound during the purification process: ^{1}H NMR (Me$_2$SO-d$_6$) δ 7.12 (d,2, $^{1}J_{H\text{-}N}$=89.84 Hz) 8.09 (s,1), 8.12 (s,1); ^{15}N NMR (Me$_2$SO-d$_6$) δ -293 (t). (Ref. 1M Na^{15}NO$_3$); m/z 137.059.

Synthesis of 3-(Acetyldistamycin)-adenine (21): a) 3-(Acetyldistamycin)-adenine, b) 3-([2-^{13}C]-Acetyldistamycin)-adenine, c) 3-(Acetyldistamycin)-[^{15}N3]-adenine, d) 3-([2-^{13}C]-Acetyldistamycin)-[^{15}N3]-adenine. A solution of 32 mM the appropriate adenine (unlabeled, **19**, or **20**) and 4mM **3** (or **8**) in dimethylformamide was refluxed for one hour. Solvent is removed under vacuo. Product is purified by preparative TLC using 1.5% NH$_4$OH/MeOH. 28% yield. The low yield is attributable to reflux conditions (degradation by heat of the tripyrrole) and traces of water in the DMF (*e.g.*, hydrolysis of **3** to **5**): ^{1}H NMR (MeSO$_2$-d$_6$) **21a** δ 1.59 (m,2), 2.12 (s,6), 2.21 (t,2), 3.18 (m,2), 3.78 (s,3), 3.81 (s,3), 3.83 (s,3), 5.18 (s,2), 6.81 (d,1, J=1.7 Hz), 6.93 (d,1, J=1.3 Hz), 7.01 (d,1, J=1.3 Hz), 7.13 (d,1, J=1.7 Hz), 7.17 (d,1, J=1.7 Hz), 7.23 (d,1, J=1.3 Hz), 7.69 (s,1), 7.91 (br s,1)7.98 (br s,1), 8.06 (t,1), 8.31 (s,1), 9.89 (s,1), 9.92 (s,1), 10.51 (s,1). $\Delta\delta_{2,8}$=0.62; Deviations from 20a due to labels: **21b** and **21d** δ 5.32, 4.96 (d,2, $^{1}J_{H\text{-}C}$=142.76 Hz) instead of 5.18 (s,2); **21c** and **21d** δ 8.30 (d, 1, **21c** $^{2}J_{H\text{-}N}$ = 6.4 Hz, **21d** $^{2}J_{H\text{-}N}$ = 6.0 Hz) instead of 8.31 (s,1); **21e** δ 7.97 (br d, 2, $^{1}J_{N\text{-}H}$ = 90.4 Hz) instead of 7.97 (br s,2); ^{13}C NMR (Me$_2$SO-d$_6$) **21b** δ 50.53, **21d** δ 50.62, 50.51 ($^{1}J_{C\text{-}N}$=11.0 Hz); ^{15}N NMR (Me$_2$SO-d$_6$) **21c** δ -221.91 (s). **21d** δ -221.88, -221 (d, $^{1}J_{N\text{-}C}$=11.0 Hz), **21e** δ -282 (t, $^{1}J_{N\text{-}H}$ = 90.9 Hz); UV max (H$_2$O) 290 (est. ε 2500); IR (KBr) 3400, 2900, 2500, 1920, 1660, 1620, 1450, 1350, 990, 830, 695; m/z **21a** 644.31, **21b** 645.32, **21c** 645.32, **21d** 646.32, **21e** 645.31.

Synthesis of 3-([2-^{14}C]-Acetyldistamycin)adenine (22). 3.1 umoles of **9** and 25 umoles of adenine in 0.78 mL of dimethylformamide was heated at 75° C for 20 hours. The DMF was removed under vacuo. The product was purified by flash chromatography two times. First with 10-20% MeOH/CH$_2$Cl$_2$ saturated with ammonia (step gradient). Second with 1% NH$_4$OH/MeOH. One umole of product was recovered (32%, 0.5 uCi/umole).

Synthesis of 3-(N-[Bromoacetamido]-N'N'-dimethyl-1,3-propane-diamine)-adenine (23). Same procedure as used to synthesize **21**, but with compound **7** as the alkylating reagent: ^{1}H NMR (Me$_2$SO-d$_6$) δ 1.63 (m,2), 2.28 (s,6), 2.47 (br s, 2), 3.14 (t,2), 4.99 (s,2), 7.72 (s,1), 7.94 (br s,1), 8.02 (br s,1), 8.27 (s,1), 8.46 (t,1). $\Delta\delta\ H_{2,8}$ = 0.55; m/z 278.17.

Proton Selective Decoupling (Jeol 400 MHz). 1) Acquire the proton spectra.

2) From the Real pattern locate the proton to be decoupled with the lightpen. Center the peak, CZ. Toggle to the data points, VEC. Identify the frequency of the peak, SS. Set the irradiation frequency offset for the selective decoupling, IRR to the desired frequency. Record the IRSET and IRFIN values. 3) Switch to the carbon-13 menu. Set the irradiation frequency offset, IRSET and IRFIN to the predetermined values. Set the ouput level of the irradiation oscillator, IRATN, between 100 to 150. 100 is more powerful. Change the pulse delay PD to 3 seconds (PW1 45 degrees, $T_1 = 8$ sec). change the experimental mode EXMOD to SGSEL and then set in the parameters, SETIN. 4) Acquire the carbon spectra.

Synthesis of 3-Methyladenine (24). This compound was synthesized from dimethyl sulfate and adenine in dimethylformamide at the refluxing temperature for one hour. The product was isolated by flash chromatography (15% MeOH/CH_2Cl_2 sat'd with ammonia): ^{1}H NMR (Me_2SO-d_6) δ 3.90 (s,3), 7.81 (s,1), 7.93 (br s), 8.32 (s,1) $\Delta\delta$ $H_{2,8} = 0.51$.

DNA Substrates. Three DNA substrates, sonicated calf thymus DNA, a 167 base pair restriction fragment from the pBR322 plasmid, and a 15 base pair synthetic oligonucleotide, were utilized in the cleavage experiments. The choice was dependent on the objective and will be indicated.

Preparation of Sonicated Calf Thymus DNA. 100 mg of calf thymus DNA was dissolved (by vortex) in 20 mL of 10 mM NaCl. The solution was purged with argon for approximately three minutes and cooled to 0° C. Sonication was done three times for 30 seconds. The solution is then divided in half. Each half is phenol extracted (the phenol is preequilibrated with water pH 8.0 by NaOH) three times. The two phases were separated by centrifugation. The bottom layer (phenol) was removed by pipette. The next extraction, one time, was with chloroform/isopropanol (24:1). The final extraction was with diethyl ether three times. The solutions were then filtered through a cellulose nitrate filter (0.45 um pore size). Filtration was done in aliquots to minimize clogging of the filter paper and to increase the speed of the process. Each solution was then dialyzed against doubly distilled water for at least 24 hours, preferably 48 hours.

Preparation of the 3' and 5' Labeled 167 base pair restriction fragment. The supercoiled pBR322 plasmid (isolated from E. coli by published procedures, see J. Sluka and R. Younguist theses) was digested with the ECO R1 restriction enzyme. Procedure: For each labeling reaction 10 ug of plasmid is digested with 30-50 units of Eco

R1 in 100 uL of the prescribed buffered solution. The incubation time is for one hour at 37°C. The enzyme is then heat denatured, 65°C for 10 minutes. After which the aqueous solution is phenol extracted two times and then ether extracted three times to remove the enzyme. The DNA is ethanol precipitated by addition of 90% EtOH/0.1M NaOAc (three times the reaction volume) and this vortexed solution is set into an ethanol/dry ice bath for 5 minutes. The precipitated DNA is centrifuged down to a pellet at an rpm >10,000 for 5 minutes. The supernatant is removed by pipette and the pellet is washed with 70% EtOH. Finally the pellet is dried under vacuum.

The linear plasmid was labeled at the 3' end with $[\alpha\text{-}^{32}P]$dATP using the Klenow fragment of DNA Polymerase I. Procedure: The pelleted linearized plasmid is resuspended into 10 uL of the concentrated enzyme buffer (10x) to which 50 uL of H_2O, 10 uL of $[\alpha\text{-}^{32}P]$-dATP, 10 uL of DTT (1mg/mL), 10 units of Klenow enzyme, and10 uL of either 10 mM dTTP or thio-dTTP is added. The reaction mixture is then incubated for 15 minutes at 37°C, after which the enzyme is heat denatured and extracted as described for Eco R1. The labeled DNA is pelleted by ethanol precipitation and dried under vacuum.

A separate batch of ECO RI digested plasmid was 5' labeled by removing the 5' phosphate with calf intestine alkaline phosphatase (CAP) and replacing it with a hot phosphate using $[\gamma\text{-}^{32}P]$dATP and T4 Polynucleotide Kinase. Procedure: The pelleted linearized plasmid is resuspended into 10 uL of the concentrated CAP buffer (10x) to which 88 ul of H_2O and 1 unit of CAP is added. The reaction mixture is incubated at 37° C for 30 minutes after which the enzyme is heat denatured and extracted as previously described. The DNA is repelleted. The pelleted dephosphorylated plasmid is then resuspended into 5 ul of 10x Kinase buffer to which 35 uL of H_2O, 800 uCi of $[\gamma\text{-}^{32}P]$dATP, 5 uL of DTT (1 mg/100 uL), and 3 units of T4 Kinase is added. The reaction mixture is then incubated for 30 minutes at 37° C after which the enzyme is heat denatured and extracted as described. The labeled DNA is then repelleted.

After labeling, the DNA was digested with RSA I to yield four restriction fragments. Procedure: Each labeled fragment is resuspended into 10 uL of 5x RSA I buffer to which 30 uL of H_2O, 5 ul DTT (1 mg/100 ul), and 30 units of RSA I is added. The reaction mixture is incubated at 37° C for one hour. The DNA is either pelleted or the appropriate amount of loading buffer is added. The 516 and 167 fragment are isolated by gel electrophoresis (1% agarose or 5% polyacrylamide).

MPE Footprinting of the Ligand Binding Sites. Metal activated MPE was made up from a lyopholized sample, which at a volume of 100 uL is 100 uM MPE, by addition of 96 uL of double distilled water, then 4 uL of 5 mM $(NH_4)_2Fe(SO_4)_2{\cdot}6H_2O$. This mixture was diluted 1:4 to make a 10x stock solution (25 uM MPE). The footprinting reaction involved 1) equilibration of the compound with the DNA for 15 minutes, 2) addition of and equilibration of MPE for 5 minutes, 3) addition of dithiothreitol, and 4) incubation at 37°C for 12 minutes (The incubation time may vary depending on the activity of the MPE). Final concentrations in a 10 uL reaction volume were: 100 uM Calf Thymus DNA, 5 uM ligand, 2.5 uM MPE-Fe (II), 4 mM DTT, 10 mM NaPhosphate pH 7.0, and the end labeled DNA.

Comparison of Binding Sites of Distamycin A and N-Bromoacetyldistamycin on the 167 b.p. Restriction Fragment. Following the MPE footprinting procedure outlined above the binding sites for distamycin A and N-bromoacetyldistamycin were determined on the 167 base pair restriction fragment from the pBR322 plasmid. The autoradiogram of the high resolution denaturing gel which indicates the binding sites are shown in Figure 1, page 181. Lanes 1-9 are the restriction fragment end labeled with ^{32}P at the 3' end and lanes 10-18 are the restriction fragment labeled at the 5' end. Lanes 1 and 10 are intact DNA controls and lanes 2 and 11 are the MPE controls (no ligand). Laser densitometric analysis indicates that the binding sites for the two ligands are identical.

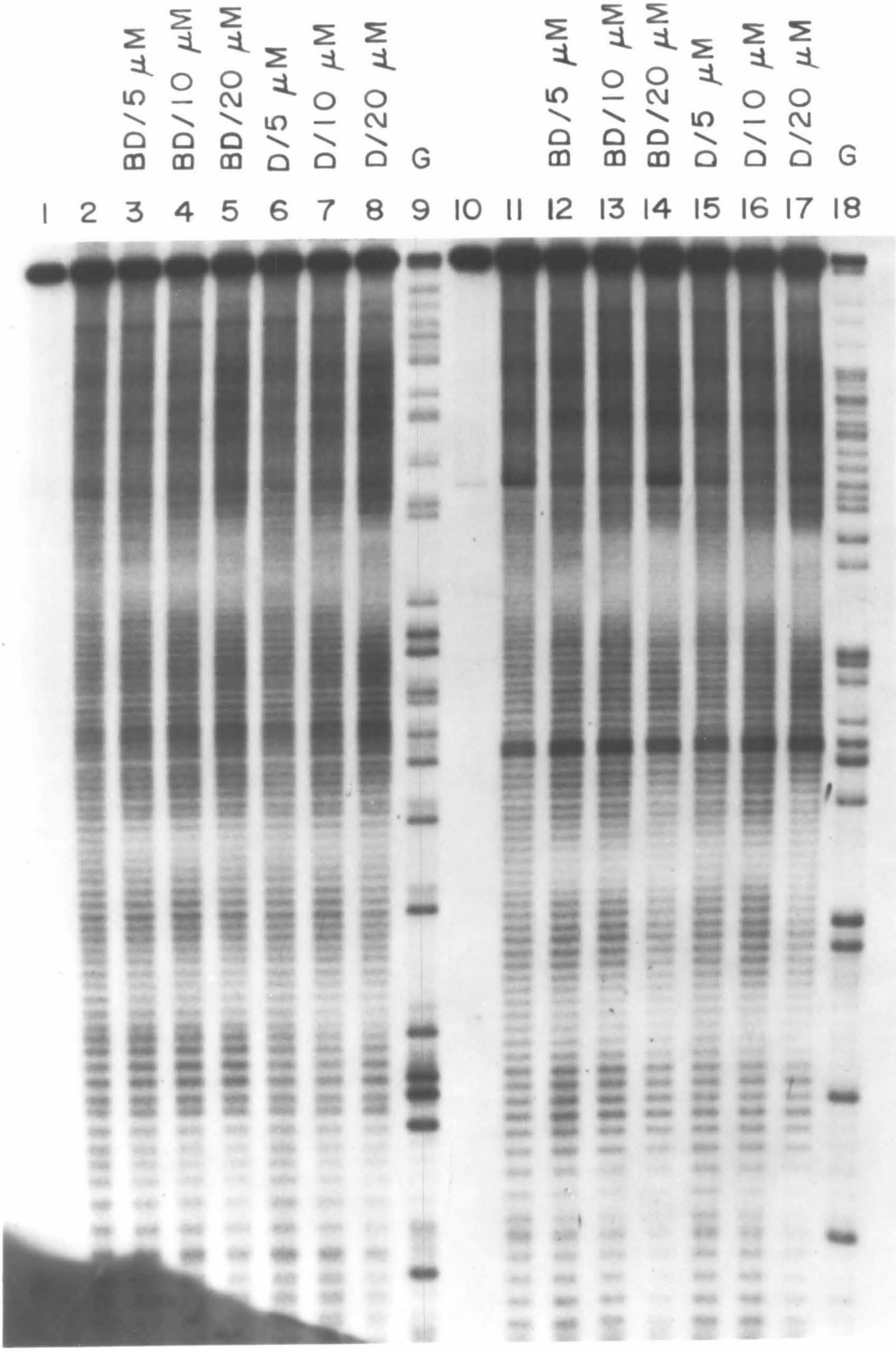
BD/5 μM
BD/10 μM
BD/20 μM
D/5 μM
D/10 μM
D/20 μM
G
BD/5 μM
BD/10 μM
BD/20 μM
D/5 μM
D/10 μM
D/20 μM
G
1
2
3
4
5
6
7
8
9
10
11
12
13
14
15
16
17
18

Workup Conditions for Optimizing Cleavage. Fourteen different workup procedures were implemented after incubation of the 167 restriction fragment (100 uM calf thymus) with BD (5 uM) at 45° C for 3 hours in order to assess the best means following incubation to maximize cleavage of the backbone. The gel is shown in Figure 2 below. Odd and even lanes are 3' and 5' labels respectively. Lanes 1 and 2) Control (DNA only) no workup, Lanes 3 and 4) Control (DNA only) -- ethanol precipitation; 1M piperidine 30 minutes at 90° C, Lanes 5 and 6) G reaction, Lanes 7 and 8) BD -- ethanol precipitation, Lanes 9 and 10) BD -- ethanol precipitation; resuspend in buffer and heat 15 minutes at 90°C; lyopholize, Lanes 11 and 12) BD -- ethanol precipitation; resuspend in buffer and heat 30 minutes at 90°C; lyopholize, Lanes 13 and 14) BD -- ethanol precipitation; resuspend in buffer and heat 15 minutes at 90° C; 1M piperidine 15 minutes at 90° C, Lanes 15 and 16) Same as 13 and 14 except 1M piperidine 30 minutes at 90° C, Lanes 17 and 18) Same as 13 and 14 except 0.5M piperidine 15 minutes at 90°C, Lanes 19 and 20) Same as 13 and 14 except 0.5M piperidine 30 minutes at 90° C, Lanes 21 and 22) BD -- ethanol precipitation; 1M piperidine 15 minutes at 90° C, Lanes 23 and 24) same as 21 and 22 except 1M piperidine 30 minutes at 90° C, Lanes 25 and 26) same as 21 and 22 except 0.5M piperidine 15 minutes at 90° C, and Lanes 27 and 28) same as 21 and 22 except 0.5M piperidine 30 minutes at 90° C. Based on this data, *i.e.*, the relative intensities of cleavage, it is evident that heat is a necessity after which the additional piperidine treatment enhances cleavage significantly. Therefore I chose the quickest and most effective workup procedure -- heat for 15 minutes at 90° C in buffer followed by heat for 15 minutes at 90° C in 1M piperidine.

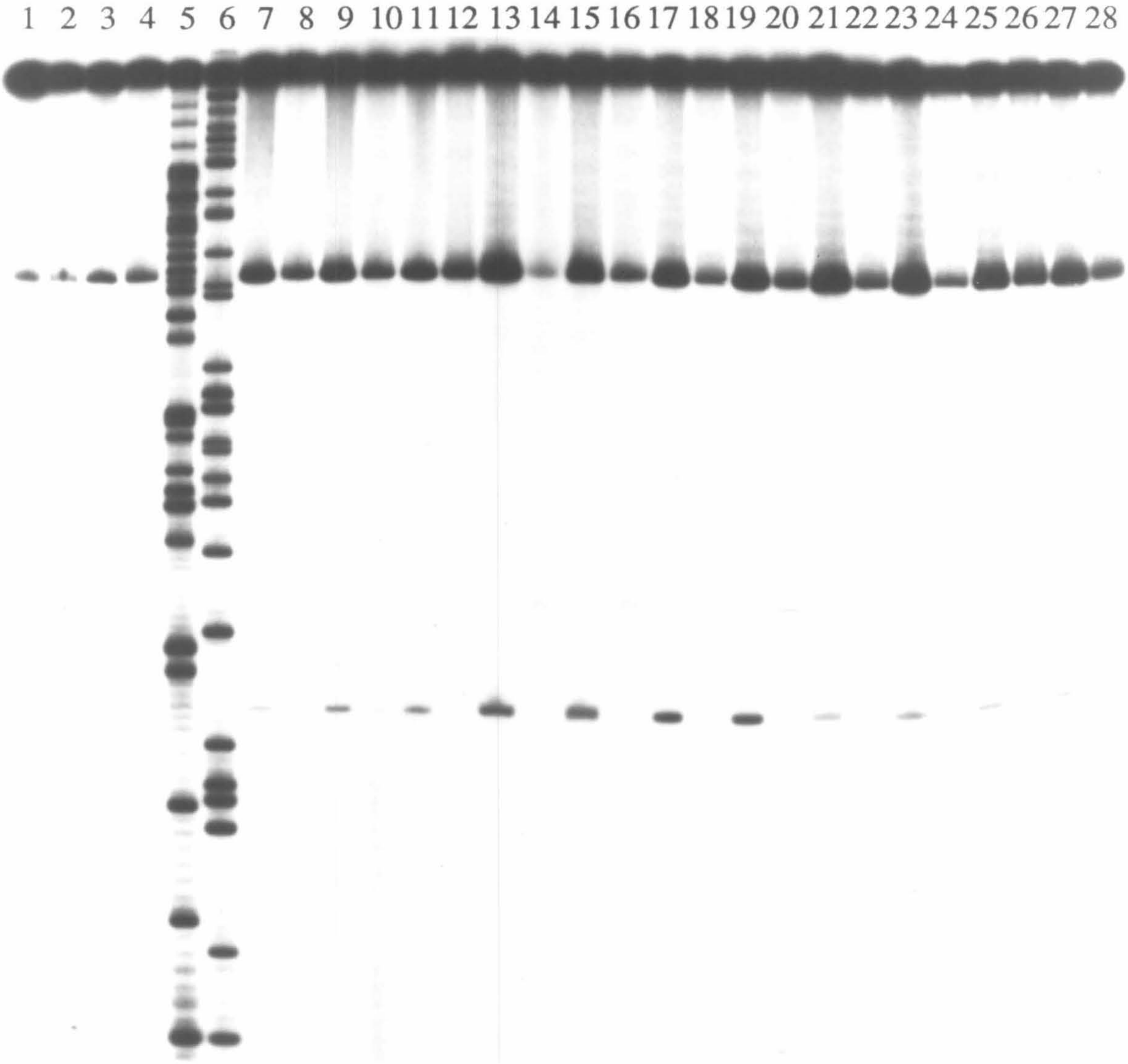
1 2 3 4 5 6 7 8 9 10 11 12 13 14 15 16 17 18 19 20 21 22 23 24 25 26 27 28

Cleavage of the 167 base pair restriction fragment by BD at 37° C. 5 uM BD was allowed to incubate at 37° C with the labeled restriction fragment (100 uM b.p. calf thymus DNA) in 10 mM NaPhosphate pH 7.0 for 0.5, 5.0, and 10 hours. The DNA was ethanol precipitated, resuspended in phosphate buffer (10 uL) and heated at 90° C for 15 minutes. Piperidine was then added to a concentration of 1M in 50 uL and the mixture was heated for 15 minutes at 90° C. At least three lyopholizations (15 uL of H_20) were carried out before loading on to the 8% polyacrylamide gel.

Time Dependence of Cleavage Specificity. Sites of DNA cleavage over time were examined on the 167 b.p. restriction fragment (ECOR1/RSA I) of pBR322 plasmid. BD at 5 uM concentration was reacted at 37° C with both the 3' and 5' labeled restriction fragment (100uM in b.p. sonicated calf thymus DNA) in 10 mM sodium phosphate buffer (pH 7.0) for 0, 1, 5, 10, 20 and 40 hours. The control reaction (no BD) was for 40 hours. The reactions were ethanol precipitated. The precipitates were resolubolized in 10 uL of 10mM sodium phosphate buffer and heated for 15 minutes at 90° C. 40 uL of 1.4 M piperidine was added and the solution heated again at 90° C. Solvent was removed by several lyopholizations.

Temperature Dependence of Cleavage Specificity. BD at 5 uM concentration was reacted for 5 hours with both the 3' and 5' labeled restriction fragment (100 uM in b.p. sonicated calf thymus DNA) in 10 mM sodium phosphate buffer (pH 7.0) in 10° C increments from 5 to 65° C. The control reaction was at 65° C. The reactions were worked up under the same procedure as the preceeding time reactions.

Dependence of Cleavage on the Leaving Group. The cleavage specificity of CD, BD, and ID were compared on the 167 b.p. restriction fragment. Each compound at 5 uM concentration was reacted with the 3' and 5' labeled fragment (100 uM CT) in 10 ul of 10 mM sodium phosphate (pH 7.0) at 37° C for 20 hours. The aqueous solution was extracted two times with water saturated phenol (pH 7.0) and then three times with diethyl ether. The DNA was ethanol precipitated, resuspended in 10 ul of 10 mM sodium phosphate and heated at 90° C for 15 minutes. 40 uL of 1.4 M piperidine was added and the solution was again heated at 90° C for 15 minutes. The piperidine was removed by several lyopholizations.

Cleavage of the 167 b.p restriction fragment by BD and CC1065. A stock solution of CC1065 in DMSO, 1.2 mM, was made up and stored in a glass container at -20° C. A comparison of the cleavage specificity of BD and CC1065 was done on the 167 b.p. restriction fragment (ECO RI/ RSA I) of pBR322 plasmid. BD and CC1065 at 5uM concentration were reacted at 37° C with both the 3' and 5' labeled restriction fragment (100 uM in b.p. sonicated calf thymus DNA) in 10mM sodium phosphate buffer (pH 7.0). The CC1065 reaction time was one hour and the BD reaction times were one and ten hours. The control (no drug) was done for 10 hours. The reactions were ethanol precipitated. The precipitates were resolubolized in 10 uL of 10mM sodium phosphate buffer and heated for 15 minutes at 90° C. 40 uL of 1.4M piperidine was added and the solution heated again at 90° C for 15 minutes. Solvent was removed by several lyopholizations.

Gel Electrophoresis of the 167 b.p. restriction fragment. Samples were taken up into 3 ul of 75% formamide, heat denatured at 90° C for one minute, chilled immediately to 0° C, and electrophoresed through an 8% polyacryamide gel (50% urea, 1:20 crosslinkage, 0.4 mm thick, 40 cm long) at 1200 volts until the bromophenol blue in the marker lane migrated 40 cm. The gels were transferred to Whatman 3mm cellulose paper and dried under vacuo at 60° C for one hour. Autoradiography was done at -50° C on Kodak x-Omat AR film.

Synthesis of Oligonucleotides. The 15 base pair oligonucleotide, 5'-CGGTAGTTTATCACA, the 21 base pair oligonucleotide, 5' TCACAGTTAAATTGC-TAACGC, and their complementary strands were synthesized on the Beckman System 1 Plus DNA Synthesizer.

Purification of Oligonucleotides. Two methods were utilized for purification of the oligonucleotides. Polyacrylamide gel electrophoresis followed by electroelution and anion exchange HPLC or FPLC. Oligos were electrophoresed on 20% polyacrylamide (2 mm thick, 42% urea, 1:28 crosslinkage) at 550 volts for 20 hours with a fan. The loading buffer may be as low as 50% formamide and does not contain the marker dyes. Migration was monitored with dyes in a separate marker lane. The gel boogies until the bromophenol blue has danced at least 20 cm. Bands were detected and cut out under a UV lamp using a thin layer flourescent silica plate backing. The oligos were electroeluted out of the gel slices with an IBI electroelutor -- Model UEA (100 ul 10M ammonium acetate salt cushion, 100 volts for 15 minutes, three times). The DNA was ethanol precipitated (95% EtOH:salt soln 10:1), reconstituted, filtered (0.45um millipore) and dialyzed for 48 hours against doubly distilled water. Purification by HPLC was done using a Synchropak AX100 column (10 mm x 25 cm). Solvent A 0.05M NaH_2PO_4 (pH5.9)/15% CH_3CN. Solvent B 0.05M NaH_2PO_4 (pH 5.9)/ 1M $(NH_4)_2SO_4$/15% CH_3CN. Gradient program: 40% B 20 min., 40-100% B 30 min. Flowrate 1.5 ml/min. Purification by FPLC was done using a Pharmacia MonoQ column. Solvent A: 20mM Tris-HCl pH 8.3/20%CH_3CN. Solvent B: 20mM Tris-HCl/1M KCl/20% CH_3CN. Gradient program: 20-80%B in 45 min.

Flowrate 2.0 ml/min. Chromatographed oligonucleotides were dialyzed against doubly distilled H_2O for 48 hours, filtered, lyopholized, and reconstituted to desired concentration (ε $1.47 x 10^5$/ss 15mer, ε 2.06 x 10^5/ss 21mer).

Reannealment of Oligonucleotides. One equivalent each of the two complementary strands was mixed in 100 mM NaPhosphate buffer (pH 7.0) and then heated at 65° C for 15 minutes. The mixture is cooled to room temperature for 15 minutes and then to 4° C for 15 minutes. Before addition of other reactants the annealed oligos were warmed to room temperature.

5' Labeling of Oligonucleotides. Ten pmole of each single stranded oligo was reacted with 2 units of polyNucleotide kinase and 20 pmole [γ-^{32}P]-dATP for 30 minutes at 37° C. Recipe: 5 uL 2uM DNA, 3 uL 10x kinase buffer (500 mM Tris pH 7.0, 100 mM $MgCl_2$), 3 uL 0.1M DTT, 15 uL H_2O, 2 units of PNK. Excess ATP was removed by centrifuging the reaction mixture through Sephadex G-10-120 two times. Solvent was removed by lyopholization. Purification was attained by polyacrylamide gel electrophoresis (no marker dyes in the loading buffer) followed by electroelution.

3' Labeling of Oligonucleotides. 3.5 nmoles each of the single stranded 15mer, 5'-CGGTATTATCACA, and the complementary 12mer, 5'-TGTGATAAATA, were mixed and reannealed at a concentration of 60 uM in 100 mM sodium phosphate buffer pH 7.0. The following compounds were then added to a final volume of 100 uL and the specified final concentrations $MgCl_2$ (6.6 mM), mercaptoethanol (1 mM), 2'-Deoxycytidine-5'-triphosphate (1mM), [α-^{32}P]-2'-Deoxyguanosine-5'-triphosphate (100 uCi), and DNA Polymerase I-Klenow (15 units). This reaction was incubated at 37° C for 20 minutes then mixed 1 to 1 with 100% formamide and loaded onto a 20% (28:1) polyacrylamide preparative gel (700 volts). Bands were excised and the labeled fragment extracted by electroelution.

Sequencing Reactions (G+A) of Oligonucleotides. The labeled oligonucleotide was heated at 65° C in 10% piperidine-formate solution (86% formic acid, 5% piperidine stock soln.) for 10 minutes. Solvent is removed by lyopholization. Cleavage is completed by heating the DNA for 30 minutes at 90° C in 1M piperidine. Piperidine was removed by lyopholization (3x) and one spin through G10-120 sephadex.

Melting Temperatures of the 15mer. Melting temperatures were determined for the 15 base pair oligonucleotide (2.5 uM) in 10 and 100 mM sodium phosphate buffer (pH7.0), with and without BD (2.5 and 25 uM). The single strand complements (5uM) were mixed together in 400 uL of the appropriate buffer. They were reannealed by heating at 57° C for 15 minutes, cooling to room temperature for one hour and then to 0° C for one hour. An additional 400 uL of the buffer only or the appropriate concentration of BD in buffer was added. The BD was allowed to equilibrate at room temperature for 20 minutes. Absorbtion was monitored from 10 to 70° C in 10 degree increments with equilibration times of 30 minutes on a Beckman Model 25 UV-Vis Spectrophotometer at 260 nm.

Sequential Analysis of Oligonucleotide Products. 10 uM 15mer:BD (1:1) in 100 mM NaPhosphate buffer (pH7.0) was incubated at 37° C for 0 and 24 hours. Aliquots for gel analysis were removed at each stage of the workup procedure, *i.e.,* 1) reaction 2) heat, 15 min at 90° C 3) 1M Piperidine, 5 min at r.t. 4) 1M Piperidine, 15 min at 90° C 5) 1M Piperidine, 30 min at 90° C.

Enzymatic Characterization of DNA Termini. 10 uM 15mer:BD (1:1) in 100mM NaPhosphate buffer (pH 7.0) was incubated at 37° C for 48 hours. Reaction mixtures were worked up by standard cleavage procedures. Salts, such as NaPhosphate (an enzyme inhibitor), were removed by chromatography through G10-120 Sephadex. In order to detect a phosphate group at the DNA cleavage site, each fragment (3' and 5' labeled) was reacted with the appropriate phosphatase to yield a hydroxyl group -- calf intestine alkaline phosphatase removes 5' phosphates and polynucleotide kinase removes 3' phosphates. For 5' end analysis the cleaved 3' labeled oligonucleotide was dissolved in CAP buffer (50 mM Tris-HCl, 0.1 mM EDTA, pH 8.0) then heated at 65° C for 5 minutes and chilled immediately to 0° C. Ten units of CAP were added and the reaction mixture incubated at 37° C for 30 minutes. Water was removed by lyopholization and the sample was prepared for gel electrophoresis. Cleaved 3' labeled oligonucleotide after a G+A sequencing reaction was tested under the same conditions. For 3' end analysis the cleaved 5' labeled oligonucleotide was dissolved in 50mM Tris-HCl, 10mM $MgCl_2$, heated for 5 minutes at 65° C, and then chilled immediately to 0° C. DTT (5 mM) and 10 units of polynucleotide kinase were added and the reaction was incubated at 37° C for one hour. Water was removed by lyopholization and the sample prepared for gel electrophoresis. The same procedure was done on the 5' labeled G+A reaction. Gel electrophoresis was conducted on a 20% polyacrylamide gel (0.4mm thick, 40 cm long, 1:20 crosslinkage, 50% urea) at 1200 volts until the bromophenol blue marker migrated 20 cm.

BD Product Analysis [^{14}C]-BD/15mer. The two single strands of the 15mer (133 uM) were mixed in 133 mM NaPhosphate buffer pH 7.0 (0.6 mL). The double stranded oligonucleotide was reannealed by heating the mixture at 65° C for 15 minutes, cooling to room temperature for 15 minutes, and then to 4° C for 15 minutes. After warming the solution to room temperature (10 minutes) one equivalent of [^{14}C]-BD (0.07 mg/0.4 mL H_2O) was added, giving a final concentration of 100 uM BD and 100 uM oligomer in 100 mM Na Phosphate. The complex was allowed to equilibrate at room temperature for ten minutes and then heated to and maintained at 37° C for 96 hours. A 200 uL aliquot was removed and lyopholized. BD and products were extracted two times from the dried DNA reaction with 100 uL of 1% NH_4OH/MeOH. The extract was condensed to approximately 20 uL and spotted on 0.25 mm Silica Gel 60 plate (Merck). The control (no oligonucleotide) was done under the same reaction conditions and workup procedure. Two to four nCi was spotted per lane. The TLC solvent used was 1% NH_4OH/MeOH. The solvent front moved 4 cm from the origin. Autoradiography of the TLC plates was done at room temperature on Kodak X-Omat AR film.

Calf Thymus DNA/BD Reaction with Isolation and Purification of the Adenine Adduct. In 1380 mL of 10 mM sodium phosphate solution (pH7.0) 911 mg sonicated calf thymus DNA and 48 mg of N-bromoacetyldistamycin were stirred for 56 hours at 48° C. Water was removed by lyopholization. BD products were extracted from the DNA with 1.5% NH_4OH/MeOH two times 125 milliters. The extract was condensed and flash chromatographed (1.5% NH_4OH/MeOH) to isolate the product, which by TLC corresponded to the adenine adduct. Further purification of the targeted adduct was done by semipreparative HPLC using an Altex Ultrasphere ODS column (10 mm x 25 cm). Solvent A: 100 mM triethylammonium formate pH3.1. Solvent B: acetonitrile. The gradient program was 5-30% Solvent B over 15 minutes followed by 30-100% B in 10 minutes. The flow rate was 14 mL/min: Partial H1 NMR δ 5.15 (s), 6.81 (d), 6.93 (d), 7.01 (d), 7.13 (d), 7.17 (d), 7.23 (d), 7.71 (s), 8.06 (s), 8.31 (s), 9.88 (s), 9.91 (s), 10.50 (s).

Equilibrium Dialysis. System: The apparatus utilized has a five cell carrier which rotates at 5, 10, or 20 revolutions and can be placed inside of a temperature controlled lucite water bath. The membrane between each cell compartment was Spectra/Por 3, which has a molecular weight cutoff of 3500 (the 15mer has a weight of 9900 and the ligands are approximately 600). The dry membranes were prepared as described by the manufacturer. For the final step of conditioning, the membranes were soaked in the dialysis buffer, 100 mM NaPhosphate pH 7.0, for at least 15 minutes (Note: hand or glove contact with the membranes was not permissable). After assembly of the five cells the compartments were washed once with the dialysis buffer. Each compartment has an effective volume of one mL. All experiments were conducted at 37° C at a rotation rate of 10 rpm. Two compounds were examined, N-[1-^{14}C]-Acetyldistamycin and N-[2-^{14}C]-Bromoacetyldistamycin, for their affinity towards the 15 base pair oligonucleotide, 5'-CGGTAGTTTATCACA.

Equilibration Time: Determination of the equilibration time was done with the nonreactive N-[1-^{14}C]-Acetyldistamycin (AcD). One compartment of each cell was filled with 1 mL of the dialysis buffer. The other compartment was filled with 1 mL of 10 uM AcD in 100 mM NaPhosphate pH 7.0 (amount of radioactivity is controlled by spiking with the unlabeled compound). After times of 1, 2, 4, 6 and 8 hours the solutions in each compartment of one of the (remaining) five cells was removed and transferred to scintillation vials. The empty compartments were then washed two times with 1 mL of dialysis buffer and the washes were transferred to the appropriate and complimentary vial. To each vial containing 3 mL of the aqueous carbon 14 solution was added 7 mL of the scintillation fluid. Vials were capped and thoroughly mixed to assure homogeneity, which is essential for counting purposes. The quenching affects in counting were monitored by the H Number method and the confidence level for channel two on the instrument was set to 2%, which means that 95 of 100 times, the counts obtained will be within +/- 2% of the mean and 5 out of 100 will be outside the 2%. This results from the randomness of the decay process. The initial cpm value, time zero, was 50,930 (approximately 75 nanocuries).

Measurement of Ligand Bound and Ligand Free: The reannealed 15mer was mixed with the ligand to a total volume of 1.2 mL by the following addition procedure with vortexing between each step. 1) 600 uL of 15mer (200 uM in 100 mM NaPhosphate), 2) 420 ul of H_2O, 4) 60 uL of 1M NaPhosphate pH 7.0, and 5) 120 uL of the labeled ligand (100 uM). As before, 1 mL of the dialysis buffer was put in one compartment of the cell and 1 mL of the oligo/ligand mixture was placed and sealed in the other compartment. Based on the equilibration time experiment, samples were dialyzed for 8 hours at 37°C. Samples were removed and counted by the same procedure as given above.

Rate of Alkylation / Disappearance of the Reactant. Reaction Procedure: The reaction mixtures were made up separately in the following order of addition at room temperature in 0.6 mL Robbins Scientific polypropylene microcentrifuge tubes 1) reannealed double stranded oligonucleotide in 100 mM NaPhosphate, 2) H_2O, 3) 1M NaPhosphate, 4) XD, and 5) 3-nitrobenzenesulfonic acid. As an example the following protocol was used for determination of the absolute rate of alkylation of adenine #48 (100 uM 15mer : 10 uM BD) The total volume was 100 uL for each sample. The style of solution transfer by pipette was kept consistent -- one preflush of the tip. 52 uL of H_2O was added to a 20 uL solution of the reannealed 15mer (500 uM) in 100 mM NaPhosphate pH 7.0. (Note: Removal of the 20 uL solution of the DNA/NaPhosphate from the stock solution requires vortexing followed by immediate transfer to the reaction tube.

Prevortexing is an essential step prior to the transfer of any and all of the reactants to the reaction vessel). After the addition of water the solution is vortexed and then 8 uL of 1M NaPhosphate pH 7.0 was added. (Note: Vortexing of the reaction tube between additions is also essential). Next, 10 uL of BD (100 uM) was added. And, finally 10 uL of the internal standard, 3-Nitrobenzenesulfonic acid (140 uM), was transferred to the reaction tube. The complete mixture was vortexed, the initial injection volume (10 uL) was removed by pipette and tranferred to a polypropylene autosampler tube. The remaining solution was immediately placed into the 37^o C temperature bath. Based on kinetic data the equilibration time is fast with respect to the time it takes to place the tubes in the bath, i.*e.,* no equilibration time is required. Injection of the sample onto the column was done automatically by an HPLC autosampler. This complete method is optimal and was applied to the other alkylation experiments on the 21mer and 15mer with CD, ID, and BD at 37, 45, and 65^o C.

Method of Rate Measurements: The disappearance of XD overtime was monitored by two techniques, TLC/Scintillation Counting and HPLC/UV Spectroscopy.

1) TLC/Scintillation Counting: Initially carbon 14 labeled BD was utilized for quantitative analysis by scintillation counting. TLC plates from the product analysis experiment (previous section) were mapped out by combining the autoradiogram with the UV detection of compounds. The plates were then dipped into EtOH and the spotted wet silica was carefully scraped off with glass capillary tubing into scintillation vials containing 2 mL of Beckman Ready-Solv MP aqueous scintillation cocktail. Due to the amount of compounds (oligonucleotides, carbon 14 labeled cleaving reagents) necessary for each experiment and the attainment of a detailed analysis, a technique was developed to monitor the reaction by HPLC.

2) HPLC/UV spectroscopy: At each time interval 10 uL of the reaction mixture was injected onto a Hewlett Packard Hypersil ODS 5 micron column (100 x 2.1 mm). Solvent A: 100 mM Triethylamineformate pH 3.0. Solvent B: Acetonitrile. Gradient Program: 5 to 30% B in 15 minutes, 30 to 100% B in 10 minutes, 100 to 5% in 5 minutes, 10 minute equilibration time. The response level of the photodiode array detector in an 80 nanometer window (264-344 nm, centered at 304 nm) for BD is 1.72 mA per 20 pmoles. In a 4 nanometer window centered around 260 nm the level is 1.4 mA per 20 pmoles. Therefore, 5 times this amount (100 pmoles) was chosen as the lower limit for the initial injection (reaction time zero) to monitor the rate of disappearance of the reactant, XD (10 ul injection volume, 10 uM starting concentration)

Data Analysis: The amounts of compounds in the injected samples were determined by peak area at 260 nm, band width of 4 nm. Final calculations were made with respect to the internal standard peak area.

Relative Rates of Cleavage, ID and BD, on the 15mer. Reaction Procedure: Each labeled strand was mixed 1:1 with its complement in sodium phosphate buffer (pH 7.0) and reannealed. The cleaving reagent (BD or ID) was added and allowed to equilibrate 20 minutes at room temperature. The DNA-drug complex was then incubated at 37° C from 1 to 60 hours. The reaction was stopped by addition of 1mM sonicated calf thymus DNA (1/10 the reaction volume) followed by ethanol precipitation. The precipitated DNA was resuspended in 10 mM sodium phosphate buffer (pH 7.0) and heated at 90° C for 15 minutes. Piperidine was then added increasing the total volume by five and finalizing the concentration of piperidine at 1M. The solution was heated at 90° C for 15 minutes and the solvent removed by lyophilization.

Method of Measurement: In order to measure the relative rates of cleavage by BD and ID the reactions were spiked before ethanol precipitation with the 5' labeled markers dA_4, dA_6, dA_8, and dA_{10} (2.5 uM unlabeled strands) at 1:1, 1:200, 1:100, and 1:10 the radioactivity of the labeled oligonucleotide, respectively. The lyopholized products were resuspended in loading buffer (85% formamide) and electrophoresed through 20% polyacrylamide at 1400 volts until a marker lane of bromophenol blue migrated approximately 15 cm. The relative rates were obtained from a comparison of the ratios of radioactivity for the marker bands and cleavage band of each reaction as measured by a scintillation counter.

Relative Rates of Cleavage by BD and ID on the 21mer/Adenine 58 and 59. Reaction Procedure: The 5' labeled 21mer 5'-^{32}P-TCACAGTTAAATTGCTAACGC was mixed with the reannealed unlabeled duplex and the mixture was reannealed a second time. The amount of the labeled strand is miniscule in comparison to the unlabeled oligo. Fourteen separate reactions were set up, each at a radioactivity level of approximately 500,000 cpm. The volume of each was 20 ul. The same addition procedure was followed as dicussed in the previous sections. (1), (2), and (3) 10 uM 21mer : 10 uM ID; (4), (5), and (6) 10 uM 21mer: 10 uM BD; (7) and (8) 50 uM 21mer : 10 uM ID; (9) and (10) 50 uM 21mer : 10 uM BD; (11) and (12) 100 uM 21mer : 10 uM ID; (13) and (14) 100 uM 21mer : 10 uM BD. All reactions were 100 mM NaPhosphate pH 7.0 and incubated at 45°C. After 2 and 3 days a 2 uL aliquot was removed from each sample and diluted to 10 uL with H_2O. After which the sample was heated at 90°C for 15 minutes, followed by 1M piperidine for 30 minutes at 90° C. A 20% polyacrylamide gel was utilized for product separation. The reaction samples were loaded every other lane. Exposure of the X-ray film to the gel only required 15 minutes. This autoradiogram was utilized as a template for slicing out by razor blade the uncleaved and cleaved strands of the oligonucleotide.

Method of Measurement: Gel slices were placed in scintillation vials and 2 mL of scintillation fluid was added to each. The confidence level was set to 1%. The amount of quenching was not accounted for. It is believed that the high energy β particles emitted from phophorous 32 will compensate for this neglect, in other words, there probably is not a significant amount of quenching occurring, if at all.

Measurement of the Extinction Coefficients (BD and DA). Each compound, BD and DA, in the solid form was put on a vacuum line inside a dessicator along with phosphorous pentoxide for 48 hours. For this experiment only one sample weight was measured for each. The extinction coefficients for BD and DA were determined in their respective HPLC elution solvents as determined by the elution time and the corresponding gradient program. For BD this occurs at 17% acetonitrile in 100 mM triethylammonium formate pH 3.1. 0.441 mg of BD was dissolved into 1.0 mL of the buffer. Four aliquots of 31.9 ul were removed and diluted to 1000 ul of buffer to give a sample concentration of 20 uM. For DA the solvent composition at elution is 11% acetonitrile in 100 mM triethylammonium formate pH 3.1. 0.600 mg of DA was dissolved in 1.0 mL of absolute methanol to give a 932 uM solution. Four aliquots of 21 uL were diluted to 1000 uL with the elution buffer to yield a concentration of 20 uM. The blank sample was 21 uL of methanol diluted to 1000 uL with the elution buffer. In addition the extinction coefficients for DA were determined in pure H_2O. Absorbances were measured at wavelengths of 304, 270, and 260 nm for each compound and sample.

Rate of Depurination. The rate of depurination was determined from the data collected for the alkylation experiments of BD at 37° C. Calculations were based on the areas of the internal standard peak and the DA peak at a wavelength of 304 nm and band width of 80 nm.

References

1. a) Watson, J.D. and Crick, F.H., A Structure for Deoxyribose Nucleic Acid. Nature 171, 737-738 (1953).
   b) Franklin, R.E. and Gosling, R.G., Molecular Configuration in Sodium Thymonucleate. Nature 171, 740-741 (1953).
2. Saenger, W., Principles of Nucleic Acid Structure, Springer Verlag (1984).
3. a) Dickerson, R.E., Drew, H.R., Conner, B.N., Wing, R.M., Fratini, A.V., and Kopka, M.L., The Anatomy of A-, B-, and Z-DNA. Science 216, 475-485 (1982).
   b) Drew, H.R., Wing, R.M., Takano, T., Broka, C., Tanaka, S., Itakura, K., and Dickerson, R.E., Structure of B-DNA dodecamer: Conformation and dynamics. Proc. Natl. Acad. Sci. 78, 2179-2183 (1981).
4. Lomonossoff, G.P., Butler, P.J.G., and Klug, A., Sequence Dependent Variation in the Conformation of DNA. J. Mol. Biol. 149, 745-760 (1981).
5. McGhee, J.D. and von Hippel, P.H., Formaldehyde as a Probe of DNA Structure II: Reaction with Endocyclic Imino Groups of DNA Bases. Biochemistry 14, 1297-1303 (1975).
6. Breslauer, K.J., Frank, R., Blöcker, H., and Marky, L.A., Predicting DNA duplex stability from the base sequence. Proc. Natl. Acad. Sci. USA 83, 3746-3750 (1986).
7. Patel, D.J., Pardi, A., and Itakura, K., DNA Conformation, Dynamics, and Interactions in Solution. Science 216, 581-590 (1982).
8. Patel, D.J., Kozlowski, S.A., Hare, D.R., Reid, B., Ikuta, S., Lander, N., and Itakura K., Conformation, Dynamics, and Structural Transitions of the TATA Box Region of Self-Complementary d[(C-G)$_n$-T-A-T-A-(C-G)$_n$] Duplexes in Solution. Biochemistry 24, 926-935 (1985).
9. Gueron, M., Kochoyan, M., Leroy, J., A single mode of DNA base pair opening drives imino proton exchange. Nature 328, 89-92 (1987).
10. Dickerson, R.E. and Drew, H.R., Structure of a B-DNA Dodecamer. II. Influence of Base Sequence on Helix structure. J. Mol. Biol. 149, 761-786 (1981).
11. Record, M.T., Anderson, C.F., and Lohman, T.M., Thermodynamic Analysis of Ion Effects on the Binding and Conformational Equilibria of Proteins and Nucleic Acids: The Roles of Ion Association or Release, Screening and Ion Effects on Water Activity. Quart. Rev. Biophys. 11, 103-178 (1978).

12. Reuben, J., Shporer, M., and Gabby, E.J., The Alkali Ion-DNA Interaction as Reflected in the Nuclear Relaxation Rates of ^{23}Na and ^{87}Rb. Proc. Natl. Acad. Sci. 72, 245-247 (1975).

13. Anderson, C.F. and Record, M.T. Jr., Sodium-23 NMR Studies of Cation-DNA Interactions. Biophys. Chem. 7, 301-316 (1978).

14. a) Povirk, L.F. and Goldberg, I.H., Stoichiometric Uptake of Molecular Oxygen and Consumption of Sulfhydryl Groups by Neocarzinostatin Chromophore Bound to DNA. J. Biol. Chem. 258, 11763-11767 (1983).

    b) Chin, D.H., Carr, S.A., and Goldberg, I.H., Incorporation of $^{18}O_2$ into Thymidine 5'-Aldehyde in Neocarzinostatin Chromophore Damaged DNA. J. Biol. Chem. 259, 9975-9978 (1984).

    c) Kappen, L.S. and Goldberg, I.H., Activation of Neocarzinostatin Chromophore and Formation of Nascent DNA Damage do not Require Molecular Oxygen. Nuc. Acids Res. 13, 1637-1648 (1985).

15. Stubbe, J. and Kozarich, J.W., Mechanisms of Bleomycin-Induced DNA Degradation. Chem. Rev. 87, 1107-1136 (1987).

16. Hertzberg, R.P. and Dervan, P.B., Cleavage of Double Helical DNA by (Methidiumpropyl-EDTA) iron(II). J. Am. Chem. Soc. 104, 313-315 (1982).

17. Sigman, D.S., Nuclease Activity of 1,10 Phenanthroline-Copper Ion. Acc. Chem. Res. 19, 180-186 (1986).

18. Basile, L.A. and Barton, J.K., Design of a Double-Stranded DNA Cleaving Agent with Two Polyamine Metal-Binding Arms: Ru(DIP)$_2$Macro^{n+}. J. Am. Chem. Soc. 109, 7548-7550 (1987).

19. Basile, L.A., Raphael, A.L., and Barton, J.K., Metal-Activated Hydrolytic Cleavage of DNA. J. Am. Chem. Soc. 109, 7550-7551 (1987).

20. Tomasz, M., Lipman, R., Verdine, G.L., and Nakanishi, K., Reassignment of the Guanine Binding Mode of Reduced Mitomycin C. Biochemistry 25, 4337-4344 (1986).

21. Hurley, L.H. and Needham-VanDevanter, D.R., Covalent Binding of Antitumor Antibiotics in the Minor Groove of DNA. Mechanism of Action of CC1065 and the Pyrrolo(1,4)benzodiazepines. Acc. Chem. Res. 19, 230-237 (1986).

22. Schultz, P.G., Ph.D. Thesis. California Institute of Technology, Pasadena, California, 1984.

23. Hertzberg, R.P. and Dervan, P.B. Cleavage of DNA with Methidiumpropyl-EDTA-Iron(II): Reaction Conditions and Product Analysis. Biochemistry 23,

3934-3945 (1984).

24. Linn, S.M. and Roberts, R.J., Nucleases Cold Spring Harbor (1982).
25. Dugas, H., Bioorganic Chemistry: A Chemical Approach to Enzyme Action, Springer-Verlag (1981).
26. a) Maxam, A.M. and Gilbert, W., Sequencing End-Labeled DNA with Base-Specific Chemical Cleavages. Methods in Enzymology 65, 499-560 (1980).
    b) Maxam, A.M. and Gilbert, W., A New Method for Sequencing DNA. Proc. Natl. Acad. Sci. USA 74, 560-564 (1977).
27. Beranek, D.T., Weis, C.C., and Swenson, D.H., A Comprehensive Quantitative Analysis of Methylated and Ethylated DNA Using High Pressure Liquid Chromatography. Carcinogenesis 1, 595-606 (1980).
28. Manoharan, M., Ransom, S.C., Mazumder, A., Gerlt, J.A., Wilde, J.A., Withka, J.A., and Bolton, P.H., The Characterization of Abasic Sites in DNA Heteroduplexes by Site Specific Labeling with ^{13}C. J. Am. Chem. Soc. 110, 1620-1622 (1988).
29. Shirahata, K. and Hirayama, N., Revised Absolute Configuration of Mitomycin C. X-ray Analysis of 1-N-(p-Bromobenzoyl)mitomycin C. J. Am. Chem. Soc. 105, 7199-7200 (1983).
30. Andrews, P.A., Pan, A., and Backur, N.R., Electrochemical Reductive Activation of Mitomycin C. J. Am. Chem. Soc., 108, 4158-4166 (1986).
31. Tomasz, M., Lipman, R., Chowdary, D., Pawlak, J., Verdine, G.L., and Nakanishi, K., Isolation and Structure of a Covalent Cross-Link Adduct between Mitomycin C and DNA. Science 235, 1204-1208 (1987).
32. Egbertson, M. and Danishefsky, S.J., Modeling of the Electrophilic Activation of Mitomycins: Chemical Evidence for the Intermediacy of a Mitosene Semiquinone as the Active Electrophile. J. Am. Chem. Soc. 109, 2204-2205 (1987).
33. Petrusek, R.L., Anderson, G.L., Garner, T.F., Fannin, Q.L., Kaplan, D.J., Zimmer, S.G., and Hurley, L.H., Pyrrolo-[1,4]-benzodiazepine Antibiotics. Proposed Structures and Characteristics of the in Vitro Deoxyribonucleic Acid Adducts of Anthramycin, Tomaymycin, Sibiromycin, and Neothramycins A and B. Biochemistry 20, 1111-1119 (1981).
34. Hertzberg, R.P., Hecht, S.M., Reynolds, V.L., Molineus, I.J., and Hurley, L.H., DNA Sequence Specificity of the Pyrrolo[1,4]benzodiazepine Antitumor Antibiotics. Methidiumpropyl-EDTA-Iron(II) Footprinting Analysis of DNA Binding Sites for Anthramycin and Related Drugs. Biochemistry 25, 1249-1258

(1986).

35. Graves, D.E., Pattaroni, C., Krishnan, B.S., Ostrander, J.M., Hurley, L.H., and Krugh, T.R., The Reaction of Anthramycin with DNA: Proton and Carbon Nuclear Magnetic Resonance Studies on the Structure of the Anthramycin-DNA Adduct. J. Biol. Chem. 259, 8202-8209 (1984).
36. Reynolds, V.L., McGovren, J.P., and Hurley, L.H., The Chemistry, Mechanism of Action and Biological Properties of CC-1065, a Potent Antitumor Antibiotic. J. Antibiotics 39, 319-334 (1986).
37. Harshman, K.D. and Dervan, P.B., Molecular Recognition of B-DNA by Hoechst 33258. Nuc. Acids. Res. 13, 4825-4835 (1985).
38. Hurley, L.H., Reynolds, V.L., Swenson, D.H., Petzold, G.L., and Scahill, T.A., Reaction of the Antitumor Antibiotic CC1065 with DNA: Structure of a DNA Adduct with DNA Sequence Specificity. Science 226, 843-844 (1984).
39. Hurley, L.H., Needham-VanDevanter, D.R., and Lee, C-S., Demonstration of the asymmetric effect of CC-1065 on local DNA structure using a site-directed adduct in a 117 base pair fragment form M13mp1. Proc Natl. Acad. Sci. USA 84, 6412-6416 (1987).
40. Hurley, L.H., Lee, C-S., McGovren, J.P., Warpehoski, M.A., Mitchell, M.A., Kelly, R.C., and Aristoff, P.A., unpublished results.
41. Reynolds, V.L., Molineux, I.J., Kaplan, D.J., Swenson, D.H., and Hurley, L.H., Reaction of the Antitumor Antibiotic CC-1065 with DNA: Location of the Site of Thermally Induced Strand Breakage and Analysis of DNA Sequence Specificity. Biochemistry 24, 6228-6237 (1985).
42. Dervan, P.B., Design of Sequence-Specific DNA-Binding Molecules. Science 232, 464-471 (1986).
43. Schultz, P.G., Taylor, J.S., and Dervan, P.B., Design and Synthesis of a Sequence-Specific DNA Cleaving Molecule. (Distamycin-EDTA)iron(II). J. Am. Chem. Soc. 104, 6861-6863 (1982).
44. Youngquist, R.S. and Dervan, P.B., Sequence-specific recognition of B-DNA by oligo-(N-methylpyrrolecarboxamide)s. Proc. Natl. Acad. Sci. USA 82, 2565-2569 (1985).
45. Zimmer, C., Effects of the Antibiotics Netropsin and Distamycin A on Structure and Function of Nucleic Acids. Prog. Nuc. Acid Res. Mol. Biol. 15, 285-318 (1975).
46. Gurskaya, G.V., Grokhovsky, S.L., Zhusze, A.L., and Gottikh, B.P.,

DNA-Binding Antibiotics: X-Ray Structure of the Distamycin A Analog. Biochim. Biophys. Acta. 563, 336-342 (1979).

47. Van Dyke, M.W. and Dervan, P.B., Footprinting with MPE-Fe(II). Complementary-strand Analyses of Distamycin and Actinomycin Binding Sites on Heterogeneous DNA. Cold Spring Harbor Symposia on Quantitative Biology, V. XLVII 347-353 (1983).
48. Van Dyke, M.W. and Dervan, P.B., Methidiumpropyl-EDTA-Fe(II) and DNase I footprinting report different small molecule binding site sizes on DNA. Nuc. Acids. Res. 11, 5555-5567 (1983).
49. Taylor, J.S., Schultz, P.G. and Dervan, P.B., DNA Affinity Cleaving: Sequence Specific Cleavage of DNA by Distamycin-Edta·Fe(II) and EDTA-Distamycin·Fe(II). Tetrahedron 40, 457-465 (1984).
50. Klevit, R.E., Wemmer, D.E., and Reid, B.R., ^{1}H NMR Studies on the Interaction between Distamycin A and a Symmetrical DNA Dodecamer. Biochemistry 25, 3296-3303 (1986).
51. Kopka, M.L., Yoon, C., Goodsell, D., Pjura, P., and Dickerson, R.E., The molecular origin of DNA-drug specificity in netropsin and distamycin. Proc. Natl. Acad. Sci. USA 82, 1376-1380 (1985).
52. Patel, D. J., Antibiotic-DNA interactions: Intermolecular nuclear Overhauser effects in the netropsin-d(CGCGAATTCGCG) complex in solution. Proc. Natl. Acad. Sci. USA 79, 6424-28 (1982).
53. Coll, M., Frederick, C.A., Wang, A.H.-J., and Rich, A., A bifurcated hydrogen-bonded conformation in the d(A-T) base pairs of the DNA dodecamer d(CGCAAATTTGCG) and its complex with distamycin. Proc. Natl. Acad. Sci. USA 84, 8385-8389 (1987).
54. Marky, L.A. and Breslauer, K.J., Origins of netropsin binding affinity and specificity: Correlations of thermodynamic and structural data. Proc. Natl. Acad. Sci. USA 84, 4359-4363 (1987).
55. Storm, D.R. and Koshland, D.E. Jr., Effect of Small Changes in Orientation on Reaction Rate. J. Am. Chem. Soc. 94, 5815-5825 (1972).
56. Menger, F.M., Directionality of Organic Reactions in Solution. Tetrahedron 39, 1013-1040 (1983).
57. Kirby, A.J., Effective Molarities for Intramolecular Reactions. Adv. in Physical Organic Chem. 17, 183-279 (1980).
58. Harris, J.M. and McManus, S.P. (ed.), Nucleophilicity, Adv. in Chemistry Series v.

215 (1987).

59. Hughes, E.D., Juliusburger, F., Masteran, S., Topley, B., and Weiss, J., Aliphatic Substitution and the Walden Inversion Part I. J. Chem. Soc. 1525 (1935).

60. Tenud, L., Farooq, S., Seibl, J., Eschenmoser, A., Endocyclische S_N-Reaktionenam gesattigten Kohlenstoff. Helv. Chim. Acta. 53, 2059-2069 (1970).

61. Coniglio, B.O., Giles, D.E., McDonald, W.R., and Parker, A.J., Solvation of Ions. Part VII. Solvation of Transition States for S_N2 and S_NAr Reactions of Azide and Thiocyanate Ions in Methanol and Dimethylformamide. J. Chem. Soc. (B0 152-160 (1966).

62. Bialer, M., Yagen, G., and Mechoulam, R., A Total Synthesis of Distamycin A an Antiviral Antibiotic. Tetrahedron 34, 2389 (1979).

63. Lown, J.W. and Krowicki, K., Efficient Total Synthesis of the Oligopeptide Antibiotics Netropsin and Distamycin. J. Org. Chem. 50, 3774-3779 (1987).

64. Sluka, J. P., Ph.D. Thesis, California Institute of Technology, Pasadena, California, 1988.

65. Emmons, W.D., McCallum, K.S., and Ferris, A.F., The Preparation of Acyl Trifluoroacetates from Trifluoroacetic Anhydride. J. Am. Chem. Soc. 75, 6047-6048 (1953).

66. McLafferty, F.W., Interpretation of Mass Spectra, 3rd ed. University Science Books (1980).

67. Calladine, C.R., Mechanics of Sequence-dependent Stacking of Bases in B-DNA. J. Mol. Biol. 161, 343-352 (1982).

68. Lomonossoff, G.P. Butler, P.J.G., and Klug, A. Sequence-dependent Variation in the Conformation of DNA. J. Mol. Biol. 149, 745-760 (1981).

69. Dickerson, R.E., Base Sequence and Helix Structure Variation in B and A DNA. J. Mol. Biol. 166, 419-441 (1983).

70. Tullius, T.D. and Dombroski, B.A., Iron(II) EDTA Used to Measure the Helical Twist Along Any DNA Molecule. Science 230, 679-681 (1985).

71. Ueki, M. and Inazu, T., Synthesis of Peptides Containing Hydroxyamino Acids by the Mixed Anhydride Method without Protecting the Hydroxyl Functions. Chemistry Letters, 45-48 (1982).

72. Sheenan, J.C., Goodman, M., and Hess, G.P., Peptide Derivatives Containing Hydroxyamino Acids. J. Am. Chem. Soc. 78, 1367-1369 (1956).

73. Montgomery, J.A. and Thomas, J.H., On the Alkylation of Adenine. J. Heterocycl. Chem. 1, 115-120 (1964).

74. a) Fujii, T. and Leonard, N.J., 3-(3-Methyl-2-butenyl)-adenine (Triacanthine): Direct Alkylation of Adenine at the 3-Position. Synthetic Procedures in Nucleic Acid Chemistry Vol. I, 13-15 (19xx).

    b) Leonard, N.J. and Fujii, T., The Synthesis of 7-Substituted Adenines through the Use of a Blocking Group at the 3-Position. J. Am. Chem. Soc. 85, 3719 (1963).

75. Cantor, C.R. and Schimmel, P.R., Biophysical Chemistry. Part II: Techniques for the Study of Biological Structure and Function. p.349, W.H. Freeman and Company (1980).

76. Fasman, G.D., Handbook of Biochemistry Vol. 1, CRC Press (1975).

77. a) Singer, B., Sun, L., and Fraenkel-Conant, H., Reaction of Adenosine with Ethylating Agents. Biochemistry 13, 1913-1920 (1974).

    c) Singer, B. and Grunberger, D., Molecular Biology of Mutagens and Carcinogens, Plenum Press (1983).

78. Ishino, M., Sakaguchi, Morimoto, I., Okitsu, T., Protonation Sites of Adenine Derivatives. I. Nuclear Magnetic Resonance Investigation of Adenine N-3 Derivatives in Dimethyl Sulfoxide-d_6. Chem. Pharm. Bull. 29, 2403-2407 (1981).

79. Yang, N.C. and Chang, C., Selective Alkylation of Carcinogenic 9-Anthryloxirane at the N-3 Position of Adenine in DNA. Proc. Natl. Acad. Sci. USA 82, 5250-5254 (1985).

80. Balaban, J.E. and Pyman, F.L., Bromo-derivatives of Glyoxaline. J Chem. Soc. 121, 947-958 (1922).

81. Barrio, M.C.G., Scopes, D.I.C., Holtwick, H.B., and Leonard, N.J., Syntheses of all Singly labeled [^{15}N]adenines: Mass spectral fragmentation of adenine. Proc. Natl. Acad. Sci. USA 78, 3986-3988 (1981).

82. Leonard, N.J., Carraway, K.L., and Helgeson, J.P., Characterization of N_x, N_y-Disubstituted Adenines by Ultraviolet Absorption Spectra. J. Heterocycl. Chem. 2, 261-297 (1965).

83. Witanowski, M., Stefaniak, L., and Webb, G.A., Nitrogen NMR Spectroscopy. Ann. Reports on NMR Spec. 11B, 115 (1981).

84. Wiemer, D.F., Scopes, D.I.C., Leonard, N.J., ^{15}N-^{13}C Coupling for Determination of the Site of N-Alkylation of Nitrogen Heterocycles: Linear-Benzopurines. J. Org. Chem. 41, 3051-3053 (1976).

85. Gonnella, N.C. and Roberts, J.D., Studies of the Tautomerism of Purine and the Protonation of Purine and Its 7- and 9-Methyl Derivatives by Nitrogen-15 Nuclear

Magnetic Resonance Spectroscopy. J. Am. Chem. Soc. 104, 3162-3164 (1982).

86. Chenon, M.T., Pugmire, R.J., Grant, D.M., Panzica, R.P., and Townsend, L. B., Carbon-13 Magnetic Resonance. XXV. A Basic Set of Parameters for the Investigation of Tautomerism in Purines Established from Carbon-13 Magnetic Resonance Studies Using Certain Purines and Pyrrolo[2,3-d]pyrimidines. J. Am. Chem. Soc. 97, 4627-4636 (1975).

87. Gonnella, N.C., Nakanishi, H., Holtwick, J.B., Horowitz, D.S., Kanamori, K., Leonard, N.J., and Roberts, J.D., Studies of Tautomers and Protonation of Adenine and its Derivatives by Nitrogen-15 Nuclear Magnetic Resonance Spectroscopy. J. Am. Chem. Soc. 105, 2050-2055 (1983).

88. Becker, E.D., Miles, H.T., and Bradley, R.B., Nuclear Magnetic Resonance Studies of Methyl Derivatives of Cytosine. J. Am. Chem. Soc. 87, 5575-5582 (1965).

89. Roberts, J.D., Sullivan, G.R., Pang, P.P., and Leonard, N., Nitrogen-15 Nuclear Magnetic Resonance Spectroscopy of 5-Azacytidine. J. Org. Chem. 46, 1014-1016 (1981).

90. Voet, D. and Rich, A., The Crystal Structures of Purines, Pyrimidines and Their Intermolecular Complexes. Prog. Nuc. Acid Res. Mol. Biol. 10, 183-265 (1970).

91. Gao, X. and Jones, R.A., Nitrogen-15-Labeled Deoxynucleosides: Synthesis of [6-^{15}N] and [1-^{15}N]Deoxyadenosines from Deoxyadenosine. J. Am. Chem. Soc. 109, 1275-1278 (1987).

92. Gao, X., and Jones, R.A., Nitrogen-15-Labeled Oligodeoxynucleotides: Characterization by ^{15}N NMR of d[CGTACG] Containing ^{15}N6- or ^{15}N1-Labeled Deoxyadenosine. J. Am. Chem. Soc. 109, 3169-3171 (1987).

93. Carlsen, P.H.J., Katsuki,T., Martin, V., and Sharpless, K.B., A Greatly Improved Procedure for Ruthenium Tetraoxide Catalyzed Oxidations of Organic Compounds. J. Org. Chem. 46, 3936-3938 (1981).

94. Beasley, A.E., and Rasmussen, M., Heterocyclic Ambident Nucleophiles. II. The Alkylation of Adenine. Aust. J. Chem., 34, 1107-1116 (1981).

95. Breitmaier, E. and Voelter, W., Carbon-13 NMR Spectroscopy: High Resolution Methods and Applications in Organic Chemistry and Biochemistry , VCH (1987).

96. Leonard, N.J. and Henderson, T.R., Purine Ring Rearrangements Leading to the Development of Cytokinin Activity. Mechanism of the Rearrangement of 3-Benzyladenine to N6-Benzyladenine. J. Am. Chem. Soc. 97, 4990-4999 (1975).

97. a) Uesugi, S. and Ikehara, M., Carbon-13 Magnetic Resonance Spectra of 8-substituted Purine Nucleosides. Characteristic Shifts for the Syn Conformation. J. Am. Chem. Soc. 99, 3250-3253 (1977).

b) Jones, A.J., Winkley, M.W., Grant, D.M., and Robins, R.K., Carbon 13 Nuclear Resonance of Naturally Occurring Nucleosides. Proc. Natl. Acad. Sci. 65, 27-30 (1970).

98. Hurley, L.H., unpublished results.

99. a) McGhee, J.D., Theoretical Calculations of the Helix-Coil Transition of DNA in the Presence of Large, Cooperatively Binding Ligands. Biopolymers 15, 1345-1375 (1976).

b) Record, M.T., Mazur, S.J., Melancon, P., Roe, J.-H., Shaner, S.L., and Unger, L., Double Helical DNA: Conformations, Physical Properties, and Interactions with Ligands. Ann. Rev. Biochem. 50, 997-1024 (1980).

100. Baker, B.R., Design of Active Site Directed Irreversible Enzyme Inhibitors. The Organic Chemistry of the Enzymic Active Site. John Wiley and Sons Inc. 1967.

101.a) VanEtten, R.L., Sebastian, J.F., Clowes, G.A., and Bender, M.L., Acceleration of Phenyl Ester Cleavage by Cycloamyloses. A Model for Enzymatic Specificity. J. Am. Chem. Soc. 89, 3242-3252 (1967).

b) VanEtten, R.L., Clowes, G.A., Sebastian, J.F., and Bender, M.L., The Mechanism of the Cycloamylose-Accelerated Cleavage of Phenyl Esters. J. Am. Chem. Soc. 89, 3253-3262 (1967).

c) Breslow, R., Czarniecki, M.F., Emert, J., and Hamaguchi, H., Improved Acylation Rates within Cyclodextrin Complexes from Flexible Capping of the Cyclodextrin and from Adjustment of the Substrate Geometry. J. Am. Chem. Soc. 102, 762-770 (1980).

102. Laird, R.M. and Whitfield, S.E., An Infrared Study of the Rotational Isomerism of Phenacyl Bromide and Chloride in Methanol adn Pentan-1-ol. J. Chem. Res. (S) 288-289 (1983).

103. RamaRao, M. and Bothner-By, A.A., Determination of Conformation of Halomethyl Ketones from the Temperature Dependence of Geminal H,H Coupling Constants. Org. Magn. Reson. 8, 329-331 (1976).

104. Loeb, L.A. and Preston, B.D., Mutagenesis by Apurinic/Apyrimidinic Sites. Ann. Rev. Genet. 20, 201-30 (1986).

105. Lindahl, T. and Nyberg, B., Rate of Depurination of Native Deoxyribonucleic Acid. Biochemistry 11, 3610-3618 (1972).

106. Grossman, L. and Grafstrom, R., AP sites and AP endonuleases. Biochimie 64, 577-580 (1982).

107. Levine, Ira N., Consecutive First Order Reactions, p. 506-507 of Physical Chemistry, 2nd Ed., McGraw-Hill Book Company 1983.